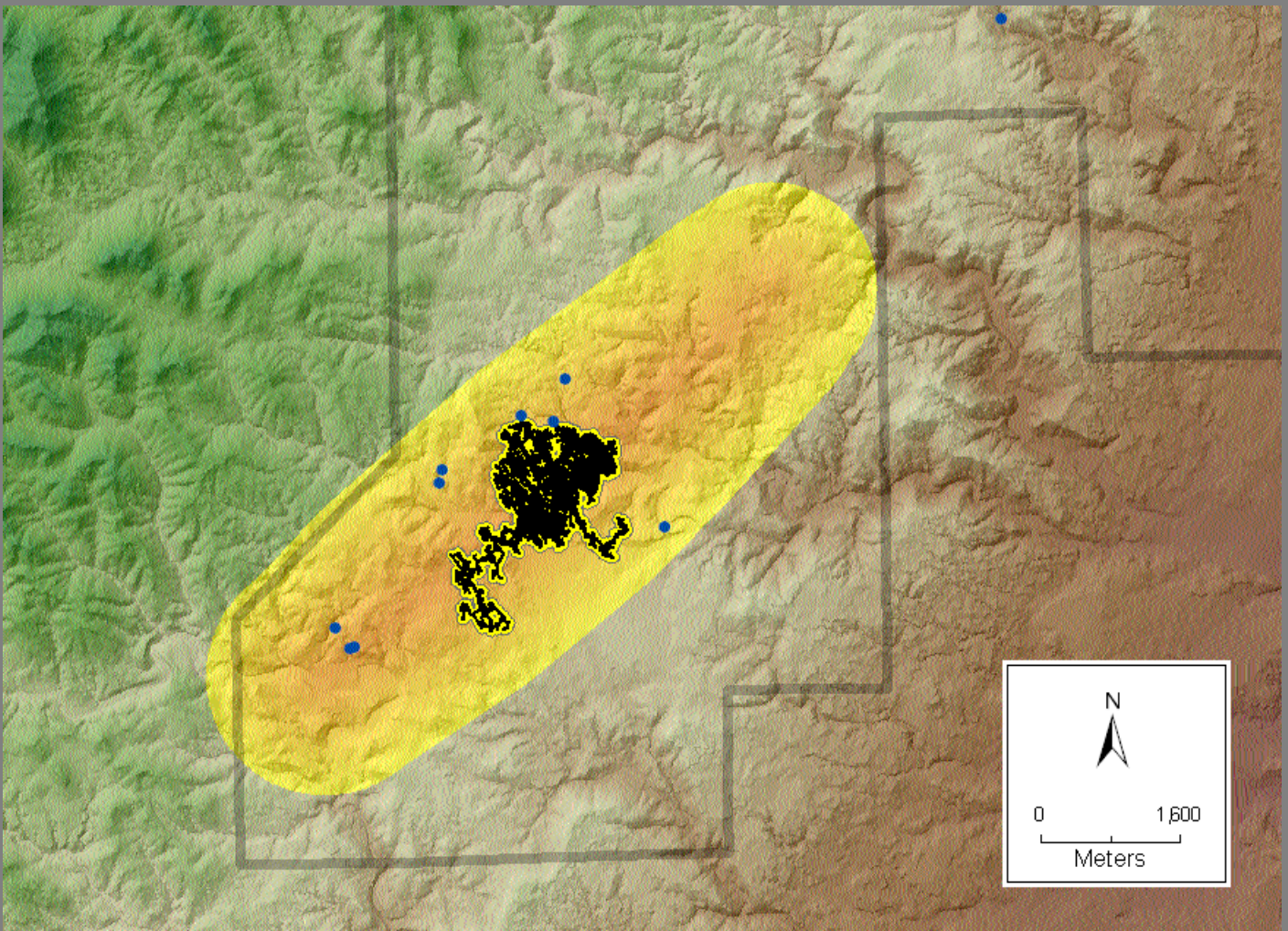


JOURNAL OF CAVE AND KARST STUDIES

April 2002
Volume 64 Number 1
ISSN 1090-6924
A Publication of the National
Speleological Society



CAVE AND KARST GIS SPECIAL ISSUE

Journal of Cave and Karst Studies of the National Speleological Society

Volume 64 Number 1 April 2002

CONTENTS

Introduction to cave and karst GIS <i>Bernard W. Szukalski</i>	3
Using GIS to manage two large cave systems, Wind and Jewel Caves, South Dakota <i>Rene Ohms and Matthew Reece</i>	4
The use of GIS in the spatial analysis of an archaeological cave site <i>Holley Moyes</i>	9
GIS applied to bioarchaeology: An example from the Río Talgua Caves in northeast Honduras <i>Nicholas Herrmann</i>	17
Remote sensing and GIS-based analysis of cave development in the Suoimuoi Catchment (Son La - NW Vietnam) <i>L. Q. Hung, N.Q. Dinh, O. Batelaan, V. T. Tam, and D. Lagrou</i>	23
Implementation and application of GIS at Timpanogos Cave National Monument, Utah <i>B.E. McNeil, J.D. Jasper, D.A. Luchsinger, and M.V. Rainsmier</i>	34
The application of GIS in support of land acquisition for the protection of sensitive groundwater recharge properties in the Edwards Aquifer of south-central Texas <i>Dan Stone and Geary M. Schindel</i>	38
Revising the karst map of the United States <i>George Veni</i>	45
The development of a karst feature database for southeastern Minnesota <i>Yongli Gao, E. Calvin Alexander, Jr., and Robert G. Tipping</i>	51
Karst GIS advances in Kentucky <i>Lee J. Florea and Randall L. Paylor, Larry Simpson, and Jason Gulley</i>	58
Using geographic information systems to develop a cave potential map for Wind Cave, South Dakota <i>Rodney D. Horrocks and Bernard W. Szukalski</i>	63
Hurricane Crawl Cave: A GIS-based cave management plan analysis and review <i>Joel Despain and Shane Fryer</i>	71
Public datasets integrated with GIS and 3-D visualization help expand subsurface conceptual model <i>Terri L. Phelan</i>	77
An examination of perennial stream drainage patterns within the Mammoth Cave watershed, Kentucky <i>Alan Glennon and Chris Groves</i>	82
Cave Science News	93

The *Journal of Cave and Karst Studies* (ISSN 1090-6924) is a multi-disciplinary, refereed journal published three times a year by the National Speleological Society, 2813 Cave Avenue, Huntsville, Alabama 35810-4431 USA; (256) 852-1300; FAX (256) 851-9241, e-mail: nss@caves.org; World Wide Web: <http://www.caves.org/~nss/>. The annual subscription fee, worldwide, by surface mail, is \$18 US. Airmail delivery outside the United States of both the *NSS News* and the *Journal of Cave and Karst Studies* is available for an additional fee of \$40 (total \$58); The *Journal of Cave and Karst Studies* is not available alone by airmail. Back issues and cumulative indices are available from the NSS office. POSTMASTER: send address changes to the *Journal of Cave and Karst Studies*, 2813 Cave Avenue, Huntsville, Alabama 35810-4431 USA.

Copyright © 2002 by the National Speleological Society, Inc. Printed on recycled paper by American Web, 4040 Dahlia Street, Denver, Colorado 80216 USA

Front cover: Cave potential map, Wind Cave, South Dakota. See Horrocks and Szukalski, p. 63.

Back cover: Geologic cross-section of the Edwards Aquifer, Texas. See Stone and Schindel, p. 38.

Editor

Louise D. Hose

Department of Physical Sciences
Chapman University
Orange, CA 92866
(714) 997-6994 Voice
(714) 532-6048 FAX
hose@chapman.edu

Production Editor

James A. Pisarowicz

Wind Cave National Park
Hot Springs, SD 57747
(605) 673-5582
pisarowi@gwtc.net

BOARD OF EDITORS

Anthropology

Patty Jo Watson

Department of Anthropology
Washington University
St. Louis, MO 63130
pjwatson@artsci.wustl.edu

Conservation

Julian J. Lewis

J. Lewis & Associates, Biological Consulting
217 West Carter Avenue
Clarksville, IN 47129
(812) 283-6120
lewisbioconsult@aol.com

Earth Sciences-Journal Index

Ira D. Sasowsky

Department of Geology
University of Akron
Akron, OH 44325-4101
(330) 972-5389
ids@uakron.edu

Exploration

Andrea Futrell

987 Dow Creek Road
Pembroke, VA 24136
(540) 626-5349
karstmap@hotmail.com

Life Sciences

Steve Taylor

Center for Biodiversity
Illinois Natural History Survey
607 East Peabody Drive (MC-652)
Champaign, IL 61820-6970
(217) 333-5702
staylor@inhs.uiuc.edu

Social Sciences

Marion O. Smith

P.O. Box 8276
University of Tennessee Station
Knoxville, TN 37996

Book Reviews

Ernst H. Kastning

P.O. Box 1048
Radford, VA 24141-0048
ehkastni@runet.edu

Proofreader

Donald G. Davis

JOURNAL ADVISORY BOARD

David Ashley	Rane Curl
Malcolm Field	Andrew Flurkey
John Ganter	Donald MacFarlane
Diana Northup	Art Palmer
William White	

INTRODUCTION TO CAVE AND KARST GIS

BERNARD W. SZUKALSKI

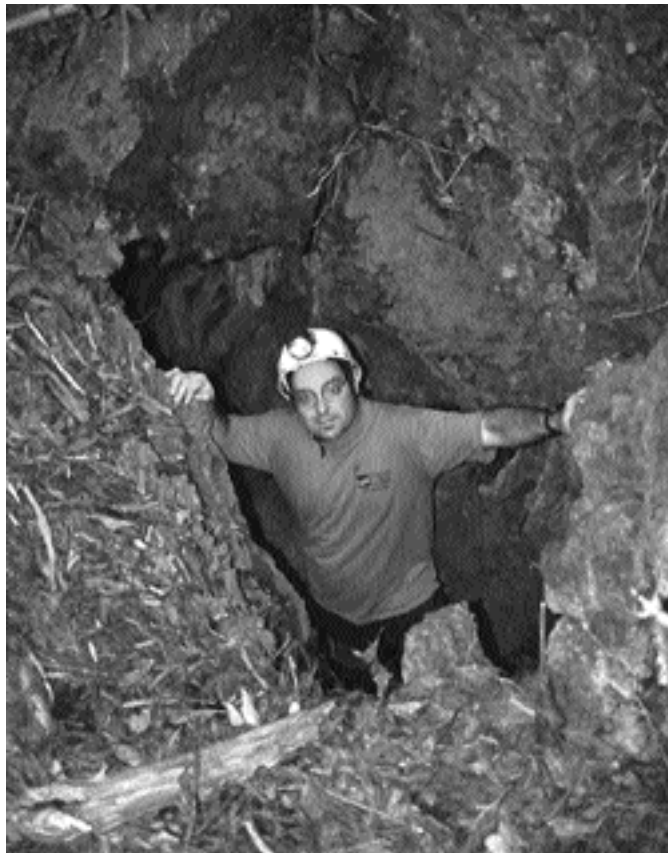
ESRI Cave & Karst Program, ESRI, 380 New York Street, Redlands, CA 92373-8100, USA

A geographic information system (GIS) is a software system that stores, analyzes, and displays geographic data and related information. GIS is a relatively new science and technology that brings together many different disciplines. It is based on the fact that much of the data and information we need to use has an inherent geographic location and is related spatially. GIS delivers the capabilities to store, manage and query geographic data, and produce maps and reports. More importantly, GIS provides the analytical tools to help understand the spatial distribution of geographic information and model its interactions, in many cases finding patterns and relationships previously unrecognized.

Once used only by a select few organizations and research institutes, today GIS is used by many cities and towns, states,

most government agencies, businesses, schools, universities, and many other organizations worldwide. GIS is used in a diverse range of applications such as environmental management, health care, telecommunications, archaeology, forestry, transportation, agriculture, local government, law enforcement, marine ecology, electric utilities, education, petroleum exploration, and more. The list of users continues to grow as GIS technology and the supporting computing environment evolves and becomes more powerful and less costly.

Although GIS has been used by environmental managers for decades, the use of GIS to study and manage caves and karst is a relatively new and rapidly growing area. Many environmental consulting companies now use GIS to solve problems in karst areas. State and local government agencies incorporate karst layers in their GIS databases and use that information in daily activities. Since the adoption of the Federal Cave Resources Protection Act of 1988, federal government agencies such as the National Park Service, Bureau of Land



Management, and US Forest Service have begun to explore the ways that a GIS can help to manage and protect cave resources. Even independent caving organizations and cave and karst conservancies have begun to explore GIS.

Cave and karst GIS has proven to be useful and effective in many ways. GIS is used to integrate and manage different kinds of karst data and to create high quality maps that incorporate many other layers of information. Advanced rendering capabilities are used to visualize caves and karst features in 3D. Beyond simple tasks, GIS analytical and modeling capabilities are increasing our knowledge of caves and karst and helping make informed decisions. GIS is used to understand and mitigate the impacts of proposed landfills,

highway construction, housing development, and landuse changes in karst areas. GIS is used to determine cave potential and for groundwater management and modeling. At a more detailed level, GIS is used to query and manage cave inventory data and is being employed to understand the spatial relationships within the cave and also to identify relationships with the external environment as a whole. Many of these applications present new technical challenges as well as insight.

The full potential of cave and karst GIS has only begun to be explored. The papers in this issue demonstrate just some of the variety of ways it is being used today. Many of the topics represent new and unique applications of GIS in cave and karst research, conservation, and management. We can learn much and gain inspiration from these examples and can look forward to the continuing evolution and expansion of GIS in the cave and karst domain. The results will be better understanding, management, and conservation of these unique resources.

USING GIS TO MANAGE TWO LARGE CAVE SYSTEMS, WIND AND JEWEL CAVES, SOUTH DAKOTA

RENE OHMS

Jewel Cave National Monument, RRI Box 60AA, Custer, SD 57730 USA

MATTHEW REECE

Lava Beds National Monument, 1 Indian Wells Headquarters, Tulelake, CA 96134 USA

The length and complexity of Wind and Jewel Caves offer unique challenges for cave managers. Determining the location of specific cave passages in relation to surface features is a key management tool, which is now greatly facilitated by Geographic Information Systems (GIS). This has been particularly useful at Wind and Jewel, where the complexity of the caves and their lack of obvious relation to the overlying surface make visualization of their locations difficult. GIS has also been used at both Wind and Jewel to display data tied to cave survey stations (such as feature inventories and control points). At Jewel Cave, GIS has been used to aid in management decisions regarding the use of herbicides above cave resources, and to better identify where the cave crosses political boundaries. At Wind Cave, GIS has been used to plan a parking lot replacement project and to create a model of the cave's potential extent.

South Dakota's Wind Cave, over 160 km, and Jewel Cave, over 200 km, are complex network mazes with several distinct levels of passage in a vertical extent of just over 190 m. Wind Cave is more complex than Jewel, averaging 150 survey stations per kilometer to Jewel's 105 stations per kilometer (Fig. 1). Both caves have over 21,000 total survey stations.

Prior to the use of GIS, the location of the caves in relation to surface features was roughly determined by processing the cave survey data, printing a scaled line plot, then overlaying the print-out on a topographic map or aerial photograph. Known locations of the caves' entrances were used to correctly align the overlay. This provided important information about the relation of the caves to surface features, but provided little flexibility to work with multiple layers or to change the scale of the overlay.

Overburden for specific survey stations could not easily be calculated or visualized with the two-dimensional overlay. Calculations for particular stations of interest could be made by adding the Z value in the cave survey software (the vertical relationship with the survey origin) to the known elevation of the origin, then subtracting this value from the elevation of the surface above the station (as determined by the rough overlay). This was a time-consuming process, and could not easily be done for all 21,000+ stations.

A wealth of data associated with cave survey stations has been collected over the years at both caves. Survey teams also collect cave feature inventory information. Each recorded feature (speleothems, biological resources, etc.) is associated in the database with the nearest survey station. Queries of the inventory databases can return a list of all stations near designated items or combinations of items, but this list is not particularly useful without the ability to put these relationships in a broader context.

Cave radiolocations have tested survey accuracy at both caves, and are also associated with the nearest survey station.

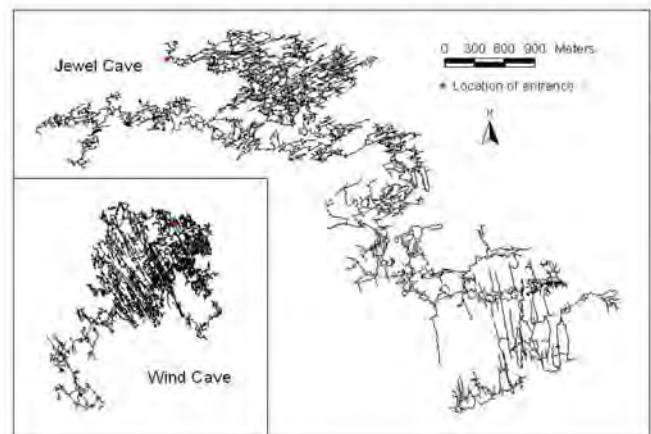


Figure 1. Line plots of Wind Cave (161.91 km) and Jewel Cave (203.20 km), illustrating complexity and passage density.

These data have been used to adjust the cave survey by entering control points into the cave survey software, but in the past there had been no easy way to graphically compare corrected and uncorrected data.

GIS technology has provided the link between these databases of information, the cave survey, and surface features. These combinations have provided managers with the ability to view and analyze spatial relationships of features located inside the caves, as well as accurate spatial distribution of the cave passages with respect to overlying surface features.

CAVE-SURFACE RELATIONSHIPS

The first step to determining a cave's location in relation to other GIS layers is to export the cave survey data to GIS soft-

ware and register (or tie) the data to a known location. At both Wind and Jewel, ArcView GIS 3.2 is used, in conjunction with CaveTools 5.0 (an ArcView extension), and COMPASS 3.01 cave survey software.

CaveTools imports a COMPASS plot file, then creates ArcView shapefiles representing the cave line plot and the cave survey stations. Two or three-dimensional shapefiles can be created. The line plot shapefile provides a more pleasing graphic representation of the cave, whereas the stations shapefile is more suited to querying data tied to specific survey stations.

The line and point shapefiles can then be registered separately to a known location (such as the cave entrance) using CaveTools. Geographic coordinates in the appropriate projection are needed for a specific survey station. These can be determined by Global Positioning Systems (GPS) or by a survey run from a known benchmark.

At Jewel Cave, a surface transit survey to the cave entrance was done in 1997, but by this time the survey station at the entrance (originally set in 1936) had been obliterated. The 1997 surface survey also included a monumented radio location point above station 40. To register the cave survey as accurately as possible in the GIS, these X and Y coordinates for station 40 were used, and the Z coordinate was determined by using the elevation of the entrance and correcting with the appropriate Z value from the cave survey (station 40 is 25.2 m below the entrance). At Wind Cave the registration point is AU!4, at the natural entrance. The coordinates for AU!4 were determined by GPS, as well as a surface survey from known control points.

Once the caves were correctly registered in the GIS, they were combined with other layers representing hydrography, roads, political boundaries, and topographic contours. They were also overlain on images supported by ArcView, such as Digital Raster Graphics (DRGs) and Digital Orthophoto Quadrangle (DOQs) (Figs. 2 & 3).

CaveTools can add the geographic coordinates of every survey station to the data attribute table. The X and Y coordinates for any station can then be input in a GPS unit and used to navigate to the point on the surface directly above that station. The interpretation division at Wind Cave has used this tool to provide new opportunities for park visitors, offering them a "surface hike to the water table," which follows the in-cave route to Wind Cave's Calcite Lake. This technique has also been used by the cave management staff to locate potential blowholes in an area where the cave is very near the surface. At Jewel Cave, GPS was used to find the approximate surface location above a chosen site for a new radiolocation. This made it easier to locate the magnetic signal.

SURVEY ACCURACY AND CONTROL POINT ADJUSTMENT

When surface land use, such as construction of roads, installation of sewer lines, or chemical treatment of vegetation, is influenced by the known extent of the cave, such manage-

ment decisions need to be based on an accurate cave survey. To check the accuracy of the Jewel Cave survey, radio-located control point data were brought into the GIS. A total of 34 monumented radiolocations above Jewel Cave have been surveyed from benchmark locations. To display these, a spreadsheet of surface coordinates was first converted to a database file (.dbf), then added to ArcView as an Event Theme.

The corresponding in-cave radiolocation points (survey stations), were selected from the attribute table for the survey stations shapefile and converted to a new shapefile. Displaying both the surface control point locations and the corresponding in-cave locations showed the distance and direction of offset between the points determined by the cave radio and those determined by the cave survey (Fig. 4a).

As expected, the surface and in-cave points closest to the entrance overlap almost perfectly. The offset between the radio-located points and the survey-determined points increases as the survey moves farther from the entrance, becoming as great as 60 m at the far southeastern end of the cave. This suggests a compounding survey error. The direction of the offset is nearly the same for all points, however, which could point to an as-yet-undetermined systematic error rather than survey error.

In COMPASS, the X and Y coordinates from the radiolocations were entered as control points. The depth determined by the radiolocation was not used to calculate a control Z coordinate (elevation) because this measurement is subject to large, non-systematic errors (Mixon & Blenz 1964). Instead, the elevation determined by the cave survey was used as the Z value. The cave was then re-plotted with the fixed control points and brought into ArcView. A portion of the unadjusted cave line plot is shown in Figure 4b, together with the plot adjusted for the radiolocations.

OVERBURDEN DETERMINATION

Determining the depth of cave passages beneath the surface is an important cave management tool. Prior to the use of GIS, depths beneath the entrance could easily be calculated from the cave survey, but overburden could not. GIS provides the means to find the elevation of the surface above any point in the cave, as well as the elevation of every cave survey station. Subtracting the in-cave elevation from the surface elevation yields the overburden.

The method used by both Wind and Jewel to match each station with its corresponding surface elevation is known in ArcView as a spatial join. Digital Line Graphs (DLGs) of 20-foot (~6 m) topographic contours were used to determine surface elevations. The Shape field from the DLG attribute table was joined to the Shape field of the cave survey stations attribute table. The resulting table lists, for each station, the record from the topographic attribute table located closest to the station (i.e., the closest contour line). The surface elevation above the station is listed in one of the fields, in feet. The ArcView field calculator can then be used to convert this ele-

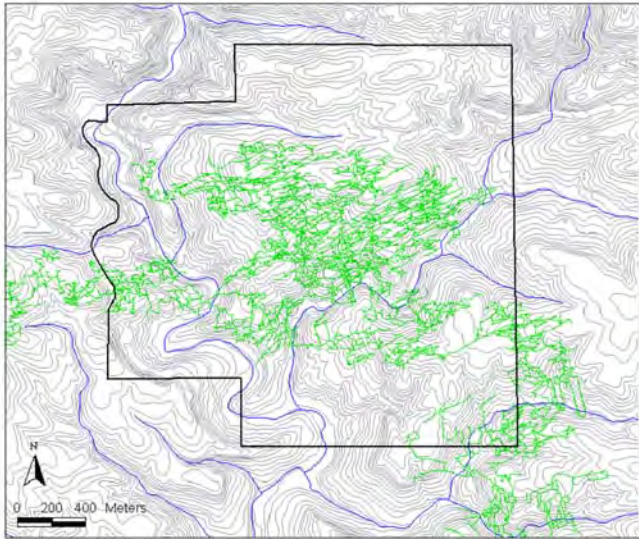


Figure 2. A portion of the Jewel Cave line plot, overlain on Digital Line Graphs representing the Monument boundary, surface elevation contours, and surface drainages.

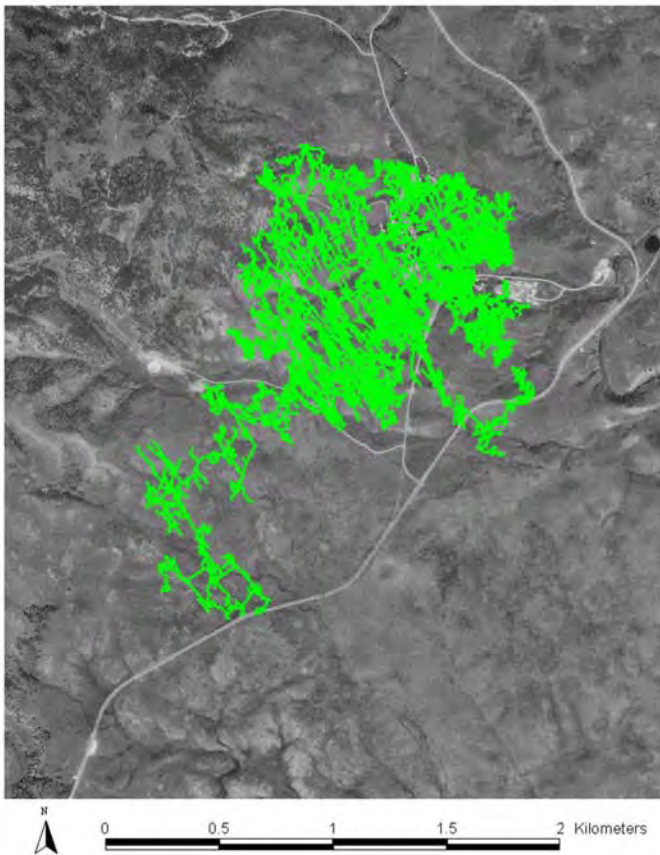


Figure 3. A view showing the location of Wind Cave relative to surface features. The surface feature image is a DOQ (Digital Orthophoto Quadrangle).

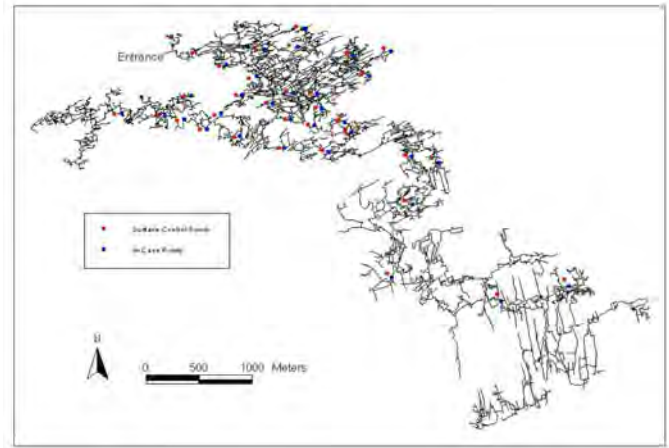


Figure 4a. Figure shows a portion of Jewel Cave, with surface control points (red) and corresponding in-cave locations (blue).

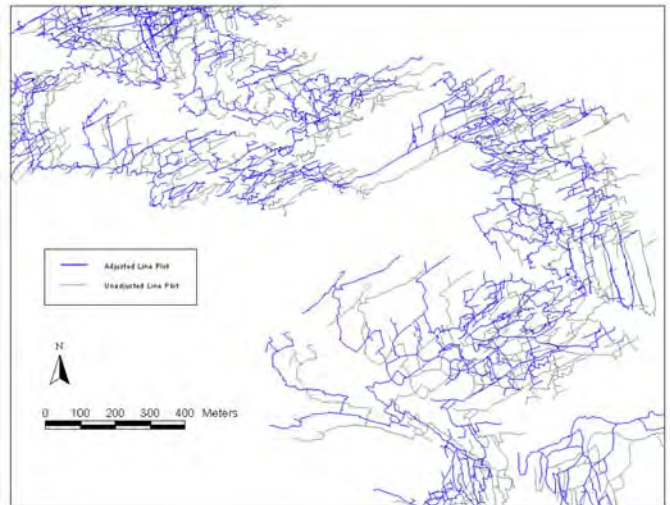


Figure 4b. Bottom figure shows a portion of the Jewel Cave line plot adjusted to fit radio location data (blue) and unadjusted (gray).

vation to meters and subtract from it the station's elevation. The resulting field gives the overburden for each station.

The accuracy of this depth determination is limited by the accuracy of the surface elevations and the accuracy of the cave survey. The DLGs used were digitized from USGS topographic maps, created from benchmark surveys, aerial overflights, and interpolation. By USGS Map Accuracy Standards, at least 90% of all tested points must be within ± 10 feet of the actual elevation (for 20-foot contours). Therefore, with the exception of $\leq 10\%$ of all points, the surface elevation can be determined within ± 10 feet.

A high-resolution Digital Elevation Model (DEM) could have been used to determine surface elevations, and this may be attempted in the future. The surface data available were the

DLGs used, and the error range of these is acceptable for the broad management applications of the overburden determination. Wind and Jewel both hope to refine the methodology when better data are available.

Cave survey accuracy will also influence the overburden determination. At Jewel Cave, survey data corrected for cave radiolocations was used when calculating overburden. Although the survey can be corrected in the X and Y directions to match the radiolocations, the Z coordinate from the original cave survey was used (as discussed in the previous section). Using the surveyed elevations could introduce error to the depth determination, particularly in the far southeastern part of Jewel Cave, where known survey error is the greatest. Less work has been done at Wind to correct survey data with radio locations, primarily based on some question of the surface survey coordinates and some missing data. Once these issues are resolved, similar corrections will be made for Wind Cave.

At Jewel Cave, the deepest point was determined to be nearly 230 m below the surface. Due to the errors described above, one survey station was found to be 2.5 m above ground! At Wind Cave, the deepest point (at the level of the water table) is 161 m, and some survey data points are as much as ~7 m above the surface. Overall, Wind Cave is much closer to the surface than Jewel, and has much greater potential for multiple surface connections (Fig. 5).

DATABASE LINKAGES

Both SMAPS and COMPASS include utilities to graphically display information from databases, such as feature inventories, on the cave line plot (Nepstad 1991; Knutson 1997). Integrating these data with other GIS layers and searching for relationships between them, however, is only possible with more powerful GIS software such as ArcView.

Feature inventory data has been collected at both Wind and Jewel. While the parks use slightly different techniques in collecting data, the fundamentals are the same: features such as speleothems, hydrologic items of note, geologic items of note, cultural artifacts, and the like are recorded with reference to the nearest survey station. These data can then be linked to attribute tables in ArcView. The inventory is now a fully-functional spatial database, and all of the functionality of ArcView is available for use on these data. Relationships between features, which may not intuitively exist, can be discovered.

It is important to note that not every surveyed passage in Wind and Jewel has been inventoried. The inventory program at both caves is relatively young, and complete coverage has not yet been achieved. Wind has much better coverage than Jewel, with over 20,000 inventoried survey stations. Over 6,000 survey stations have been inventoried at Jewel Cave.

In both Wind Cave and Jewel Cave, bat scratches have been found on the ceilings of many cave passages. The GIS inventory linkage at Jewel Cave has shown that many of the inventoried bat scratch locations are very far from the cave entrance. One rather isolated bat scratch site is near the Big

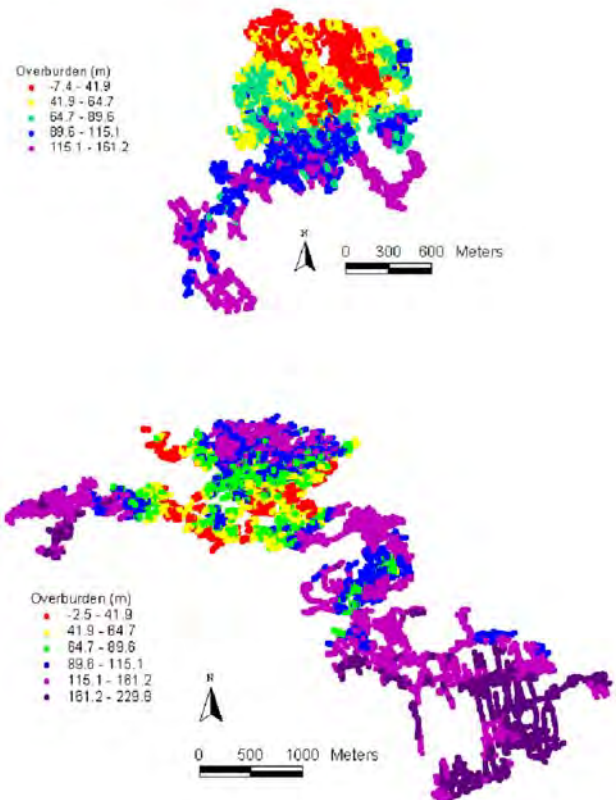


Figure 5. Wind and Jewel Caves, shaded by ranges of overburden. Wind Cave is shallower than Jewel.

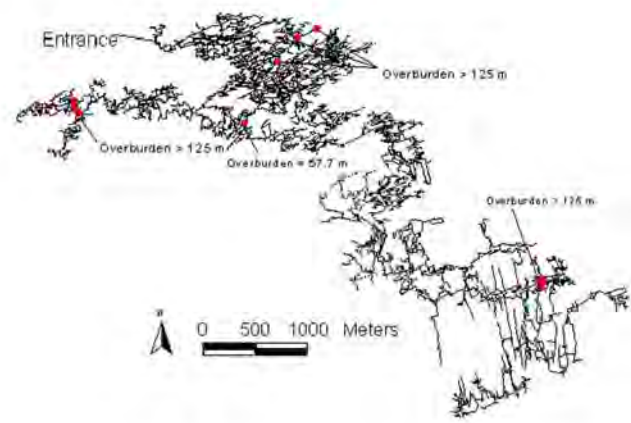


Figure 6. Locations of bat scratches in Jewel Cave (red) as determined by cave feature inventory linkage. These may be locations of old entrances that have since been naturally filled. Note overburden and distance from entrance for each area.

Duh, ~8 km (travel distance through the cave) southeast of the natural entrance. Another isolated site is in the western extent of the cave, a travel distance of ~5 km from the entrance. The overburden of these areas, as determined by the GIS analysis described in the previous section, is >125 m (Fig. 6). These

sites could be locations of past entrances that have since been naturally filled. Combining the feature inventory with other GIS layers has drawn attention to this mystery, which may have otherwise gone unnoticed.

Examples from Wind Cave include the location of water drip sites below surface drainages and the presence of helictite bushes along a distinct line across the cave. The geologic/hydrologic influences guiding the alignment of helictite bushes have not yet been understood, and the use of GIS analysis may soon help to explain this pattern.

The inventory linkage was only recently completed at both Wind and Jewel, but shows great potential to help unlock some of the secrets held, until now, by the caves. Once more data are included in the GIS, it is likely that more striking relationships will be discovered.

GIS AS A MANAGEMENT TOOL

Although GIS is in its infancy at Wind and Jewel Caves, the technology is already being used to guide management decisions. At Jewel Cave, GIS has been used to show the location of noxious weed sites relative to the cave, to calculate the depth of the cave below these sites, to evaluate their proximity to drainages and other potential infiltration zones, and to find locations of in-cave water drips near these sites. This analysis has helped the resource management staff make decisions regarding the use of herbicides to treat non-native plants.

GIS has also been used to more precisely determine where Jewel Cave leaves the National Monument boundary (Fig. 2). Currently, over 40% of Jewel Cave lies beneath U.S. Forest Service land.

A graduate student has used Jewel Cave's GIS to determine that cave passages trend beneath faults identified on the surface. He has then been able to look for evidence of faulting in those passages. This is the first step ever taken at Jewel Cave to assess surface/subsurface geologic relationships (Brian Fagnan, pers. comm., 2001).

At Wind Cave, the cave management staff has used GIS to show the relationship between the current parking lot and the cave. Plans are underway for a complete remodeling of the main parking lot at the Wind Cave Visitor Center, including a runoff treatment system. It was important to know the relationship of the cave to the overlying parking lot, particularly the amount of overburden in that area.

Likewise, the GIS has been used to create a "cave potential" model for Wind Cave (Horrocks & Szukalski 2000; 2002), in order to show the area of highest potential for cave development. This may help to guide continuing exploration, which will contribute to our knowledge of the cave and its extent. The GIS has also been used to show the relationship of Wind to other caves in the park.

As exploration of both caves progresses, more data will be collected, which will increase the knowledge base on these two world-class cave systems. At Wind Cave, researchers have already expressed interest in investigating the distribution of bat scratches, orientation of boxwork veins, and the arrangement and distribution of helictite bushes. All of these projects may be aided by use of the GIS.

A detailed geologic map of the area above Jewel Cave was recently created and will soon be digitized for use with GIS. Structural geologic contours of the top of the Mississippian Pahasapa Limestone, the cave-forming unit, were also determined and will be included as a GIS layer. The cave maps are currently hand-drafted and will be digitized in the coming years. Once this is done, passage shape, size, and orientation can be related to layers representing the surrounding geology.

The main benefit that managers have gained from the development of GIS at Wind and Jewel Caves is a way to combine datasets that were previously somewhat incompatible. This ability has allowed us to investigate relationships that would otherwise not have been apparent. As more data are made available, GIS will continue to aid in the understanding and management of these unique resources.

REFERENCES

- Horrocks, R.D. & Szukalski, B.W., 2000, Developing a cave potential map to guide surface land use management decisions at Wind Cave National Park [abst.]: *Journal of Cave and Karst Studies*, v. 62, no. 3, p. 189.
- Horrocks, R.D. & Szukalski, B.W., 2002, Using geographic information systems to develop a cave potential map for Wind Cave, South Dakota: *Journal of Cave and Karst Studies*, v. 64, no. 1, p. 63-70.
- Knutson, S., 1997, Cave maps as geographical information systems: An example from Oregon Caves National Monument: 1997 Cave and Karst Management Symposium Proceedings, p. 116.
- Mixon, W. & Blenz, R., 1964, Locating an underground transmitter by surface measurements: *Windy City Speleoneers*, v. 4, no. 6, p. 47-53.
- Nepstad, J., 1991, An inventory system for large cave systems: Proceedings of the 10th National Cave Management Symposium, p. 222-234.

THE USE OF GIS IN THE SPATIAL ANALYSIS OF AN ARCHAEOLOGICAL CAVE SITE

HOLLEY MOYES

University at Buffalo, Department of Anthropology, Box 610005 MFAC 360, Buffalo, NY 14261-0005 USA

Current Address: 609 Castillo, Santa Barbara, CA 93101 USA

Although archaeologists traditionally have viewed geographic information systems (GIS) as a tool for the investigation of large regions, its flexibility allows it to be used in non-traditional settings such as caves. Using the example of Actun Tunichil Muknal, a Terminal Classic Maya ceremonial cave in western Belize, this study demonstrates the utility of GIS as a tool for data display, visualization, exploration, and generation. Clustering of artifacts was accomplished by combining GIS technology with a K-means clustering analysis, and basic GIS functions were used to evaluate distances of artifact clusters to morphological features of the cave. Results of these analyses provided new insights into ancient Maya ritual cave use that would have been difficult to achieve by standard methods of map preparation and examination.

Archaeological studies using geographic information systems (GIS) have most often been employed in regional analyses (Petrie *et al.* 1995). One explanation is that the original GIS was designed by government planners to solve regional planning problems on large tracts of land. However, the general spatial infrastructure of GIS is not scale dependent (Aldenderfer 1996), and the flexibility of the system allows it to be used in smaller geographic spaces. For this reason, it is hardly surprising that archaeology is witnessing a growing trend of intrasite (within site) use that includes innovations in digitally recorded excavation data (Craig 2000; Edwards 2001; Levy *et al.* 2001).

Even though archaeological excavations are conducted in three-dimensional space, archaeologists traditionally conceive of units as discrete, horizontal, stratigraphic levels. Divisions between levels may be arbitrarily assigned or may represent temporal or cultural changes. The convention has been to map units as multiple levels using two-dimensional top plans (plan views). Because a GIS does not represent a major cognitive departure from paper mapping traditions, it easily represents the world as static, two-dimensional (or two and one-half dimensional) surfaces. In a GIS, each stratigraphic layer within a unit is represented as a separate view or data layer. This custom is acceptable to the archaeologist who has traditionally conceived of stratigraphic levels as discrete units of analysis. Often in intrasite analyses, archaeologists are interested in artifacts and features. For this reason, object or *vector* data models are commonly chosen to represent these entities. Objects and features are classed and each class receives its own *coverage* or *theme* that may or may not be displayed within the view.

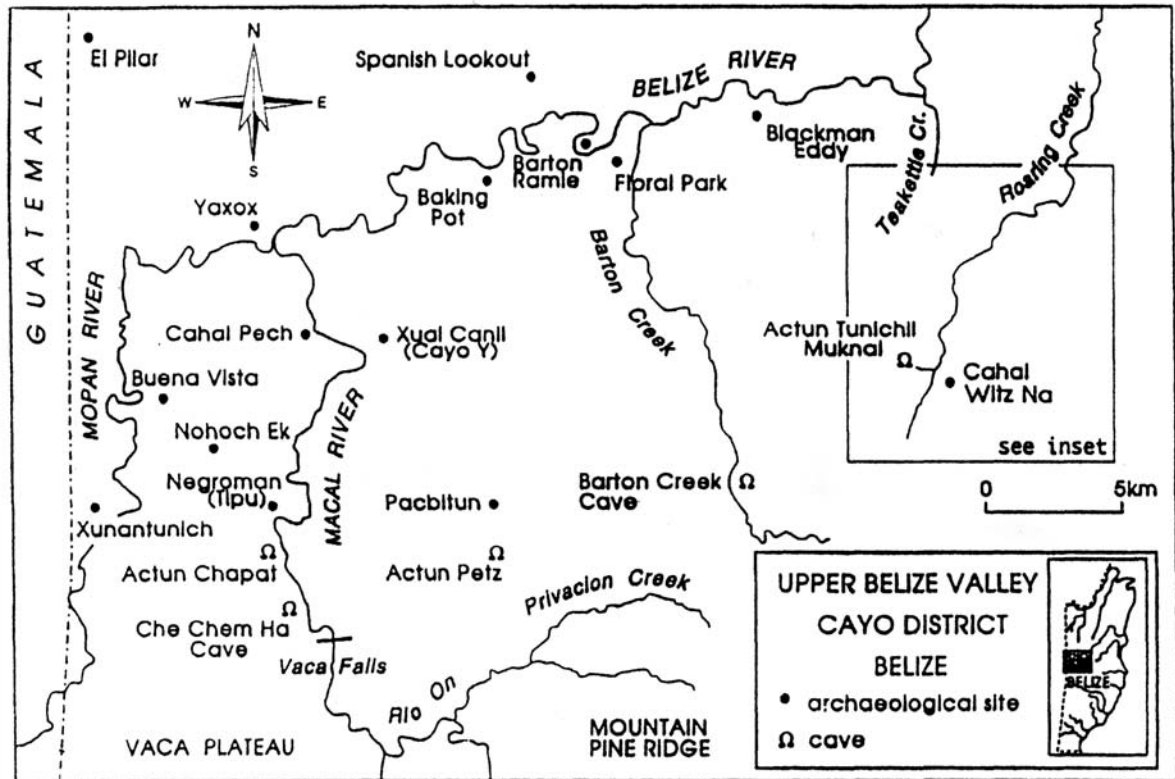
Unfortunately, this cognitive model is not always appropriate for archaeology in caves. Although archaeologists may conduct cave excavations, in many instances artifacts and features are located in tunnels that may wind back upon themselves, creating a situation in which one sits directly on top of another. To illustrate this problem, imagine a winding stairway.

The steps are vertically separated but horizontally overlapping. Problems arise in creating a GIS when tunnels and chambers vertically overlap because, in these cases, units of analysis are not layers of strata but continuous surfaces. Additionally, caves may contain complex topology in which objects share subsets of each other's volumes. For instance, along the same wall, artifacts may sit on overhanging shelves positioned directly on top of undercut niches containing objects of interest. These types of spaces are difficult to model because they are three-dimensional. The commercially available GIS software cannot yet account for these real world situations, since it is not designed to both display and conduct quantitative analyses in *truly* three-dimensional space.

This problem may be addressed by treating overlapping tunnels as separate views within a GIS, in effect making each tunnel or chamber equivalent to a discrete entity. Each area of the site matrix could be analyzed separately but displayed on a single coordinate system. However, it is not an ideal solution because the spatial relationships between the entities are not maintained, since this method forces the user to make arbitrary distinctions as to where to "cut" the space into layers. In order to facilitate quantitative analyses, it would be possible to produce map projections of overlapping areas on the same grid system, but doing so would adversely affect visualization. Although both of these solutions could work fairly well, their biggest drawback is that they compromise spatial relationships that may be important to analyses.

For display and visualization, dimensionality may be achieved using TINs (triangulated irregular network) or DEMs (Digital Elevation Models), but these produce two and one-half dimensional graphics. This can be visualized by imagining the draping of a cloth over a geographic area. Additionally, numerous other software programs can successfully represent and display objects in three dimensions. Of particular note is the CaveTools extension for ArcView that is capable of representing underground tunnels as lines (Pratt 1998; Szukalski 2001). Likewise CAD (computer assisted design) representa-

Figure 1.
Map showing
the location of
Actun Tunichil
Muknal in
western Belize.



tion of caves can be drawn. However, none of these approaches has the ability to quantify points or conduct basic GIS functions such as the creation buffers. Although display should not be underestimated as an important tool of scientific visualization for the archaeologist, geo-referencing and quantitative analyses of the distribution and spatial patterning of objects (such as artifacts or other features) are of primary interest. These analyses require the use of the quantitative analysis functions of a GIS.

For now, the decision on whether to create a GIS for analyses and display is heavily predicated on the topology of the space and goals of the research. Despite some of the problems that may be encountered, a GIS is still the most powerful tool available for geo-referencing objects and conducting two-dimensional spatial analyses. Caves or areas of caves that can be represented by horizontal planes are particularly good candidates for the creation of geographic information systems because they require minimal adaptations.

A case study of the Main Chamber of Actun Tunichil Muknal (ATM), or Cave of the Stone Sepulcher, illustrates these issues. The cave is an ancient Maya site located on the Roaring Creek River in western Belize near Teakettle village (Fig.1). It was discovered and named by geomorphologist Thomas Miller (Miller 1989), who produced a map of the 5 km system. The Western Belize Regional Cave Project, under the direction of Jaime Awe, conducted archaeological investigations there in 1996-1998. The Main Chamber of the cave functioned as a ritual space for the ancient Maya during the Terminal Classic Period (A.D. 830-950).

The chamber is a high-level passage that splits off from the

tunnel system 500 m from the cave entrance. It provided an almost ideal spatial context for the implementation of a GIS because there were no overlapping tunnels and few problem areas containing artifacts. The area could be represented as a two-dimensional flat plane, which made it possible to create a GIS using commercially available software without modifications.

THE PROJECT

WHY GIS?

Although archaeological research has demonstrated that the ancient Maya used caves as ritual spaces (Brady 1989; MacLeod & Puleston 1978; Thompson 1959), the nature of the actual rituals is unknown. Archaeologists suspect that there may have been considerable variation in ritual practice both between and within caves. Because artifact deposition in ritual contexts is not expected to be haphazard or structurally amorphous, an examination of their distributional patterns should reflect ritual structure.

The goal of the project was to analyze the placement of artifacts within the cave's interior using visualization and quantitative methods. The project entailed geo-referencing and tallying artifacts, examining their spatial distribution, and assessing artifact proximity to the morphological features of the cave. Comparing results generated by the study with ethnographic, iconographic, and ethnohistoric data should help to clarify the function and meaning of ancient Maya caves.

Achieving project goals required a means of data visualization, a high level of accuracy in mapping and analysis, and

a method by which to group the objects. GIS was instrumental in solving problems and eliminating obstacles that stood in the way of each goal. For instance, there were a number of problems with visualization. In the field, visual assessments of artifact distributions were prevented due to the limited range of our lights, large size of the chamber, and complex topology of the space. The long axis of the chamber is 183 m long and varies from 5-35 m wide, producing a total floor area of ~4450 m² (Awe *et al.* 1996; Moyes 2001; Moyes & Awe 1998, 1999). Large areas of breakdown, stalagmitic columns, and isolated boulders partition the space. Simple visual inspection was impossible, and the only mechanism by which to view the area was via a map, which led to further difficulties.

A total of 1408 artifact fragments were distributed throughout the chamber. The objects were piece-plotted at a scale of 1:60 to enhance detail and accuracy. The resulting paper map measured almost 4 m long. Viewing the document was difficult, but to reduce its size sacrificed legibility and introduced new distortions. By creating a GIS, it was possible to view the entire chamber on a single screen. A further advantage was that the GIS allowed the viewer to zoom into areas for close-up views with greater detail at an infinite number of scales. Representation of the same data at different display scales permits better visual inspection for patterning.

Proximity or associations between objects was important to understanding ritual activity. Therefore, a number of buffer areas surrounding cave features were needed for the analysis. These items included a diversity of sizes ranging between 10 cm - 1.5 m. Although it was possible to render these by hand, both the time required for such an undertaking and the compromise in expected accuracy due to line thickness and human error was prohibitive. The GIS provided a high level of accuracy for analyses and had the capability to create a variety of buffer zones surrounding specific morphological features within minutes.

Another problem was the development of a method for the quantitative analysis of the artifact assemblage. Over 99% of the artifacts were broken fragments, with some having been smashed into halves whereas others were broken into as many as 30 pieces, thus causing unequal weighting of the data. An *in situ* examination of the artifacts revealed that the fragments from single objects were deposited in close spatial proximity to one another. Often several objects were stacked together in piles or scattered in what appeared to be intentional groupings.

Clusters of artifacts offered a better unit of measurement than artifact fragments because they solved the problem of unequal weighting and were likely to represent specific isolated events. In many areas, such as small niches or rimstone dam pools, clusters were well bounded, but in large open spaces they were sometimes more difficult to define. This necessitated a formal cluster program to determine the cluster configurations mathematically. To create optimal, accurate, geo-referenced clusters, GIS technology was combined with statistical techniques.

MAPPING THE CHAMBER

The chamber was mapped and artifacts recorded during the 1996-1997 field seasons. Due to the difficulty in accessibility and wet, humid, conditions, no electronic mapping devices were employed and measurements were taken using tape and compass. To record artifacts, a system of 1-m grids was drawn over the base map, each grid assigned a number. Grid squares were located in the cave, and artifacts were piece-plotted on grid maps. These data were recorded on data sheets that were transferred to the base map.

CREATING A GIS

The success of the study relied heavily on the design of the system. Because the primary goal of the project was to measure distances between objects, a vector model, representing features as points, lines, and polygons, was used. Points were used to represent artifacts and lines or polygons to represent morphological features of the cave. One of the most difficult tasks was to categorize features. The primary consideration was to devise a typology that reflected how the ancient Maya might have conceptualized interior cave space. A review of ethnohistoric and ethnographic documents, as well as archaeological reports, provided guidance for the creation of feature classes. Based on these data, as well as personal observations, features were divided into the following categories: 1) alcoves; 2) walls & walkways; 3) boulders; 4) breakdown; 5) niches; 6) pools; and 7) stalagmitic or stalacto-stalagmitic columns.

For purposes of the study, alcoves were defined as recessed or partially enclosed areas, accessible for human entry, opening onto a room, passageway, or tunnel. Alcoves could be at floor levels, sub-floor levels, or elevated. An alcove could not open onto another alcove, therefore it was partitioned on three sides. The category of "walls and walkways" was defined as the exterior boundaries of the chamber, or vertical structures that created interior partitioning. These might include large stalagmitic or stalacto-stalagmitic columns, areas of breakdown, or any other feature that delineates a passable route. Boulders were defined as detached rocks larger than 10 inches (~16 cm) in diameter and breakdown as "the debris accumulated from the process of collapse of the ceiling or walls of a cave" (Gary *et al.* 1972: 86, 112). Niches were described as very small alcoves that did not permit human entry. In the cave, they are usually recesses within walls or spaces under rock overhangs. Pools referred to gour pools and areas in the cave where standing water was observed during flooding. Stalagmitic or stalacto-stalagmitic columns are large stalagmites, groups of fused stalagmites, or those that formed a union of a stalagmite with its complementary stalactite (Gary *et al.* 1972).

Each category was represented by its own coverage. Walls and walkways were represented in the GIS by line coverages, and all others by polygons. Pools were represented using both lines and polygons. Maps were digitized using PC Arc/Info. To prepare for digitizing, paper maps were color coded by feature category. The paper map was divided into 6 segments to fit the

Actun Tunichil Muknal Main Chamber

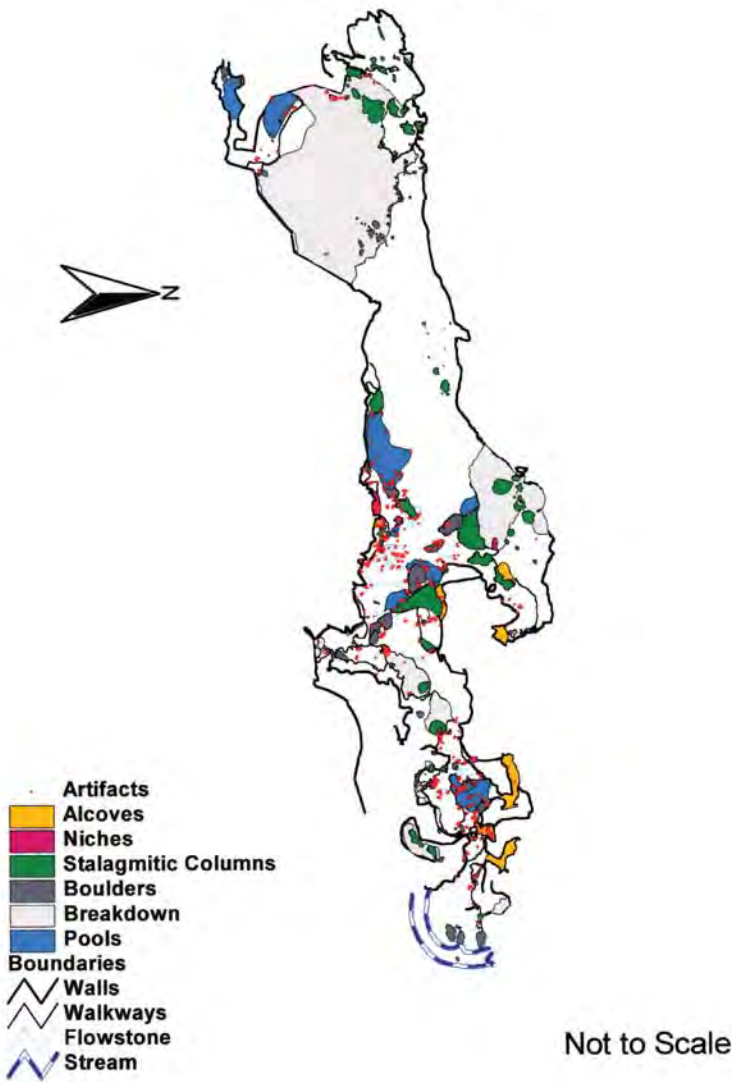


Figure 2. Map produced in ArcView 3.1 of the global artifact distribution in the Main Chamber of Actun Tunichil Muknal.

digitizing board. Between 4 and 6 tics were placed in each segment, corresponding to the previously developed 1-m grid system used for *in situ* recording. Once digitized, coverages were inspected, errors in digitizing were corrected, and polygon labels were examined for accuracy. Maps were then appended, edge-matched and transformed using Arc/Info. Transformation was accomplished by using grid coordinates from the original grid system. Once the coverages were edited, topology was built using Arc/Info and imported into ArcView 3.1 for manipulations of attribute tables, analyses, and data display. Maps of the cave were generated in order to view both global (Fig. 2) and local (Fig. 3) artifact deposition.

Actun Tunichil Muknal Central Area of Main Chamber

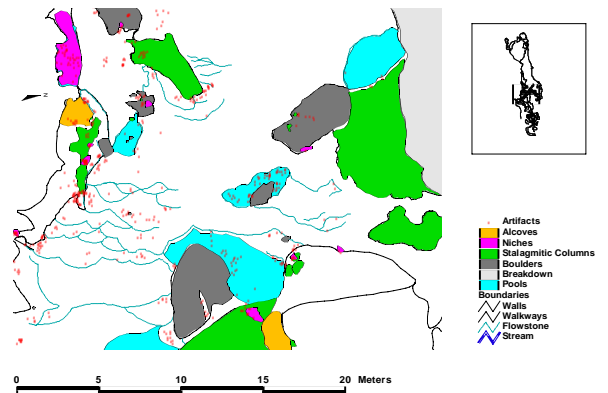


Figure 3. Detail map produced in ArcView 3.1 of local artifact distribution in the Main Chamber of Actun Tunichil Muknal.

Actun Tunichil Muknal Central Area of the Main Chamber

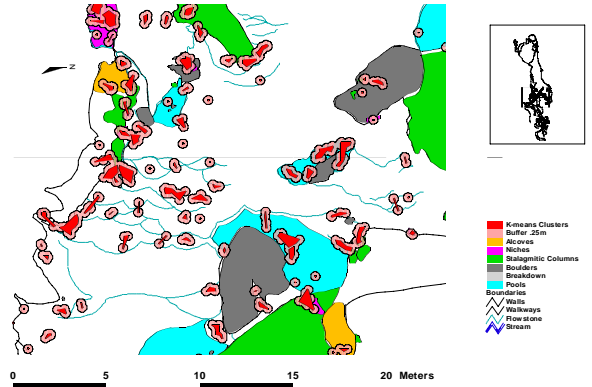


Figure 4. Detail map illustrating shape and size differences between clusters created by dissolving buffers in ArcView 3.1 and those generated by combining the K-means method with GIS functions.

CLUSTER ANALYSIS

K-MEANS CLUSTERING

Clusters of artifacts were generated based on pure locational analysis using the *K-means* cluster program developed by Kintigh and Ammerman (1982). This method was employed because it is a simple, non-hierarchical program that can be applied to two-dimensional spatial coordinates of a set of points. Its application in this context was to determine whether specific artifact classes could be formed into a set of groups based on their pure spatial location. These groups, should they exhibit robust patterning, could then be related to specific morphological features in the cave using a GIS. In this research context, the approach was superior to point pattern methods such as nearest neighbor analysis.

Point pattern methods are generally concerned with the evaluation of the degree to which the individual members of a single artifact class have a tendency to be distributed randomly, homogeneously, or clumped, across a space with reference only to members of that class (Bailey & Gatrell 1995). These methods are powerful because they are based on the assumption that the spatial relationship of the members of that single class of artifacts *vis-à-vis* one another is *intrinsically* more important than the degree of spatial proximity of those artifacts to members of different artifact classes.

In contrast, pure locational clustering is not specifically concerned with a single artifact class, but instead the degree to which members of different artifact classes are found in close spatial proximity. The content of these clusters can then be evaluated to gain insights into past behaviors. This approach has the advantage of not weighing *a priori* any specific artifact class more than another. Instead, the method seeks to define “natural” groupings of objects across a space. While it is necessary to acknowledge that these methods often impose a structure on a data set, experimental studies have shown that *K-means* clustering generally provides excellent recovery of known data structure, especially when patterning is strong within the data (Aldenderfer & Blashfield 1984).

The number of clusters to be generated by the *K-means* program is determined by the user. The *K-means* algorithm allocates each point to one of a specified number of clusters and attempts to minimize the global goodness-of-fit measures by using an SSE (sum squared error). This measure is the distance from each point to the centroid of the cluster. Some programs allow the operator to view plot files of the SSE data to determine which number of clusters used produces the best goodness-of-fit configuration, but these programs can handle only small datasets. In order to handle the large ATM dataset, it was necessary to run the program in SPSS. Unfortunately, SPSS does not generate SSE plots, and although SSEs were numerically generated, they were produced by using a linear function, ill suited to the ATM spatial data.

New techniques were developed to determine the ideal number of clusters used for the *K-means* analysis. Although one option was to estimate the number based on perusal of the data, this was rejected for two reasons. First, it would have introduced bias to the data and defeated the purpose of numerical clustering, and second, not all of the points were well clustered and decisions on the number of clusters present in these areas would have been difficult, if not arbitrary. To resolve these issues, another quantitative method, LDEN (local density analysis) was enlisted.

LOCAL DENSITY ANALYSIS

The LDEN, or local density analysis, proposed by Johnson (1976) is a global measure designed to compute densities of artifact classes within a fixed radius of each point. The GIS program was used to generate *x,y* spatial coordinates for the 1408 artifact fragments and a LDEN was conducted on the data. The LDEN was iterated in .25 m increments, beginning

at 25 cm and increasing to 3 m. The program was directed to produce a plot file of the results. The plot file that showed the highest local density coefficients of the spatial data occurred within the 25-cm radii. Using ArcView, a 25 cm buffer was created around each of the 1408 artifact points, and overlapping buffers were dissolved by the program, resulting in 252 polygons.

TEST OF BEST FIT

The *K-means* analysis was then initiated using the spatial data (*x,y* coordinates) and directed to generate 252 clusters. Before importing these data into ArcView for further analysis, the number of clusters was tested for best fit against higher and lower numbered configurations using the coefficient of variation (CV). The CV is defined as the ratio of the standard deviation to the mean:

$$CV = s/X$$

It is used to compare variables with unequal means by comparing the relative variability of a frequency distribution. Relatively less dispersed variables have lower coefficients of variation.

K-means clusters were created for 8 cluster configurations using the spatial coordinates. These were based on the original number of clusters generated by the ArcView buffers (252) and included numbers above and below that value. The cluster configuration numbers chosen were: 240, 250, 251, 252, 253, 254, 255, and 264. Seven numbered clusters from each configuration generated by the *K-means* were chosen at random for analysis. The CVs for the *x,y* coordinates for cluster numbers of each cluster configuration were added together and compared. The result showed that cluster configuration 252 had the lowest combined CV (.026554), demonstrating least variability in the data, therefore producing the best goodness-of-fit.

CREATING A CLUSTER COVERAGE IN GIS

Using the 252 *K-means* cluster configuration, a cluster attribute table was produced in ArcView. Each of the 1408 artifacts was assigned a cluster number. Numbers were highlighted and polygons were created using artifact points as nodes. This graphic was converted to a *shapefile* and imported into ArcInfo. Topology was built and the newly built coverage was re-introduced into ArcView.

The advantage of the new cluster coverage was that the clusters were smaller and more clearly defined than those generated by dissolving buffers around individual artifact points in the GIS program. This provided more accurate units of analysis and allowed for a better spatial resolution. Figure 4 illustrates shape and size differences between the two sets of clusters.

Using the 252 *K-means* clusters, buffers surrounding cave features were created using GIS. Results were generated for a variety of buffer sizes ranging from 10 cm to 1 m. As one would expect, spatial overlap of artifact clusters was present at

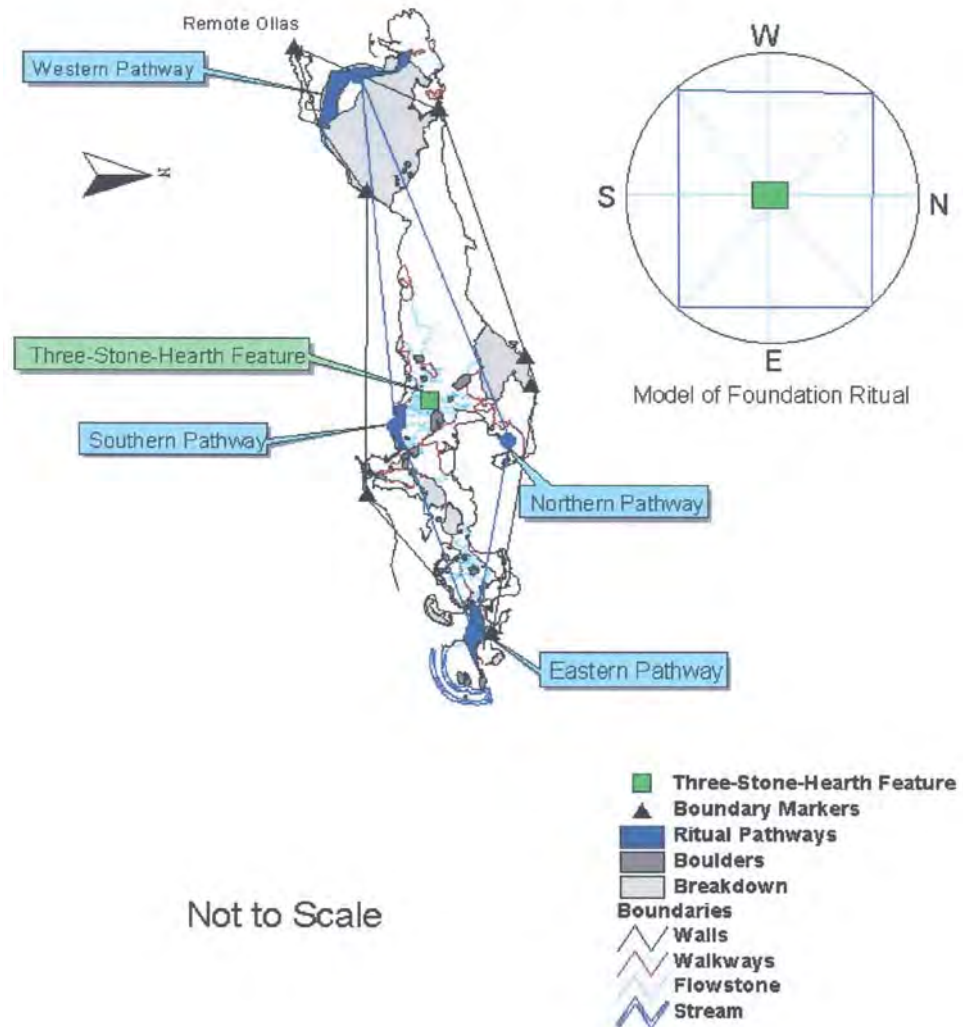
Figure 5.
Map of the Main Chamber illustrating ritual pathways, Three-Stone Hearth feature, and boundary markers juxtaposed with García-Zambrano's spatial model for rituals of foundation (after García-Zambrano 1994:220, Fig. 3).

all size levels. It was noted in the field that many artifacts were placed in pools, but also that a significant amount of the floor space was covered with intermittent standing water. If the pools category was considered separately, then the remaining categories accounted for 94% of the artifact clusters at the 25 cm buffer level. This demonstrates a reduction in category overlap at this level, suggesting that this buffer level is the best fit because it is the closest to 100%. Results were obtained using 25 cm buffers on the following feature classes: walls & walkways, stalagmitic/stalacto-stalagmitic columns, and boulders. Niches and alcoves were evaluated by determining clusters that intersected features. Because pools were represented by both lines and polygons, clusters were tallied manually on a presence/absence basis. The data are reported as a percentage of the total number of clusters found in association with each feature class: 1) pools (60%); 2) walls & walkways (28%); 3) boulders (23%); 4) stalagmitic/stalacto-stalagmitic columns (17%); 5) niches (12%); 6) alcoves (7%); and breakdown (7%).

FINDINGS

The data created by the generation of buffers was instructive because artifact depositional patterns that were not immediately obvious appeared in quantitative analyses. For instance the number of objects placed near or on boulders was unexpected. Ethnographic literature and iconography suggest that freestanding stones were used as altars or benches for the deities. Although rocks in caves are not morphologically similar to altars used in surface contexts, the data suggest that they serve as analogs to these features (Moyes & Awe 1998; Moyes 2001).

Actun Tunichil Muknal Model of Cluster Distribution Patterns Compared with Model of Rituals of Foundation



Additionally, the quantitative data generated will aid in establishing methodology to evaluate variation in the ritual function of sites, one of the most pertinent questions facing Maya cave archaeologists. Quantifying objects and assessing their placement in relation to morphological features of the cave provide concrete units of analyses. These analytical units may be used to compare sites within and outside of the region.

This study also reinforces the importance of visualization in assessing artifact assemblages. Viewing artifact clusters was instrumental in determining global spatial patterns, and areas of intense as well as sparse usage were easily identified. For instance, analysis revealed that 24% of the clusters were located in the central area. This area also contained the greatest variation in artifact classes as well as 40% of the total artifact assemblage. This ritual center of the chamber was, in fact, demarcated by the ancient Maya who placed what may be a

Three-Stone-Hearth in the middle of the area (Moyes 2000). The Three-Stone-Hearth is a salient concept in Maya cosmology representing the center of the universe and relating to the creation of the world (Friedel *et al.* 1993). This find suggest that centrality was an important feature in the use pattern of the Main Chamber, was instrumental in spurring an investigation into the possibilities that creation and renewal rituals took place in the cave (Moyes 2001). Although it has been well recognized that rituals conducted in caves were often related to rain or water deities, this new finding suggests that, in this instance, water rituals may have referenced the flood event of the Maya creation myth.

Three global cluster patterns were identified as well: concentrated clusters, linear distributions, and isolated clusters located in peripheral areas. By comparing these configurations with ethnographic and ethnohistoric data, it became clear that linear distributions were most likely to represent ritual pathways (Moyes & Awe 1998, 1999), and isolated clusters most likely functioned as boundary markers.

Much of our knowledge of modern Maya spatial cognition comes from the work of Hanks (1984, 1990) who studied the Maya of Yucatan. He recognized that there is an important cognitive spatial component at the heart of all ceremonies performed by shamans. The model is a quincuncial configuration based on the four cardinal directions and a central area. Hanks (1990) described the ritual cognitive model as a centroid surrounded by a four-sided polygonal structure whose sides are created by joining the four intercardinal points.

This cognitive model has ancient roots. Evidence for its presence among the pre-Columbian Maya can be found in the Codex Madrid, in the layout of tombs at Río Azul (Adams & Robichaux 1992), and in site construction typified by the twin pyramid complexes at Tikal (Ashmore 1991). Ethnohistoric texts demonstrate the use of an elaborated quincuncial model in rituals of foundation intended to identify and sanctify community boundaries (García-Zambrano 1994). Note the similarity of the placement of linear scatters and boundary markers in the Main Chamber to the spatial model of the rituals of foundation illustrated by García-Zambrano (Fig. 5). This agreement suggests that interior cave space was ritually bounded and that establishing these boundaries may have been an important means of ritually defining a social universe within the cave (Moyes & Awe 1999; Moyes 2001).

CONCLUSION

Despite disadvantages that two-dimensional analyses may present when working with three-dimensional spaces, GIS is still the most powerful tool available for the analysis and display of archaeological data at every spatial scale. Although studies such as this could have been accomplished using paper maps, analyses such as the creation of buffers would not have been undertaken due to the time involved as well as the loss of accuracy and precision entailed in hand-drawing these entities. Although visualization would have been possible using other programs, no other system was capable creating geo-refer-

enced data *and* conducting quantitative analyses. As this study illustrates, the strength of a GIS is demonstrated by its utility as a tool for visualization, data exploration, and data generation. There is no doubt that the GIS of the future will possess three-dimensional capabilities that will open up new lines of inquiry for spaces such as topologically complex caves.

ACKNOWLEDGMENTS

The Western Belize Regional Cave Project was funded by a grant from the Social Science and Humanities Research Council of Canada to Jaime Awe. I would particularly like to thank Dr. Awe for his support and encouragement. The permit for the project was provided by the Belize Department of Archaeology, and thanks go to Allen Moore, Brian Woodeye and John Morris.

Special thanks is extended to the 1997 staff of the WBRCP, Sherry Gibbs, Cameron Griffith, Christophe Helmke, Mike Mirro, Caitlin O'Grady, Vanessa Owens, Rhanju Song, Jeff Ransom, and Kay Sunihara. Additionally, I am grateful to Keith Kintigh for his assistance in the early stages of this work, and to Ezra Zubrow and Nathan Craig for helpful comments. Thanks also to James Brady for his encouragement and assistance in the development of my work. Finally, I would like to thank Mark Aldenderfer for his comments and suggestions in the preparation of this paper. Although I have received insights from a number of people and valuable criticism from five anonymous reviewers for which I am grateful, the content of this paper is my responsibility.

This article is based upon work supported by National Science Foundation Grant No. DGE 9870668, "Integrative Graduate Education and Research Training in Geographic Information Science," awarded to the University at Buffalo.

REFERENCES

- Adams, R.E. & Robichaux, H.R., 1992, Tombs of Río Azul, Guatemala: National Geographic Research & Exploration, v. 8, no. 4, p. 412-427.
- Aldenderfer, M., 1996, Introduction, *in* Aldenderfer, M., & Maschner, H., ed., Anthropology, space, and geographic information systems: New York, Oxford University Press, p. 3-18.
- Aldenderfer, M. & Blashfield, R., 1984, Cluster analysis: Beverly Hills, CA, Sage Publications.
- Ashmore, W., 1991, Site planning principles and concepts of directionality among the ancient Maya: *Latin American Antiquity*, v. 2, no. 3, p. 199-226.
- Awe, J., Gibbs, S., & Griffith, C., 1996, Evidence for Late Classic elite ritual activity at Actun Tunichil Muknal, Belize, Paper presented at the 61st Annual meeting of the Society for American Archaeology, Nashville, TN.
- Bailey, T. & Gatrell, A., 1995, Interactive spatial data analysis: Essex, England, Longman Scientific and Technical.
- Brady, J.E., 1989, Investigation of Maya ritual cave use with special reference to Naj Tunich, Peten, Guatemala [PhD dissertation]: University of California.
- Craig, N., 2000, Real-time GIS construction and digital data recording of the Jiskairumoko Excavation, Peru: *The Society for American Archaeology Bulletin*, v. 18, no. 1, p. 24-28.
- Edwards, D., 2001, Excavations at Khirbet Cana, Israel, <http://www.nexfind.com/cana>

- Freidel, D., Schele, L., & Parker, J., 1993, *The Maya cosmos*: New York, William Morrow.
- García-Zambrano, A.J., 1994, Early colonial evidence of Pre-Columbian rituals of foundation, in Robertson, M.G. & Field, V., ed., *Seventh Palenque Round Table*: San Francisco, Pre-Columbian Art Research Institute, p. 217-227.
- Gary, M., McAfee, Robert Jr., & Wolf, C., 1992, *Glossary of geology*: Washington, D.C., American Geological Institute.
- Hanks, W., 1984, Sanctification, structure, and experience in a Yucatec ritual event: *Journal of American Folklore*, v. 97, no. 384, p. 131-166.
- Hanks, W., 1990, *Referential practice: Language and lived space among the Maya*: Chicago, University of Chicago Press.
- Johnson, I., 1976, *Contribution méthodologique à l'étude de la répartition des vestiges dans des niveaux archéologiques* [Thesis for obtaining a Diplôme des Études Supérieures]: Université de Bordeaux I.
- Kintigh, K. & Ammerman, A.J., 1982, Heuristic approaches to spatial analysis in archaeology: *American Antiquity*, v. 47, p. 31-63.
- Levy, T.E., Anderson, J.D., Waggoner, M., Smith, N., Muniz, A., & Adams, R.B., 2001, *Digital archaeology 2001: GIS-based excavation and recording in Jordan*: The Society for American Archaeology Archaeological Record, v. 1, no. 3, p. 23-29.
- MacLeod, B. & Puleston, D., 1978, Pathways into darkness: The search for the road to Xibalba, in Robertson, M.G. & Jeffers, D.C., ed., *Tercera Mesa Redonda de Palenque*, Vol. 4: Monterey, Hearld Peters, p. 71-77.
- Miller, T., 1989, Tunichil Muknal: Caves and Caving, v. 46, p. 2-7.
- Moyes, H., 2000, The cave as a cosmogram: Function and meaning of Maya speleothem use, in Colas, P.R., Delvendahl, K., Kuhnert, M., & Schubart, A., ed., *The sacred and the profane: Architecture and identity in the Maya lowlands*: Acta Mesoamericana vol. 10: Germany, Anton Saurwein.
- Moyes, H., 2001, The cave as a cosmogram: The use of GIS in an intrasite spatial analysis of the main chamber of Actun Tunichil Muknal, A Maya ceremonial cave in western Belize [M.A. thesis]: Florida Atlantic University.
- Moyes, H. & Awe, J., 1998, Spatial analysis of artifacts in the main chamber of Actun Tunichil Muknal, Belize: Preliminary results, in Awe, J., ed., *The Western Belize Regional Cave Project: A report of the 1997 field season*: Department of Anthropology Occasional Paper No. 1: Durham, University of New Hampshire.
- Moyes, H. & Awe, J., 1999, Cultural constructs and the binding of space: Ritual pathways at Actun Tunichil Muknal, Belize, in Awe, J. & Lee, D.F., ed., *The Western Belize regional Cave Project: A report of the 1998 field season*: Department of Anthropology Occasional Paper No. 2: Durham, University of New Hampshire.
- Moyes, H. & Awe, J., 2000, Spatial analysis of an ancient cave site: *ArcUser*, v. 3, no. 4, p. 64-68.
- Petrie, L., Johnson, I., Cullen, B. & Kvamme, K., 1995, *GIS in archaeology: An annotated bibliography*, Sydney University Archaeological Methods Series 1: Archaeological computing laboratory, archaeology: Prehistoric and historical, Australia, University of Sydney 2006.
- Pratt, M., 1998, Mapping underground treasure: *ArcUser*, v. July-Sept, p. 60-62.
- Szukalski, B., 2001, <http://www.mindspring.com/~bszukalski/cavetools/cavetools.html>
- Thompson, J.E., 1959, The role of caves in Maya culture, *Mitteilungen Aus dem Museum Für Völkerkunde in Hamburg* 25: Hamburg, Kommissionsverlag Ludwig Appel, p. 122-129.

GIS APPLIED TO BIOARCHAEOLOGY: AN EXAMPLE FROM THE RÍO TALGUA CAVES IN NORTHEAST HONDURAS

NICHOLAS HERRMANN

Department of Anthropology, The University of Tennessee, Knoxville, TN 37996 USA

The presence of human skeletal remains in caves is a common phenomenon throughout the world. In an effort to preserve these remains, researchers often document the material in situ. The application of a geographic information system (GIS) in combination with a flexible recording system provides an efficient means of recording the context of the burial or ossuary. Two caves, La Cueva del Río Talgua and Cueva de las Arañas, in eastern Honduras, provide a case study for the application of a GIS to human skeletal remains from cave environments. A GIS-based investigation offers the ability to visualize the relationships and context of the ossuary. It also provides a means to estimate specific population parameters, such as the minimum number of individuals and the Lincoln Index.

When confronted with osteological remains in cave environments, archaeologists must realize the significance of the skeletal material and appreciate the context of these remains. In Binford's (1971) essay on mortuary practices, he assumes that a "burial" with all its associated attributes reflects the individual's social persona and expresses the communal "debt" owed the deceased. Deep cave interments may result from a complex social context, or may simply document the fate of an unlucky adventurer, as in the case of prehistoric miners in Mammoth Cave (Meloy 1971). The deposition of bodies within vertical shafts or sinks may be the most convenient mode of interment for a local community, or this process may be a symbolic ritual (e.g., for returning the body of the deceased to the underworld). In either situation, the archaeologist must evaluate the remains from both cultural and biological frameworks within the context of the burial environment. Cave archaeologists and skeletal biologists should work together to devise logical, reliable, and efficient methods of data collection for the documentation of these unique archaeological resources. One useful system of recording karst mortuary facilities is within a geographic information system (GIS) framework enabling bioarchaeologists to reconstruct and examine the burial context outside the cave. This paper reviews Honduran cave mortuary practices, describe obstacles and confounding factors involved in cave bioarchaeology, and details the application of a GIS in the analysis of osteological remains from La Cueva del Río Talgua and Cueva de las Arañas in eastern Honduras. Finally, it summarizes the osteological data derived from Cueva de las Arañas.

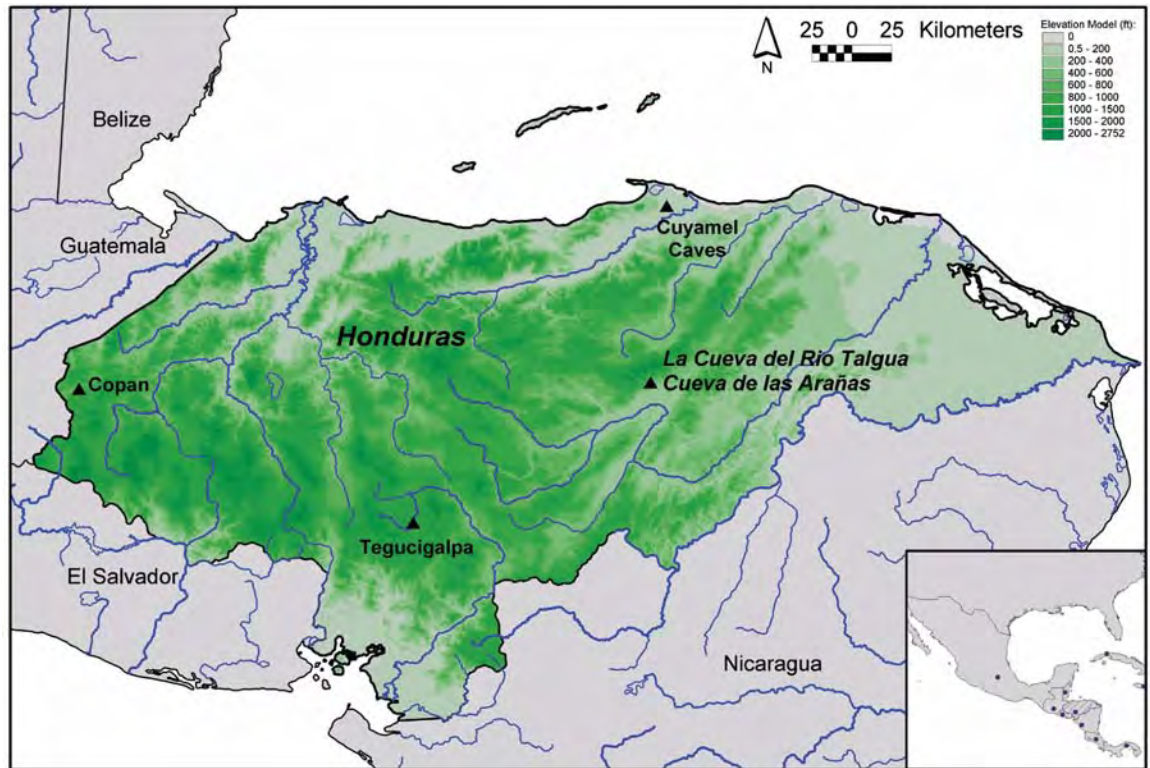
LA CUEVA DEL RÍO TALGUA AND CUEVA DE LAS ARAÑAS

Human osteological remains were discovered in 1994 in a cave above the eastern bank of the Talgua River, 7 km from Catacamas in the Olancho Valley of northeastern Honduras (Brady 1994; Fig. 1). With permission of the Instituto Hondureño de Anthropología e Historia and under the direc-

tion of James Brady as part of a joint archaeological field school of George Washington and Western Kentucky Universities, basic skeletal data were collected during a three-week period in June 1996. The ossuary in Cueva del Río Talgua, or "The Cave of the Glowing Skulls", was the primary focus of the osteological fieldwork. Hereafter, this cave is referred to as Talgua. Prior to the arrival of the osteological research team, a second mortuary cave with human skeletal remains was discovered. Recent explorers had not disturbed the ossuaries within this cave, and only limited prehistoric disturbance had occurred. The survey team named the cave "Cueva de las Arañas" (or "Cave of the Spiders") for the arachnids prominently present throughout it. This cave is referred to as Arañas.

Mortuary activities in both caves date to the Formative Period, also referred to as the Preclassic period (Brady *et al.* 1995a; 1995b; 2001). Five uncalibrated radiocarbon dates derived from bone and charcoal samples from both caves cluster within a 600 year period between 3110 BP and 2510 BP (Brady *et al.* 2001), but the calibrated two-sigma ranges of these dates span a 1000-year window. The Arañas assay (Beta-95367 2790±100 BP: Brady *et al.* 2001) falls nicely among four Talgua dates, which strongly suggests that the caves are contemporaneous and may represent the mortuary program of one population. A sixth radiocarbon date from Talgua (WG286 1385±75 BP: Brady *et al.* 2001) suggests that later populations in the region may also have used the cave. Additional mortuary caves have been found in this area, but the bioarchaeological significance and temporal placement of these sites have not been determined. Two of the radiocarbon dates are Accelerator Mass Spectrometry (AMS) determinations on human bone from the cave. As a result of AMS dating, basic carbon ratios (¹³C/¹²C) were calculated, which provide valuable evidence for dietary inferences (Buikstra 1992). The δ¹³C indicate that the Río Talgua populations were not consuming substantial quantities of maize (corn). This determination is important because diets of later Mayan populations in western

Figure 1.
General elevation model of Honduras with the locations of the Río Talgua Caves, Copan, and the Cuyamel Caves.



Honduras (Copan), Guatemala, and Mexico relied heavily on maize. Subsistence in the Talgua population may have been based on a variety of non-domesticated plants, tubers, and fauna. Manioc is a likely candidate for a primary staple of these groups, similar to a pattern documented in many Central American populations (Piperno & Holst 1998).

MORTUARY PROGRAM

Human interment within cave environments is a common approach to the disposal of the dead. Throughout the world, caves have been used as burial facilities. In North and Central America, cave passages and vertical shaft pits have been exploited (Robbins 1974; Walthall & DeJarnette 1974; Willey & Crothers 1986; Turpin 1988; Haskins 1990; Bement 1994). For example, the Woodland Period Copena mortuary complex of northern Alabama exhibits a diverse burial tradition, including extended inhumations and cremations in cave passages and shaft pit interments (Webb & Wilder 1951; Walthall 1974; Walthall & DeJarnette 1974). These mortuary caves often include numerous grave offerings and elaborately prepared burial facilities. The Archaic Period cave mortuary program of central Texas, on the other hand, differs significantly from the Copena example. In central Texas, Bement (1994) documents a mortuary pattern that entailed the interment of partially or completely defleshed individuals into vertical pit shafts and sinks, such as Seminole Sink (Turpin 1988). In the case of the Talgua caves, it appears that the indigenous population transported the skeletonized remains of numerous individuals into the back passages of these caverns. Individuals of all ages were

either disarticulated or allowed to decompose away from the caves. These remains were then bundled into some type of container, into which copious amounts of red ocher/hematite were added. The bundles were carried into the caves to fairly inaccessible areas and stacked in small piles in niches, within flowstone pools, and on shelves (Fig. 2). Multiple individuals and, in many cases, multiple ages are represented at all loci. Burial offerings were included with some, but not all, of the bundles. Offerings include ceramic vessels, jade pendants and beads, and shell beads. Talgua contained a number of these mortuary items, but burial goods were noticeably absent from Arañas, where only four beads were recorded.

The full mortuary program of Preclassic peoples in north-eastern Honduras is not well understood because few Preclassic open-air sites in this region have been investigated. However, the archaeological context and ceramic evidence appears similar to those recorded by Healy (1974) from the Cuyamel caves in the Department of Colon in northeastern Honduras (Fig. 1). Healy's (1974, 1984) work indicates that the mortuary program of the Cuyamel caves was quite similar to that of the Río Talgua region. No formal skeletal analysis or basic bone inventory has ever been conducted on the remains in these former caves, however. Gordons Cave #3 is a well-reported ossuary cave near Copan in northern Honduras (Fig. 1). Most research (Gordon 1898; Rue *et al.* 1989) has suggested that the large ossuary in the back room (Chamber #3) of the cave dates to the Middle Preclassic period of the Copan valley (ca. 900-300 B.C.), but this chronology has come under question by Brady's (1995) excavations in the other two chambers of the cave. The skeletal analysis for this material provides evi-



Figure 2. View of Lot III-03 near the back of Arañas.

dence of a select mortuary population comprised primarily of subadults. Brady suggests the biased demographic profile may have resulted from the offering of young children and infants as sacrifices, or as companions for the deceased adults. Brady and colleagues propose a unique Honduran Preclassic cave mortuary program differing significantly from those of the lowland Mayan communities (Brady 1995; Dixon *et al.* 1998; Brady *et al.* 2001). Typically, the lowland Mayan mortuary use of caves focuses on a relatively limited number of individuals that may represent sacrifices (Roberts 1990; Brady 1995). The eastern Honduran examples, specifically the Río Talgua data, differ in that no evidence of the trauma usually associated with sacrifice has been identified. Poor preservation and calcite deposits limit observations of bone surfaces, however.

CAVE BIOARCHAEOLOGY

The basic principle followed here is that cave bioarchaeology is the same as bioarchaeology undertaken anywhere else (compare to Watson 1997). Osteological data collection from caves varies from complete excavation and removal of skeletal material to simple documentation and conservation. Excavations in rock shelters and in some deep caves are no different from excavations of human remains at open-air archaeological sites. With prior legal permission, material is exposed, documented, removed, and analyzed. Thus, a majority of the osteological data is ideally derived in the laboratory outside the cave environment. Dealing with the skeletal materials from Río Talgua did not afford such a luxury, however. Hence, a well defined, but flexible means of data collection needed to be employed.

The Río Talgua samples are fraught with analytical problems. Because these samples are ossuaries, many of the skeletal elements are fragmented, and all are commingled. Furthermore, the Honduran government requested that all *in situ* material remain in the caves, and that the majority of the analysis be conducted within the caves as well. In most cases,

elements were cemented in place by calcite, especially in Arañas. Thus, encrusted remains could not be moved, examined, or assessed for the presence of pathological lesions. In addition, skeletal elements above the old waterlines are typically reduced to bone meal due to taphonomic factors and/or looting activities.

For the Río Talgua ossuaries, a specific data collection strategy for human remains was adapted from the work of Church and Burgett (1996). Burgett (1990) initially developed this information recording and retrieval system to document *in situ* commingled and fragmentary faunal remains. The system offers a quick and efficient format to gather data from the Honduran ossuary caves that minimizes impacts to the *in situ* and disturbed material.

The coding system is an alphanumeric “*integrated identification hierarchy*” within which element, portion, and segment of the bone are identified (Church & Burgett 1996). In addition to the identification hierarchy, Church and Burgett (1996) incorporate basic bone properties and taphonomic attributes. The *properties* fields constitute size, age, sex, fusion/development, and pathological conditions. The *taphonomic* attributes include weathering, gnawing, modification, breakage, burning, and trauma. Based on our initial visits to the caves, an assessment of calcite encrustation was added. This information was entered into the Río Talgua Specimen database within *Paradox*©. These variables can readily be visualized within a GIS platform for examining patterns in the distribution of the various skeletal and taphonomic attributes.

Standard osteological techniques cannot always be applied to cave ossuary samples. Due to commingling and other taphonomic processes, researchers are often restricted to an elemental level analysis, an approach often employed by zooarchaeologists (Grayson 1984; Reitz & Wing 1999). One of the primary objectives of any bioarchaeological research is to inventory and quantify the number of individuals in the skeletal sample. In most burial situations, determining the number of individuals is fairly straightforward. These estimations can be more problematic for cave ossuaries, however. For most commingled human skeletal assemblages, researchers quantify the sample through a Minimum Number of Individuals (MNI) estimate. Skeletal material is sorted according to element, age, and bilateral symmetry, and then counted. The most frequently occurring element provides the MNI estimate.

Research has demonstrated that MNI estimates are generally biased, and dependent upon skeletal recovery rates. Therefore, MNI estimates derived from poorly preserved samples are highly suspect. An alternative to MNI estimates when addressing commingled human remains is the Lincoln Index (LI), also known as the Peterson Index (Grayson 1984). Adams (1996) has demonstrated that the use of the LI for commingled human remains may provide a better estimate of the death assemblage than does an MNI estimate. The LI is calculated from any paired skeletal element, usually long bones because they preserve fairly well. First, the number of observed left and right elements is multiplied, then the product is divided by the

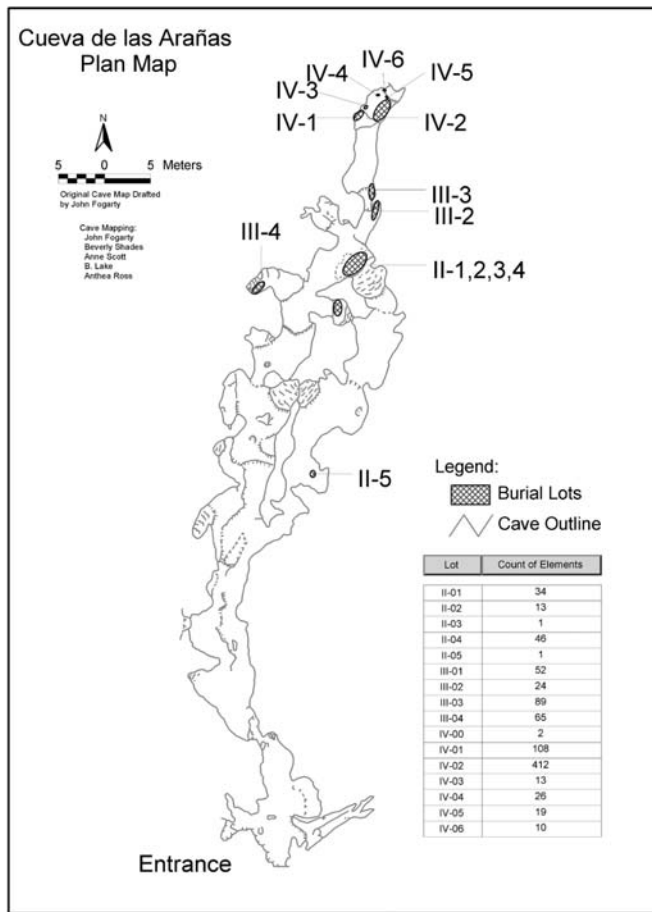


Figure 3. Plan map of Cueva de las Arañas with burial lots marked.

number of matched pairs within the sample. “Matched pairs” refers to the number of left and right elements that were determined to be from the same individual (either through visual assessment or some quantitative method). The LI is also susceptible to error, however. For example, extreme fragmentation can severely bias LI estimates. When dealing with small samples (less than 20 individuals) and relatively high recovery rates, the LI and MNI usually provide similar estimates.

The analysis of the Río Talgua mortuary caves used MNI estimates supplemented in some cases with LI information. A combination of calcite encrustation, severe fragmentation, and degradation of the skeletal material in both caves restricted to pair-matching of elements, thus limiting the use of LI. In some instances, specific individuals could be identified, but skeletal material in Talgua was so disturbed that elements could not be paired. Therefore, MNI estimates were used for Talgua. In Arañas, however, skeletal preservation of several lots was sufficient to use MNI and LI to estimate the burial population. The LI estimates were derived from visually examining ArcView themes and counting the number of paired and unpaired elements.

Several unique methods were employed to facilitate rapid data recovery from both caves. This discussion focuses on the work in Arañas because GIS applications were used more extensively there and Talgua was extensively disturbed. During the 1996 season, digital images were taken of all burial lots in Arañas with an Epson *PhotoPC* digital camera. At the time of the field investigations, widespread use of digital imagery was just beginning and the resolution of the images is low (640x480 pixels). Nevertheless, field osteologists used printed copies of the digital images for each lot to aid in the inventory and mapping process. These images enhanced the efficiency of data collection by providing preliminary maps for each location. Notes and specimen numbers could be placed on the printed images during data collection. The digital photographs furnished a quick reference resource and location control. In instances of small bone clusters, the digital image served as the field map, and a line drawing could then be generated within ArcView by digitizing the geo-referenced image. In addition, each lot was closely examined for *in situ* deposits or articulated skeletal material. Intact deposits were mapped on graph paper and tied to a specific datum on the cave map.

Various data sources combined within ArcView reconstructed the cave system and ossuary locations within the cave. John Fogarty, one of the lead cavers working on the project in Honduras, drafted the cave map. During survey and mapping, Fogarty divided the cave into several areas termed *Operations*. These operations were then subdivided into discrete *Lots*. Skeletal data was recorded by the original operation and lot identifications. Areas discussed in this paper are identified by the Operation-Lot designation (e.g. Operation IV, Lot 2 is IV-2).

Original cave mapping data entered into COMPASS (<http://www.fountainware.com/compass/>) created a three-dimensional plan map of the cave. These data could be imported into ArcView using the Cave Tools extensions (<http://www.mindspring.com/~bszukalski/cavetools/cavetools.html>). Next, the various individual burial lots were digitized and imported into ArcView, rotating, scaling, and moving each polyline themes into position relative to an associated cave datum. Although the example from Arañas is small, these methods could be employed for larger ossuaries, either subterranean or open-air sites.

ArcView extension Edit Tools (http://www.ianko.com/EditTools/et_main.htm) converted the digitized polylines to polygons. Each polygon was assigned a specific Specimen Number. Next, the polygon theme was linked to the Río Talgua Specimen Database, as described earlier. Once the tables were joined, the ossuary could be queried to examine specific elemental, taphonomic, or demographic patterns in the bone scatters.

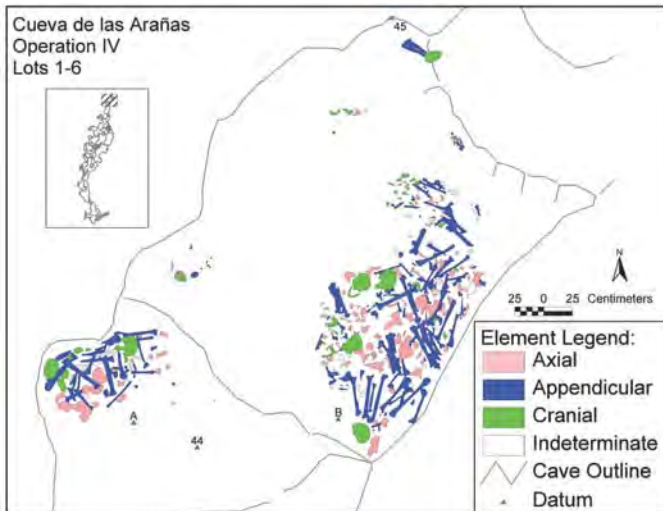


Figure 4. Coded plan map of Lot IV in Arañas. Elements are coded by skeletal divisions (cranial, axial, appendicular, or indeterminate).

RESULTS FOR CUEVA DE LAS ARAÑAS

In Arañas, several discrete burial areas, or lots, were identified. The larger bone scatters were in the back of the cave (Fig. 3). Typically, bones appear to have been placed behind flowstone dams, possibly within pools of water. In the case of Lots IV-1 and IV-2, bone concentrations are quite dense with moderate to heavy calcite encrustation. Other lots were located in niches or along the walls in small passages. Preservation in most locations varied according to the duration of water exposure. In Lot III-3, nearly all elements were located below the old water line. The elements are heavily encased in calcite but some data could be collected, including cranial metrics and dental pathology.

The maps produced for these lots assisted in the determination of the MNI for the cave. In Figure 4, the lots in the back of the cave are plotted by skeletal region (cranial, axial [mid-line], appendicular [limbs], or indeterminate). This visualization technique aids in interpreting the distribution of elements within the ossuary. Typically, a cranium is surrounded by a series of appendicular elements with the axial elements randomly distributed.

The ossuary theme was then filtered for two specific elements, in this case femora and tibiae. These lower limb bones were then coded by side and plotted. Based on observations from Talgua, it appears that bundles of bones were brought into the cave and placed in the ossuary areas. Typically, the cranium was placed next to or on top of the bundle. Therefore, we expected linear clusters of elements that probably came from the same individual. In Figure 5, the distribution of sided femora and tibiae is depicted. In general, the expected pattern of clustered elements is present. Several distinct clusters of elements, possibly former bundles of bones, are evident. These bone clusters were counted to provide the number of “paired”

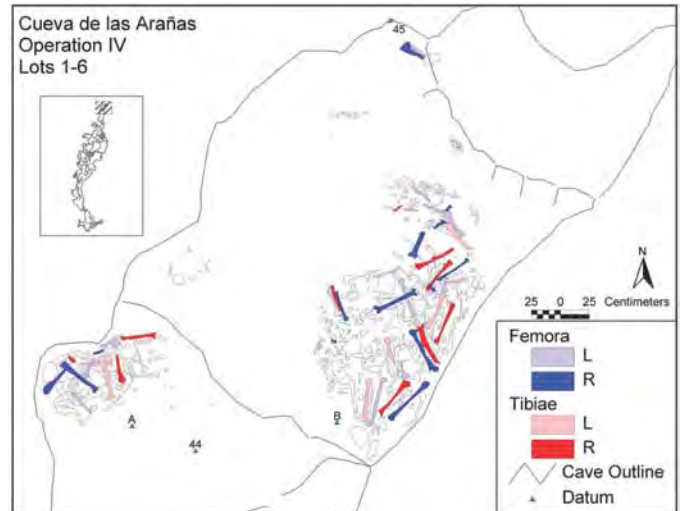


Figure 5. Filtered plan map of Lot IV in Arañas. Femora and Tibiae are identified and coded by side.

elements, and this value can be factored into the LI determination. Elements not associated with a specific cluster were considered as unpaired. I use the paired and unpaired values to calculate the LI. Also, each element could be counted by size to estimate the MNI.

Combining observations from skeletal element MNIs, dental remains, and the visualized pair matching using GIS derives a burial population of 22 individuals for Arañas. The LI estimate for femora in Operation IV is 12.2 (with 9 pair matches), whereas the MNI is 11. The slight difference results from “unpaired” elements in Lot IV-2. All the other elements within the Operation IV produce LI and MNI estimates that were lower than the femur values. A combination of elements can be used to estimate the LI (Grayson 1984; White 1996), but the counts per element at Arañas were so low that this approach was deemed unnecessary. If the ossuary sample was larger, a multi-element LI approach would provide a better estimate of the burial population size as compared to a basic MNI.

Three individuals identified at Arañas are subadults (less than 15 years) and the remaining 19 individuals are adults. A similar demographic pattern was observed in the Talgua sample, where a minimum of 73 individuals was identified based on the osteological analysis. A total of 15 subadults were present in this sample. The age distributions of these caves are not significantly different ($X^2 = 0.1721$, $df = 1$, $p\text{-value} = 0.68$) and support the conclusion that the skeletal samples from these two caves are derived from the same population.

CONCLUSION

The Río Talgua ossuaries represent a rare cultural and archaeological resource. The method detailed here was devised to preserve this resource through documentation and recording of skeletal material *in situ*. By means of GIS applications, we

can examine the ossuaries outside the cave. A GIS based analysis provides “quick retrieval and flexible display” of the spatially referenced skeletal data (Green 1990: 3). If skeletal material is extremely fragmented, unidentifiable, or disturbed, as in the case of Talgua, the application of GIS is difficult and unproductive. Elemental mapping and LI estimates are not possible. On the other hand, the undisturbed burial lots found at Arañas do allow the application of a GIS, as illustrated in this paper. High-resolution digital imaging and improved mapping software will permit quicker and more detailed documentation of such cave resources without disturbing the deposit. The example presented from Arañas is small, but it demonstrates the utility of an adaptable data collection system for recording human skeletal material within cave interiors.

ACKNOWLEDGMENTS

I would like to acknowledge James Brady for directing this project. Valerie Haskins coordinated Western Kentucky University students and osteological investigation in Talgua. The project was made possible by a generous grant from Dole-Standard Fruit, which was arranged by Laurence August, CEO of Geoventures, Inc. In addition, Discovery Channel, Nissan Motors, and Taca Airlines made financial contributions. Olga Joya Sierra, director of the Instituto Hondureño de Antropología e Historia, and the late George Hasemann are acknowledged for their support of this project. Several cavers and archaeologists participated in the documentation of these remains including John Forgarty, Ann Scott, Brad Adams, and Valerie Haskins. I also wish to thank the four anonymous reviewers who provided excellent comments, which greatly improved the manuscript.

REFERENCES

- Adams, B., 1996, The use of the Lincoln/Petersen index for quantification and interpretation of commingled human remains [MA thesis]: University of Tennessee.
- Bement, L.C., 1994, Hunter-Gatherer mortuary practices during the Central Texas Archaic: Austin, University of Texas Press, 165 p.
- Binford, L., 1971, Mortuary practices: Their study and their potential: *Memoirs of the Society for American Archaeology*, v. 25, p. 6-29.
- Brady, J.E., 1994, A report to the Instituto Hondureño de Antropología e Historia on the investigations carried out at La Cueva del Río Talgua, District of Olancho, Honduras.
- Brady, J.E., 1995, A reassessment of the chronology and function of Gordon's Cave #3, Copan, Honduras: *Ancient Mesoamerica*, v. 6, p. 29-38.
- Brady, J.E., Hasemann, G. & Fogarty, J., 1995a, Harvest of skulls and bones: *Archaeology*, v. 48, p. 36-40.
- Brady, J.E., Hasemann, G. & Fogarty, J., 1995b, Buried secrets, luminous find: *Américas*, v. 47, p. 6-15.
- Brady, J.E., Begley, C., Fogarty, J., Stierman, D.J., Luke, B. & Scott, A., 2001, Talgua Archaeological Project: A technical assessment: Web-based report, http://nss.calstatela.edu/anthro/Talgua_pre.htm.
- Buikstra, J.E., 1992, Diet and disease in late prehistory, in Verano, J.W. & Ubelaker, D.H., ed., *Disease and demography in the Americas*: Washington D.C, Smithsonian Institution Press.
- Burgett, G.R., 1990, The bones of the beast: Resolving questions of faunal assemblage formation processes through actualistic research [PhD thesis]: University of New Mexico, 394 p.
- Church, M.S. & Burgett, G.R., 1996, An information recording and retrieval system for use in taphonomic and forensic investigations of human mortalities: *Proceedings of the 48th Annual Meeting of American Academy of Forensic Sciences*, v. 2, p. 167-8.
- Dixon, B., Hasemann, G., Gómez, P., Brady, J.E. & Beaudry-Corbet, M., 1998, Multi-ethnicity or multiple enigma: Archaeological survey and cave exploration in the Río Talgua drainage, Honduras: *Ancient Mesoamerica*, v. 9, p. 327-40.
- Gordon, G.B., 1898, *Caverns of Copan, Honduras*: Peabody Museum of Archaeology and Ethnology Memoirs, v. 1, p. 137-48.
- Grayson, D.K., 1984, *Quantitative zooarchaeology: Topics in the analysis of archaeological faunas*: Orlando, Academic Press, 202 p.
- Green, S.W., 1990, Approaching archaeological space: An introduction to the volume, in Allen, K.M.S., Green, S.W. & Zubrow, E.B.W., ed., *Interpreting space: GIS and archaeology*: London, Taylor & Francis.
- Haskins, V.A., 1990, *The prehistory of Prewitts Knob, Kentucky* [MA thesis]: Washington University, 164 p.
- Healy, P.F., 1974, The Cuyamel Caves: Preclassic sites in northeast Honduras: *American Antiquity*, v. 39, p. 435-47.
- Healy, P.F., 1984, Northeast Honduras: A Precolumbian frontier zone, in Lange, F.W., ed., *Recent developments in Isthmian archaeology: Advances in the prehistory of Lower Central America*: London, BAR International Series, p. 227-41.
- Meloy, H., 1971, *Mummies of Mammoth Cave: An account of the Indian mummies discovered in Short Cave, Salts Cave, and Mammoth Cave, Kentucky*: Shelbyville, Indiana, Micron Publishing Company, 40 p.
- Piperno, D.R. & Holst, I., 1998, The presence of starch grains on prehistoric stone tools from the humid neotropics: Indications of early tuber use and agriculture in Panama: *Journal of Archaeological Science*, v. 25, p. 765-76.
- Ramsey, C.B., 1998, OxCal program v3.0: Oxford, Oxford Radiocarbon Accelerator Unit, 111 p.
- Reitz, E.J. & Wing, E.S., 1999, *Zooarchaeology*: New York, Cambridge University Press, 455 p.
- Robbins, C.A., 1974, Prehistoric people of the Mammoth Cave area, in Watson, P.J., ed., *The archaeology of the Mammoth Cave area*: New York, Academic Press.
- Roberts, C.A., 1990, Observations of Mayan cave archaeology in Belize: *Cave Science*, v. 17, p. 123-9.
- Rue, D.J., Freter, A. & Ballinger, D.A., 1989, The caverns of Copan revisited: Preclassic sites in the Sesesmil River Valley, Copan, Honduras: *Journal of Field Archaeology*, v. 16, p. 395-404.
- Turpin, S.A., 1988, Seminole Sink: Excavation of a vertical shaft tomb, Val Verde County, Texas: *Plains Anthropologist*, v. 33, Memoir 22, p. 1-156.
- Walthall, J.A., 1974, A possible copena burial cave in Blount County, Alabama: *Journal of Alabama Archaeology*, v. 20, p. 60-2.
- Walthall, J.A. & DeJarnette, D.L., 1974, Copena burial caves: *Journal of Alabama Archaeology*, v. 20, p. 1-59.
- Watson, P.J., 1997, Theory in cave archaeology, in 62th Annual Meeting of the Society for American Archaeology, Nashville.
- Webb, W.S. & Wilder, C.G., 1951, *An archaeological survey of Gunter's Basin on the Tennessee River in northern Alabama*: Lexington, University of Kentucky, 278 p.
- White, G.C., 1996, NOREMARK: population estimation from mark-resighting surveys: *Wildlife Society Bulletin*, v. 24, p. 50-2.
- Wiley, P. & Crothers, G., 1986, *Archeological and osteological survey of Bull Thistle Cave (44Tz92), Virginia*: The University of Tennessee, Knoxville, Archaeological Research Corporation Midsouth.

REMOTE SENSING AND GIS-BASED ANALYSIS OF CAVE DEVELOPMENT IN THE SUOIMUOI CATCHMENT (SON LA - NW VIETNAM)

L.Q. HUNG, N.Q. DINH

Department of Remote Sensing and Geomatic, Research Institute of Geology and Mineral Resources, Thanhxuan, Hanoi VIETNAM

O. BATELAAN

Department of Hydrology and Hydraulic Engineering, Vrije Universiteit Brussel, Pleinlaan 2, 1050 Brussels BELGIUM

V.T. TAM

The VIBEKAP Project, Research Institute of Geology and Mineral Resources, Thanhxuan, Hanoi VIETNAM

D. LAGROU

VITO, Boeretang 200, 2400 Mol BELGIUM

Integration of remotely sensed imagery with ground surveys is a promising method in cave development studies. In this research a methodology was set up in which a variety of remote sensing and GIS techniques support cave analysis in the tropical karst area of the Suoimuoi catchment, NW Vietnam. In order to extract the maximum information from different remotely sensed data, the hue invariant IHS transformation was applied to integrate Landsat multi-spectral channels with the high resolution Landsat 7 ETM panchromatic channel. The resulting fused image was used, after enhancement, to visually and digitally extract lineaments. Aerial photos evaluated the extracted lineaments. Based on lineament density indices a fracture zone favorable for cave development is defined. The distance between caves and faults was investigated as well as the correspondence between the cave occurrence and the fracture zone.

During the last decade, Vietnam experienced a rapid economic growth. Sustainable growth, however, also requires an improvement in the quality of life. Rural water supply and sanitation are, therefore, priority issues for the Vietnamese government and of international donors. Since 1998, the Vietnamese-Belgian research project "Rural development in the mountain karst area of NW Vietnam by sustainable water and land management and social learning: Its condition and facilitation" (Masschelein & Swennen 1997) aims at increasing knowledge and expertise regarding the assessment and evaluation of karst systems in Son La and Lai Chau provinces (NW Vietnam). In this karst area, short supply of domestic water in the dry season and flooding in the rainy season are two of the main issues. Both problems can be better managed with better knowledge of the underground rivers and reservoirs. The project has gained a lot of information from several speleological expeditions, organized by the Research Institute of Geology and Mineral Resources, Belgian Geological Survey, Belgian-Vietnamese Karst and Cave Association, and the Speleological Association of the University of Leuven (Dusar *et al.* 1994; Coessens *et al.* 1996; Mrose *et al.* 1998; Spekul *et al.* 2000). During three expeditions, 129 caves and 35 km of cave development have been surveyed.

The main purpose of the study is to examine the relationship between the development of caves and the tectonic structures in the karst area of Son La. The tools for this study have been remote sensing for fault and lineament extraction and

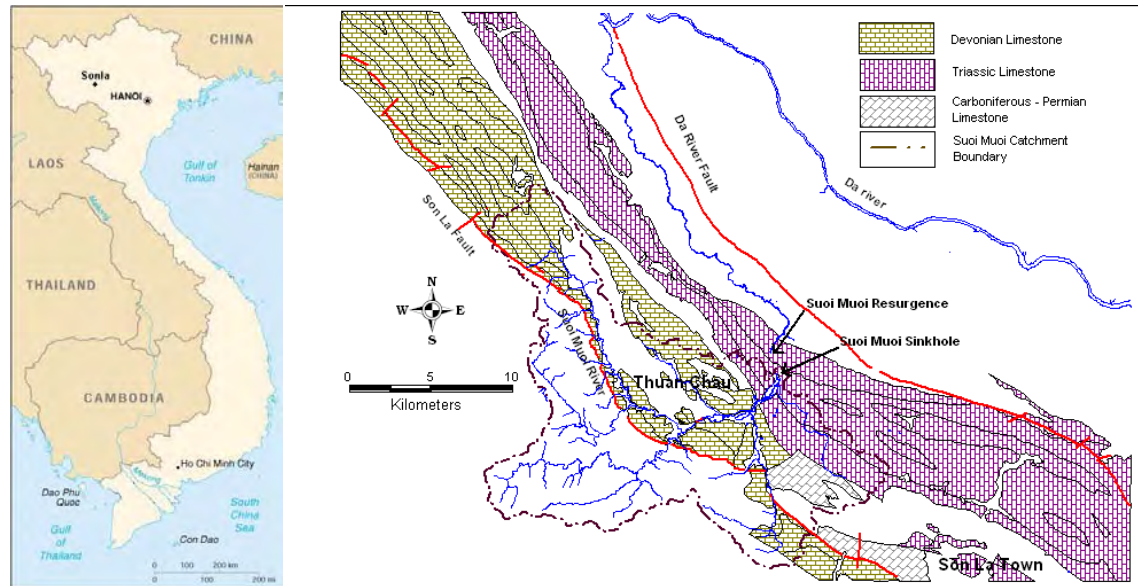
GIS spatial analysis of cave passages corresponding with these faults and lineaments.

The study area, the Suoi Muoi River catchment, is situated northwest of the city of Son La, between longitude 103°33' E and 104°00' E and latitude 21°20' N and 21°29' N, covering 284 km² (Fig. 1). The population of the Son La province is 650,000 inhabitants, resulting in an average density of 48 inhabitants/km². Natural hazards, droughts and floods are frequent threats to daily life.

The Son La karst area is part of the Son La-Thuan Chau karst highland, a mountain range extending over 300 km in NW-SE direction and with an average width of 10-30 km. The karst landscapes include the absence of permanent surface flow, closed depressions, caves, the existence of large springs, and the presence of sinkholes into which entire streams, like the Suoimuoi River, disappear underground. In the Suoimuoi catchment, the karst landscape occurs mainly in the central part and stretches from northwest to southeast, averaging 10 km wide and ranging from 500-850 m high. The landscape is characterized by a peak cluster morphology (*cf.* Chinese Fengcong), blind valleys, deep dolines, narrow valleys, chained sharp peaks and many swallow holes exiting underground into caverns. In the middle part of the area, mainly peak forest landscape dominates with residual karst peaks and tower karst, which emerge here and there above the dissolution-erosion valleys (Tuyet 1998).

Vietnam has a humid tropical climate, heavily influenced

Figure 1. Map of study area, indicating the Triassic ($T_{2a}dg_1$ and $T_{2a}dg_2$), Carboniferous (C_3-P_{1bd}), Devonian (D_{2bp_1} , D_{2bp_2} , D_{2bp_3}) and Cambrian (E_{3hr}) karst formations, mapped cave locations and faults in the Suoimuoi catchment, digitized from geological map (Hop 1997).



by the monsoon regime and characterized by two seasons: a hot and rainy summer and a colder and dry winter (Dieu 1992). In Son La, the annual mean temperature is 21°C, maximum and minimum recorded temperatures are 40°C and 1°C, respectively. The average humidity of the air is 80%, but may drop in winter to an all-time low of 6%. Eighty-five percent of the 1413 mm mean annual rainfall occurs during the rainy season (from April to September).

GEOLOGY

The Son La-Thuan Chau karst area consists mainly of two sub-areas. The southwestern parts are composed of karst water-bearing carbonate rocks of Paleozoic age, Banpap (D_{2bp}) and Early Permian-Carboniferous Chienpac ($C-P_{1cp}$) Formations. The northeastern part is of Middle Triassic age with the Dong Giao Formation (T_{2dg}). Table 1 presents a summary of the stratigraphic description of the carbonate rocks in the area. In the Suoimuoi catchment, karst occurs in limestones and dolomites of Late Cambrian, Middle Devonian, Carboniferous - Early Permian and Middle Triassic age. These carbonates have a favorable composition, texture, and structure for karstification (Hung 2001).

Many different tectonic phases and neotectonic movements have intensively affected these rocks. The present Son La karst highland is dissected by NW-SE, SW-NE, sublatitudinal, and submeridional trending faults. The NW-SE fault system resulted from the collision of continental crust in the Precambrian. The region then was affected by NW-SE oriented folding due to Indosinian closure of the Paleotethys, starting in Late Permian and culminating during Middle Triassic. All the deposits were finally uplifted during the Neogene Himalayan collision event (Tri *et al.* 1977; Tri & Tung 1979; Tien *et al.* 1991). A series of sub-parallel strike-slip faults can be recognized in the Son La fault zones. Furthermore, Son La town is

located on the active Tuan Giao-Son La seismic zone where many destructive earthquakes with intensities of up to 7.0 on the Richter scale have been recorded in this zone. Damage to property has included rockfalls, ground cracking, and landslides (Dusar *et al.* 1994). Along the NW-SE faults, the width of fractured zone ranges from 1 - 2 km.

The SW-NE fault system is younger than the NW-SE one. The continuous tectonic activity in the Son La region accompanied by strong uplift and associated tilting towards the Da River valley to the east, has resulted in the destruction of the Miocene-Pliocene peneplane surface and the creation of deeply incised valleys. This system modifies the block structures formed by the faulting. These SW-NE transform faults are discontinuous. The width of fractured zone ranges from 800-1200 m (Hop 1997).

The development and characteristics of karst depends on many interacting factors such as: composition, texture and solubility of carbonate rocks, folding, faulting, neotectonic activity, quality and quantity of water, availability of CO₂ gas from various sources, character of vegetative cover, as well as environmental conditions, including human impacts. Tam *et al.* (2001) concluded that the karst groundwater aquifers in the Suoimuoi catchment are determined by fractured/fissured media whilst the cavern conduits, although abundantly occurring in the region, act as groundwater galleries and/or conveyers.

DATA

A Landsat 7 ETM satellite image of February 27th, 1999, has seven multispectral bands and additionally a panchromatic band of 15 m resolution. Additionally, 36 aerial photographs, along four flight lines, were available for January 1975 and January 1999. The nominal scale of the aerial photographs is 1:33,000. All photos were scanned with a resolu-

Table 1.

A summary of the stratigraphic column for the Suoimuoi catchment. The Triassic (T_{2adg₁} and T_{2adg₂}), Carboniferous (C_{3-P_{1bd}}), Devonian (D_{2bp₁}, D_{2bp₂}, D_{2bp₃}) and Cambrian (E_{3hr}) karst formations have been indicated in bold.

AGE	CODE	THICKNESS (M)	DESCRIPTION	
CENOZOIC	Quaternary Holocene	Q	Alluvium and deposit of temporal flows include cobbles, gravels, mixed composition, badly rounded, sand and clay upward.	
		Cretaceous Middle	K _{2yc₃}	Upper Yenchau sub-Formation: sandstone, gravelstone and calcareous sandstone, red color.
			K _{2yc₂}	Middle Yenchau sub-Formation: sandstone, siltstone and some lenses of calcareous conglomerate and gravelstone, red color
MESOZOIC	Cretaceous Middle	K _{2yc₁}	Lower Yenchau sub-Formation: conglomerate with gravelstone lenses, light grey color.	
		Triassic Middle	T _{3n-sb}	Suolbang Formation: lower: dark grey siltstone, sandstone, calcareous shale, siliceous limestone lenses, fossil-bearing tufaceous sandstone. Upper: siltstone, dark grey sandstone with fine sandstone rich in organic calcareous clay and thin lenses of coal.
			T _{2₁mt₃}	Upper Muongtral sub-Formation: shale, dark grey oolitic siltstone, sericite sandstone with moderate to thick bedding and calcareous sandstone. Rich in fossils.
	T _{2₁mt₂}		Middle Muongtral sub-Formation: calcareous claystone, limestone breccia in block structure or thick bedding. Upper Namthan sub-Formation: lower part: black shale, thin bedding siliceous limestone. Middle part: light grey, white limestone, irregular bedding, and clayish intercalations. Upper part: limestone, dolomitized limestone, thick bedding and rich in fossils.	
	Triassic Early	T _{2₁mt₁}	Lower Muongtral sub-Formation: lower part: thin layers of dark grey shale, porphyry basalt and continental basalt. Lower Namthan sub-Formation: lower part: dark-to-light grey, partly dolomitized limestone, thick bedding and rich in fossils. Middle part: sandstone, sandy siltstone, gravelstone and fauna fossils. Upper part, marl, black-coaly shale and flora fossils.	
		T _{2adg₂}	Upper Dong Giao sub-Formation: lower part: dark grey limestone intercalated with the light grey, irregularly dolomitized, thick bedding and rich in fossils. Upper part: light grey limestone, partly domomitized, thick bedding to massive structure and rich in fossils.	
		T _{2adg₁}	Lower Dong Giao sub-Formation: calcareous schist, siltstone, black oolite-limestone intercalations and upwards: dark grey clayish limestone, siliceous bituminiferous limestone, thin bedding and rich in fossils.	
		T _{1tl}	Taniac Formation: lower part: conglomerate with majority of basalt cobbles, tufaceous sandy cement, tufaceous sandstone and siltstone upwards. Upper part: siltstone, claystone with clayish limestone, oolite, wormlike textured limestone and rich in fossils.	
	Permian Middle	T _{1vn}	Viennam Formation: lower part: alkaline olivine basalt, trachybasalt, plagiobasalt and green basalt. Upper part: rhyolite, trachydacite, trachyrhyolite and lava breccia.	
		P _{2yd}	Yenduyet Formation, lower part: banded siltstone, schist ferrous allite and tufaceous sandstone. Middle part: organic oolite limestone, dark grey siliceous deposit and rich in fossils. Upper part: black schist with siliceous intercalations, limestone and rich in fossils.	
P _{2T₁nm}		Camthuy Formation, lower part: porphyryte basalt, green basalt, dolomite breccia, tuff and clayish limestone lens. Upper part: laminations of tufaceous siltstone, few basalts and allite lenses.		
Carboniferous Late			Nammuoi Formation: mafic and neutral extrusive rock with high magnesium. Low titanium, mainly: komatite, basaltkomatite, picrite basalt, boninite, okeanite and ankaramite.	
		C _{3P₁bd}	Bandiet Formation, lower part: mafic extrusive rock, black siliceous deposit, tuff sandstone and coaly claystone. Upper part: dark grey limestone, schist laminations, limestone breccia, regular bedding to massive structure and rich in fossils.	
PALEOZOIC	Devonian Middle		Chiengp ac Formation, lower part: light grey, fine grained limestone with organic limestone and dark spots, breccia, oolite, thick to massive structure and rich in fossils. Upper part: green grey limestone, thin bedding and rich in fossils.	
		D _{2bp₃}	Upper Benp ap Formation: light grey limestone, thick bedding to massive structure, micro-grained and partly dolomitized limestone, clayish limestone, thin layers of siliceous limestone, contains fossils.	
		D _{2bp₂}	Middle Benp ap Formation: dark grey and ash-grey limestone, thick bedding to massive structure, clayish oolite limestone with thin bedding, grayish limestone intercalations, irregularly calcitized and rich in fossils.	
	Devonian Early	D _{2bp₁}	Lower Banp ap Formation: dark grey, black and partly dolomitized limestone, siliceous limestone, clayish limestone, thin bedding and rich in fossils (corals).	
		D _{1np}	Nampia Formation: quartz-sericite schist, sericite-quartz-chlorite schist and thin-bedded sandy siltstone with lenses of sandstone.	
Cambrian Middle	O _{1ds}	Dongson Formation, lower part: quartzitized arkose sandstone and sandstone laminations. Upper part: quartz-sericite schist, sericite sandstone intercalations, contains fossils.		
	E _{3hr}	Hamrong Formations, Lower part: pale grey, fine limestone, partly dolomitized limestone, oolite and clayish limestone. Upper part: clayish limestone, schist with few calcareous siltstones and sandstones, contains fossils.		
	E _{2sm}	Songma Formation, divided into 3 parts including: conglomerate, coaly schist, mica-quartz-sericite-chlorite, quartz-feldspars-biotite, schist, green schist, amphibolite schist, quartzitic sandstone and limestone lenses.		
LATE PROTEROZOIC	PR _{3-E₁nc₃}	500-550	Upper Namco sub-Formation: mica-quartz, mica-quartz-sericite, chlorite schist with quartzitic, siliceous sandstone and intercalations. Upper part: quartz-sericite-chlorite with quartzitic sandstone intercalations.	
		800-1000	Middle Namco sub-Formation: lower: mica-quartz-garnet schist, biotite-staurolite schist (andalusite) with micaceous, mica-quartz intercalations. Upper: quartz-feldspar-biotite schist containing garnet with quartzite, sericite, siliceous intercalations.	
		400-450	Upper Namco sub-Formation, lower part: biotite-quartz schist bearing cordierite and staurolite with some black siliceous schist. Upper part: micaceous-quartz and quartz-sericite-chlorite schist.	

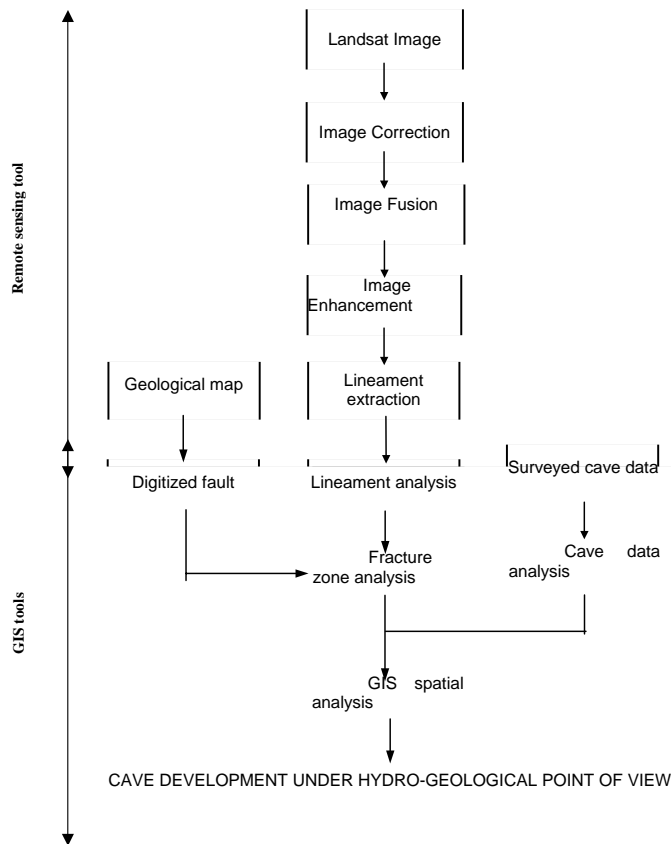


Figure 2. Flow-chart for RS and GIS based methodology of cave development analysis.

tion of 600 dpi, resulting in digital aerial images with high-resolution features. Reference data available over the study area comprise the geological map, a digital elevation model (DEM) with a spatial resolution of 20 m and four 1:50,000 scale topographic maps with UTM projection (zone 48N).

The geological map (Hop 1997) provided a data layer indicating the faults and lineaments. The caving data consist of the description of the mapping of 97 caves in Suoimuoi catchment and direct surroundings as reported from caving expeditions (Dusar *et al.* 1994; Coessens *et al.* 1996; Mrose *et al.* 1998). Using the dataset, a cave database was built using CaveTools (Szukalski 2001), ArcView, and MS-Access.

METHODOLOGY

REMOTE SENSING

The combination of remote sensing and GIS provides a set of tools for cave development analysis. In Figure 2, the major analysis steps for cave development based on analyzed Landsat ETM and a cave database are given. In a first step, the Landsat image was geometrically corrected, followed by image fusion. Image fusion is defined as combining two or more different images to form a new image with a certain algo-

rithm (Carper *et al.* 1990). It is clear that the selection of an image fusion approach depends on the desired application (Zhang *et al.* 1999). Our purpose was to integrate images from different sensors to facilitate visual interpretation. For this purpose, pixel-based statistical/numerical or color related fusion techniques are an appropriate tool. Statistical/numerical fusion uses the statistics of individual image bands for correlation analysis. The color related fusion methods were used here and deal with the transformation between display-device and perceptual color spaces. The most popular color related technique is the transformation of image data from the red-green-blue (RGB) color space to the intensity-hue-saturation (IHS) space and vice versa (Fig. 3).

The intensity relates to the brightness, hue represents the dominant wavelength, while the saturation is defined by the purity of the color. In the first transformation step, a multispectral RGB composite image was encoded to the IHS space. In the manipulation stage, intensity was substituted by another image or “replacement intensity”. In this stage, saturation can be enhanced by multiplying it with a scale factor (e). During fusing of the two datasets, the saturation enhancement scale factor “e” is controlled in order to reduce over-range pixels. When multispectral channels are fused with the panchromatic band, saturation can be enhanced up to e=3 (Ha 2001). Care should be taken with the enhancement of hue because it may result in spectral distortions (Schetselaar 2001). The principle of image fusion can be written as a single transformation, which allows control on the enhancement and over-range with respect to the faces of the RGB cube and limits hue distortions (Schetselaar 2000):

$$\begin{pmatrix} R \\ G \\ B \end{pmatrix} = \begin{pmatrix} I' \\ I \end{pmatrix} \begin{pmatrix} \frac{1}{3} + \frac{2}{3}e & \frac{1}{3} - \frac{1}{3}e & \frac{1}{3} - \frac{1}{3}e \\ \frac{1}{3} - \frac{1}{3}e & \frac{1}{3} + \frac{2}{3}e & \frac{1}{3} - \frac{1}{3}e \\ \frac{1}{3} - \frac{1}{3}e & \frac{1}{3} - \frac{1}{3}e & \frac{1}{3} + \frac{2}{3}e \end{pmatrix} \begin{pmatrix} x_1 \\ x_2 \\ x_3 \end{pmatrix}$$

$$I = (1/\sqrt{3})(x_1 + x_2 + x_3)$$

Where (x₁, x₂, x₃) is the multispectral feature vector of a pixel, I is the intensity of that pixel, I' is the replacement intensity, e is saturation enhancement. The technique can be applied to fuse images from a single sensor, or multisensor data, or image data with ancillary data, like geophysical, geochemical, thematic data, and data compiled from fieldwork (Harris *et al.* 1990; Schetselaar 2000). By fusing multispectral channels with high spatial resolution channels, enhancements are expected with respect to geographical features, boundaries between different lithological units and the relationship between the multispectral and high spatial resolution information.

In the next step of remote sensing analysis, lineaments were detected and extracted (Hung 2001). A lineament is a

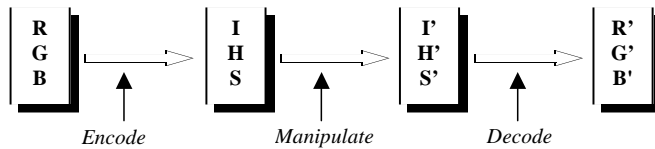


Figure 3: The IHS principle (Lillesand and Kiefer 1994).

mappable linear or curvilinear feature of a surface whose parts align in a straight or slightly curving relationship. They may be an expression of a fault or other line weakness. The surface features making up a lineament may be geomorphological (caused by relief) or tonal (caused by contrast differences). Straight stream valleys and aligned segments of a valley are typical geomorphological expressions of lineaments. A tonal lineament may be a straight boundary between areas of contrasting tone. Differences in vegetation, moisture content, and soil or rock composition account for most tonal contrast (O'Leary *et al.* 1976). In general, linear features are formed by edges, which are marked by subtle brightness differences in the image and may be difficult to recognize.

Directional and non-directional filters have been developed to enhance edges in images. Laplacian filters are non-directional filters because they enhance linear features having almost any orientation in an image. The exception applies to linear features oriented parallel with the direction of filter movement; these features are not enhanced. Directional filters are used to enhance specific linear trends in an image. Sabins (1997) shows some major directional filters that can enhance any specific direction. Since image noise can create linear features, edge enhancement is strongly dependent on the pre-processing of the images.

In the last remote sensing analysis step, lineaments are extracted visually or digitally (automatically). Both methods have certain advantages and disadvantages (Table 2). Because of the complexity of the process, only a few automatic lineament extraction schemes exist and most lineament extractions still depend on the researcher's experience. In order to study the tectonic fracture zone in Suoimuoi catchment, both visual and digital lineament extraction were applied. The digital extraction used Laplacian and directional filters to enhance the lineaments; consequently the enhanced image was converted to Boolean images using different threshold values. Lineaments from these images were extracted by OCR-tracing software, combined, and further processed by lineament specific software (Hung 2001).

STRUCTURAL DEFORMATION

Through brittle deformation, two mechanisms or modes of propagation, shear and extension, generate fractures. Frequently, the shear fractures occur as a conjugate pair and the extension fractures bisect the acute angle in pair. The extension features are oriented parallel to the direction of the maximum compressive stress (σ_1), and perpendicular to the

Table 2: Some major characteristics of visual and digital lineament extraction.

Visual processing	Digital processing
- Relatively higher quality if image quality is low	- Relatively higher quality if image quality is high
- Higher quality if the research area has high complexity	- Lower quality if the research area has high complexity
- Strongly depends on human experience	- Strongly depends on software functionality
- Slow	- Fast
- Easy to distinguish the type of lineament	- Cannot distinguish the type of lineament
- Simple but subjective method	- Complex but objective method

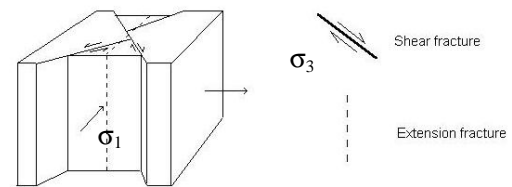


Figure 4: Stress orientation and corresponding types of fractures.

minimum stress (σ_3) (Fig. 4). As a result of propagation mode, the apertures of the extension fractures tend to be larger than those of shear fractures. Groundwater flow may be more significant along the extension fractures. Fernandes and Rudolph (2001) concluded that tectonic activities, which result in brittle deformation, generate: 1) shear fractures that remain under compression and are not very transmissive; and 2) more permeable extension structures tend to be associated with wide-aperture fractures. The recognition of these extension fractures would be valuable for groundwater resources development. Lineament analysis may be the most effective method to map these types of features.

By understanding the orientation of the stress field that generated the structures in the study area, it is possible to evaluate which lineaments can be associated with mostly shear fractures or conjugated faults and which with extension fractures. Figure 4 depicts the stress field and the general position in space of the shear and extension fractures that are generated by a strike-slip tectonic regime.

CAVE ANALYSIS

In order to investigate the relationship between the occurrence of caves and geologic structures, a spatial GIS analysis was performed using the ArcView software (ESRI 1996). In the first step, an ArcView shape file, indicating the cave entrances, was transformed to a grid by using the "Find distance" function. Each resulting grid cell with a spatial resolution of 10 m bears the value indicating the distance between itself and the nearest cave. Then by reclassification, a buffer

zone with a radius of 20 m or two grid cells is defined around the cave grid cell. The purpose of the buffer zone around the cave is to cover the area of the cave entrance or doline as well as to take into account the effect of errors in locating the caves (Dinh 2001).

In the second step, the digitized fault sheet from the geological map and the visually extracted lineament maps as polyline shape files are transformed to grids with a resolution of 10 m. Similar to the cave map, a map showing the distance to the nearest fault or lineament was created. The resulting fault distance zone map was reclassified in 6 distance zones, where each of the first 5 zones have a width of 100 m adding up to 500 m, while the last zone covers the remaining area. The maximum buffer zone was defined as 500 m since this is half of the width of the commonly found fractured zone bordering a fault (Hop 1997). In the third step, statistics for each zone were calculated. The ArcView Spatial Analyst "Histogram by Zone" function was used to identify the percentage of cave pixels that fall within each buffer zone bordering the faults.

In the final step, the comparison of the direction of cave development and fault direction was performed. Although each cave has its own properties, characterized by its own unique speleogenetic history, general directions can be observed. Classification of direction was based on the maximum length of the cave in a certain direction; that means the cave is considered to be developed in the direction along which most cave passage developed. One can determine the direction of the cave by using a rose diagram, a built-in function of the COMPASS software (Fish 2001).

RESULTS AND DISCUSSION

LINEAMENT AND FRACTURE ZONE ANALYSIS

The results of the visual and digital lineament extraction, after directional and non-directional enhancement of the fused image, are given respectively in Figures 5a and 5b. Randomly selected visually extracted lineaments were visually compared with observed lineaments from the high-resolution aerial photos to improve the visual selection procedure. The DEM was also used to verify the location of the extracted lineaments. The lineaments resulting from visual processing are relatively continuous lines. Since visual lineament extraction selects lineaments based on morphological characteristics, they correspond well to the mapped faults from the geological map (Fig. 1). However, the visual extraction results in more lineaments and with a higher spatial accuracy than faults present in the geological map. The digitally extracted linear features are considered as lineaments if they are longer than 100 m (6 pixels). Two lineaments will combine into one, if they have a maximum difference in direction of 3° and/or if the space between them is less than 45 m (3 pixels). The resulting digitally extracted lineaments are still relatively short compared to the visual lineaments, but they have a high density (Fig. 5b). Non-tectonic linear features (roads, etc.) and, especially, the shadow in the image are the cause of this high density. In visual

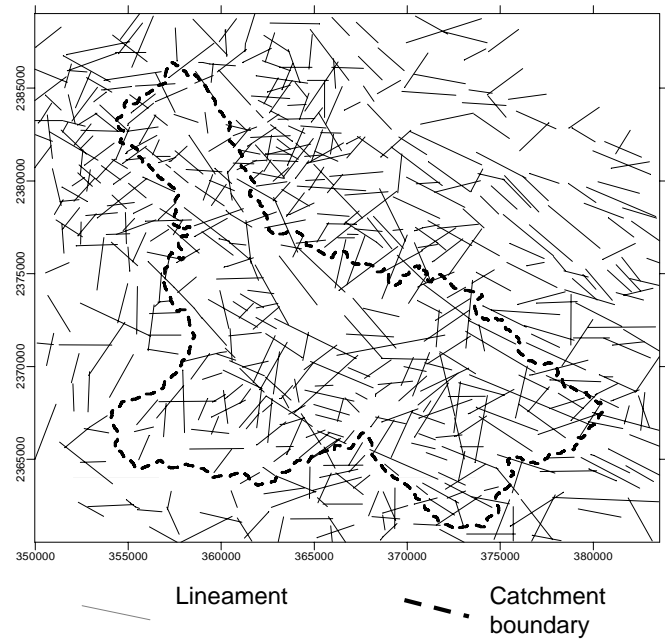


Figure 5a: The result of visual lineament extraction from the fused, transformed Landsat images.

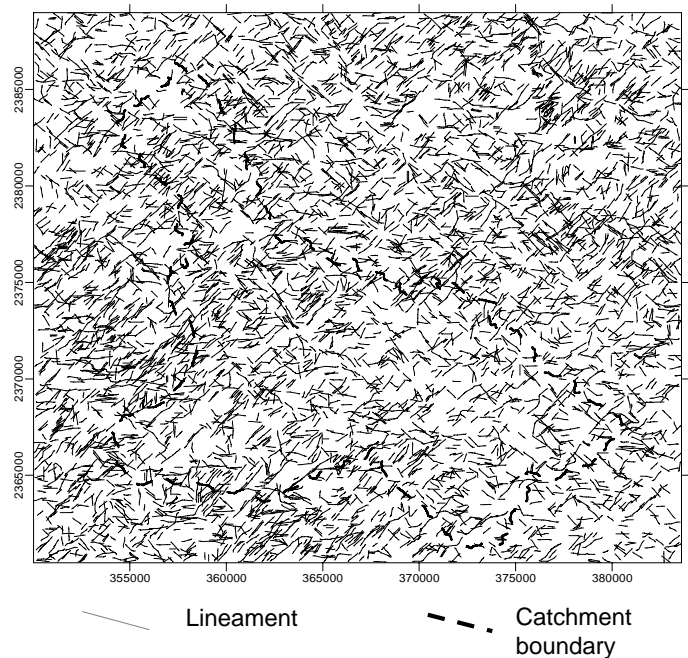


Figure 5b: The result of digital lineament extraction from the fused, transformed Landsat images.

processing shadow is much less of a problem.

In order to define the fracture zone, the map with digitally extracted lineaments was used to calculate the density of lineaments in the Suoimuoi catchment under the hypothesis that

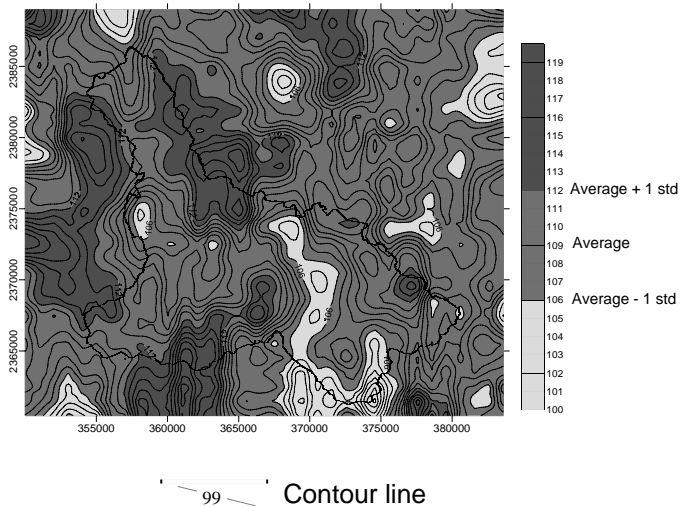


Figure 6: Contour map of the average of lineament length (meters) per km².

a higher density of lineaments indicates a higher intensity of deformation. The most common method is to calculate lineament density as the number of lineaments per unit area (n/km^2), or as the number of lineament intersections per unit area (n/km^2), or as the total length of lineaments per unit area (m/km^2). In order to avoid the effect of non-tectonic lineaments here, two other indices are used: the average of the lineament length per km² and the ratio between number of intersections of lineaments and the number of lineaments per km². These lineament density indices are calculated for a raster with a grid cell resolution of 1 km² and can be reclassified into ranges of values and presented as an isopleth map (Figs. 6 and 7). The major statistical characteristics of the two density maps are listed in Table 3.

Since the Suoimuoi catchment can be considered as a homogeneous tectonic region, the fracture zone can be defined on basis of the statistical characteristics of the two indices: average length of lineaments and ratio between number of intersections of lineaments and the number of lineaments per km². In zones with a low value of these indices, caves cannot develop. In zones with a very high density, rock stability is too low for cave development. Therefore, the fracture zone is defined as the zone where the two indices have a value between the average plus and minus one standard deviation.

Two main types of conjugate fracture patterns are recognized for the Suoimuoi catchment, depicted by the diagrams in Figure 8a. Hop (1997) supposed that both fracture types (E-W and NW-SE) generated faults (shear fractures) and extensional fractures that affected the rocks from Precambrian up to Middle Triassic. The E-W fracture type is accompanied by shear fractures with a NW-SE and NE-SW direction and extension fractures with a sub-E-W direction. The NW-SE fracture type is accompanied by shear fractures of sub-N-S and sub-E-W direction and extension fractures with a NW-SE direction. The correspondence of the NW-SE shear and extension direc-

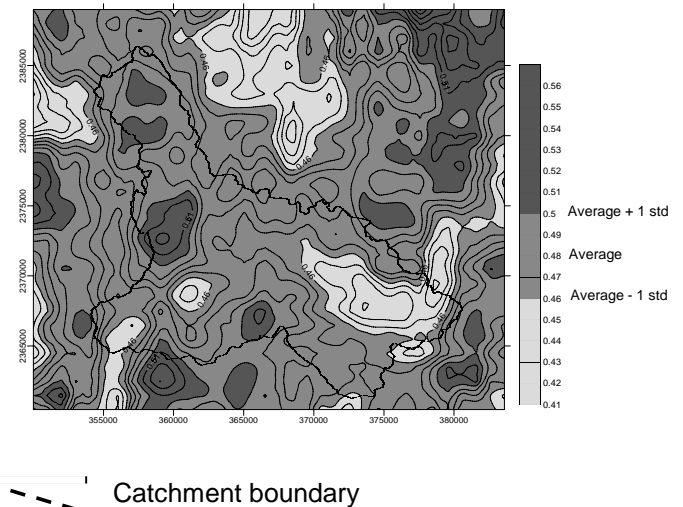


Figure 7: Contour map of the ratio between the number of lineament intersections and the number of lineaments per km².

Table 3: Statistical characteristics of digitally extracted lineaments.

Lineament index	Statistical characteristics			
	Max	Min	Average	Standard deviation
Total length (m)	119526	11285	75486	21231
Intersection	521	46	331	95
Ave. length (m)	120	99	109	3
Inter/number	0.56	0.41	0.48	0.02

tions and the E-W correspondence of shear and extension directions, make these two directions most favorable for groundwater development.

In Figure 8b, the rose diagram is given for the visually extracted lineaments. It is clearly observed that the directions correspond to the results of Hop (1997) as given in Figure 8a. The density of the lineaments differs. The visual extraction results in more sub-N-S and sub-E-W lineaments than in Figure 8a. Figure 8c shows the rose diagram for the digitally extracted lineaments. The very high density of NW-SE and NE-SW lineaments in this figure is due to additional lineaments caused by the effect of shadow in the image. The densities of the sub-N-S and sub-E-W lineaments are, therefore, relatively reduced.

CAVE DEVELOPMENT STUDY BASED ON LINEAMENT ANALYSIS

Figure 1 shows the location of the 97 mapped caves. The caves cluster in the southeast and northwest of the catchment. This is partly due to the fact that the cave mappings were not performed systematically over the area due to the inaccessibility of the terrain, e.g. in the northern central karst part. From Figure 1, it is observed that the occurrence of the caves corresponds to the areas with a relatively high number of intersec-

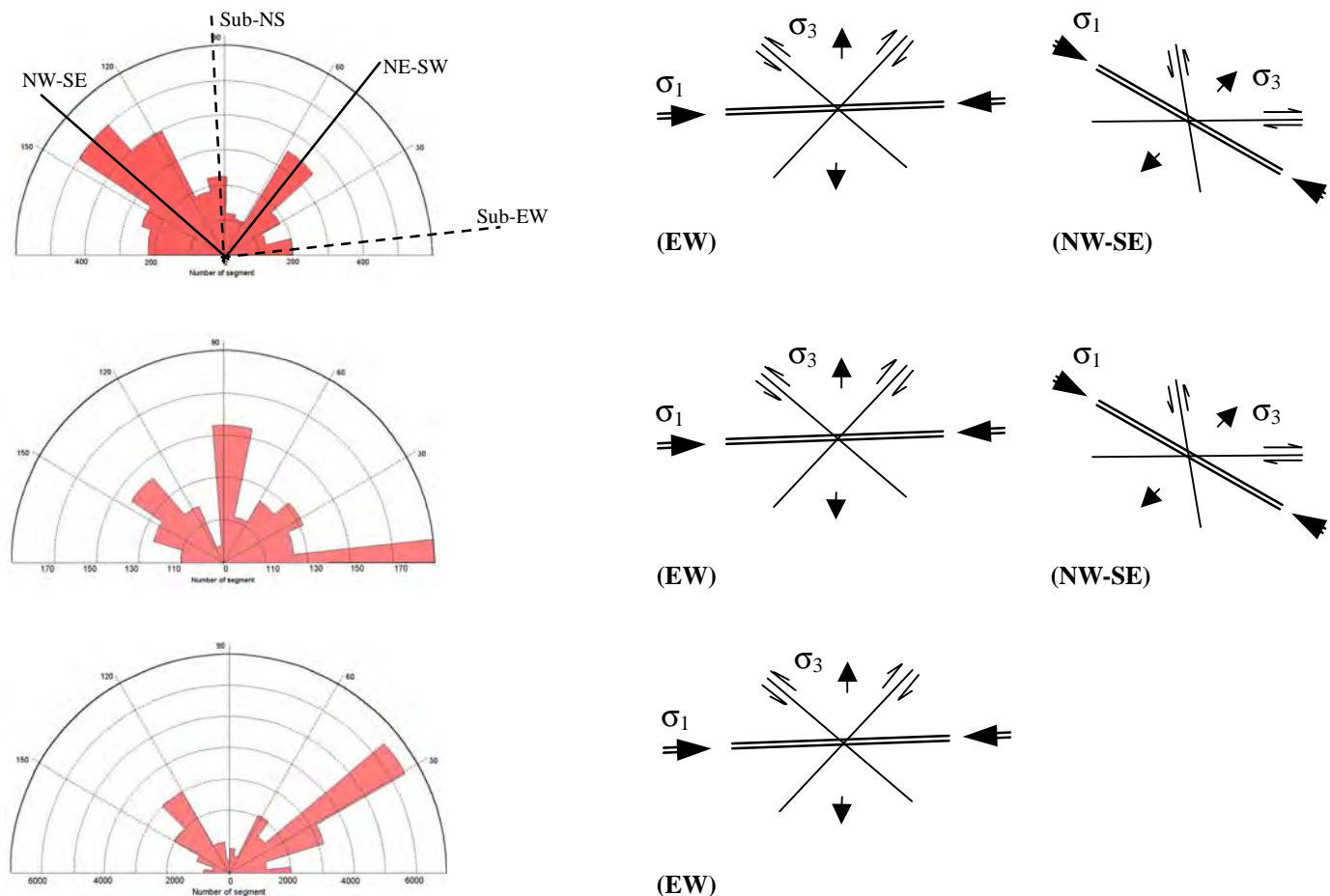


Figure 8a (top): Rose diagram depicts the distribution of lineaments on geological map (Hop 1997). Also shown are the orientations of shear and extension fractures.

Figure 8b(center): Rose diagram of visually extracted lineaments and related directions of shear and extension fractures.

Figure 8c (bottom): Rose diagram of digitally extracted lineaments and related directions of shear and extension fractures.

tions of NW-SE, NE-SW, and E-W faults. In the southeast the caves occur favorably at the contact of limestone and non-limestone formations. In the narrow karst band running from northwest to southeast cave development is not favorable since the Late Cambrian formations only contain thin carbonate lenses, which are partly dolomitized and separated by conglomerates and metamorphic rocks.

In Figure 9a, the results of the analyses of the distance between the caves and the faults, which were derived from the geological map, are presented. The bar chart indicates the percentage of caves occurring within a certain distance zone from the faults. It is concluded that more than 80% of caves are situated within the fractured zone (< 500 m), pointing to a high likelihood of tectonic control in the development of the caves. The fault map shows only faults that play a controlling factor to the regional structure and the faults that are not covered by the Quaternary sediments. If non-regional and non-superficial faults had been included, likely a higher percentage of cave-fault correspondence would have been achieved. In Figure 9b, the diagram shows the results from distance analyses of the

cave to the visually extracted lineaments. Ninety-seven percent of the caves are located within 500 m of the fractures. Lineaments represented all the features caused by tectonic activities, not only faults but also folds and edges, which may explain why a higher percentage of caves located close to the lineaments compared to the faults.

In Figure 9c, the results are shown from the analysis of the direction of cave development and the fault direction. From the caves that have been surveyed, 58% of the caves developed in NW-SE direction, corresponding to the most pronounced regional tectonic direction. Nineteen percent of the caves developed along high density SW-NE lineament direction, while only 15% and 8% of the caves developed, respectively, along N-S and W-E directions. Most of the active caves, which have developed along NW-SE direction, have horizontal passages or very slightly inclined passages, while most of the caves developed along NE-SW direction have inclined passages (Dusar *et al.* 1994). The inclination of those caves somewhat follows the dipping of carbonate rocks. In those cases, the bedding planes may also provide routes for groundwater

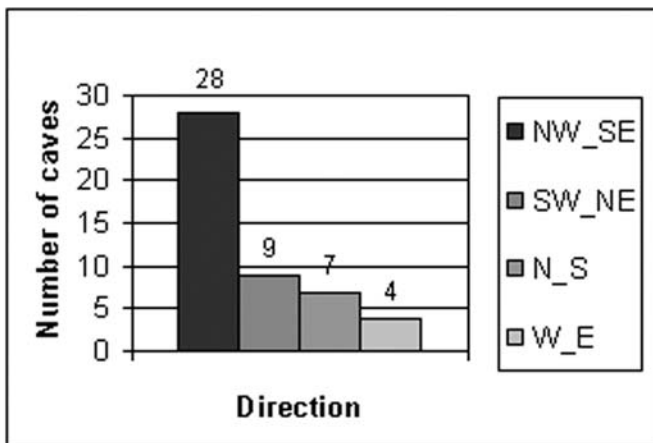
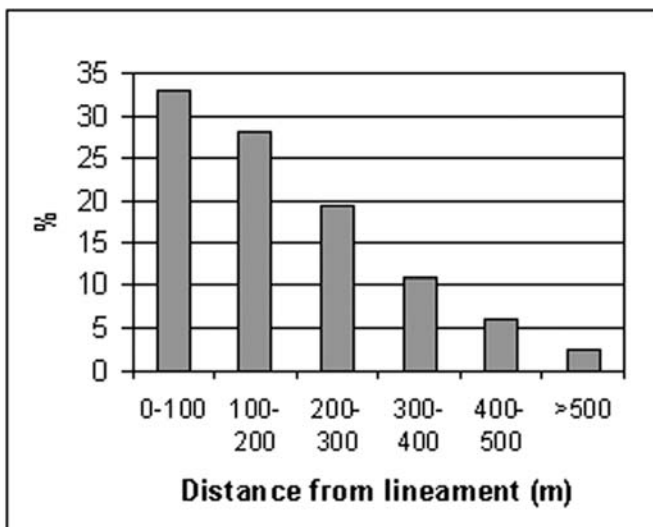
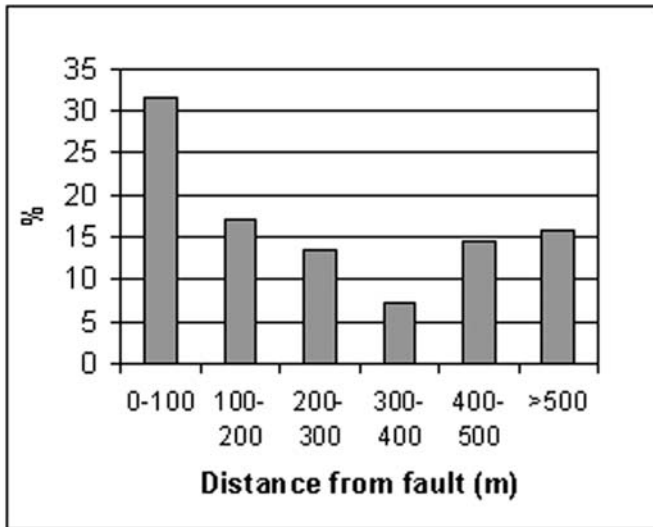


Figure 9: Bar graph showing the number of mapped caves (a - top) with respect to fault distance, based on faults from the geological map (Hop 1997), (b - center) with respect to lineament distance, based on map of visually extracted lineaments, (c - bottom) versus main fault direction.

eaments. The crosshatched area in Figure 10 is the most favorable fracture zone for cave development since it is the overlap of the two extracted fracture zones of Figures 6 and 7. Most caves are located in the favorable fracture zone. In the central-southeast part, some caves do fall outside the favorable fracture zone; however, they have developed on the contact of limestone and non-limestone formations. The absence of caves in the central-northern part of the karst belt can be explained from the fact that only a very small part of the area belongs to the favorable fracture zone. The favorable fracture zone in Figure 10 can be used to suggest zones for finding new caves in the Suoimuoi catchment.

CONCLUSIONS

A methodology has been set up, involving remote sensing and GIS analysis to map, predict and explain the occurrence of caves in a tropical karst region. Based on a geologic analysis, it is concluded that tectonic activity was very strong in the Suoimuoi catchment. The tectonics resulted in a NW-SE dominated fault system.

The integration of Landsat 7 ETM imagery with high-resolution panchromatic data provided complementary information with respect to the discrimination of major geologic features and allowed lineament extraction in detail. A favorable fracture zone for cave development is determined through the analysis of the lineaments.

The cave correspondence with the fractured zone was very high. Outside the fractured zone caves occurred at the formation contact between limestones and non-limestones. The majority of the caves developed along the major structural NW-SE direction. It is suggested that the favorable fracture zone for cave development can be used to predict cave occurrences.

ACKNOWLEDGMENTS

This work results from the MSc theses of the first and second author and frames within the project "Rural development in the mountain karst area of NW Vietnam by sustainable water and land management and social learning: Its conditions and facilitation (VIBEKAP)", funded by the Flemish Interuniversity Council (VL.I.R.). Koen Van Keer and the Research Institute of Geology and Mineral Resources are acknowledged for their cooperation within this project and for making it a success. The Speleological Association of the University of Leuven (SPEKUL) is thanked for providing the data of the cave mappings. VL.I.R. and the Vrije Universiteit Brussel, Development Cooperation Council are acknowledged for their sponsorship of the MSc studies of, respectively, L.Q.

movement. However, in such cases movement is often controlled by fracture patterns and hydrological regimes.

Figure 10 combines density data for average lineament length, number of lineament intersections, and number of lin-

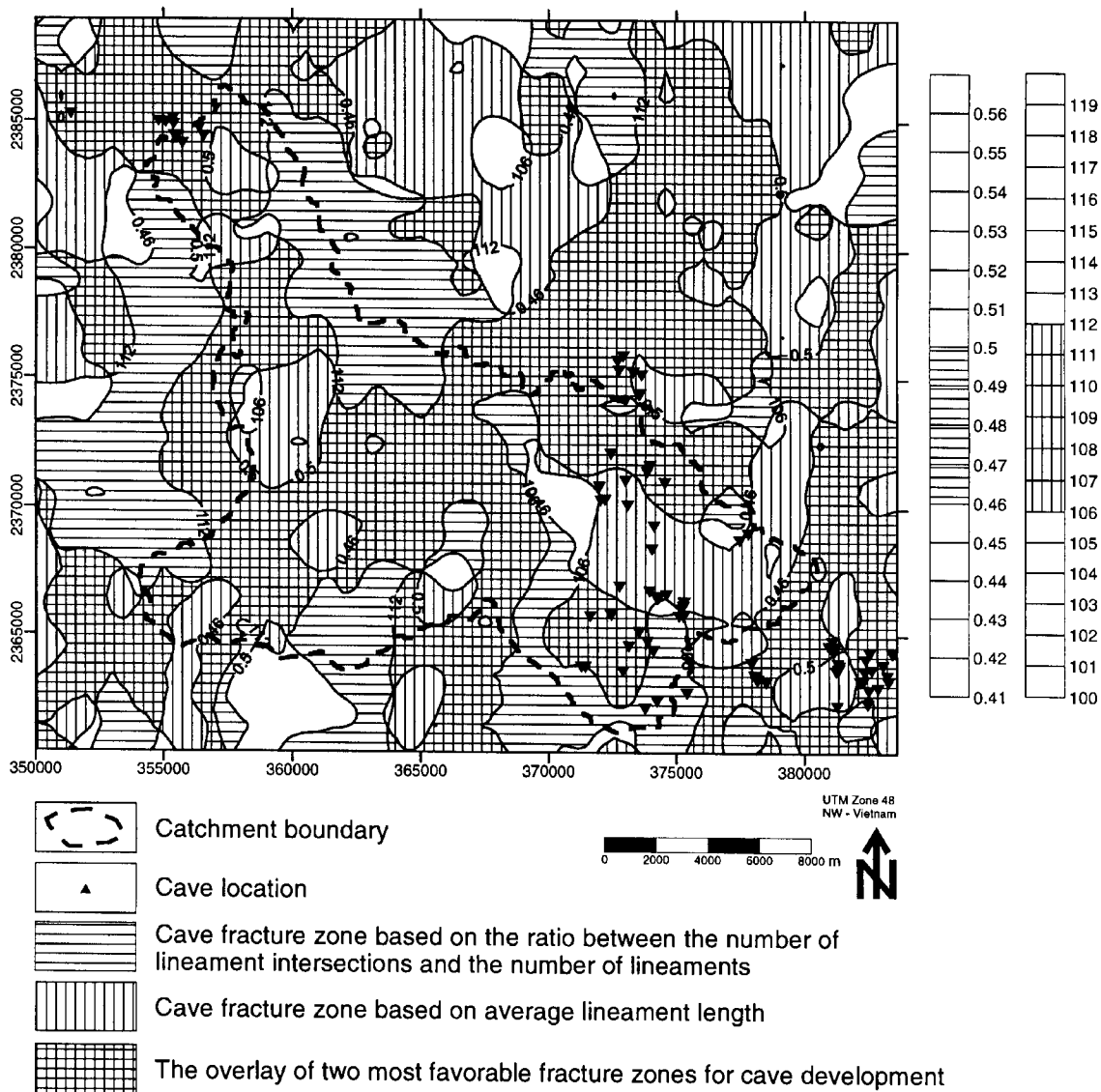


Figure 10. Overlay of the density map of average lineament length with the density map of the ratio between the number of lineament intersections and number of lineaments. The horizontal and vertical hatched areas are the fracture zones favorable for cave development. Overlain, the cross-hatched area is the most favorable fracture zone for cave development.

Hung and N.Q. Dinh. Finally the reviewers of the article are acknowledged for improving the text.

REFERENCES

Carper, W.J., Lillesand, T.M., & Kiefer, R.W., 1990, The use of intensity-hue-saturation transformations for merging SPOT panchromatic and multi-spectral image data: *Photogrammetric Engineering and Remote Sensing*, v. 56, p. 457-467.

Coessens, V., Deblaere, C., Lagrou, D., Masschelein, J., Tien, P.C., & Tuyet, D., 1996, Belgian-Vietnamese speleological expedition Son La 1995-1996: Cave investigation, a start for research on sustainable development, BVKCA, SPEKUL, RIGMR report, 63 p.

Dieu, N.T., 1992, *Geography of Vietnam: Hanoi*, The Gioi Foreign Languages Publishing House.

Dinh, N.Q., 2001, Cave database development, spatial analysis and 3D visualization with GIS, case study in Sonla - Vietnam [MSc thesis]: Vrije Universiteit Brussel, 114 p.

Dusar, M., Masschelein, J., Tien, P.C., & Tuyet, D., 1994, Belgian-Vietnamese speleological expedition Son La 1993, Professional Paper Belgian Geological Survey 1994/4-N.271, 60 p.

Fernandes, A.J., & Rudolph, D.L., 2001, The influence of Cenozoic tectonics on the groundwater-production capacity of fractured zones: A case study in Sao Paulo, Brazil: *Hydrogeology Journal*, v. 9, p. 151-167.

- Fish, L., 2001, COMPASS - software package for processing cave survey data, <http://www.fountainware.com/compass/>.
- Ha, L.T.C., 2001, Integrating landsat ETM7, aerial photographs and field data for geological mapping - the Tabernas basin - Southeast Spain [MSc thesis]: ITC, 174 p.
- Harris, J.R., Murray, R., & Hirose, T., 1990, IHS transform for the integration of radar imagery and other remotely sensed data: Photogrammetric Engineering and Remote Sensing, v. 56, p. 1631-1641.
- Hop, N.D., 1997, Geological map of Thuan Chau - Son La (Vietnam): Hanoi, The Geological Survey of Vietnam, p. 600.
- Hung, L.Q., 2001, Remote sensing based hydrogeological analysis of Suoimuoi catchment Vietnam [MSc thesis]: Vrije Universiteit Brussel, 87 p.
- Lillesand, T.M., & Kiefer, R.W., 1994, Remote sensing and image interpretation: New York, John Wiley & Sons, Inc, 750 p.
- Masschelein, J. & Swennen, R., 1997, Project proposal: Rural development in the mountain karst area of NW Vietnam by sustainable water and land management and social learning: Its conditions and facilitation, VIBEKAP documents, <http://www.vub.ac.be/vibekap/>.
- Mrose, N., Van Baars, M., Coessens, V., Deblaere, C., Lagrou, D., Masschelein, J., Tien P.C., & Tuyet, D., 1998, Belgian-Vietnamese speleological expedition Son La 1997-1998: Report of the third expedition in the northern provinces of Son La and Lai Chau, SPEKUL, BVKCA, RIGMR, 68 p.
- O'Leary, D.W., Friendman, J.D., & Pohn, H.A., 1976, Lineaments, linear, lineation - some proposed new standards for old items: Geological Society of America Bulletin, v. 87, p. 1463-1469.
- Sabins, F.F., 1997, Remote Sensing: Principles and interpretation: California, W.H. Freeman and company, 494 p.
- Schetselaar, E.M., 2000, Integrated analyses of granite-gneiss terrain from field and multisource remotely sensed data. A case study from the Canadian Shield [PhD thesis]: Technische Universiteit Delft, 269 p.
- Schetselaar, E.M., 2001, On preserving spectral balance in image fusion and its advantages for geological image interpretation: Photogrammetric Engineering and Remote Sensing, v. 67, p. 925-934.
- SPEKUL, BVKCA, & RIGMR, 2000, Preliminary report of the 4th Vietnamese-Belgian speleological expedition February-March 2000, SPEKUL, BVKCA, RIGMR, 51 pp. & app p.
- Szukalski, B.W., 2001, CaveTools version 5.0 for ArcView GIS, <http://www.mindspring.com/~bszukalski/cavetools/cavetools.html>.
- Tam, V.T., Vu, T.M.N., & Batelaan, O., 2001, Hydrogeological characteristics of a karst mountainous catchment in the northwest of Vietnam. Acta geologica sinica (English Edition): Journal of the Geological Society of China, v. 75, no. 3, p. 260-268.
- Tien, P.C., An, L.D., Bach, L.D., Bac, D.D., Bosakham Vongdara, Bountheung Phengthavongsa, Danh, T., Dy, N.D., Dung, H.T., Hai, T.Q., Khuc, V., Sauv Chiv Kun, Long, P.D., Mak Ngorn Ly, My, N.Q., Ngan, P.K., Ngoc, N., Nokeo Ratanavong, Quoc, N.K., Quyen, N.V., Somboun Duang Aphaymani, Thanh, T.D., Tri, T.V., Truyen, M.T., & Thach Soval Xay, 1991, Geology of Cambodia, Laos and Vietnam. Explanatory note to the geological map at 1:1,000,000 scale 2nd edition: Hanoi, Geological Survey Vietnam, 158 p.
- Tri, T.V., & Tung, N.X., 1979, Geotectonic evolution of northern Vietnam (in Russian): XIV Pacific Scientific Congress, Com. B, Sect. II: Khabarovsk, p. 48-49.
- Tri, T.V., Chien, N.V., Cu, L.V., Hao, D.X., Hung, L., Khuc, V., Luong, P.D., Ngan, P.K., Nhan, T.D., Quy, H.H., Thanh, T.D., Thi, P.T., Tho, T., Thom, N., Tung, N.X., & Uy, N.D., 1997, Geology of Vietnam-the north part. Explanatory note to the geological map at 1:1,000,000 scale: Hanoi, Science-Technical Publishing House, 335 p.
- Tuyet, D., 1998, Karst geology investigation of the northwest region: Hanoi, Research Institute of Geology and Mineral Resources, 251 p.
- Zhang, X.M., Cassells, C.J.S., & Van Genderen, J.L., 1999, Multi-sensor data fusion for the detection of underground coal fires: Geologie en Mijnbouw, v. 77, p. 117-127.

IMPLEMENTATION AND APPLICATION OF GIS AT TIMPANOGOS CAVE NATIONAL MONUMENT, UTAH

B.E. McNEIL^{a*}, J.D. JASPER^b, D.A. LUCHSINGER^a, AND M.V. RAINSMIER^a

^aDepartment of Geography, University of Denver, Denver, CO, 80210 USA

^bTimpanogos Cave National Monument, American Fork, UT, 84003 USA

*Present address: Department of Geography, Syracuse University, Syracuse, NY 13244 USA bemcneil@maxwell.syr.edu

Recent advances in accessibility and functionality of geographic information systems (GIS) have allowed Timpanogos Cave National Monument (TICA), Utah, to implement and apply this valuable management and interpretive tool. This implementation is highlighted by successful collaborations and the development of a 2-m resolution Digital Terrain Model. Applications of GIS at TICA are useful for the interpretation, resource management, and maintenance areas of park management. Specific applications with importance to the management decisions of TICA include interpretive mapping, 3-D visualization, cave resource management, and surface rockfall hazard.

Timpanogos Cave National Monument (TICA), a 100 hectare site surrounded by U.S. Forest Service Wilderness areas, is easily accessible by over one million people along the Wasatch Front, Utah (Fig. 1). It is set in American Fork Canyon, a limestone gorge with spectacular cliffs, avalanche chutes, pinnacles, and caves. The Monument was created in 1922 to protect the Timpanogos Cave system, a set of three caverns perched in a cliff band 460 m above the canyon floor. The cave system is known for its spectacular colors and abundant helictites. Over 70,000 visitors tour the caves each year and are placing increasing demands on the resources.

APPLICATIONS

Geographic information systems (GIS) has long been known as a valuable tool to better manage, interpret, and maintain resources as well as a proven decision support system. Data collection and development is paramount to applications in a GIS and must be customized to study area requirements and limitations. At TICA, all data must be high resolution, highly accurate, and function relative to the extreme topography and/or three-dimensional cave environment. Data have been collected and developed from a variety of sources, including GPS, hard copy maps, existing information databases, and aerial photography. Many applications are made possible through the development of a high resolution Digital Terrain Model (DTM). This DTM serves as the key base layer for TICA's GIS (Fig. 2). This 2-m resolution DTM has been created through digitizing and interpolating 10-ft contour lines obtained from a hard copy, 1 inch = 100 feet scale map (Eklundh & Martensson 1995). This terrain model has been checked for accuracy through the collection of 75 randomly distributed, highly accurate GPS control points (Holmes *et al.* 2000). This process found a mean elevation error of 3.216 m ($1\sigma = 3.219$ m). The errors are assumed to be randomly distributed to topographic variation as error is not found to be cor-

related to slope ($r^2 = 0.1441$). The accuracy and resolution of the DTM allows the GIS at TICA to visualize features and model phenomena in ways not possible with commonly available terrain models (e.g., USGS 30 m DEM).

A demonstration of the power and usefulness of the DTM has come through the completion of a rockfall hazard model. The unstable Deseret Limestone, steep topography, and multitude of visitors all combine to make rockfall a grave concern for managers at TICA (Fig. 3). While rockfall chutes and many hazard prone areas along the trail to the cave are well known, the GIS is now a powerful tool to quantify and objectify the rockfall hazard to TICA visitors, employees, and structures. The relative hazard model uses the DTM to delineate rockfall paths and determine slope while incorporating a vegetation map to account for friction. Van Dijke and Van Westen (1990) showed that the velocity of falling rocks can be calculated for every location (grid cell) in a hazard area. Using their method, the rock's velocity is calculated at each cell using a mathematical equation accounting for friction, gravity, horizontal distance, and vertical distance of the rock's fall. As the equation was translated into an ArcInfo GRID modeling environment, the velocity was calculated through running the FLOWLENGTH GRID command over a cost-distance surface simulating resistance to rockfall (McNeil 2002). Because it was not possible or necessary to obtain exact rockfall velocities, the model results in output maps representing hazard in relative terms (e.g. Low, High, and Extreme) and identifying dangerous rockfall paths (Fig. 4). These maps are used by TICA management as planning and decision-making tools for source area stabilization and hazard mitigation.

The DTM and the GIS now allow the management at TICA to visualize the cave and overlying terrain for purposes ranging from interpretation to natural resource management. A virtual field trip was created using the DTM and cave maps as background images. While this field trip is structured and realized in a web-based design, it is inherently a GIS application,



Figure 1: Location of Timpanogos Cave National Monument.

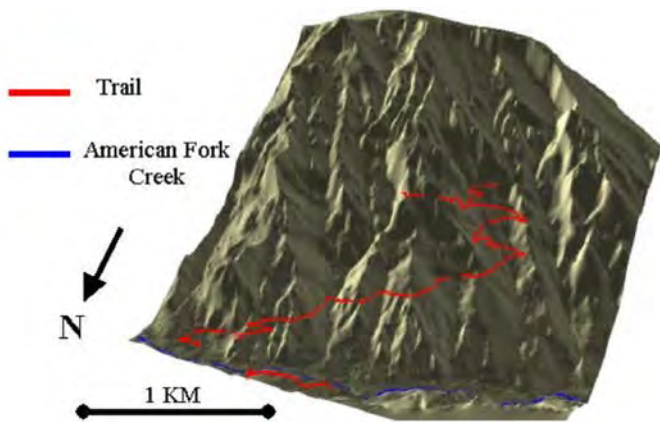
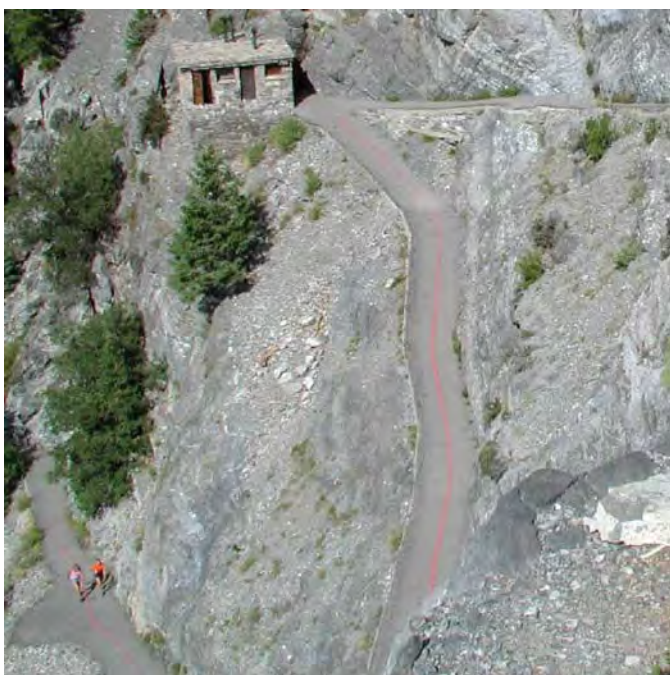


Figure 2: A visualization result showing the DTM, cave trail, and American Fork Creek.



interactively displaying and managing spatial information in the form of maps. The TICA virtual field trip is designed in a web based format in order to embrace the largest possible virtual visitor population and allow that population the freedom to explore the cave and cave trail from anywhere at anytime.

The inspiration to create a virtual field trip for TICA arose largely out of the limited accessibility of the caves and the limited nature of interpretation along the trail leading to the caves' entrance. Because the Timpanogos cave system is located high on the south wall of the American Fork Canyon, visitors must climb 325 m over 2.4 km of hard surfaced trail in order to reach the entrance to the caves. This climb is challenging for most visitors and prevents a significant population from being able to reach the caves. During the late fall and winter months, the cave is closed to the public because of dangerous ice and snow on the trail as well as increased rockfall hazard. Virtual field trips enable people to experience the full resources of TICA regardless of their physical condition or time of year. It is hoped that TICA will soon be able to provide access to the virtual field trip from their visitor center so that visitors will be able to enjoy the park during times of inclement weather or even if unable to hike the trail. Visitors to TICA's virtual field trip may choose to "Hike the Trail" or "Tour the Cave" from the home page: http://www2.nature.nps.gov/grd/parks/tica/tica_virtual_fieldtrip/Index.htm

The trail leading from the visitor center to the caves is depicted on this three dimensional visualization of the DTM in order to give visitors a clear understanding of the steep terrain adjacent to the cave system. Points of interest along the trail have been marked and linked to photographs and educational descriptions of identified resources (Fig. 5). Visitors can choose to move directly from one point of interest to the next or return to the map and select only the places that interest them. Visitors may enter the cave portion of the virtual tour either by returning to the home page and choosing "Tour the Cave," or linking to a map of the cave from the entrance shown on the trail map. Once visitors have reached the map of the cave, they will be able to navigate through points of interest in the same manner as the trail to the cave (Figure 6).

Virtual field trips like the one created for TICA promise to become valuable interpretive tools because of the freedom they give to visitors and interpreters alike. Maps play a vital role in this and other virtual field trips by allowing visitors to better understand the spatial relationships between resources. These virtual visitors can explore the caves at their leisure, taking time to read the educational descriptions accompanying photographs taken at the monument, or quickly glance at the pictures that interest them. Additionally, virtual field trips provide a wide range of interpretive possibilities unavailable in the past because of their ability to be accessed from a remote

Figure 3 (left). Rockfall danger to the trail as seen from the cave entrance looking northeast. Note the visitors on the trail in the bottom left and the loose rockfall debris directly above and below them. Red lines on trail warn visitors of dangerous rockfall areas. (Photo by J. Jasper)

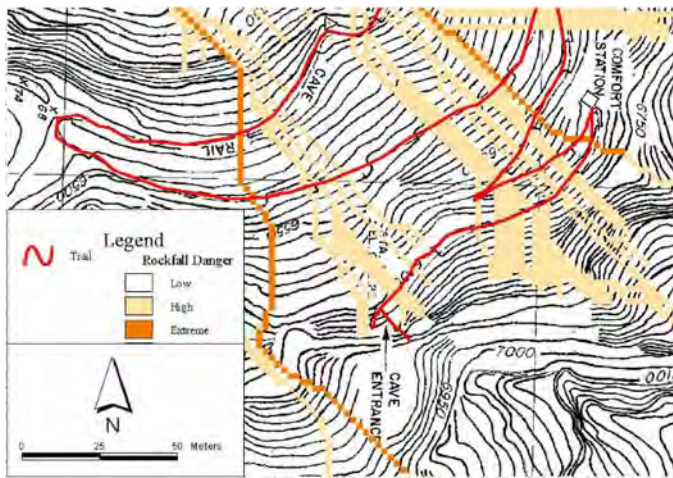


Figure 4: Hazardous rockfall paths to the upper portions of the cave trail with 10 foot contour lines. Note the comfort station visible in Figure 3.

location. Now interpreters are able to share resources located deep within wilderness areas or in fragile environments such as caves. Virtual field trips also allow interpreters to explain features in thorough detail seldom afforded by time constraints during visits. GIS has enabled the virtual field trip concept to be realized at TICA and presents a new paradigm for the interpretation of cave resources.

Natural resource management has also benefited greatly from the visualization opportunities of the GIS at TICA. One

of the most basic gains in understanding the cave resource comes through visualizing the cave and its overlying topography (Fig. 7). The 3-D cave lineplot is created through reading the survey coordinates (distance, bearing, and altitude) into COMPASS software (Fish 2002). The CAVETOOLS extension of ArcView (Szukalski 2002) will then convert the COMPASS data to a 3-D ArcView shapefile (the standard output format in ArcView). GPS locations of surface features identifiable on the original cave survey are used to geo-reference the 3-D shapefile.

Creating GIS layers of cave features is problematic since aerial photography and GPS techniques are not possible. To overcome these obstacles, a scanned Timpanogos Cave map was geo-referenced to the lineplot shapefile. This map provides an excellent base for recording and planning management actions. The cave map is the ultimate utility for management of cave-related data (Fig. 8). Currently, the park is documenting its cave cleaning efforts, photomonitoring points, cave habitat zones, electrical corridors, place names, and significant cave features. GIS provides the framework for managing all these data in its natural, spatially interconnected environment. This more spatially aware information management facilitates powerful resource management decisions and conclusions. All of these utilities allow TICA to increase their understanding of the active cave processes and use this knowledge to make better management decisions.



Figure 5: Virtual field trip web screens.

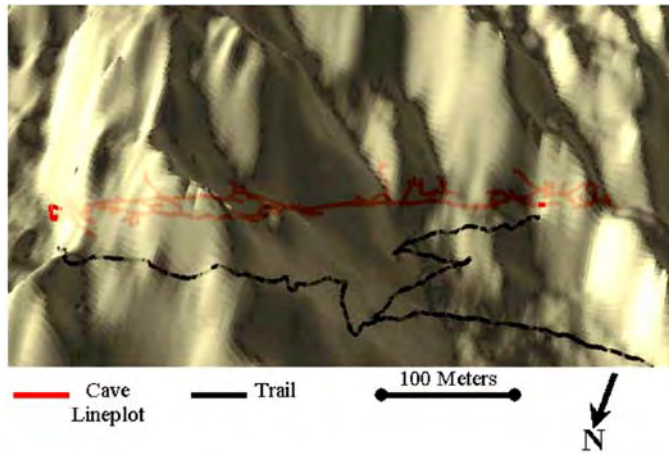


Figure 6: A 3-D visualization of the cave lineplot, cave trail, and the overlying topography as represented by the DTM.

CONCLUSIONS

GIS has been implemented at TICA because of its utility to effectively and efficiently manage and interpret cave and aboveground resources. Collaborations between TICA staff and academic researchers have catalyzed the implementation of a GIS framework that provides valuable applications and decision making support. To date, many unique and powerful datasets have been developed, facilitating rockfall hazard modeling, a virtual field trip, and a host of cave resource management applications. With high quality data, software, and hardware, the GIS at TICA is a glimpse of the vast possibilities that GIS holds for the management and interpretation of cave and karst ecosystems.

ACKNOWLEDGMENTS

B.E. McNeil wishes to thank the many people who generously provided technical support, fieldwork, and professional advice for this project. Especially Jon Jasper, Quincy Bahr, Camille Pullam, and Mike Gosse at TICA; Brian Carlstrom, Theresa Ely, and the rest of the National Park Service Intermountain Region GIS Support Office; and Neffra Matthews at the BLM Photogrammetry Lab. GIS software at TICA was obtained with the assistance of an ESRI Conservation Program grant. D.A. Luchsinger wishes to thank Red Hen Systems, developer of the VMS 2000 Video Mapping System, and Joe Berry, for the use of his equipment. We are grateful for the original cave survey and cave map cartography completed by Rodney Horrocks. We wish to thank Bernard Szukalski at ESRI for his helpful review and continued interest in TICA and cave and karst GIS in general. Our manuscript was strengthened by comments and suggestions of the anonymous reviewers.

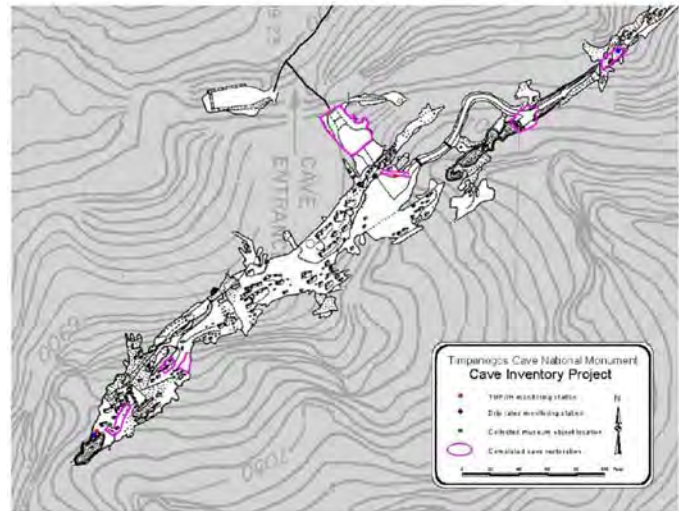


Figure 7: The geo-referenced cave map showing with overlying 10 foot contour lines. Note the scale and legend.

REFERENCES

- Eklundh, L. & Martensson, U., 1995, Rapid generation of digital elevation models from topographic maps: *International Journal of Geographic Information Science*, v. 9, no. 3, p. 329-340.
- Fish, L., 2002, COMPASS, www.fountainware.com/compass/
- Holmes, K.W., Chadwick, O.A., & Kyriakidis, P.C., 2000, Error in a USGS 30-meter digital elevation model and its impact on terrain modeling: *Journal of Hydrology*, v. 233, p. 154-173.
- McNeil, B.E., 2002, Implementation and application of a 3-D enterprise GIS at Timpanogos Cave National Monument [MS thesis]: University of Denver.
- Szukalski, B., 2002, Cave Tools version 5.0, www.mindspring.com/~bszukalski/cavetools/cavetools50.html
- Van Dijke, J.J. & Van Westen, C.J., 1990, Rockfall hazard: A geomorphological application of neighborhood analysis with ILWIS: *ITC Journal*, v. 1, p. 40-44.

THE APPLICATION OF GIS IN SUPPORT OF LAND ACQUISITION FOR THE PROTECTION OF SENSITIVE GROUNDWATER RECHARGE PROPERTIES IN THE EDWARDS AQUIFER OF SOUTH-CENTRAL TEXAS

DAN STONE

ESRI – San Antonio, 14100 San Pedro Avenue Suite 210, San Antonio, Texas 78232 USA

GEARY M. SCHINDEL

Edwards Aquifer Authority, 1615 North St. Mary's Street, San Antonio TX, 78215 USA

In May 2000, the City of San Antonio passed a \$45 million bond issue to purchase land or conservation easements of sensitive land in the recharge zone of the Edwards Aquifer in south central Texas. The Edwards Aquifer is the primary source of water for over 1.7 million people in the region. The application of geographic information systems (GIS) methods allowed for the objective comparison of all properties within the recharge and contributing zones of the aquifer for possible purchase. A GIS matrix was developed and applied in the process of prioritizing sensitive karst lands.

The San Antonio segment of the Balcones fault zone section of the Edwards Aquifer is one of the most productive karst aquifers in the United States. Located in south-central Texas, the San Antonio segment extends from the groundwater divide in Kinney County (Brackettville), east through Bexar County and the City of San Antonio, then northeast to the groundwater divide in Hays County (near the town of Kyle). The Edwards Aquifer is the primary source of water for over 1.7 million people in the greater San Antonio area and supports a broad base of agricultural, municipal, industrial, and recreational uses (EAA 2001). The need to protect the water quality of the Edwards Aquifer was highlighted in 1987 when the U.S. Environmental Protection Agency designated the Edwards as the first “Sole Source Aquifer” in the United States. Various state, regional, and local regulatory programs have been initiated to protect water quality in the Edwards’ region.

In May 2000, the citizens of San Antonio passed a \$65 million sales tax initiative to collect 1/8 cent sales tax up to \$65 million to purchase open space within the city and for land acquisition for aquifer protection in Bexar County. Approximately \$40.5 million from the sales tax initiative will be used to directly purchase land or conservation easements for aquifer protection. Another \$4.5 million will be put aside for operations management. The San Antonio City Council directed city staff to develop a process to allow for the fair and adequate selection and evaluation of eligible properties.

GEOLOGIC SETTING

The Edwards Aquifer is named after and contained in the Lower Cretaceous Edwards Limestone. Secondary porosity and permeability, resulting from both meteoric water and deep circulation mixing corrosion, have dominated the flow regime. The Edwards Limestone and associated units range from 130

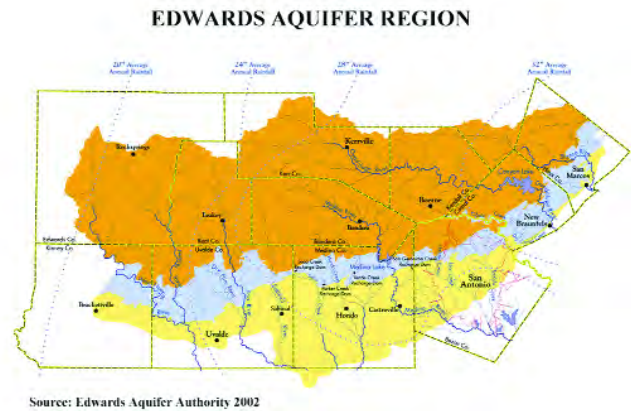


Figure 1. Edwards Aquifer region.

m to over 270 m thick with an average thickness of ~180 m. A series of faults in the Balcones fault zone has exposed the Edwards Limestone at the surface along the boundary between the dissected Edwards Plateau (Texas Hill Country) and the Gulf Coastal Plain. En echelon faulting has dropped the Edwards Limestone to great depth below the surface along the aquifer’s southern and eastern boundary (Maclay 1995).

Generally, the Edwards Aquifer is divided into three zones: the drainage zone or contributing zone, the recharge zone, and the artesian zone (Fig. 1) (EAA 2002). Surface streams forming on the contributing zone (the dissected Edwards Plateau), flow south or east and cross the Edwards Limestone outcrop (recharge zone) (Fig. 2). During low flow conditions, most surface water is captured by the aquifer as it crosses the outcrop. In addition, rainfall that occurs directly on the recharge zone also enters the aquifer. Groundwater entering the aquifer generally flows south and east into the artesian zone. In the artesian zone, regional flow paths are from west to east where the aquifer discharges at two primary springs – Comal Springs and

San Marcos Springs. Comal Springs is the largest spring in the southwest with an average discharge of 8.3 m³/s. However, wells tapping the aquifer in the artesian zone withdraw >500,000,000 m³ of water each year. Residence time of water in the aquifer ranges from a few hours or days to many years depending upon depth of circulation, location, and related aquifer parameters (Maclay 1995).

Water quality in the aquifer is generally very high; however, human activities in the contributing and recharge zone have resulted in degraded

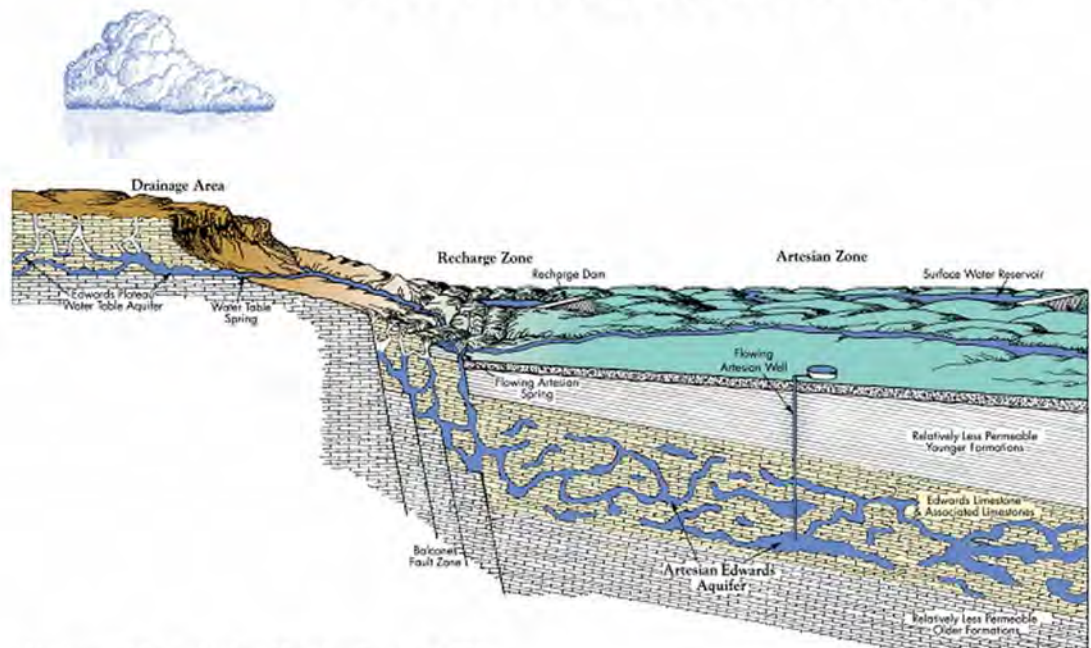
water quality in some areas. Of particular concern is the northern growth of San Antonio onto the recharge zone. Land use is quickly changing from ranching to mixed residential and commercial development. Wells that exceed safe drinking water limits are generally associated with point contamination sources such as releases from above or underground storage tanks.

PROPOSITION 3

On May 6, 2000, the citizens of San Antonio passed a "Parks Development and Expansion Venue Project Proposition" (Proposition 3) to raise \$65 million through a 1/8 cent sales tax increase for the acquisition of open space over the Edwards recharge zone and linear parks along Salado and Leon Creeks. Of the four propositions in the May election, only Proposition 3 passed. A total of \$40.5 million was reserved for the purchase of land or conservation easements over the recharge and contributing zones of the aquifer. Another \$4.5 million was created for a maintenance endowment fund for management of acquired properties and easements.

Upon passage of Proposition 3, the San Antonio City Council instructed City staff to create a process for the fair and adequate evaluation of properties. City staff proposed and the City Council approved the creation of two committees: the Scientific Evaluation Team (SET) and the Conservation Advisory Board (CAB).

GEOLOGIC CROSS-SECTION OF THE EDWARDS AQUIFER



Source: Edwards Aquifer Authority 2002

Figure 2. Geologic cross-section of the Edwards Aquifer.

The purpose of the SET was to develop a "scientific data matrix" outlining and prioritizing the characteristics of the area for use by the CAB in property evaluation. This group was composed of representatives from public agencies and one private environmental consulting firm as follows: Texas Parks & Wildlife, Edwards Aquifer Authority, San Antonio Water Systems, City of San Antonio Public Works Department, City of San Antonio Parks & Recreation Department, United States Geological Survey, University of Texas San Antonio, National Resources Conservation Service, San Antonio River Authority, and George Veni and Associates.

The Conservation Advisory Board was created to review the SET's scientific data matrix, establish additional criteria to be considered for land acquisition (i.e., property size, cost, proximity to other public property, open space linkages, etc.), transmit the final matrix to the land agents, evaluate properties identified by the land agent, make recommendations for land purchases to the Planning Commission and City Council, and to work with City staff to determine appropriate park land use intensity after purchase. The CAB is composed of representatives from the following groups: Texas Parks & Wildlife, Edwards Aquifer Authority, San Antonio River Authority, San Antonio Water Systems, City of San Antonio Public Works Department, City of San Antonio Parks & Recreation Department, Open Space Advisory Board (conservation community representative), Parks and Recreation Advisory Board (neighborhood representative), and a business representative.

The City of San Antonio (COSA) staffed the SET and the

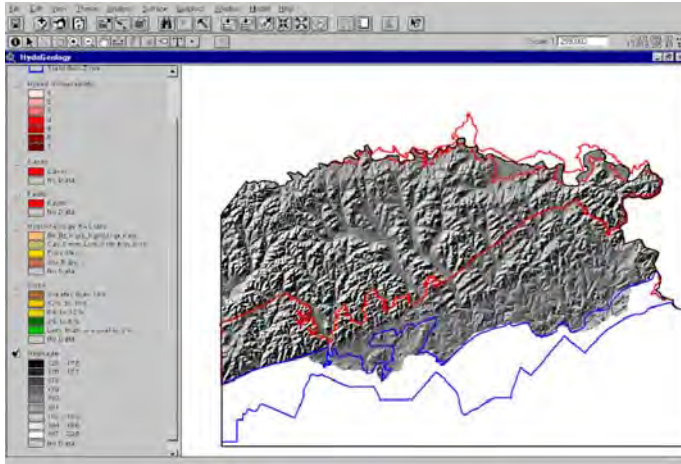


Figure 3. Digital elevation model (DEM) of the study area.

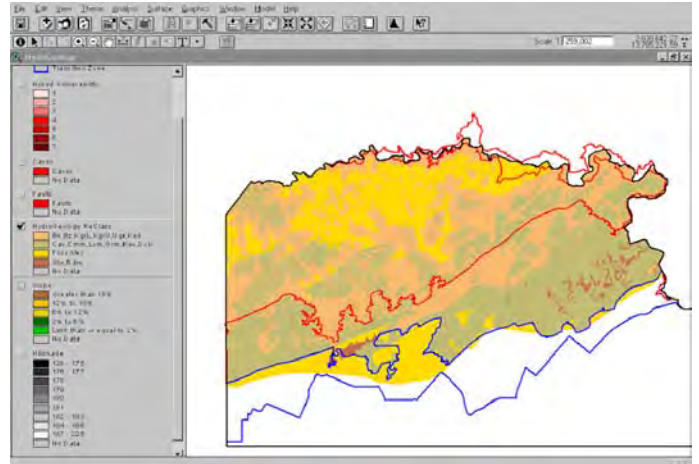


Figure 5. Geologic classifications.

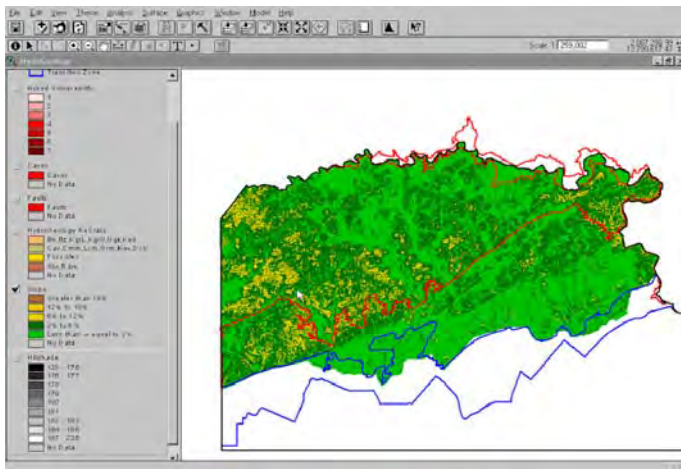


Figure 4. Calculated slope ranking.

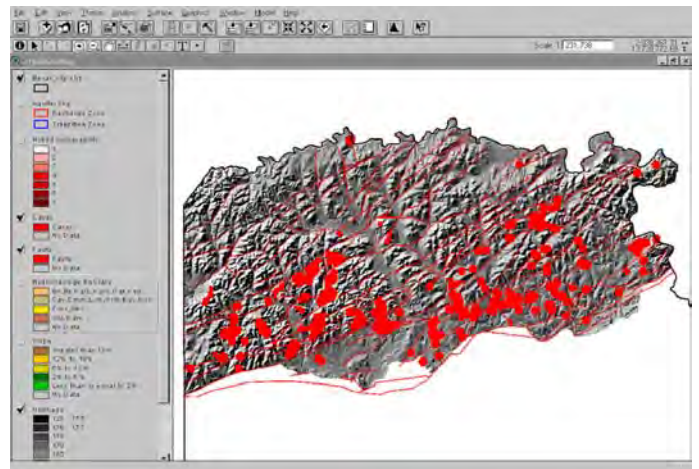


Figure 6. Buffered faults, sinkholes, and caves.

CAB. Susan Crane, a landscape architect with COSA was named project manager. In addition, COSA contracted with software developer ESRI to provide Geographic Information System (GIS) support.

The first meeting of the SET addressed various methods to rank and score individual properties. However, it was determined that this offered no guidance to the land agents in pre-selection of properties and potentially wasted considerable time and money. In addition, the scoring of individual properties could be very subjective, especially if properties would not or could not be compared to a larger population set. The SET Committee determined that developing a matrix using GIS offered the best solution to this problem and allowed for the objective comparison of all properties within the recharge and contributing zones.

The use of GIS allows spatial information to be stored in a computer based on different themes or layers. A layer is data organized by subject matter. For example, land surface elevation data can be grouped together into a single layer. As relevant data sets are identified and gathered, the GIS technology allows the various layers to be queried to determine relation-

ships, or quantified for scoring and ranking purposes. For example, the process can be used to indicate all properties within 60 m of an existing park that are at least 24 hectares in size, and contain specific geologic formations.

The SET then identified the variables, criteria for inclusion of the datasets, and weighting for each layer for use in the spatial model. Three primary data categories were selected for inclusion in the model: geologic, biologic, and watershed data. Each major category contained a number of subcategories. It was also necessary for each dataset to cover the entire study area. Advances in computational power and existing datasets allowed a 1-m data cell resolution.

GEOLOGIC DATASETS

The following geologic criteria were selected for use in the GIS model: terrain slope, stratigraphy, mapped faults, caves and sinkholes, and soils. The United States Geological Survey (USGS) had just completed a 2-year study of the recharge zone and created a dataset using the above listed layers. However, this data set was limited to the recharge zone only. At the

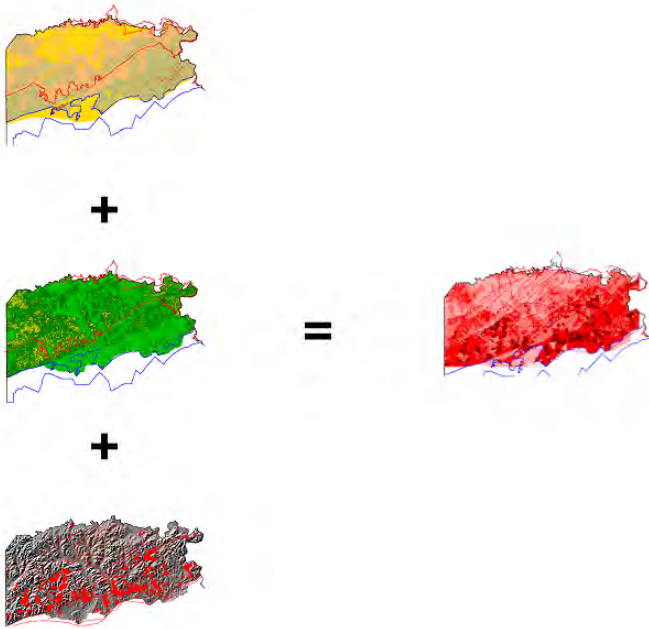


Figure 7. Vulnerability model spatial overlay process.

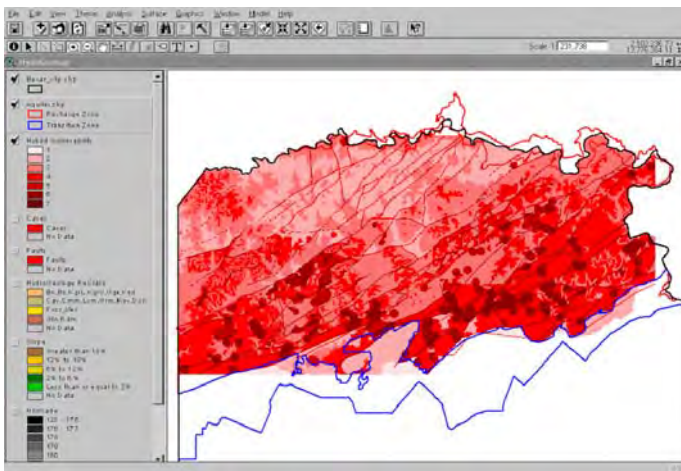


Figure 8. Vulnerability model showing areas of highest permeability in darker red.

request of the SET, the USGS prepared a new hybrid-data set that included the contributing zone.

Table 1. Slope Classification

Class	Rating
Greater than 18%	1
Greater than 12% and less than 18%	3
Greater than 6% and less than 12%	5
Greater than 2% and less than 6%	9
Less than or equal to 2%	10

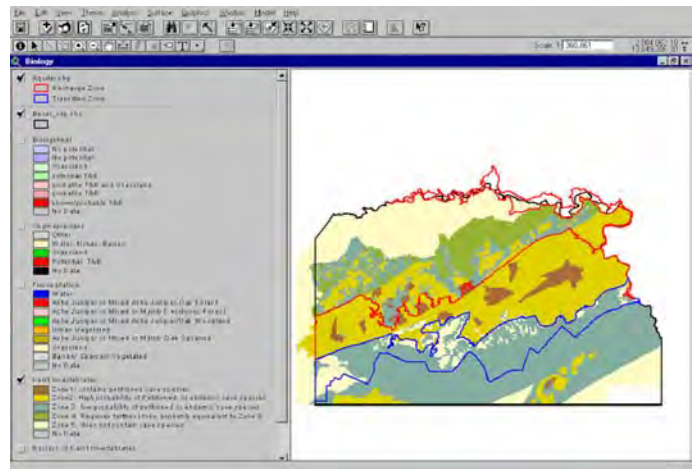


Figure 9. Endangered karst invertebrate classification zones.

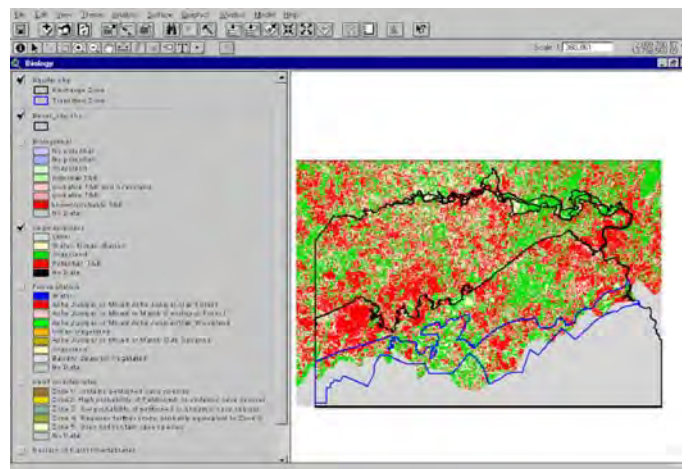


Figure 10. Vegetation habitat classification for the Golden-Checked Warbler.



Figure 11. Biological model spatial overlay process.

TERRAIN SLOPE

Slope plays an important roll in controlling rainfall runoff with the greatest slope having the least potential for infiltration. Properties with little or no slope would have the greatest potential for infiltration and would therefore be more important to protect through purchase. The GIS was able to analyze the Digital Elevation Model (DEM) and calculate the differences in elevation between every square meter in the data set (McCoy & Johnston 2001). Using the criteria established for slope in Table 1, it was easy to calculate a ranking of slope for

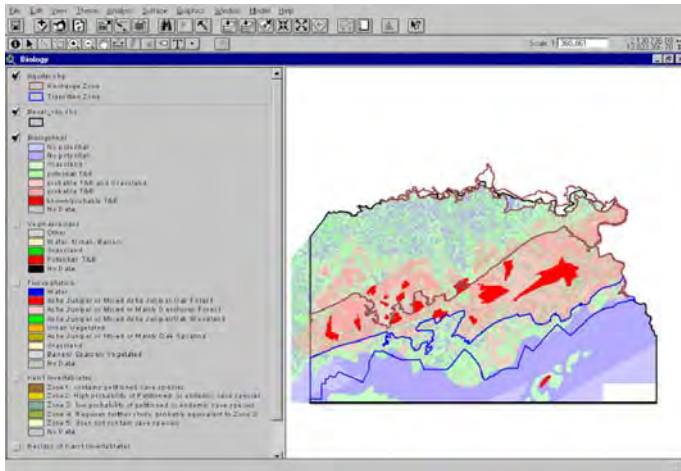


Figure 12. Biological model showing areas of highest potential for threatened and endangered species in dark red.

the region. Figure 3 shows the DEM for the study area. The resulting slope calculation by the GIS is displayed in Figure 4. Areas indicated in light green have relatively flat slopes and are indicative of highest rating.

STRATIGRAPHY

The recharge zone of the Edwards Aquifer is generally defined as the outcrop area of the Edwards Limestone and associated units (Georgetown Formation). The Edwards Limestone is composed of a number of mappable units or strata, each exhibiting varying degrees of susceptibility to dissolution processes. The location of each unit has been defined within a GIS dataset. The contributing zone is composed of the Glen Rose Limestone, the geologic unit located stratigraphically beneath the Edwards Limestone. Units within the Glen Rose also display varying susceptibility to karstification. The SET, based upon a consensus of experience, assigned each unit a classification related to its primary and secondary porosity and permeability. Under the guidance of the SET geologists, the geology was classified into the following categories with areas of higher relative permeability given a higher ranking than areas of lower relative permeability. The resulting data layer is displayed in Figure 5.

The last variable in the hybrid-vulnerability model was the inclusion of fault, sinkhole, and cave data. The SET made an assumption that all faults, sinkholes, and caves were areas of enhanced permeability and, therefore, should receive separate coverage and given a high ranking. Faults, sinkholes, and caves were identified from data provided from the USGS, the Texas Bureau of Economic Geology, the terrain model, and from the Texas Speleological Survey files. The areas around faults, sinkholes, and caves were “buffered” in the model to cover some uncertainty regarding their locations and the concern that adjacent areas may not have been identified but exhibit similar physical properties related to hydrology. Faults were given a 25-m buffer on each side, caves and sinkholes

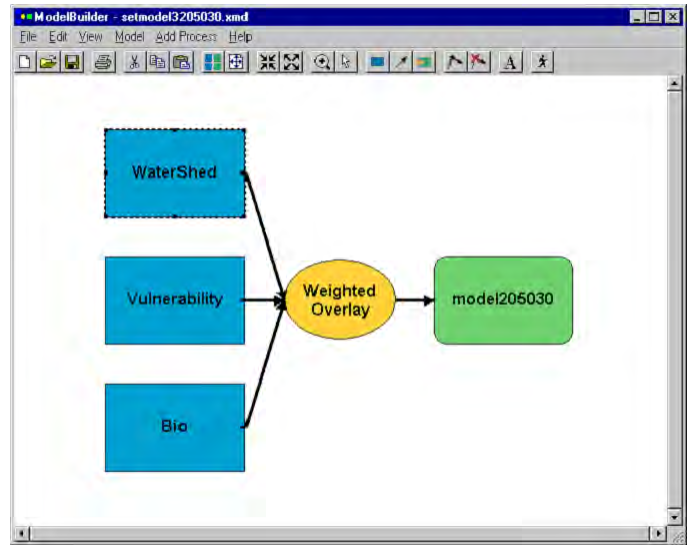


Figure 13. Model Builder diagram of the final SET model.

were given a 50-m buffer. Identified features are shown in red in Figure 6.

The final hybrid-vulnerability model was created through an operation known as a spatial overlay (ESRI 1997). All of the layers: Slope, Geology, Faults, Sinkholes, and Caves; were overlaid (Fig. 7) and the values for each square meter calculated for the output model. Figure 8 depicts the results of the overlay process. The dark red colors in Figure 8 are areas that have the highest score, thus meeting the majority of the geologic criteria established by the SET.

BIOLOGY

The second primary data category identified for inclusion in the model was biological criteria. The SET identified a surface biological component and a subsurface biological component for inclusion in the model. Datasets containing relevant material were provided by the Texas Parks and Wildlife and the U.S. Fish and Wildlife Service.

The SET selected the habitat of the Golden-Cheeked Warbler to represent surface biologic datasets. The Golden-Cheeked Warbler is a federally listed endangered species that only nests in mature, central Texas mixed ash juniper and oak woodlands. The species was listed because of declining populations resulting from land use changes.

In 1992, several groups petitioned the U.S. Fish and Wildlife Service to add 9 species of karst invertebrates to the list of Threatened and Endangered Wildlife. The 9 species of invertebrates are known only from caves in the northern and northwest parts of Bexar County. The SET selected the karst invertebrate dataset to represent the subsurface component for the model. In December 2000, U.S. Fish and Wildlife listed the 9 species, which includes three beetles, five spiders, and one harvestman. Figure 9 indicates the GIS coverage for the biologic subsurface datasets. The data are partitioned into 5 zones with Zone 1 (highest ranking) to Zone 5 (lowest ranking).

Table 2. Geologic Classification Based On Relative Permeability

Geologic Strata	Class
Basal Nodular (Edwards) Member Bullis Zone Lower Glen Rose Upper Glen Rose Edwards	1
Upper Glen Rose "Cavernous Zone" Edwards (Cyclic and Marine Members) Edwards (Leached and Collapsed Member) Edwards (Grainstone Member) Edwards (Kirschberg Member) Edwards (Dolomitic Member)	2
Upper Glen Rose "Fossiliferous Zone" Upper Confining Unit Undivided 3	3
Georgetown Formation Regional Dense Member (Edwards)	4

Table 3. Karst Invertebrate Zones

Zone	Classification
Zone 1	Contains petitioned cave species
Zone 2	High probability of petitioned or endemic cave species
Zone 3	Low probability of petitioned or endemic cave species
Zone 4	Requires further study
Zone 5	Does not contain petitioned species

Zone 1 containing listed cave species, Zone 2 probably containing species, Zone 3 having a low probability of containing species, Zone 4 requiring further study, and Zone 5 not containing listed species. The classification is described in Table 3.

Vegetation data for the study area was reclassified to identify potential endangered species habitat. The SET acquired a vegetative dataset prepared cooperatively by Texas Parks and Wildlife and U.S. Fish and Wildlife Service. From the dataset, vegetation was reclassified from 8 classifications to 3 classifications. The reclassification is described in Table 3. The results of the reclassification are shown in Figure 10.

The final biology model was created through spatial overlay. The vegetation and karst invertebrate layers were combined to form the final biologic layer (Fig. 11). The result of the overlay process is shown in Figure 12. The red areas in Figure 12 represent areas that have the highest potential for threatened and endangered species.

Table 4. Reclassification of Vegetative Data Sets

Original	Reclassified
Ashe Juniper or Mixed Ashe Juniper Oak Forest Ashe Juniper or Mixed Ashe Juniper or Mainly Deciduous Forest Ashe Juniper or Mixed Ashe Juniper/ Oak Woodland Ashe Juniper or Mixed or Mainly Oak Savanna	Potential Threatened and Endangered Species
Water Urban vegetated Barren, Sparsely Vegetated	Water, Urban, Barren
Grassland	Grassland

WATERSHED

The third primary data category was a watershed component. The watershed component consisted of several variables such as property size, adjacency, and proximity of a property to other "Open Space" properties.

The SET decided to set a minimum property size for property consideration at 60 acres. The 60 acres minimum was based upon the minimum area necessary for effective wildlife management. Properties were then reclassified by property size from data provided by the Bexar Appraisal District and included parcel number, size, ownership, and appraised value including improvements.

The SET determined that properties located either adjacent to or in proximity of other open space properties were desirable. This would improve the size of wildlife habitat as well as make management of properties easier. Existing open space areas that were considered in the model were military bases, San Antonio River Authority Dam locations, and existing parks and nature areas. This layer was used to find all properties that are adjacent to these features. A 200-foot buffer was used to select all properties in proximity to these features.

THE SET MODEL

Data layers from the geologic, biological, and watershed primary data categories were combined into a spatial overlay using the GIS model builder application (Ormsby & Alvi 1999) (Fig. 13). The SET determined the weighting for primary data categories as follows: geologic (50%), biological (20%), and watershed (30%). The modeling process assigned every square meter of the study area a value based on the weighted overlay with the higher values representing the greatest number of criteria met.

The results of the modeling were divided into 8 tiers with the 3 highest tiers meeting the overall criteria developed by the SET to be considered for evaluation for purchase. Use of the GIS SET model allowed the objective evaluation of each property and provided the public an assurance that Proposition 3 funds were being spent to support the goals of the program.

CONCLUSION

GIS allows for the processing of very large and diverse data sets to meet the goals of the SET - to established scientifically based, objective criteria to evaluate properties over the drainage and recharge areas of the Edwards Aquifer. The model was used by the Proposition 3 project manager to direct land agents to pursue properties that met the objectives of the program. As land purchases are negotiated with the owners, they are evaluated by the Conservation Advisory Board. If the CAB gives a land purchase a favorable rating, the property acquisition was forwarded to the Planning Commission and City Council for review and approval.

In December 2000, the first purchase of "sensitive" land was made using funds generated by Proposition 3, a 1/8 cent sales tax that took effect in October 2000. The San Antonio City Council voted to spend almost \$6.8 million to acquire 414 hectares of ranch land adjacent to Government Canyon State Natural Area in northwest Bexar County. Almost all the property lies within the recharge zone. The city is now creating a management plan for the property in cooperation with the CAB.

The Proposition 3 program continues to purchase property in the recharge and contributing zone and is now considering increasing the funding as well as the ability to purchase lands outside of Bexar County for inclusion in the program. Since December, the city has acquired 4 additional properties. A total \$22.5 million was spent for 1416 hectares. Prior to the proposition program the park acreage was 3298 hectares. With the proposition program the park lands have increased 43%.

REFERENCES

- EAA, 2001, Edwards Aquifer hydrogeologic report of 2000: Edwards Aquifer Authority Report 01-02: San Antonio, Texas, 102 p.
- EAA, 2002, Map of the Edwards Aquifer Region, Edwards Aquifer Authority.
- ESRI, 1997, Getting to know ArcView GIS: Cambridge, UK, GeoInformation International, 434 p.
- Maclay, R.W., 1995, Geology and hydrology of the Edwards Aquifer in the San Antonio area, Texas: US Geological Survey, Water-Resources Investigations Report 95-4168, 69 p., 12 sheets.
- McCoy, J., & Johnston, K., 2001, Using ArcGIS spatial analyst: Redlands, CA, ESRI, 230 p.
- Ormsby, T., & Alvi, J., 1999, Extending ArcView GIS: Redlands, CA, ESRI Press, 526 p.

REVISING THE KARST MAP OF THE UNITED STATES

GEORGE VENI

George Veni & Associates, 11304 Candle Park, San Antonio, Texas 78249-4412 USA, gveni@satx.rr.com

The production of the recently published Living with karst: A fragile foundation required a map showing the distribution of karst in the United States. William Davies et al. (1984) produced the last such map. I used their work as the basis in developing a revised US karst map, but delineated karst primarily on lithology rather than cave lengths. The categories are: exposed and buried carbonate and evaporite karst, and volcanic and unconsolidated pseudokarst. The new US karst map updates the previous map with data from more detailed regional karst maps. Scale and information availability limited the accuracy of the new map. Buried evaporites and unconsolidated pseudokarst are underrepresented due to insufficient delineation. I had to interpolate from available information to adjust for discrepancies due to different map projections and differences between maps. The new US karst map improves on earlier versions but is still incomplete and of low precision in some areas. Production of detailed karst maps with drainage basins and other land management factors is best left to state agencies. The US Geological Survey is developing a new US karst map and the NSS Section of Cave Geology and Geography is assisting with that effort. Uniform standards need to be established for definitions, scale, and map projections. Section members include the country's most knowledgeable karst geoscientists and they play key roles in developing an accurate and definitive US karst map.

This report describes the process and rationale for the development of the United States (US) karst areas map recently published by the American Geological Institute (AGI) in *Living with karst: A fragile foundation* (Veni *et al.* 2001). Also discussed are the applications and limitations of the map and recommended directions for future refinements in delineating US karst.

Well before most people who were interested in caves knew the term "karst," maps were drawn showing the location of caves and occasionally their underlying geology. Some of the earliest examples were published in *Caverns of Virginia* (McGill 1933). Initially, these maps were meant to illustrate cave locations to facilitate further visitation and study. As time went on, the intent of the maps began to focus on spatial relationships between caves, typically to support exploration and hydrogeologic analysis. Maps of karst were not produced until late in the 20th Century because detailed, regional geologic maps were not broadly available until that time.

Most "karst" mapping has been the illustration of cave locations or the density of known caves and sinkholes within given areas. This was done for various karst regions, but Moore and Sullivan (1978) produced the first cave density map that covered the entire country. The first attempts to geologically delineate US karst were produced for county, state, and geographic regions by outlining areas of carbonate and evaporite rocks (e.g. Smith 1971).

Davies *et al.* (1984) produced the first map showing the karst areas of the United States. The karst was color-coded into four main areas based on the following characteristics:

- many caves over 300 m long and 75 m deep;
- caves generally less than 300 m long and 15 m deep;
- caves generally absent but where present, usually less than 15 m long and 3 m deep; and

-pseudokarst features in unconsolidated sediment and volcanic rocks.

Patterns drawn within each colored area identified if the karstic rocks were dipping, folded, carbonates, evaporites, metamorphosed, and/or buried. The map was published as one large sheet by the U.S. Geological Survey (USGS) with an explanation printed on one side and has since served as the standard reference that defines US karst.

The map by Davies *et al.* (1984) is generally correct but has limitations. The one most noticed is that some small but important karst areas are excluded. For example, the lower member of the Glen Rose Formation in central Texas is excluded even though it contains two show caves that have operated since the 1930s plus Honey Creek Cave, the state's longest, with over 32 km of surveyed passages (Elliott & Veni 1994). Another drawback is that the shapes of the karst areas are smoothed and generalized so that they are not as accurate or precise as they could be at that scale. Accessibility is also a problem. The map is known primarily to karst scientists, but is poorly accessible and not well known to land managers, educators, and other people who make critical decisions about karst. In fact, it may not be easily accessible to karst researchers either, since I could not find it cited in any major text on karst or in any of four karst bibliographic publication series.

In 1991, White (2001) initiated discussion to examine the need and means of developing a more complete and accurate karst map of the US. Project KarstMap was formally organized under the National Speleological Society's (NSS) Section of Cave Geology and Geography in 1995. Little progress was made except to review the status of karst mapping throughout the country and the rapidly changing technology for performing the job. Detailed state-funded karst maps were found completed or in production for some states and regions, but producing maps of this type was beyond the level of effort that

could be met by the NSS project. Consequently, the KarstMap project languished and its viability was in doubt in 2000.

DEVELOPING THE AGI KARST MAP

Near the end of 2000, I was completing work on the *Living with karst* booklet, which the NSS Section of Cave Geology and Geography wrote for publication by AGI. The booklet is part of AGI's "Environmental Awareness Series," aimed at educators, decision-makers, and the general public to teach important principles about geologic resources. The karst booklet was the fourth in the series, and AGI and I decided that a map showing the karst areas of the US was important for the public to realize that karst is not a rare phenomenon and it directly affects many people. We initially planned to use the Davies *et al.* (1984) map but couldn't locate a high quality digital version. Other problems arose after scanning the map, such as showing the fine geologic details when reduced in size for the booklet, so I offered to redraw the map digitally.

Rather than simply trace the existing map, I sought to make as many improvements as feasible given the intended audience for the booklet and the limited time and resources available. Discussing the issue with my co-editor Harvey DuChene and AGI editor Julie Jackson, we set five goals for the new map:

1. Base the map on lithology, not cave length. Cave length is an imperfect means of measuring karst. It falsely assumes uniform levels of exploration and knowledge of cave systems, and arbitrarily gives significance only to the humanly enterable portion of the conduit system. More fundamentally, caves have been used as a surrogate for the maturity of karst landscapes when in fact, karst can be hydrologically mature and have advanced troglobitic ecosystems even where caves are small relative to human access. Mapping based on lithology allows convenient grouping of areas with similar hydrologies, chemistries, morphologies, and land management issues.

2. Include missing karst and pseudokarst areas. Davies *et al.* (1984) did not include some karst and pseudokarst areas by mistake, oversight, or because those areas had not yet been identified. As many of these areas as possible would be included.

3. Improve the illustration of exposed versus buried karst. Non-karstic strata cover much of the US karst. Mapping of additional buried karst, along with a more easily recognizable means of representing these areas, was needed to distinguish this different, but important, subset of karst.

4. Increase map accuracy and precision. Known errors in the map would be corrected and the map spot-checked for general accuracy against other available information. Improving the map's precision was important but beyond the scope of the project except in a very limited way in areas where maps showing more precise boundaries were known to exist.

5. Simplify map for easier use. A general, informative, visually attractive, and intuitively understandable map was needed for the booklet's broad audience. The map of Davies *et*

al. (1984) included a lot of detailed information that was hard to see on the map and not intuitively apparent without close examination. Those details were also not particularly useful to the general public or to researchers who would usually need even more site-specific information. The forum for the AGI karst map, publication in the nationally distributed booklet, would meet a sixth goal of making the map broadly and easily accessible for use.

The first step in drafting the AGI karst map was to select the CorelXara version 1.5 computer drawing program for the cartography. Admittedly, much of this decision was based on having the program already on my computer and my familiarity in its use. However, other important factors were its versatility in executing the drawings, importing other files, and exporting files that AGI could use.

The second step was to select basemaps for use. The map by Davies *et al.* (1984) was the foundation of the AGI map. Since it seemed basically correct, much of its information could be directly used. I scanned it into my computer and imported it into CorelXara to trace karst area boundaries. Those scans are shown in Figures 1 and 2 in this report at the resolution used to draw the new map. I also scanned karst maps of various regions into the computer that provided more precise and complete illustrations of the country's karst. I tried to review a complete range of karst maps for US areas but probably missed some regions with the limited time available. Maps that appeared to offer improvements to the Davies *et al.* (1984) map and were used in developing the AGI map were from Powell (1961) for Indiana, Daniel and Coe (1973) for Alabama, Hill, Sutherland, and Tierney (1976) for Wyoming, Quick (1979) for the Hudson River Valley, Smith and Veni (1994) for Texas, Vineyard (1997) for Missouri, Richards (1999) for Hawaii, and Werdon, Szumigala, and Davidson (2000) for Alaska.

For ease of manipulation, each scanned map was saved as its own layer in the drawing. Each layer could be made visible, invisible, editable, and uneditable as needed. The drawing itself was also saved in individual layers for each category of karst depicted: exposed carbonates, buried carbonates, exposed evaporites, buried evaporites, volcanic pseudokarst, and unconsolidated pseudokarst. The text was also saved as a separate layer, as was the map AGI provided that showed the borders of the 50 US states. A rectangular border (not shown in the final map) was added to precisely register each of the drawn layers; there were no visible variations in the borders at a magnification of 3000%.

The fourth step was to illustrate the map in a clear and easy to grasp manner. Since most of the geologic details found on the earlier map were not used, a simple application of color was possible. Red was selected as the most intuitive color for volcanic pseudokarst. Gold, blue, and green were respectively selected as distinctive colors for unconsolidated sediments, evaporite karst, and carbonate karst. Buried karst was illustrated by a lighter shade of the appropriate primary color: light blue and light green were used for buried evaporites and car-

bonates.

Several challenges arose in drafting the new map. The first was a matter of scale. Since the new map would be smaller than the Davies *et al.* (1984) map, some details had to be altered. The smallest karst areas were deleted because they would not be visible as anything more than undistinguishable dots. Karst areas in close proximity to other karst areas were connected when they would appear connected when reproduced at the scale for publication. These modifications were determined by printing out test versions of the map to see which changes, if any, were needed.

The second challenge was to adjust for different map projections. Almost every map used was drawn at a different projection or suffered some shrink-swell changes in the paper versions so that the state borders could not be perfectly overlaid. Figure 1 shows an example. Two maps are overlain: the Davies *et al.* (1984) map and the new AGI karst map drawn on a different projection of the US state borders (the projection type was not determined). The maps are registered to match the state borders in the Yellowstone area at the junction of Idaho, Montana, and Wyoming. In southwestern Wyoming, the borders are slightly off. As the nearby southern Idaho border sweeps westward past that state, it is off by nearly 30 km where it reaches California. In addition to the discrepancies in the borders, the differences in the karst areas are also apparent. The color areas reflect the karst areas traced from the older map and show them offset from those areas which are shown in black and white. The new karst map had to continually be shifted and registered in different locations relative to the older scanned maps, and only the karst areas immediately adjacent to the registered areas were then traced.

The third and more difficult challenge was to determine which karst boundary to follow when Davies *et al.* (1984) differed from other karst maps. The greatest discrepancy occurred in Wyoming, as illustrated in Figure 2. The black and white map shows the karst boundaries drawn by Davies *et al.* (1984) and the color boundaries are based on Hill, Sutherland, and Tierney (1976). While there is perfect concordance in the Black Hills area, the north-central and western parts of the state show moderate differences, and the southeastern area shows little in common between the two maps. In the case of Wyoming and other areas where I lack personal knowledge of local karst development, I did what research I could to determine which map is most likely correct and generally defaulted to the local experts who should know their areas best.

The fourth and greatest challenge was to define undefined karst areas. More precisely, I defined pseudokarst areas. Karst areas were usually delineated on lithology where it is safe to assume that most mapped carbonates and evaporites produce karst. However, the chances of pseudokarst being present in volcanic rocks and unconsolidated sediments are far lower, so such generalizations could not be made. Richards (unpub. data, 1999) provided helpful maps of volcanic pseudokarst in Hawaii, which I supplemented from maps of cave locations in other areas of the state. Bernie Szukalski (pers. comm., 2000;

2001) sent information on two unconsolidated pseudokarst areas that have recently been found by cavers in southern California. Their extents have not been well delineated, so using geologic and other maps plus Szukalski's descriptions, I conservatively delineated those areas. Cavers exploring those areas in the future will determine how well I estimated the boundaries.

When I finished drawing the map, I drew in some lines pointing to various locations around the country and added text that discussed some unique or important aspect of those areas. In order to show the diversity of karst and its importance nationwide, I sought a variety of examples and topics. I then added the following explanation and caveat, which is important to repeat here:

This map is a general representation of U.S. karst and pseudokarst areas. While based on the best available information, the scale does not allow detailed and precise representation of the areas. Local geologic maps and field examination should be used where exact information is needed. Karst features and hydrology vary from place to place. Some are highly cavernous, and others are not. Although most karst is exposed at the land surface, some is buried under layers of sediment and rock, yet still affects surface activities.

The final step in producing the map was to send it to AGI for the final graphics work. They turned it over to graphics artist Julie DeAtley of DeAtley Design. She added background color to the map, created a shadow effect, created and/or laid out the legend, caption, and other text, and used an actual rock photograph to fill in and color the letters "karst" in the title. In June 2001, the map was published in the *Living with karst* booklet as shown here in Figure 3.

FUTURE MAPPING OF US KARST

Having recently completed the AGI karst map, I state without reservation that it is an improvement over the previous map by Davies *et al.* (1984), yet it needs to be redone. The new map is deficient in five main areas.

1. "Karst" is not defined. While most outcrops of carbonate rocks can correctly be assumed to form karst, there are some areas where the presence of karst is arguable. A standard definition of karst needs to be defined and applied. For example, Worthington, Schindel, and Alexander (2001) propose the use of six specific testable properties to differentiate karst aquifers from porous media aquifers: tributary flow to springs, turbulent flow in conduits, troughs in the potentiometric surface, downgradient decreases in hydraulic gradient, downgradient increases in hydraulic conductivity, and substantial scaling effects in hydraulic conductivity. Clear and testable defining criteria should be established and applied in karst mapping.

2. "Pseudokarst" is not defined. Like karst, criteria for pseudokarst should be defined. For example, is there a sufficient density of pseudokarst features in the southern Great Plains to justify the large unconsolidated pseudokarst areas shown in Figure 3, or should those areas be shrunk to smaller

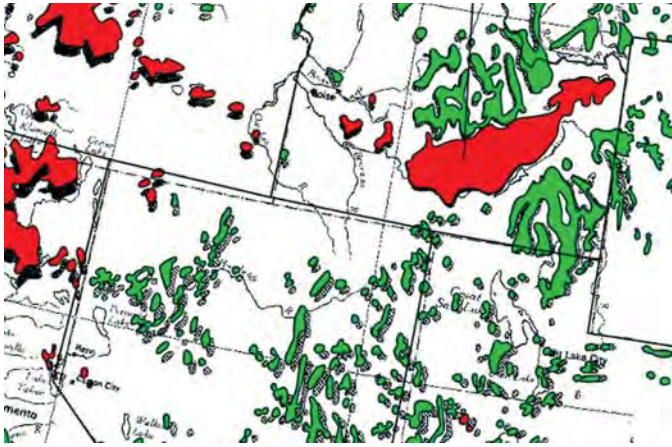


Figure 1. Projection differences in two overlaying maps become significant with increased distance from the Yellowstone area where they are aligned.

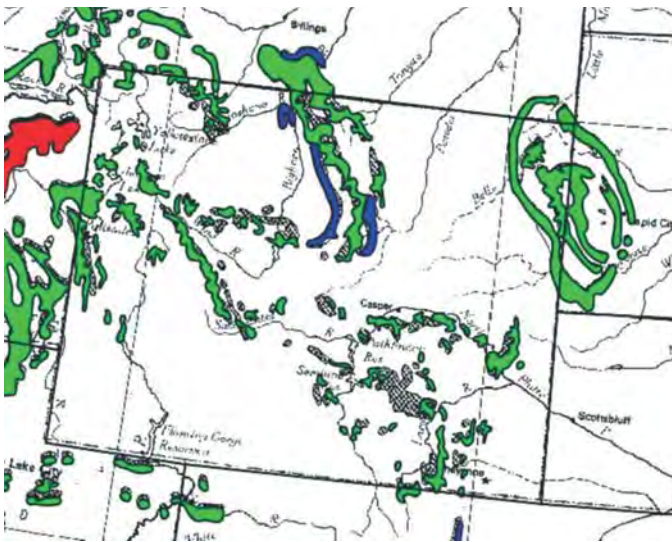


Figure 2: Two maps of Wyoming karst show considerable differences, producing a challenge to determine which map is correct.

areas where pseudokarst features are known to exist? Should the map illustrate the potential for pseudokarst or the known existence of pseudokarst? If the map will illustrate the potential for pseudokarst, that must also be defined in a clear and testable manner that is useful to scientists, land managers, and cavers, and not misleading in its implications for the potential development of pseudokarst.

3. Karst and pseudokarst boundaries are not precisely mapped. The boundaries shown in Figure 3 are generalizations and while often close, do not precisely delineate those areas. Approximations will always be made according to the scale of mapping, but greater precision is possible at the scale of Figure 3 (reduced from its original size for publication here).

4. Precise adjustments are needed for differences in map projections. Figure 3 was developed by manually shifting maps to adjust for differences in map projections or irregularities. Consequently, some areas are more precisely drawn than others. Computer programs are available and should be used to automatically and properly adjust for projection differences and to uniformly correct for other irregularities.

5. Pseudokarst and buried karst areas are underrepresented. While careful mapping in the future will reveal karst areas not previously included, the biggest changes will be in the representation of pseudokarst and buried karst areas. Numerous unconsolidated and volcanic pseudokarst areas occur for which I could not find sufficient information to add them to Figure 3. Martinez, Johnson, and Neal (1998) found evaporites, especially buried evaporites, underlying 35-40% of the 48 contiguous US states. This is far less than shown in Figure 3, and certain generalizations in their mapping prevented their inclusion in Figure 3. One aspect of buried karst that needs to be defined is the depth of burial that will be considered for mapping. The depth should be sufficient to include the reasonable potential for subsidence or other land management problems to occur.

The USGS proposed development of a national karst map in 2001 (Epstein *et al.* 2001) and has begun that work. The map may be digitally prepared and include hot-links to references of detailed source maps, generalized descriptions of the karst areas, reports on the effects of karst on land management, summaries of the geology and karst features in selected areas, and annotated bibliographies for those areas. Features that may be included on the map are exposed carbonate and evaporite units, intrastratal karst, karst beneath surficial overburden, and percentage area covered by karst. This USGS report was presented during a Project KarstMap symposium at the 2001 NSS Convention. The members of the NSS Section of Cave Geology & Geography, USGS, National Cave and Karst Research Institute, and National Park Service have since met to pursue developing a complete and accurate karst map of the US. This should prove a fruitful association; the federal agencies have the resources to develop a fine and accessible map and the NSS has the expertise to evaluate the accuracy of the karst areas they delineate.

Based on my experience, especially from developing the AGI karst map and association with Project KarstMap, I offer the following recommendations:

1. Define terms and parameters. The first task in developing a karst map should define karst and pseudokarst, identify the intended audience for the map, and set the scale, level of details, and other map parameters accordingly.

2. Consult experts to ensure completeness. Karst experts from around the country should be consulted to draw or evaluate the proposed boundaries for highest accuracy and precision in the states or regions where they have expertise. This will greatly reduce the chance for errors and help ensure that important areas are not overlooked.

U.S. Karst Map

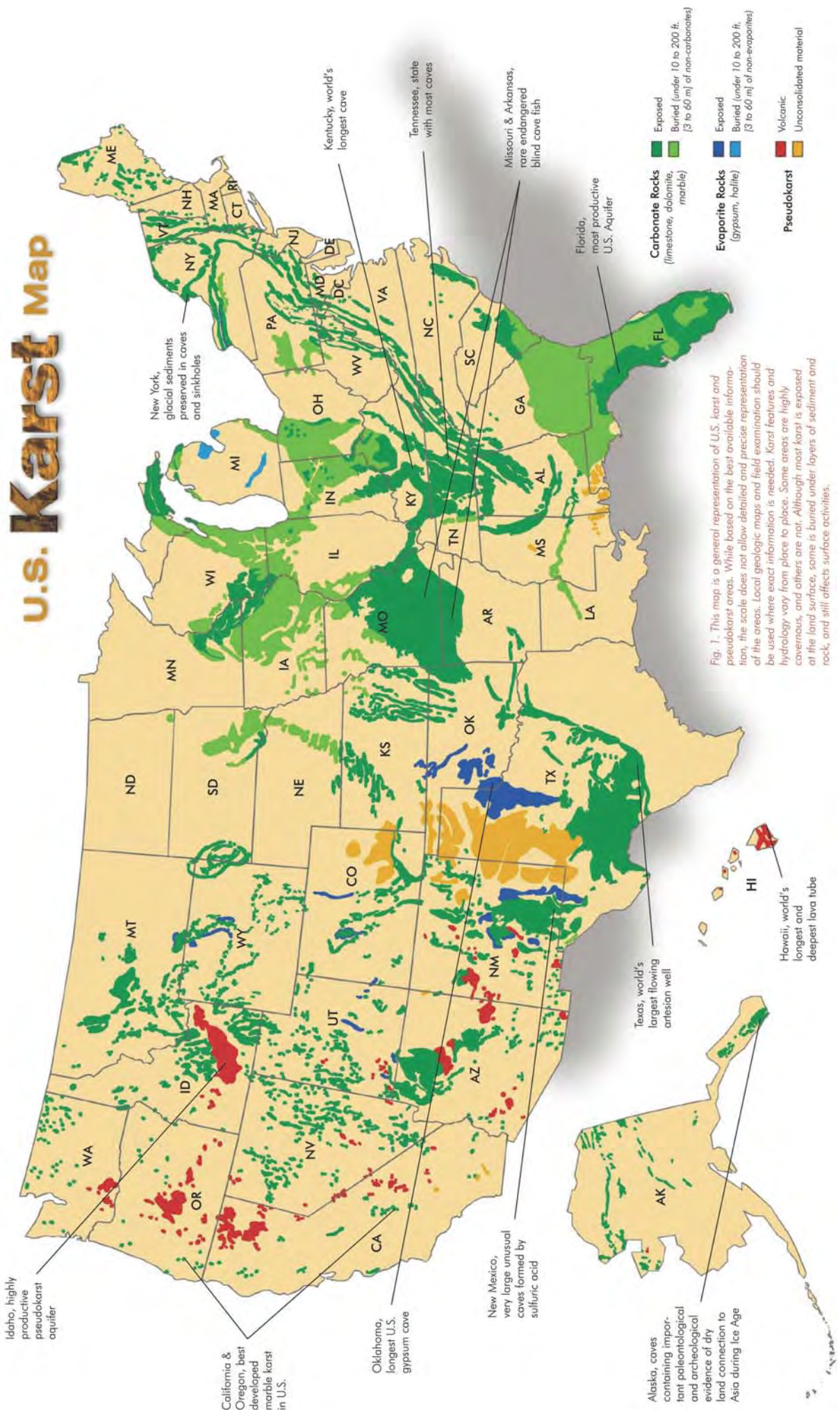


Figure 3: Karst map of the US published by AGI (Veni et al. 2001).

3. Keep it simple but versatile. The map should be prepared in simple layers identifying major karst types and their distribution. Detailed geologic information should be available in other graphic layers and/or as hot-linked text. The layering should allow development of personalized maps according to individual needs to show as many or as few layers and spatial relationships as desired. The map should be drawn as vectorized images to allow sharp enlargement and reduction of the map scale without needing to redraft it.

4. Link to specialty maps. Drainage basin, land management, and other specialty maps should be left to state and regional agencies, which in many cases are currently conducting the detailed research needed to develop those maps. However, those maps should be hot-linked to the karst map and the karst map updated as needed based on their results.

5. Keep it current and accessible. The proposed digital format of the karst map should allow easy updating to correct for errors or new information. The USGS is currently only discussing the illustration of karst on their new map, but pseudokarst areas and other information could be drawn on separate digital layers to continuously update and improve the map over time. With the increasing national interest in karst, the map should be well publicized and made easily accessible on compact disk and through the Internet.

ACKNOWLEDGMENTS

I thank the following people: William B. White for conceiving and promoting Project KarstMap; AGI and Julie Jackson for prompting me to develop a new U.S. karst map; Julie DeAtley of DeAtley Design for making my bland karst map look good in print; the USGS for recognizing the need for a new karst map, taking the lead in that effort, and working with the NSS to ensure that it will be a high quality product; three anonymous reviewers for their helpful comments; and Karen Veni for proofreading my manuscript and her unfailing support.

REFERENCES

- Daniel, T.W., Jr. & Coe, W.D., 1973, Exploring Alabama caves. Bulletin 102, Geological Survey of Alabama, 99 p.
- Davies, W.E., Simpson, J.H., Ohlmacher, G.C. Kirk, W.S. & Newton, E.G., 1984, Engineering aspects of karst, national atlas, 38077-AWNA-07M-00, 1 sheet p.
- Elliott, W.R. & Veni, G., 1994, The caves and karst of Texas. National Speleological Society Convention Guidebook: Huntsville, Alabama, 342 pp. + 13 pls. p.
- Epstein, J.B., Orndorff, R.C. & Weary, D.J., 2001, U.S. Geological Survey national karst map [abs]: National Speleological Society Convention Program Guide, Great Saltpetre Cave Preserve, Kentucky, p. 87.
- Hill, C., Sutherland, W. & Tierney, L., 1976, Caves of Wyoming: Bulletin 59, Geological Survey of Wyoming, 230 p.
- Martinez, J.D., Johnson, K.S. & Neal, J.T., 1998, Sinkholes in evaporite rocks: American Scientist, v. 86, no. 1, p. 38-51.
- McGill, W.M., 1933, Caverns of Virginia. Bulletin 35, Educational series no. 1, State Commission on Conservation and Development, Commonwealth of Virginia, 187 p.
- Moore, G.W. & Sullivan, G.N., 1978, Speleology: The study of caves: Teaneck, New Jersey, Zephyrus Press, 150 p.
- Powell, R.L., 1961, Caves of Indiana. Circular No. 8, Geological Survey, Indiana Department of Conservation, 127 p.
- Quick, P., 1979, Cave formation in western new England, An introduction to caves of the northeast: National Speleological Society 1979 convention guidebook, p. 9-10.
- Smith, A.R., 1971, Cave and karst regions of Texas, in Lundelius, E.L. & Slaughter, B.H., ed., Natural history of Texas caves, p. 1-14.
- Smith, A.R. & Veni, G., 1994, Karst regions of Texas, The caves and karst of Texas, National Speleological Society 1994 convention guidebook, p. 7-12.
- Szukalski, B., 2001, Cave development in Rainbow Basin National Natural Landmark [abs]: National Speleological Society convention program guide, Great Saltpetre Cave Preserve, Kentucky, p. 74.
- Veni, G., DuChene, H., Crawford, N.C., Groves, C.G., Huppert, G.H., Kastning, E.H., Olson, R. & Wheeler, B.J., 2001, Living with karst: a fragile foundation. Environmental awareness series, American Geological Institute, 64 pp. + 1 pl.
- Vineyard, J.D., 1997, Missouri, the cave factory: An introduction to the geology of Missouri: Exploring Missouri caves, National Speleological Society 1997 convention guidebook, p. 27-45.
- Weldon, M.B., Szumigala, D.J. & Davidson, G., 2000, Generalized geologic map of Alaska. Alaska Geological and Geophysical Surveys, 1 sheet p.
- White, W.B., 2001, The karstmap project: progress and status [abs]: National Speleological Society convention program guide, Great Saltpetre Cave Preserve, Kentucky, p. 86.
- Worthington, S.R.H., Schindel, G.M. & Alexander, E.C. Jr., 2001, Hydraulic characterization of carbonate aquifers focusing on water level data [abs]: National Speleological Society convention program guide, Great Saltpetre Cave Preserve, Kentucky, p. 87.

THE DEVELOPMENT OF A KARST FEATURE DATABASE FOR SOUTHEASTERN MINNESOTA

YONGLI GAO, E. CALVIN ALEXANDER, JR.

Department of Geology & Geophysics, University of Minnesota, Minneapolis, MN 55455 USA, gaox0011@tc.umn.edu

ROBERT G. TIPPING

Minnesota Geological Survey, 2642 University Ave., St. Paul, MN 55114 USA

A karst feature database of southeastern Minnesota has been developed that allows sinkhole and other karst feature distributions to be displayed and analyzed across existing county boundaries in a geographic information system (GIS) environment. The central Database Management System (DBMS) is a relational GIS-based system interacting with three modules: GIS, statistical, and hydrogeologic modules. Data tables are stored in a Microsoft Access 2000 DBMS and linked to corresponding ArcView shape files. The current Karst Feature Database of Southeastern Minnesota was put on a Windows NT server accessible to researchers and planners through networked interfaces.

Initial spatial analyses and visualizations of karst feature distributions in Southeastern Minnesota were conducted using data extracted from the karst feature database. A series of nearest-neighbor analyses indicates that sinkholes in southeastern Minnesota are not evenly distributed (i.e., they tend to be clustered). ArcInfo, ArcView and IRIS Explorer™ were used to generate a series of 2D and 3D maps depicting karst feature distributions in southeastern Minnesota using data exported from the GIS-based karst feature database. The resulting maps allow regional trends to be visualized and extend county-scale trends to larger state-wide scales.

Southeastern Minnesota is part of the Upper Mississippi Valley Karst (Hedges & Alexander 1985) that includes southwestern Wisconsin and northeastern Iowa. Karst lands in Minnesota developed in Paleozoic carbonate and sandstone bedrock. A significant sandstone karst has developed in Pine County (Shade *et al.* 2000). Most surficial karst features, such as sinkholes, are only in those areas with less than 50 ft (~15 m) of sedimentary cover over bedrock surface (Fig. 1). Few scientific descriptions of the Upper Mississippi Valley Karst exist. Nevertheless, the karst lands of southeastern Minnesota present an ongoing challenge to environmental planners and researchers and have been the focus of a series of research projects and studies for over 30 years.

Since the early 1980s, the Minnesota Geological Survey and Department of Geology and Geophysics at the University of Minnesota have been mapping karst features and publishing various versions of their results in the form of 1:100,000 scale County Geologic Atlases. In the mid-1990s, the Minnesota Department of Natural Resources was assigned responsibility for the hydrogeology portions of the County Atlases and is now responsible for the karst mapping. Dalgleish and Alexander (1984a), Alexander and Maki (1988), Witthuhn and Alexander (1995), Green *et al.* (1997), Shade *et al.* (2001), and Tipping *et al.* (2001) published sinkhole distribution maps for Winona, Olmsted, Fillmore Counties, Leroy Township, Pine and Wabasha Counties respectively. Published atlases of Washington, Dakota, and the counties of the Twin Cities Metro area contain limited information on sinkhole occurrences.

As geographic information systems, (GIS), global positioning systems, and web tools became more accessible to resource

managers in the 1990s, the need for a state-wide, Web-accessible, and GIS-compatible karst feature base has become increasingly evident. Several factors hindered the development of this database. Karst features have not been inventoried in significant areas. Where data exist, they are often decades old and exist as difficult to obtain paper copies in researchers' files. Several generations of students and workers have gathered the data, and the format, quality, and completeness vary greatly. The data were organized into county databases and incompatibilities between adjacent counties were introduced. All of these challenges only serve to emphasize the need for state-wide data sets and, indeed, for interstate compilations.

A successful model for such a database already exists in Minnesota. The Geological Survey's County Water-Well Index (CWI) successfully supplies current users with readily accessible information about Minnesota's millions of water wells while continually updating and improving the database and delivery system. The Database Management System (DBMS) we are building builds on the lessons that have been learned from the CWI project. Experts in GIS, computer science and geology have constructed a karst feature GIS database that displays and allows analysis of sinkhole and other karst feature distributions across existing county boundaries. The ongoing research focused on the management of the GIS-based Karst Feature Database of Southeastern Minnesota, statistical analysis of karst feature distribution and sinkhole formation, and 2D and 3D visualization of karst feature distribution in southeastern Minnesota.

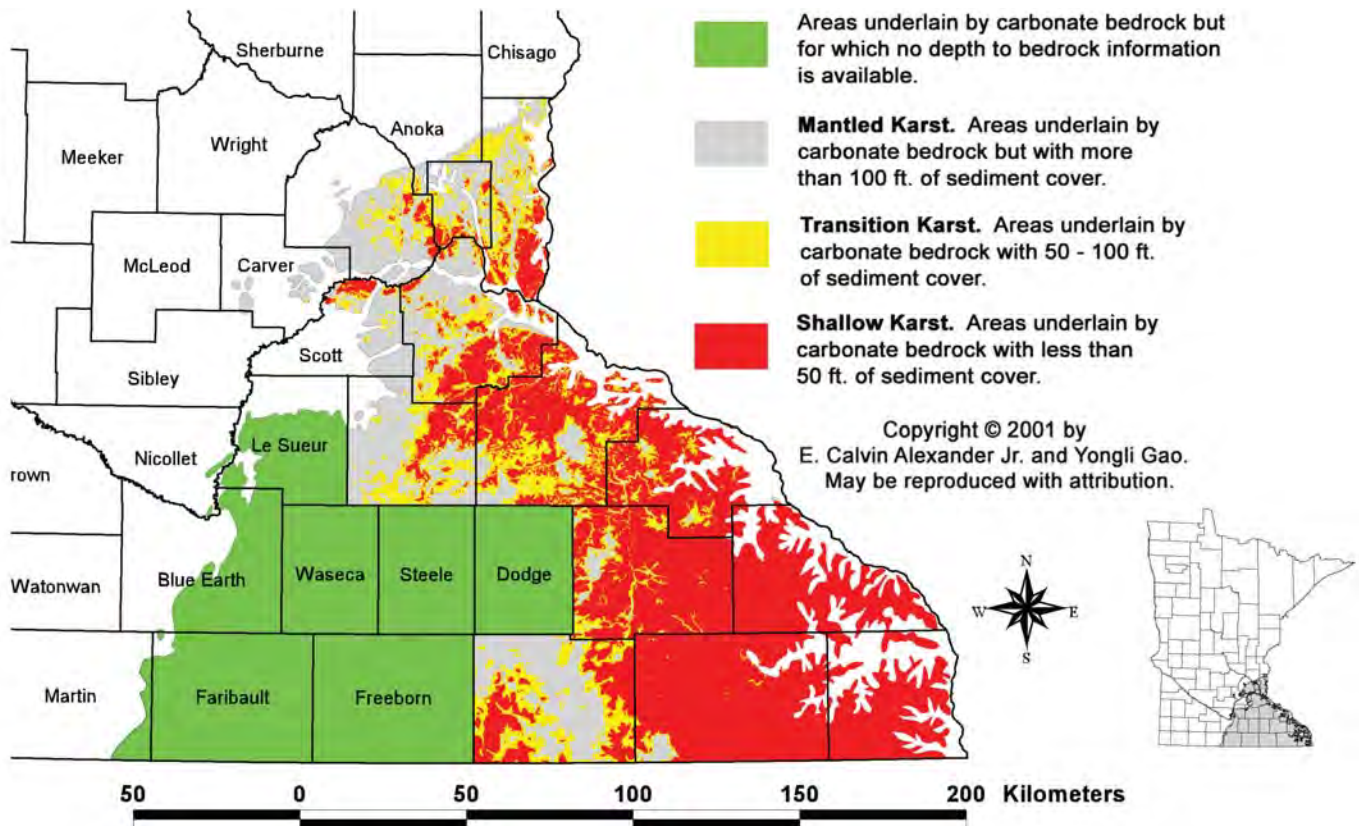


Figure 1. Minnesota Karst Lands. This map overlays the areas with < 50 feet, 50 to 100 feet, and > 100 feet of surficial cover over the areas underlain by carbonate bedrock. Featureless green counties in the southwestern portion of this map are underlain by carbonate bedrock but the depth to bedrock has not mapped with sufficient accuracy to draw informative maps. This map emphasizes the patchy nature of the thick sediment cover and the importance of site-specific information for land-use decisions.

RESEARCH GOALS

This research integrated geology, groundwater hydrology, statistics, GIS, and DBMS to study karst feature distribution in southeastern Minnesota. The main goals of this interdisciplinary research are: 1) to look for large-scale patterns in the sinkhole distribution; 2) to conduct statistical tests of hypotheses about the formation of sinkholes; 3) to create Web-accessible management tools for land-use managers and planners; and 4) to deliver geomorphic and hydrogeologic criteria for making scientifically valid land-use policies and decisions in karst areas of southeastern Minnesota.

RESEARCH APPROACH

Existing county and sub-county karst feature datasets have been assembled into a large GIS-based database capable of analyzing the entire data set. Figure 2 illustrates the logical design of the Karst Feature DBMS of Southeastern Minnesota. The central DBMS is a relational GIS-based system interacting with three modules: GIS, statistical, and hydrogeologic modules. The GIS module uses ArcInfo and ArcView to manipulate spatial transformation and map generation. The statistical

module is used to analyze and test karst feature distribution and hypothesis about the formation of sinkholes. The hydrogeologic module helps to understand groundwater flow and solute transport in carbonate aquifers and investigate the hydrogeologic controls on the sinkhole distribution. As can be seen in Figure 2, the three modules and the central DBMS are interconnected to each other instead of standing alone. A series of software packages have been developed in the last decade to integrate two or three modules in Figure 2. For example, a “close coupling” between statistics package S-Plus and ArcInfo has been developed to conduct both GIS and statistical processes (Trevor 1995).

DBMS AND GIS MODELING

GIS-based DBMS have been widely used to manage and analyze karst features on both regional and national scales (Denizman 1997; Kochanov & Kochanov 1997; Whitman & Gubbels 1999; Cooper *et al.* 2001; Lei *et al.* 2001). The databases used in this research have been built over the past 20+ years. The most complete sinkhole database was constructed by Dalglish and Alexander (1984b), and updated by Magdalene and Alexander (1995) using spreadsheet format for

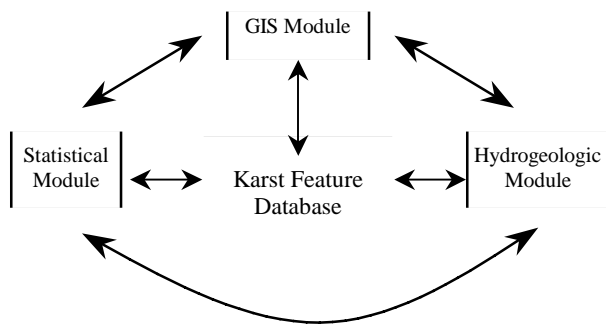


Figure 2. Logic design of Minnesota Karst Feature Database. See Figure 3 for the logical design of the central Karst Feature Database.

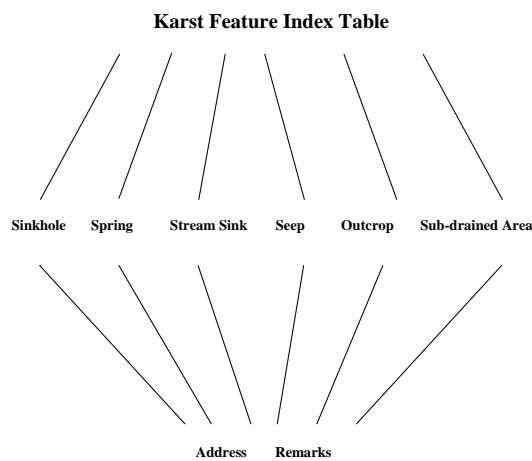


Figure 3. Database Structure of the Karst Feature Database of Southeastern Minnesota (Updated from Gao *et al.*, 2001). The top level karst feature index table stores basic and location information for each karst feature. The middle level tables, sinkhole - sub-drained area, store specific information for different features. The bottom level tables, address and remarks store owners' address and additional comments of each karst feature. See Figure 6 and 7 for applications built upon this structure.

Winona County. That inventory continues to be the model for subsequent work.

Existing county and sub-county sinkhole databases have been assembled into a large GIS-based relational database capable of analyzing the entire data set. Several other karst features in Winona County, including springs, seeps, and outcrops, have been mapped and entered into the Karst Feature Database of Southeastern Minnesota. The Karst Feature Database of Winona County is being expanded to include all the mapped karst features of southeastern Minnesota. Figure 3 illustrates the design and relationships of the Karst Feature Database of southeastern Minnesota. Tables are stored in a Microsoft Access 2000 DBMS and linked to corresponding

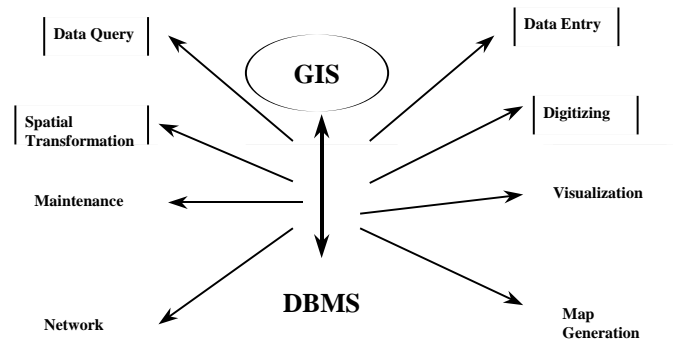


Figure 4. Applications built for GIS-based DBMS. See Figures 6 and 7 for examples of data entry, digitizing, and editing interfaces

ArcView shape files. A Karst Feature Index Table, primary table of the database, has a series of one to many and 1-to-1 cascading downward relationships to the other data tables. Codes are stored in a separate database and are accessed by Structured Query Language (SQL) requests. The code database contains lookup tables for code types. Code types are numerous, but cover all field entries where a specific text value is required. Examples would be fields such as quadrangle, stratigraphy, and surface strata. Figure 6 shows some of the codes used for sinkhole data represented by pull-down menus. Users can click the arrows of those pull-down menus and get the definitions of the codes used for different attributes. Using codes in this database significantly reduces storage space and improves performance of applications built on the DBMS.

In order to make a secure database, only the database management administrator (DBA) has the full-control permission to access all data and codes of the karst feature database. Other users will be assigned different permissions to access the database through different interfaces. Figure 4 shows some applications built for the central DBMS and the GIS module. These interfaces were written in Visual Basic, ArcInfo AML, and ArcView Avenue programming languages to interact with the karst feature database.

Most of the karst feature datasets of Southeastern Minnesota were inventoried as paper files and/or surveyed and marked on USGS 1:24,000 topographic maps (Fig. 5). Figure 5a is a paper-file record of a spring (ID number is MN85:A0261) in Lewiston, Winona County. This spring, also marked on a USGS 1:24,000 topographic map (Fig. 5b), was surveyed and recorded on April 26, 1986. Since some existing karst feature datasets are in either paper-file format or marked on topographic maps, two kinds of interfaces were created to enter and manipulate these two different dataset formats. One set of interfaces was written in Visual Basic programming language and linked to the Karst Feature Database under Microsoft Access 2000 DBMS. These interfaces were used to process karst feature records in paper-file format. The other set of interfaces was written in ArcView Avenue programming language and linked to the Karst Feature Database under

SPRING DATA SHEET

MSS No. MN 85: A0261 Name Baynton Seeps South
 County Winona Quad Lewiston
 Location SW/SW/NW/SW/NE/NE Sec 7, T 10S N, R 8 W
AACBCC (MGS)
 Owner Baynton

 _____ Telephone Number _____

Physical Parameters
 Elevation 900' Formation Jordan
 Flow _____ date _____
 _____ date _____
 Temp 12.3°C date 4/27/86
 _____ date _____

Misc: _____

Chemical Parameters
 pH _____ date _____ Turb _____ date _____
 _____ date _____ _____ date _____
 cond _____ date _____ Others _____ date _____
 _____ date _____ NO_3^-N 1.26±0.07 ppm date 4/27/86
 D.C. _____ date _____ _____ date _____
 _____ date _____ _____ date _____

Comments: _____

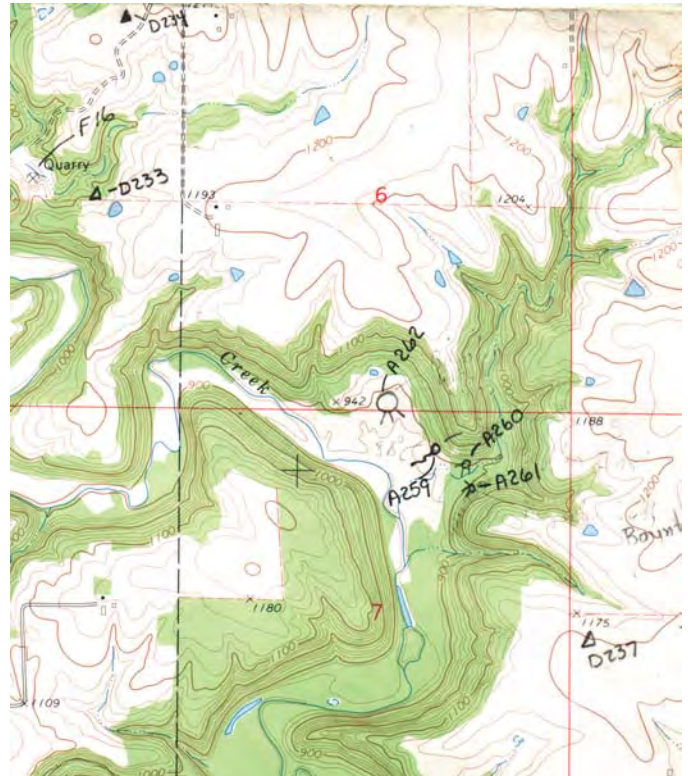


Figure 5a (left). Karst features recorded in a paper data sheet format. **Figure 5b (right).** Karst features compiled on USGS 1:24,000 topographic maps. This example is from the Lewiston Quadrangle, Minnesota - Winona Co., 7.5 minute series topographic map, 1974. The area of section 6 is 1 square mile.

ArcView 3.2 environment. These interfaces were used to process karst feature records surveyed and stored on topographic maps. Both kinds of interfaces would allow users to enter, edit, and query karst feature data stored in the karst feature database.

Figure 6 illustrates a data-entry interface for karst features in paper-file format. “BASE INFO” and “POSITIONING” in Figure 6 correspond to the top-level karst feature index table on Figure 3. The tabs (Sinkhole – Remarks) at the bottom section of Figure 6 are linked to the lower level data tables specific for each karst feature and its owner’s address and additional remarks through sub-form interfaces. These sub-form tabs correspond to the lower level tables on Figure 3.

Figure 7 shows a digitizing-editing interface written in ArcView Avenue programming language. This interface was used under ArcView 3.2 environment and connected to our karst feature database. Users can digitize karst features based on their location on USGS 1:24,000 topographic map or USGS Digital Orthoquad (DOQ). If a user clicks the “save” button on the interface, a karst feature’s location information such as geographic coordinates, quadrangle, township, and range will be automatically entered into the database. Users can also enter or modify some base information of a karst feature such as organization, digitizer, program, and data type. This information will be saved into the karst feature database when the “save” button is clicked. In addition, users can adjust the loca-

tion of a karst feature and change some attributes of a karst feature through this interface.

Figure 6 demonstrates that information about a spring in Lewiston, Winona County, (see original data on Fig. 5a), is entered through the data entry interface. Figure 7 displays that users can find this spring and its corresponding USGS 1:24,000 topographic map through the digitizing-editing interface, which allows users to adjust the spring’s location and modify some attributes of the spring.

KARST FEATURE VISUALIZATION AND DISTRIBUTION DERIVED FROM THE KARST FEATURE DATABASE

Several 2D and 3D maps showing the relationships between sinkhole distribution and bedrock geology, depth to bedrock, surficial geology, and surface topography have been created using ArcInfo, ArcView, and IRIS Explorer™. Figure 1 shows one rendering of this combined data set. This map, compiled from a series of 1:100,000 scale depth to bedrock and bedrock topography datasets developed by Minnesota Geological Survey, emphasizes the patchy nature of the thick sediment cover and the importance of site-specific information for land-use decisions. Figure 8 shows sinkhole distributions across county boundaries on top of bedrock geology. Bedrock geology information was compiled from a series of 1:100,000 scale bedrock geology datasets published by Minnesota

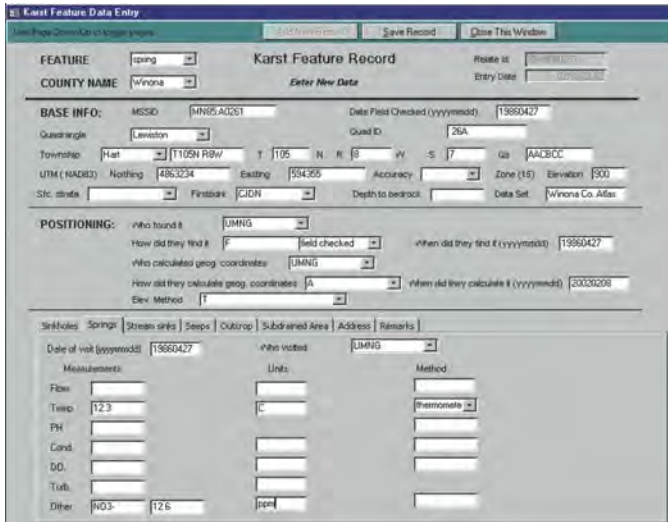


Figure 6. Data-entry interface written in Visual Basic programming language under Microsoft Access 2000 DBMS.

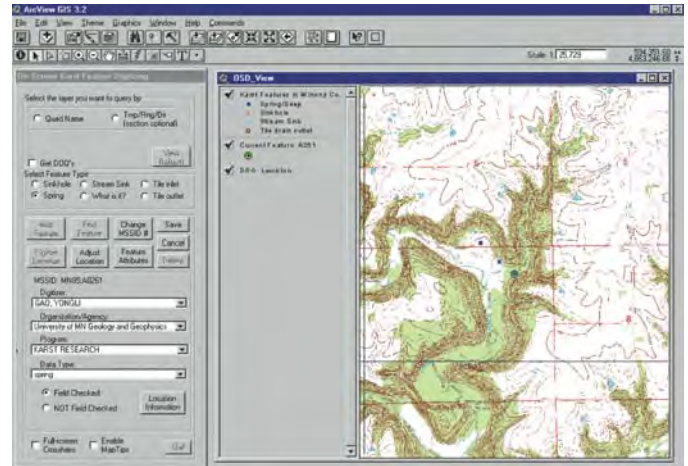


Figure 7. Digitizing-editing interface written in ArcView Avenue programming language under ArcView 3.2 environment. The background map is from the USGS Lewiston Quadrangle, Minnesota - Winona Co., 7.5 minute series topographic map, 1974.

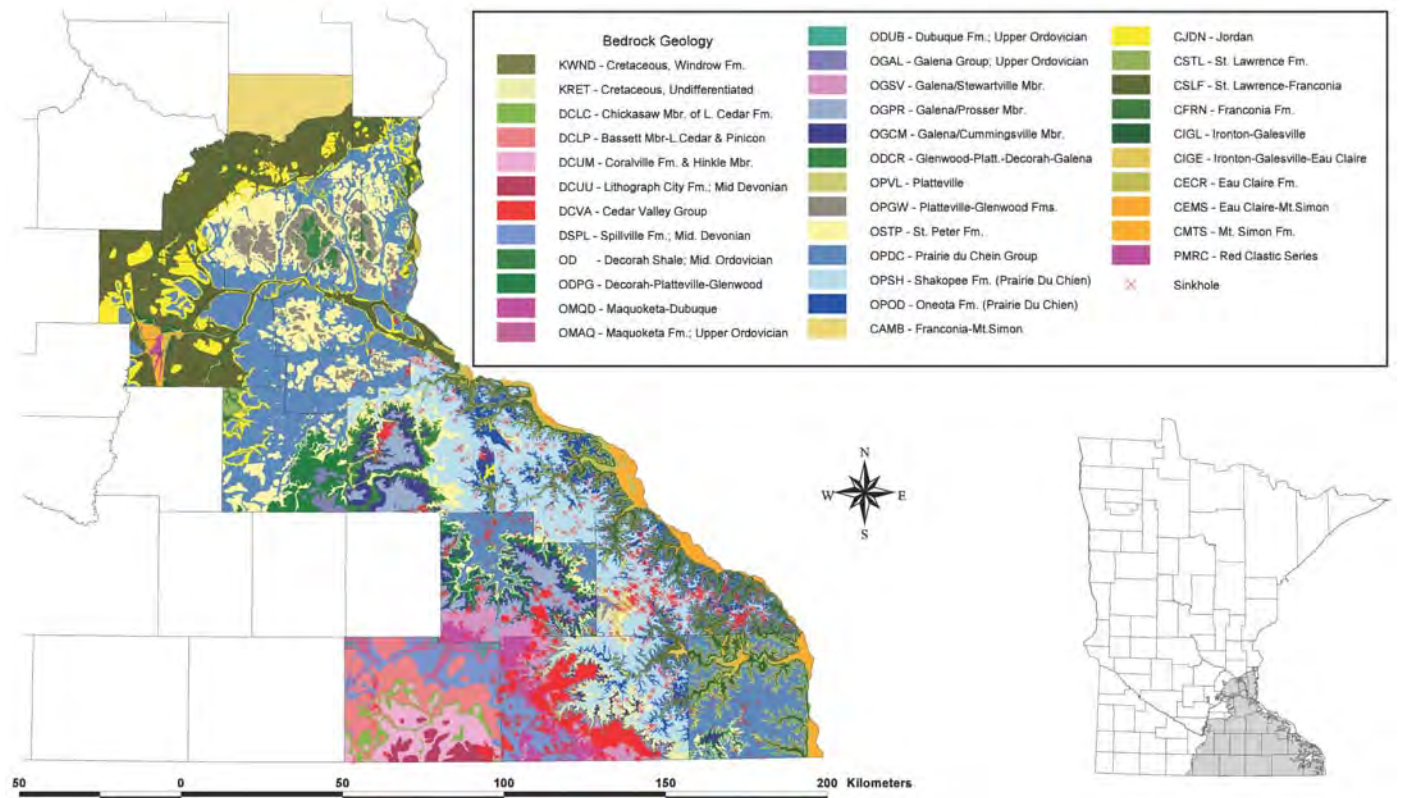


Figure 8. Sinkhole Distribution and Bedrock Geology of Southeastern Minnesota (Bedrock Geology information was compiled from 1:100,000 scale maps, Minnesota Geological Survey. Uncolored counties in the southwestern portion of this map have not been mapped with sufficient accuracy to draw informative bedrock geology maps.)

Geological Survey. A sinkhole dataset extracted from the karst feature database was superimposed on the bedrock geology map. The distributions of bedrock geology, depth to bedrock, and karst features form three bands of karst development that

are arranged parallel to the Mississippi River. These bands of karst features extend into and correlate with similar distributions in northeastern Iowa. These three bands comprise the Prairie du Chien, Galena/Spillville, and Cedar Valley Karsts.

Figure 9. Histograms and cumulative fractions of the nearest-neighbor distances of the three stratigraphically distinct populations of sinkholes in southeastern Minnesota. Note the radically different numbers of sinkholes on the vertical axes of the three graphs. There are 146 Cedar Valley sinkholes, 6,940 Galena/Spillville sinkholes, and 1,161 Prairie du Chien sinkholes in these statistical analyses (Gao and others, 2001).

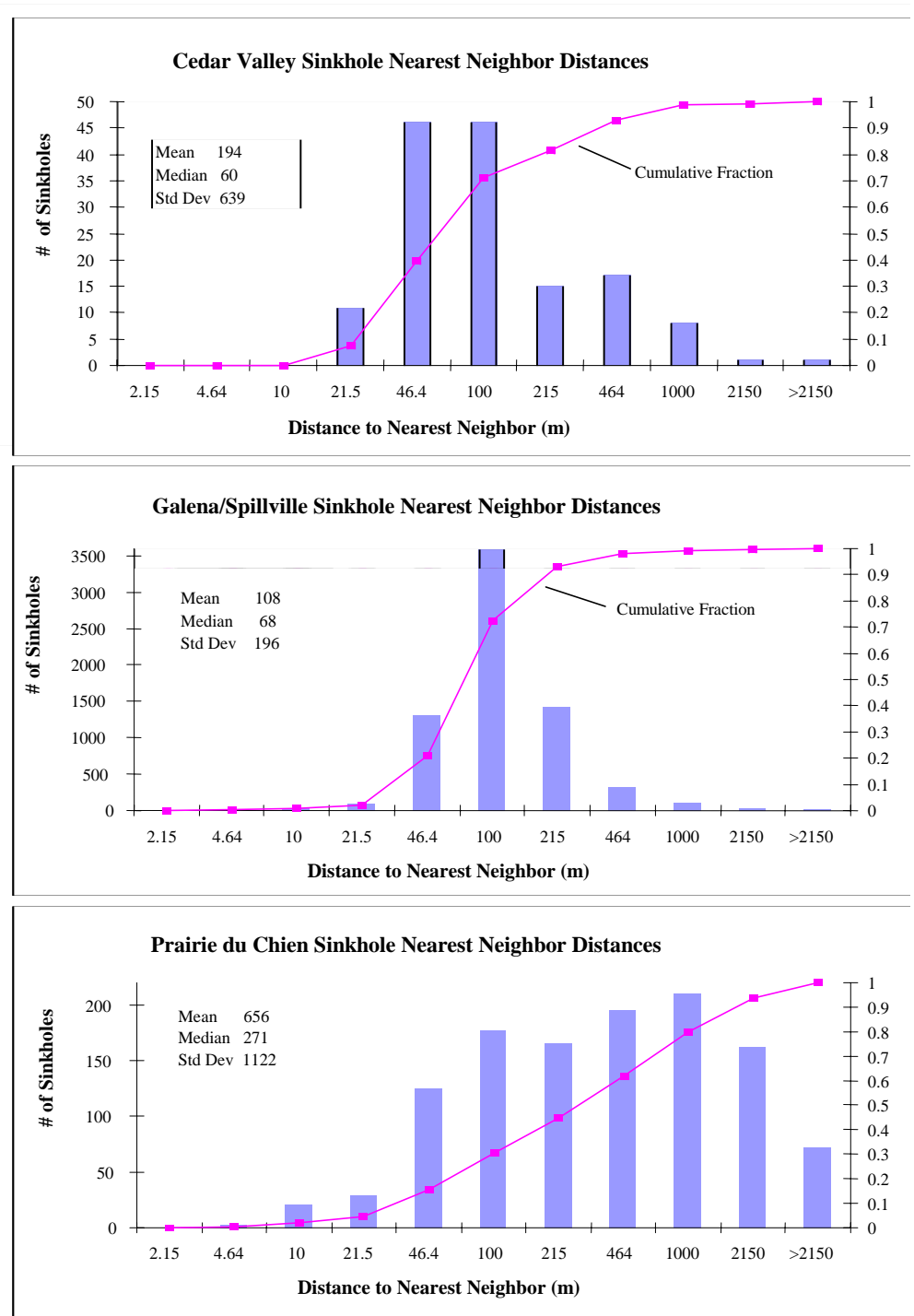


Figure 9 displays the histograms and cumulative fractions of the nearest-neighbor distances of the three sinkhole groups above. As can be seen in Figure 9, the median distance to the nearest neighbor is significantly less than the mean distance to the nearest neighbor of all the sinkhole groups. Our nearest-neighbor analyses on other sinkhole datasets all showed a highly skewed distribution. All the current nearest-neighbor analyses testify that sinkholes in southeastern Minnesota tend

to cluster. This result confirms and expands Magdalene and Alexander's (1995) conclusion of clustered sinkhole distribution in Winona County to the entire Minnesota dataset. Figure 9 also reveals that the sinkholes in the Prairie du Chien Karst are spaced about 3-5 times further apart than are the sinkholes in the Cedar Valley and Galena/Spillville Karst. This implies that more isolated sinkholes occur in Prairie du Chien Karst.

FURTHER STUDY

All current nearest-neighbor analyses demonstrate that sinkholes in southeastern Minnesota are not evenly distributed in this area. Additional statistical methods such as cluster analysis, probability estimation, correlation and regression will be implemented to study the spatial distributions of mapped karst features of southeastern Minnesota. The results of these spatial analyses will provide evidence for karst hazard assessment.

ACKNOWLEDGMENTS

This research was supported with funding from the Minnesota Department of Health. The databases used in this research have been built over the past 20+ years with support from The Legislative Commission on Minnesota Resources, Minnesota Department of Natural Resources and several counties. We thank Prof. Randall Barnes for the loan of his nearest-neighbor program and for many stimulating discussions of geostatistics. We acknowledge the assistance of Fuliang Li and Al Epp with the development of the interfaces built upon the karst feature database.

REFERENCES

- Alexander E.C., J., & Maki, G.L., 1988, Sinkholes and sinkhole probability, Geologic atlas of Olmsted County, Minnesota, County atlas series C-3: St. Paul, Minnesota, Minnesota Geological Survey, Plate 7.
- Cooper, A.H., Farrant, A.R., Adlam, K.A.M., & Walsby, J., 2001, The development of a national geographic information system (GIS) for British karst geohazards and risk assessment, in Beck, B.F., & Herring, J.G., ed., Geotechnical and environmental applications of karst geology and hydrology: Proceedings of the Eighth Multidisciplinary Conference on Sinkholes and the Engineering and Environmental Impacts of Karsts: Louisville, Kentucky, 1-4, April, A.A. Balkema, Lisse, p. 125-130.
- Dalgleish, J.D., & Alexander, E.C., Jr., 1984a, Sinkholes and sinkhole probability, in Balaban, N.H., & Olsen, B.M., ed., Geologic atlas of Winona County: County atlas series C-2: St. Paul, Minnesota, Minnesota Geological Survey, Plate 5.
- Dalgleish, J.D., & Alexander, E.C., Jr., 1984b, Sinkhole distribution in Winona County, Minnesota, in Beck, B.F., ed., Sinkholes: Their geology, engineering and environmental impact: Proceedings of the First Multidisciplinary Conference on Sinkholes, Orlando, Florida, 15-17 October: Boston, A.A. Balkema, p. 79-85.
- Davies, W.E., & Legrand, H.E., 1972, Karst of the United States, in Herak, M., & Stringfield, V.T., ed., Karst, important karst regions of the northern hemisphere: Amsterdam, Elsevier Pub Co., p. 466-505.
- Denizman, C., 1997, Geographic information systems as a tool in karst geomorphology: Abstracts with programs-Geological Society of America, v. 29, no. 6, p. 290.
- Dougherty, P.H., Jameson, R.A., Worthington, S.R.H., Huppert, G.N., Wheeler, B. J., & Hess, J. W., 1998, Karst regions of the eastern United States with special emphasis on the Friars Hole Cave System, in Yuan D., L., Z., ed., Global karst correlation: Beijing, Science Press, p. 137-155.
- Gao, Y., Alexander, E.C. Jr., & Tipping, R.G., 2001, Application of GIS technology to study karst features of southeastern Minnesota, in Beck, B.F., & Herring, J.G., ed., Geotechnical and environmental applications of karst geology and hydrology: Proceedings of the Eighth Multidisciplinary Conference on Sinkholes and the Engineering and Environmental Impacts of Karsts, Louisville, Kentucky, 1-4, April, A.A. Balkema, Lisse, p. 83-88.
- Green, J.A., Mossler, J.H., Alexander, S.C., & Alexander, E.C., Jr., 1997, Karst hydrogeology of Le Roy Township, Mower County, Minnesota, Minnesota Geological Survey open file report 97-2, scale 1:24,000: St. Paul, MN, 2 plates.
- Hedegs, J., & Alexander, E.C., Jr., 1985, Karst-related features of the upper Mississippi Valley Region: Studies in Speleology, v. 6, p. 41-49.
- Kochanov, W.E., & Kochanov, J.S., 1997, Land management practices using a relational database: the Pennsylvania sinkhole inventory: Geological Society of America, Northeastern Section, 32nd annual meeting, v. 29, no. 1, p. 59.
- Lei, M., Jiang, X., & Li, Y., 2001, New advances of karst collapse research in China, in Beck, B.F., & Herring, J.G., ed., Geotechnical and environmental applications of karst geology and hydrology: Proceedings of the Eighth Multidisciplinary Conference on Sinkholes and the Engineering and Environmental Impacts of Karsts, Louisville, Kentucky, 1-4, April: A.A. Balkema, Lisse, p. 145-152.
- Magdalene, S., & Alexander, E.C., Jr., 1995, Sinkhole distribution in Winona County, Minnesota revisited, in Beck, B.F., & Person, F.M., ed., Karst geohazards: Proceedings of the Fifth Multidisciplinary Conference on Sinkholes and the Engineering and Environmental Impact of Karst, Gatlinburg, Tenn., 2-5 April, 1995: A.A. Balkema, Rotterdam, p. 43-51.
- Shade, B.L., Alexander, S.C., Alexander, E.C., Jr., & Truong, H., 2000, Solutional processes in silicate terranes: True karst vs. pseudokarst with emphasis on Pine County, Minnesota [abs]: Abstracts with programs: 2000 GSA annual meeting, v. 32, no. 7, p. A-27.
- Shade, B.L., Alexander, S.C., Alexander, E.C., Jr., & Martin, S., 2001, Sinkhole distribution, Depth to bedrock, and bedrock topography, Geologic atlas of Pine County, Minnesota, County atlas series C-13: St. Paul, MN, Minnesota Geological Survey, Plate 6.
- Storck, P., Bowling, L., Wetherbee, P., & Lettenmaier, D., 2000, Application of a GIS-based distributed hydrology model for prediction of forest harvest effects on peak stream flow in the Pacific Northwest, in Gurnell, A.M., & Montgomery, D.R., ed., Hydrological applications of GIS: Chichester, John Wiley and Sons, p. 69-83.
- Tipping, R.G., Green, J.A., & Alexander, E.C., Jr., 2001, Karst features, Geologic atlas of Wabasha County, Minnesota, County atlas series C-14: St. Paul, Minnesota, Minnesota Geological Survey, Plate 5.
- Trevor, B.C., 1995, Interactive spatial data analysis: New York, J. Wiley, 413 p.
- Troester, J.W., & Moore, J.E., 1989, Karst hydrogeology in the United States of America: Episodes, v. 12, no. 3, p. 172-178.
- Whitman D., G., T., 1999, Applications of GIS technology to the triggering phenomena of sinkholes in central Florida, in Beck, B.F., Pettit A.J., & Herring G.J., ed., Hydrogeology and engineering geology of sinkholes and karst: Proceedings of the Seventh Multidisciplinary Conference on Sinkholes and the Engineering and Environmental Impacts of Karst, Harrisburg-Hershey, Penn., 10-14 April, A.A. Balkema, Rotterdam, p. 67-73.
- Witthuhn, M.K., & Alexander, E. C., Jr., 1995, Sinkholes and sinkhole probability, Geologic atlas of Fillmore County, Minnesota, County atlas series C-8: St. Paul, MN, Minnesota Geological Survey, Plate 8.

KARST GIS ADVANCES IN KENTUCKY

LEE J. FLOREA, RANDALL L. PAYLOR

Kentucky Speleological Survey Inc., 228 Mining and Mineral Resources Building, Lexington, KY 40506 USA, LJF: mr_chaos@hotmail.com

LARRY SIMPSON

3870 Beihl Ave., Cincinnati, OH 45248 USA

JASON GULLEY

Department of Earth and Atmospheric Sciences, Purdue University West Lafayette, IN 47907 USA

Little statewide geospatial data was available for Kentucky caves and karst in the past. Recent trends in land development have prompted a distinct need for these data in order to help minimize impact to cave and karst resources. During the past two years, the I-66 Special Project of the National Speleological Society, The Kentucky Speleological Survey, and the Kentucky Geological Survey have gathered, archived, and developed karst data for the state. Current projects include publication of karst basin maps, archiving cave entrance locations, archiving and georeferencing cave maps, creating polygon coverages of cave conduits, and a statewide sinkhole digitization project. These data have proven useful in efforts to redirect planned developments, and to further the state of our knowledge about karst resources within Kentucky.

Karst is an integral part of the Kentucky landscape with ~55% of the state underlain by karstic limestone in 3 of 7 physiographic provinces and along the margins of the Eastern and Western Kentucky Coal Fields (KGS 1985) (Fig. 1). This allows for a great diversity in the state's caves and karst since each karst region has unique characteristics due to differing hydrogeologic conditions (KGS 1985). The abundance of karst in Kentucky affects everything from the state's biodiversity (Barr 1958) to the history of human settlement (Andrews 2001; O'Dell 2001). The widespread and intense karstification of the region also poses tremendous environmental impact issues due to continued population growth and industrialization (Crawford 2001). Increasingly, the karst areas of Kentucky face rapid development and a losing battle due to lack of knowledge about our subsurface environment (Florea *et al.* 1999).

Geographic information system (GIS) data are becoming an important component of today's technology. Kentucky organizations and agencies such as the Kentucky Geological Survey and the Office of Geographic Information have developed extensive coverages and databases for geographic features in the state. Some examples of available, on-line data are Digital Raster Graphic (DRG) maps, Digital Elevation Models (DEMs), and various hydrologic and geologic coverages. Until recently, however, little or no GIS data existed for statewide cave and karst resources in Kentucky. This lack of data has seriously impacted the ability to protect and manage our caves and karst.

KENTUCKY KARST GIS

Caves and karst have been studied intensely in Kentucky for decades. Extensive studies in the Mammoth Cave region have changed our thinking on speleogenesis (White *et al.* 1970; Ford & Ewers 1978; Palmer 1981; White 1988).

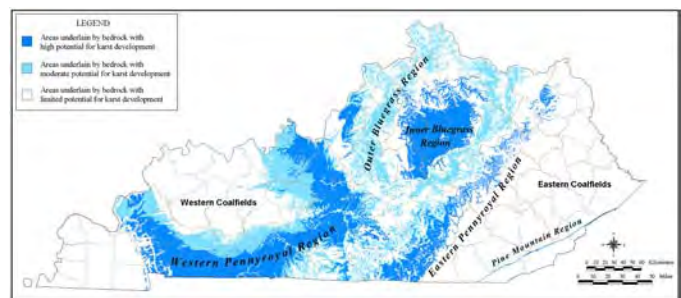


Figure 1. GIS karst map of Kentucky developed by the Kentucky Geological Survey.

Methods for karst aquifer analysis and tracer testing were perfected in the sinkhole plains of central Kentucky (Thraillkill 1972; Quinlan & Ewers 1981). Also during the 1970s and 1980s, cave systems were mapped throughout the state by various groups. Data from these studies were used in publications, theses, and dissertations, but were not widely known.

Much of the distribution problem was due to a lack of appropriate technology to expedite the transfer of these data. Data gathering was laborious, and data storage was always a point of concern. Further, holders of Kentucky karst data were widespread and not accustomed to working cooperatively. No appropriate statewide data repository existed, and the political climate was not conducive for any one organization to become a driving force to organize cave data collection.

During the course of the past several years, all of these factors challenged karst research and forced the advancement of our knowledge of karst on a statewide scale through the use of GIS technology. Recent developments in computer technology have alleviated many of these issues and have revolutionized the ways we communicate and visualize the results of our

work. The issues driving development of Kentucky's cave and karst GIS projects can be summarized in three phases.

INITIAL DATA COLLECTION EFFORTS

Various organizations and individuals have been collecting cave and karst data in Kentucky for years. These individual projects, designed with particular goals in mind, have tested various methods of cooperative data sharing and presentation, resulting in essential lessons for future projects.

In the early 1990s, the Cave Research Foundation (CRF), Central Kentucky Karst Coalition, and the American Cave Conservation Association (ACCA) coordinated with other cavers and groups to co-produce a Dripping Springs Escarpment map displaying Mammoth Cave data and other known caves. This overlay of map information addressed several data issues, such as cooperative data sharing and effective presentation methods for large quantities of karst and tracing data.

Starting in 1996, the Kentucky Geological Survey (KGS) began developing a karst atlas of Kentucky composed of various plates (Currens & Ray 1999). KGS has completed five 30 x 60-minute quadrangle maps at a scale of 1:100,000 that show karst groundwater basins. The maps were compiled using data from dye traces performed by numerous researchers. The maps depict major karst springs and swallets, and the approximate path of groundwater flow (Paylor & Currens 2001).

In a more site-specific project, the ACCA, in cooperation with CRF, has modeled the Hidden River Cave System in Horse Cave, Kentucky using

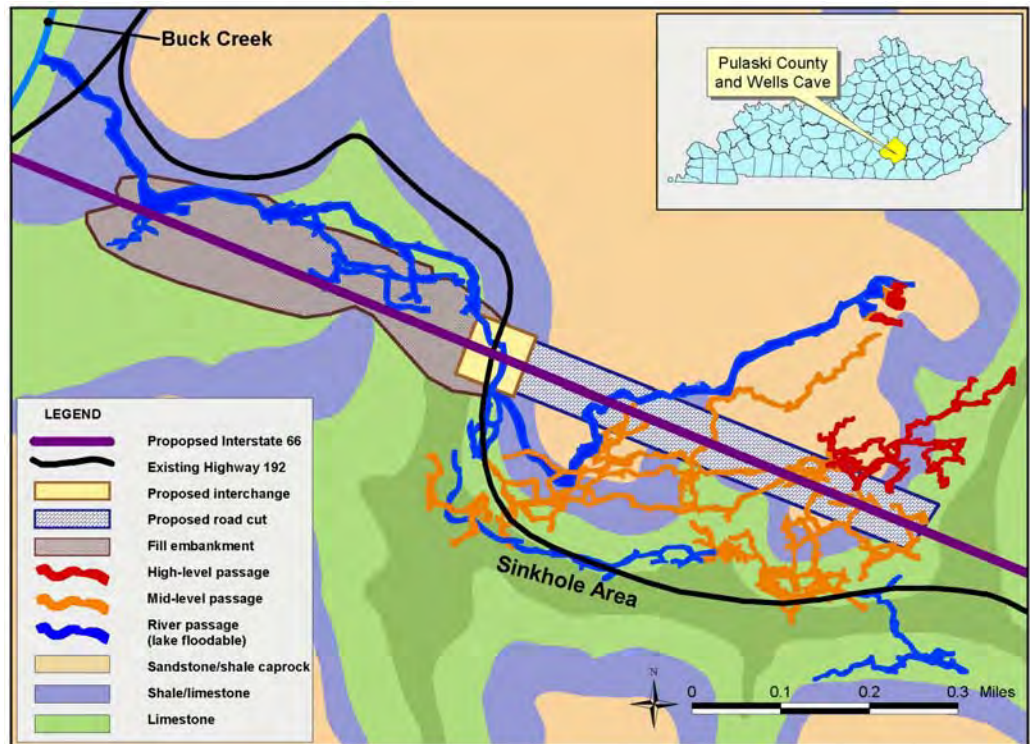


Figure 2. Relationship between the originally proposed I-66 corridor and Wells Cave (adapted from overlay by Larry Simpson).

ESRI ArcView and 3D Analyst software. This project has been useful in testing methods of incorporating Digital Line Graph (DLG), Digital Ortho Quarter Quad (DOQQ) data and cave survey data to display the relationship of the sub-surface conduits to the overlying topography and town of Horse Cave.

The Ohio Valley Region (OVR) of the NSS and the Sloans Valley Conservation Task Force have gathered and developed Sloans Valley Cave data for several years. Sloans Valley Cave, the longest mapped cave in the eastern part of the state, has a long history of environmental problems. A large landfill lies adjacent to the cave and within part of its drainage basin, and the cave receives polluted runoff in these areas. Reservoir water from Lake Cumberland permanently inundated much of the cave. As the reservoir level fluctuates as much as 12 m throughout the year, thermal pollution wreaks havoc with the cave's biological systems. The complicated system of hydrologic and biologic interactions is perfectly suited to GIS analysis.

In addition to these specific examples, much of the original data on Kentucky caves has existed for years in individual databases and boxed files in basements or attics. Over time, data loss has taken its toll on the level of our knowledge of caves and karst in Kentucky. As the state continues the current population and industrialization trend, fully operational databases of Kentucky karst will be essential for proper planning and zoning in karst regions, implementation of best management practices for karst, and advancing our knowledge about karst through well-informed research.

INTERSTATE 66 AND DEVELOPMENT ISSUES

When the Kentucky Transportation Cabinet (KTC) unveiled possible routes for the section of Interstate 66 between London and Somerset, KY (KTC 1999), karst researchers and cavers were dismayed. Of the alternatives presented in May of 1999, the KTC seemingly chose the most environmentally damaging route (the southern route) as the preferred alternative (Florea *et al.* 1999). This proposed corridor traversed undeveloped woodlands inside and outside the

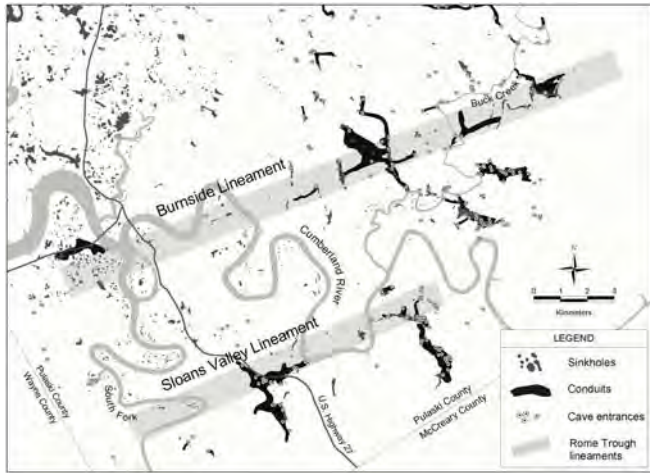


Figure 3. Karst resources in southern Pulaski County, Kentucky, showing newly recognized fracture lineaments that control cave and karst development.

Daniel Boone National Forest, crossed several high quality watersheds, and threatened severe damage to cave and karst resources including Wells Cave (20 km of surveyed passages) (Fig. 2). In response to the KTC planning study, the I-66 Special Project of the National Speleological Society in cooperation with dozens of other organizations initiated one of the first extensive cooperative data gathering campaigns in the region.

The response focused on collecting, maintaining, and presenting a GIS of karst resources in Pulaski County, Kentucky, using ESRI ArcView software. The first level of data included a point location database of cave entrances and other associated karst features provided by locals and members of the caving community. A second layer of information included scanned and georeferenced (registered to real-world coordinates) cave maps. From these raster images, polygons outlining the passages were digitized to display regions in which surveyed caves were known to lie underneath the surface. A third layer of information included sinkhole polygons digitized from depression

contours on 7.5' topographic quadrangles (Fig. 3). The final layer of information in the GIS was a vector representation of the corridor alternatives for the I-66 project. This information was provided by the KTC. All data was created using NAD 1983 datum and the Kentucky State Plane South 1983 coordinate system, chosen to maintain consistency with GIS coverages in state developed databases, and to match the State Plane zone for the proposed corridor.

The data developed by this effort were used in several ways. Overlays of the corridor alternatives with a 1000 foot [~305 m] buffer and the conduit polygons and cave entrance data were used to determine potential karst impacts for each alternative. KTC and its consultants provided conduit polygons and the sinkhole coverages for the area affected by the proposed corridors for incorporation in a second planning study being completed to address the concerns raised by the first (KTC 2000). Images produced using the data were presented in publications and at various presentations throughout the region to help others understand the concerns (Florea *et al.* 1999; Florea 2000a).

THE KENTUCKY SPELEOLOGICAL SURVEY

As a result of the cooperative atmosphere of the I-66 research, a desire to gather the extensive but disorganized karst data for all of Kentucky prompted the formation of the Kentucky Speleological Survey (KSS) during 1999 and 2000. The KSS was formed to serve as a statewide database and repository for cave and other karst related data. The establishment of the KSS was an important step toward saving and inte-

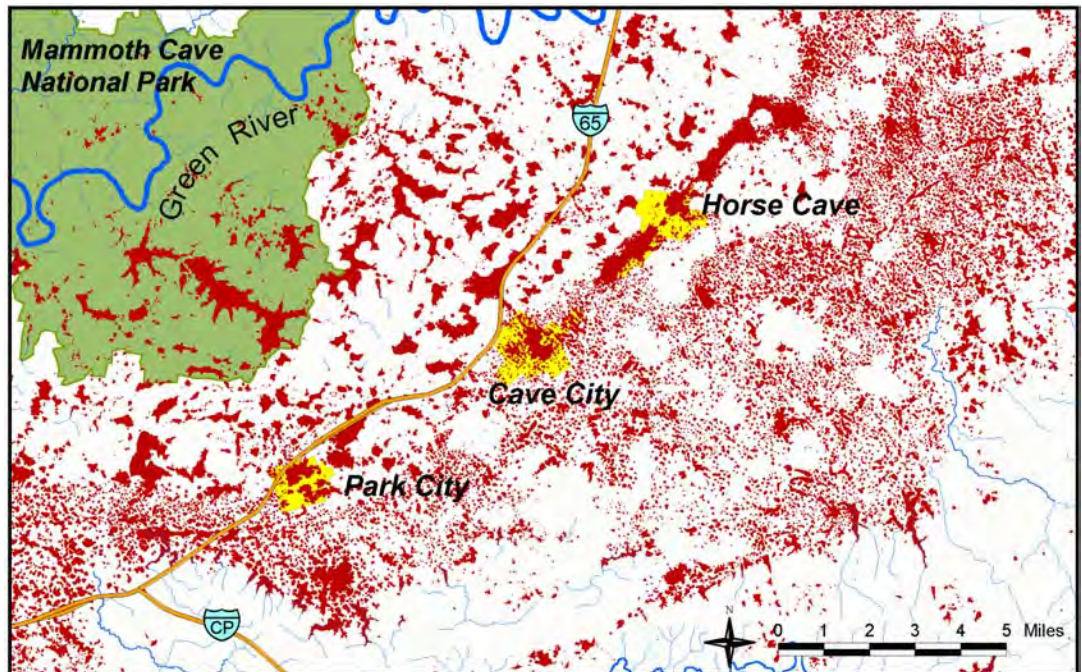


Figure 4. Portion of the Kentucky statewide sinkhole map showing sinkhole distribution near the Mammoth Cave area.

grating vital karst data before it was lost or forgotten (Florea 2000b).

The utilization of GIS as an integral component of the KSS's data gathering and archiving activities was emphasized during organization. The KSS currently uses ArcView GIS linked to Access databases and spreadsheets to manage all its spatial data, allowing users to link multimedia data such as narrative files, scanned maps and cave photographs to the primary spatial index of feature locations. This system provides the framework needed for an eventual, fully integrated database of material without the need for primary paper copies.

An example of one of the issues that KSS addressed arose during the I-66 conflict in Pulaski County. The interstate development problem illuminated the need for a detailed, statewide sinkhole delineation. Following a review of the results of the I-66 Special Project and considering the ongoing groundwater investigations occurring at KGS, a decision was made to complete a sinkhole digitizing effort for all of Kentucky on a 1:24,000 scale (Fig. 4) (Paylor & Florea 2001).

The sinkhole digitization raised several data issues, including the representation of complex uvalas (sinkholes with multiple sinkpoints), differences in contour intervals between topographic quadrangles and their effects upon data resolution, and manipulation of USGS hypsography files.

RESULTS AND CONTINUING STUDY

The impact of all the GIS work to date in Kentucky has been significant. Due to a combination of public opinion and evidence provided through karst GIS development, the second planning study for I-66 (released in June 2000) recommended a more northerly corridor, which avoid many known cave and karst resources (KTC 2000). Many concerns still exist with the current preferred corridor, and future efforts will involve continued exploration and data gathering of karst resources concurrent with the KTC environmental impact statement.

The efforts of the I-66 Special Project have opened the door to other research in the region including a cave-cricket/beetle predation study (White 2001), cave diving exploration in regional aquifers, and geomorphic studies of regional caves (Florea 2000b; 2001b). Other research stemming from this collected data has detected evidence of a previously unknown fault though sinkhole and conduit alignments (Fig. 3) (Florea 2001a).

A more recent offshoot of the I-66 effort temporarily averted a strip mine proposal in the vicinity of Wells Cave in Pulaski County. Due to the combined effort of several individuals and through use of GIS data collected during the I-66 Special Project effort, serious deficiencies were noted in the permit application. The Department for Surface Mining Reclamation and Enforcement technically withdrew the permit after the deficiencies were pointed out.

A 3D model of the Sloans Valley Cave System is being developed using ArcView GIS with the Spatial Analyst and 3D Analyst software packages (Paylor *et al.* 2001). The GIS is

nearing completion and will be used to model water levels, cave stream and reservoir water mixing, siltation, and landfill runoff routes through the cave. In addition to hydrogeologic studies, endangered and threatened species populations and migrations will be tracked, and an attempt will be made to model airflow patterns through the complicated system and its 18 entrances.

Other ongoing karst GIS activities in Kentucky are occurring at Western Kentucky University's Hoffman Institute and the KGS (Glennon & Groves 2002). Other planned elements of KGS's karst atlas series will show karst flood-prone areas, and will detail carbonate bedrock lithologies, sinkholes, and springs as well as include results of long-term dye tracing projects in the Inner Bluegrass and Western Pennyroyal regions that are being used to update the atlas maps. In addition to updates to its karst groundwater basin map series, KGS will shortly be publishing a statewide karst occurrence map developed from new 1:100,000-scale ArcInfo geology coverages.

The statistics generated by the KSS sinkhole digitization project are impressive. Nearing completion, over 62,000 sinkholes have been digitized to date for Kentucky. The combined area of these polygons suggests that ~3% (>3100 km²) of the surface of Kentucky lies within a topographically mapped sinkhole. The sinkhole digitization effort has also helped KGS develop more effective dye tracing methods due to the recognition of regional sinkhole lineaments (Paylor & Currens 2001).

The completed statewide sinkhole coverage will be published through the KSS and KGS, and will include a descriptive folio and data CD-ROM. The coverage will be useful for many purposes, including planning, resource management, cave and karst research, groundwater studies, and statistical analysis.

CONCLUSIONS

Kentucky's abundance of karst has created tremendous land use concerns as population and industrialization in karst areas rapidly increases. The lack of statewide organization for gathering karst data in Kentucky once resulted in problems with dealing with issues of planning and resource management. GIS utilization is changing the outlook for statewide karst data availability for Kentucky. The I-66 Special Project of the NSS, the Kentucky Speleological Survey, the KGS, and others have been gathering, archiving, and developing karst GIS data for the past several years. Current GIS projects include groundwater dye trace information, cave entrance archiving, map archiving and georeferencing, conduit polygon coverage development, and a statewide sinkhole digitization project. The data from these efforts have proven useful in efforts to improve the outcome of planned developments, and to further the state of our knowledge about karst resources within Kentucky.

ACKNOWLEDGEMENTS

The research conducted in this paper has been funded in part by exploration and conservation grant money awarded by the National Speleological Society and by software grants from the Environmental Systems Research Institute (ESRI) Conservation Program.

Research has also been made possible through the support of the following organizations: Blue Grass Grotto, Central Ohio Grotto, ESRI, Kentucky Department for Surface Mining Reclamation and Enforcement, Kentucky Geological Survey, Kentucky Heartwood, Kentucky Speleological Survey, Kentucky Transportation Cabinet, KICK 66, National Speleological Society: Conservation and Exploration Committees, Sloans Valley Conservation Task Force, Somerset Pulaski County Concerned Citizens, and the University of Cincinnati.

REFERENCES

- ACCA, 2000, Highways and karst: American Caves, v. Fall 2000, p. 8-14.
- Andrews, W.M., 2001, Influence of geology on the history of central Kentucky, in Braley, L., & Florea, L., ed., NSS convention 2001 guidebook: A cave odyssey, p. 216.
- Barr, T.C., 1958, Studies on the cave invertebrates of the interior lowlands and Cumberland Plateau [PhD thesis]: Vanderbilt University.
- Crawford, N.C., 2001, The proposed Kentucky trimodal transpark to be built at Bowling Green, Kentucky and other development near Mammoth Cave National Park, in Kalnitz, H., ed., 2001 National Speleological Society Convention program guide.
- Currens, J.C., & Ray, J.A., 1999, Karst atlas for Kentucky, in Beck, B.F., Pettit, A.J., & Herring, J.G., ed., Hydrogeology and engineering geology of sinkholes and karst-1999, Proceedings of the 7th Multidisciplinary Conference on Sinkholes and the Engineering and Environmental Impacts of Karst, April 10-14, 1999, Harrisburg-Hershey, PA, Rotterdam, A.A. Balkema, p. 85-90.
- Florea, L.J., Graham, B., Simpson, L., Currens, J., & Hopper, H.L., 1999, Karst impacts of the proposed route for I-66: NSS News, v. 57, no. 10, p. 307-309.
- Florea, L.J., 2000a, Interstate 66: Proposed alternatives in southern Kentucky and karst impacts [abs]: Journal of Cave and Karst Studies, v. 62, no. 3, p. 188.
- Florea, L.J., 2000b, Kentucky Speleological Survey: Concept to foundation [abs]: Journal of Cave and Karst Studies, v. 62, no. 3, p. 188.
- Florea, L.J., 2001a, Survey and exploration of Jugornot Cave, Pulaski County, Kentucky [abs]: Journal of Cave and Karst Studies, v. 63, no. 2, p. 111.
- Florea, L.J., 2001b, Geomorphic indicators of paleo-environmental conditions, Wells Cave Kentucky: Geo², v. 12, no. 1-3, p. 4-11.
- Ford, D.C., & Ewers, R.O., 1978, The development of limestone cave systems in the dimension of length and depth: Canadian Journal of Earth Science, v. 15, p. 1783-1798.
- Glennon, A., & Groves, C., 2002, An examination of perennial stream drainage patterns within the Mammoth Cave watershed, Kentucky: Journal of Cave and Karst Studies, v. 64, no. 1, p. 82-91.
- KGS, 1985, Caves and karst of Kentucky, in Dougherty, P., ed., Kentucky Geological Survey Special publication 12, Series XI, 196 p.
- KTC, 1999, Kentucky Transportation Cabinet Division of planning: Southern Kentucky corridor (I-66), Somerset to London (Planning Study), Wilbur Smith and Associates, 45 p.
- KTC, 2000, I-66 southern Kentucky corridor (Planning Study), Kentucky Transportation Cabinet Division of Planning, 93 p.
- KICK 66, 2000, Proposed routes for I-66, comments on corridor alternatives, private publication, 252 p.
- O'Dell, G., 2001, Springs and springhouses in Kentucky's Inner Bluegrass region, form and function in an evolving landscape, in Proceedings of the Kentucky Water Resources Annual Symposium, Kentucky Water Research Institute, p. 13.
- Palmer, A.N., 1981, A geologic guide to Mammoth Cave National Park: Teaneck, NJ, Zephyrus Press.
- Paylor, R.L., & Florea, L.J., 2001, The Kentucky sinkhole project. Development of a statewide sinkhole map, in Kalnitz, H., ed., 2001 National Speleological Society Convention Program Guide, p. 86.
- Paylor, R.L., & Currens, J.C., 2001, Mapping karst ground-water basins in the inner bluegrass as a nonpoint-source pollution management tool, in Beck, B.F., Pettit, A.J., & Herring, J.G., ed., Proceedings of the 2001 sinkhole conference, Louisville, Kentucky, p. 229-234.
- Paylor, R.L., Cole, J.L., & Simpson, L.S., 2001, Sloans Valley Cave System, in Braley, L., & Florea, L., ed., NSS convention 2001 guidebook, p. 216.
- Quinlan, J.F., & Ewers, R.O., 1981, Hydrogeology of the Mammoth Cave region, Kentucky, in Robers, T.G., ed., GSA Cincinnati 1981 Field Trip Guidebooks: Boulder, CO, Geological Society of America, p. 457-506.
- Thraillkill, J., 1972, Carbonate chemistry of aquifer and stream water in Kentucky: Journal of Hydrology, v. 16, p. 93-104.
- White, M.J., 2001, Study of a convergent cave beetle/cave cricket predator prey system [abs]: Journal of Cave and Karst Studies, v. 62, no. 3, p. 109.
- White, W.B., Watson, R.A., Pohl, E.R., & Brucker, R., 1970, The central Kentucky karst: Geographical Review, v. 60, p. 88-115.
- White, W.B., 1988, Geomorphology and hydrology of karst terrains: New York, Oxford University Press, 464 p.

USING GEOGRAPHIC INFORMATION SYSTEMS TO DEVELOP A CAVE POTENTIAL MAP FOR WIND CAVE, SOUTH DAKOTA

RODNEY D. HORROCKS

Wind Cave National Park, RR 1 Box 190, Hot Springs, SD 57747 USA, Rod_Horrocks@nps.gov

BERNARD W. SZUKALSKI

ESRI Cave & Karst Program, ESRI, 380 New York Street, Redlands, CA 92373-8100, USA

The cave potential map concept was originally developed to address management concerns, but other uses rose to the forefront, including the likely maximum boundaries of Wind Cave, the potential surveyable length of the cave, and the possibilities of a connection with Jewel Cave. In addition, this method may provide means to judge the exploration potential for any section of the cave and to evaluate hypotheses regarding the cave's origin. The cave potential map was based on structural geologic factors, surface contour maps, cave survey data, surface blowhole locations, and hydrologic maps. Geographic information systems (GIS) were used to combine these data with GIS-generated triangular irregular networks, slope and aspect, orthophotoquads, a park boundary map, and land ownership maps. By combining these datasets and deriving buffers and overlays, it was determined that the current cave boundaries cover 1/10 of the total potential or maximum likely extent of the cave. The likely maximum potential boundaries are 97% inside of the current boundaries of Wind Cave National Park. Based on passage density, the length of the Wind Cave survey could range from 400-1760 km. Since the current 166 km of survey represents no more than 40% of the minimum predicted length of the cave or as little as 9% of the maximum predicted length of the cave, a tremendous amount of surveyable passage remains in the system.

Since its discovery in 1881, numerous cavers have been drawn to Wind Cave to explore its complex mazes. Although the first surveys were conducted in 1902 and produced about 1.6 km of survey (Willsie 1902), it was not until the mid-1950s that significant survey work began. Between 1955 and 1963, the South Dakota School of Mines and Technology in Rapid City mapped another 1.6 km of passage. The National Speleological Society's 1959 Wind Cave Expedition mapped an additional 5 km (Brown 1959). In 1960, the Colorado Grotto surveyed 0.8 km and begun a long-standing survey project (La Borde 1960). In 1962, seasonal Wind Cave ranger Alan Howard began surveying in the cave, mapping several hundred meters of passage. In the mid-1960s, Dave Schnute, Herb Conn, and Jan Conn surveyed 3.2 km and made numerous important discoveries. The most sustained survey in Wind Cave to date was a project begun by John Scheltens and the Windy City Grotto in 1970 (Scheltens 1970). During the 1970s, Wind Cave rangers also contributed another 4.80 km of passage and during the 1980s the National Outdoor Leadership School (NOLS) surveyed in the cave. As the survey grew, the boundaries of the cave expanded to 1.3 km north/south by 1.4 km east/west. In 1990, the Wind Cave Weekend survey project was started by the Colorado Grotto. Between 1990 and 1998, 30 km was added to the survey length. Since 1999, the Wind Cave Weekend has continued and, coupled with increased survey work by park staff, an average of 12 km a year is being surveyed. The total Wind Cave survey now exceeds 166 km

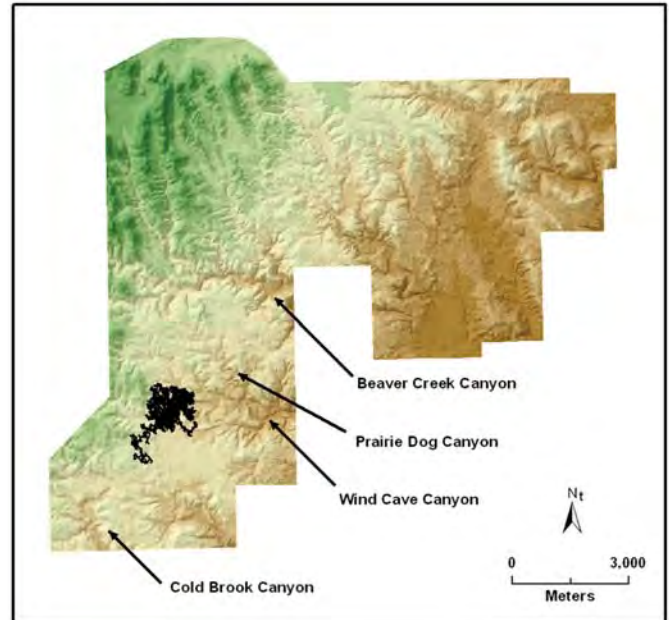


Figure 1. Location of Wind Cave within Wind Cave National Park. The Wind Cave survey lineplot (black) was generated using COMPASS software and imported to GIS format and georeferenced using the CaveTools extension for ArcView GIS. The cave data are plotted atop a digital elevation model (DEM), which has been shaded showing higher elevations in green and lower elevations in brown.

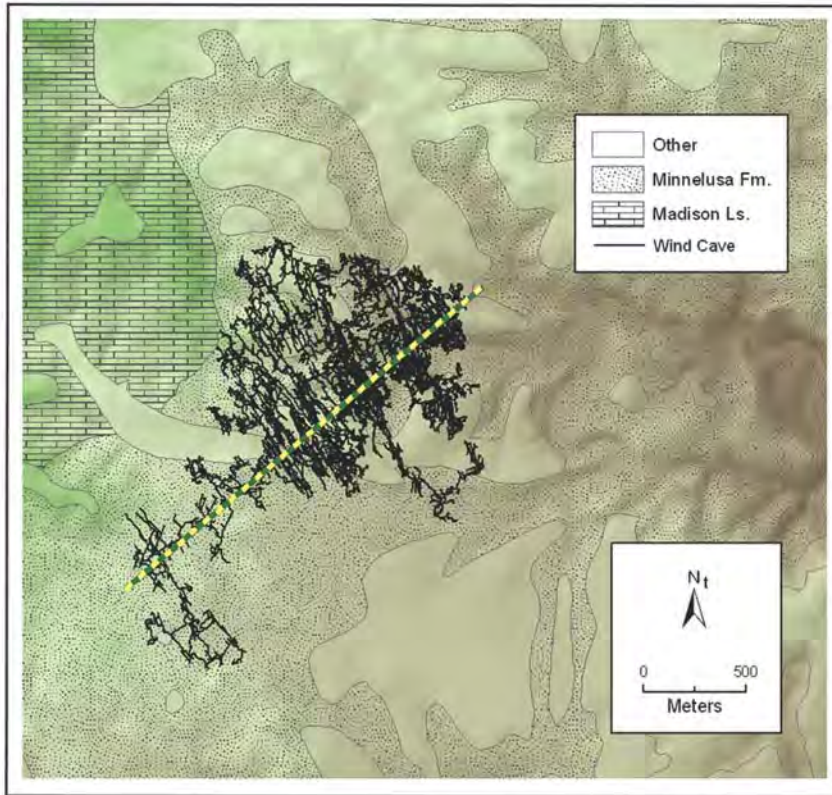


Figure 2. Relationship of the Madison Limestone outcrops to the Wind Cave survey. The major trend of the cave is marked with a yellow and green striped line. The Minnelusa Formation lies directly above the Madison limestone. This illustration was created by combining a shaded relief DEM, geology layer, and survey lineplot.

and the boundaries have expanded to fill a 1.6–1.9 km rectangle (Fig. 1).

Recently, cavers have been directed by the park cave resource management staff to concentrate their survey efforts on individual areas. This was done to facilitate the survey of the cave and to provide incentive for cavers to take ownership of “their” areas. The unforeseen result of this tactic was that the true complexity of Wind Cave was revealed. This information helped to substantiate a hypothesis that the major trend of the cave (Fig. 2) developed along a sulfate zone that paralleled the ancient shoreline (A. N. Palmer 2000 pers. comm.). It is common to hear cavers participating in the current survey effort remark about the “endless” potential of the cave. A famous diary quote by an early Wind Cave explorer, Alvin McDonald, said, “Have given up the idea of finding the end of Wind Cave” (McDonald 1891). This is as true today as it was in 1891.

For years, cavers based the potential size of Wind Cave on barometric wind studies done by Conn (1966). Those studies suggest that the current volume of surveyed cave represents only 2.5% of the total volume of $5.5 \times 10^{10} \text{ m}^3$. The current volume of the surveyed portions of Wind Cave is $1.4 \times 10^9 \text{ m}^3$ (M. J. Ohms 2001 pers. comm.). Others pointed out that the $5.5 \times 10^{10} \text{ m}^3$ calculation was actually conservative, since the Snake Pit Entrance, numerous blowholes, and the elevator leakage were not considered. Recently, surveyors have noticed that cool windy air blows in many domes throughout the cave. It is thought that this air represents surface connections too small to penetrate or notice as blowholes on the surface. Additional entrances would suggest a greater total volume. It also

is possible that the portion of Wind Cave that is accessible may be much smaller than the above estimate. The majority of the cave may be beyond unenterable cracks and small connecting passages, or it may be completely water filled and not contributing to the total airflow at all. This study speculated that a cave potential model might be a more accurate method to predict the amount of potential surveyable passage in Wind Cave than barometric wind studies could provide.

As the boundaries of the cave have enlarged, many hypotheses on passage extent have been proposed, including speculation on a connection with Jewel Cave, 29.4 km to the northwest. These hypotheses have proposed either an air-filled or a water-filled connection.

WIND/JEWEL CAVE CONNECTION HYPOTHESES

It has been hypothesized that a connection between Wind and Jewel Caves may exist based on the observation that these two huge cave systems are both located in the Madison Limestone (locally known as the Pahasapa Limestone), which forms a continuous ring around the Black Hills (Zerr 1972). Others have suggested that the connection may not be air-filled but within the phreatic zone. Either potential connection may not be passable by humans.

Proponents of the air-filled connection hypothesis suggest that the caves behave as one giant cave system based on barometric wind measurements (Zerr 2001). However, a general observation concerning the barometric winds seems to argue against this air-filled hypothesis. The barometric winds from Wind Cave react to surface changes in atmospheric pressure as a balloon-shaped void, with all the passages relatively close to the entrance. Jewel Cave behaves as a cylinder, with much of that cave a great distance from its entrance (Conn 1966). Additionally, the smaller and concentrated maze passages of Wind Cave significantly differ from Jewel Cave’s larger passages and broader footprint.

Survey data and geologic maps reveal that the southeast point of Jewel Cave is 313 m higher in elevation than the southwest corner of Wind Cave and that there are 4 folds and at least one significant fault between them. Analysis of the line plot of Wind Cave reveals an obvious concentration of passage development along a line, the major trend, roughly per-

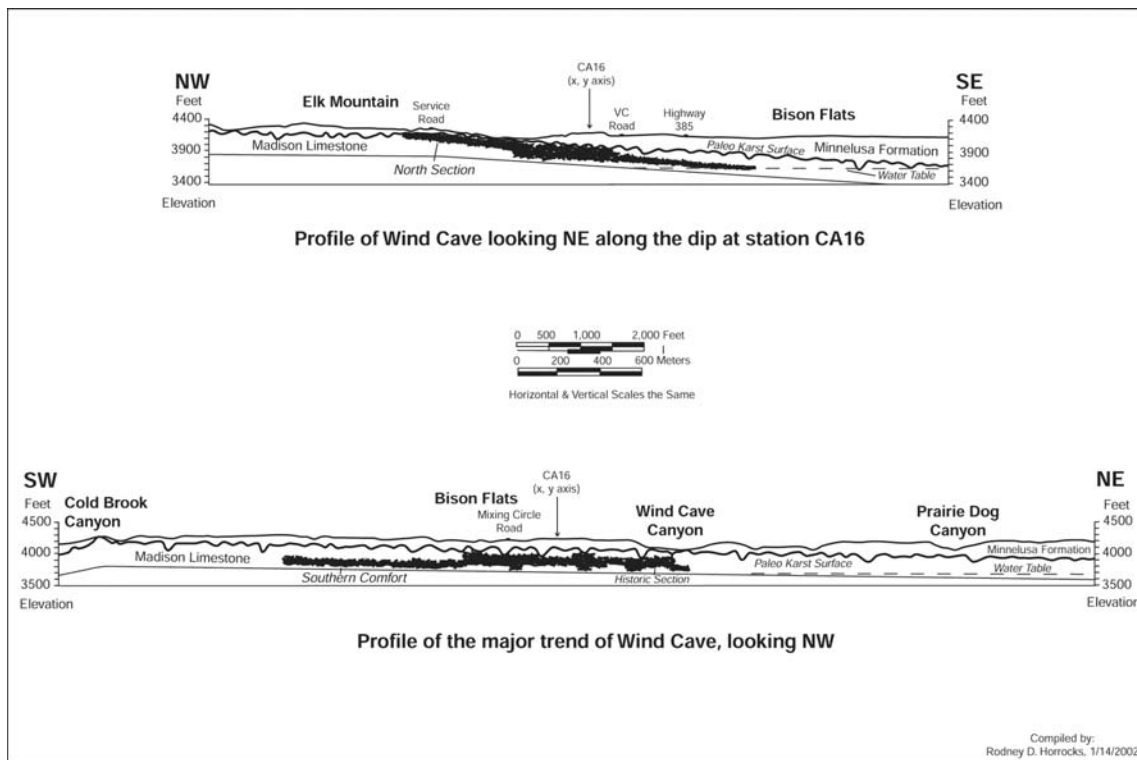


Figure 3. Profiles of Wind Cave along the major trends of the cave, showing the relationship of surveyed passages with the structural geology. Station CA16 was chosen because of its location at the intersection of the two major trends of cavern development. This illustration was compiled from the Wind Cave National Park and Vicinity 20-foot contour map, COMPASS data, geology maps, cave radio location data, and GIS hydrography layers.

pendicular to the dip of the beds (Fig. 2). When a profile of the Wind Cave survey is analyzed, it becomes apparent that the major trend of Wind Cave runs on a line extending N52°E and plunges slightly to the northeast (Fig. 3). Following this major trend to the southwest, there is no reason to believe that this pattern would be abandoned with the cave trending to the west and then up to the northwest past the folds and up the significant elevation gain to Jewel Cave.

Even though the straight-line distance between the two caves is 29.4 km, the distance following the Madison Limestone-Minnelusa Formation contact is longer, 32 km, as the limestone outcrop strikes to the west before angling northwest towards Jewel Cave. This measurement approach was chosen since both caves lie underneath the Minnelusa exposures. If such a connection actually existed, the resulting cave would be on the order of 7200 km long and largely not explorable due to human limitations. This estimate assumes the same passage density along the entire distance as is found in the Wind Cave area and may represent a high estimate since Jewel Cave currently appears less complex than Wind Cave.

Others have suggested that a hydrological connection between the two caves may be possible via a connection below the potentiometric surface. The problem with a water-filled cave connection is that the potentiometric contour that trends through Wind Cave is 18 km to the south and 400 m lower in elevation with respect to any known passages in Jewel Cave (Carter & Driscoll 2001). However, a groundwater connection between the Jewel Cave area and Cascade Springs, a large spring on the southern tip of the hills, has been observed based on potentiometric studies (Carter & Driscoll 2001). Along the

western flank of the Black Hills, the Madison aquifer flows to the southwest at 0.34-0.54 m³/s. About 32 km from Jewel Cave, that flow arcs to the east and emerges after another 41 km at Cascade Springs (Carter & Driscoll 2001). However, on the eastern edge of the Black Hills, there is no groundwater flow connection between Wind Cave and Cascade Springs as all water flows to the southeast from Wind Cave at 0.0085-0.037 m³/s (Carter & Driscoll 2001). Because the potentiometric contour that intersects Cascade Springs trends 4.0 km southeast of Wind Cave and is 120 m lower, and because it is unlikely that cave development continues much below the water table in that direction (see the Developing the Model section below), a phreatic connection between Wind Cave and Cascade Springs below the potentiometric surface is unlikely. Assuming a connection is unlikely makes it possible to analyze Wind Cave as a finite entity with definable boundaries that can be quantified in a cave potential model.

MANAGEMENT REQUIREMENTS

Traditionally, surface land management decisions have been based on whether or not activities were above known cave, but recent cave management projects have demonstrated that activities within the cave watershed could impact the cave just as easily. Not only are there sinking streams in the Park, but close hydrological connections between surface drainages and the cave system have been demonstrated through cave inventory (Nepstad 1996) and dye tracing projects (Alexander

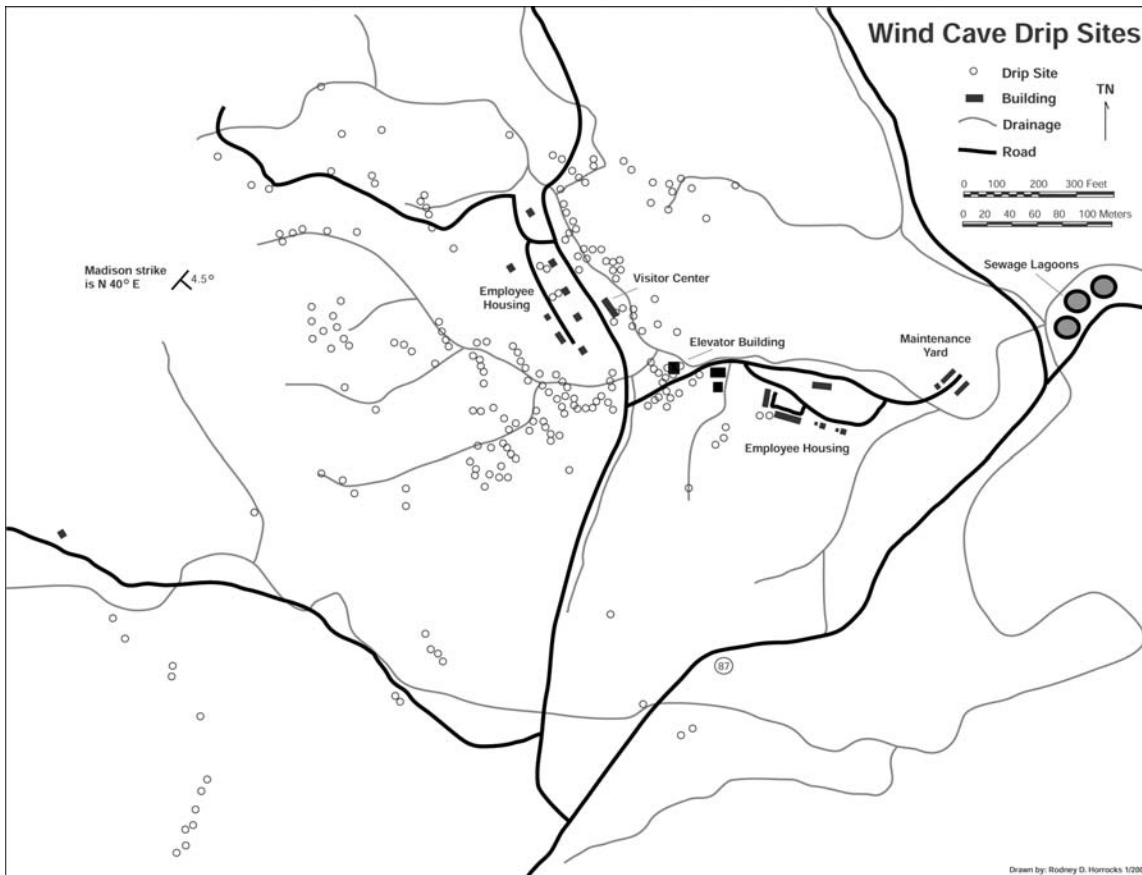


Figure 4. Relationship between dripping water in Wind Cave and the location of surface drainages. Notice that nearly all drip sites are near drainages or down dip from them. Map compiled by James Nepstad.

1986). The cave inventory demonstrated that wet spots in the cave are either located below surface drainages or just down-dip from those drainages (Fig. 4). The dye-tracing project recorded flow-through times as fast as six hours (Nepstad 1996) and documented increased hydrocarbons from parking lot runoff after a storm event (Venezky 1994).

Park facilities and infrastructure, which were built directly on top of the cave and within a window in the Minnelusa Formation that exposed the underlying Madison Limestone and produced the natural entrances (Fig. 2), historically provided the foremost threats to Wind Cave. Fortunately, the three most severe threats presented by these structures and facilities have either been mitigated or are in the process of being addressed. In 2001, 2400 m of the aging sewer system was replaced with dual-contained HDPE lines and inspection ports to check for inner line leaks. The park plans to replace the asphalt parking lot with Portland concrete and add a storm water treatment system that would catch the hydrocarbons washed off the lot during the first flush of precipitation events. It also plans to remove the inadequate sewage lagoons. Although these lagoons were outside the current boundaries of the cave, it was suspected that they could be over undiscovered cave (J. Nepstad 1999 pers. comm.).

Any scenario that would extend Wind Cave beyond the current park boundaries would necessitate partnerships with additional land managers as US Forest Service and private lands surround Wind Cave National Park. In the foreseeable

future, pressure from surrounding development may threaten the cave. Housing tracts adjacent to Beaver Creek to the north-west of the park are being planned. This creek enters the park and a large portion of its flow disappears underground into Beaver Creek Cave in the Madison Limestone. Although this water has been dye traced to the parks well in Wind Cave Canyon, it has not yet been traced to Wind Cave (Alexander 1986). Likewise, using herbicides to control exotic weeds within the Wind Cave watershed to the west of the Park is a land management activity that could potentially impact the cave.

Historically, it had been difficult to get park managers to recognize that Wind Cave may extend beyond its current boundaries. Unless the cave survey extended into an area, managers assumed that no cave existed there (J. Nepstad 1999 pers. comm.). Although this concept of a cave potential map first developed after hearing about these attitudes, actual development of the model identified its limitations as a management tool.

DEVELOPING THE MODEL

As the model developed, it was decided that this model could address four issues: 1) the maximum likely extent of Wind Cave; 2) the surveyable length of the cave; 3) the Wind/Jewel Cave connection hypothesis; and 4) surface land management shortcomings that existed near known cave.

Although previous researchers have analyzed Wind Cave's potential extent based on individual disciplines, no one has attempted to use geology, hydrology, airflow, and cave survey data together to quantify the potential extent of Wind Cave. We initially analyzed the region surrounding Wind Cave and identified some preliminary large-scale factors that could limit cave passage development. We theorized that the current erosional surface and the water table could provide those limiting boundaries. Blowholes and the cave survey data also provided additional clues on the potential extent of the cave.

The Madison Limestone has been eroded away 2100 m to the northwest of the cave, eliminating the possibility that the cave could extend in that direction by more than 2100 m (Fig. 2). Additionally, 1100 m to the southwest of the known cave, a moncline dips 11° to the south. To the west of this moncline, the drainages north of Cold Brook Canyon have removed the upper 30-m of the Madison Limestone, probably representing the upper unit. This does not preclude the possibility of cave underneath those drainages, it only limits that potential. About 3200 m to the northeast of known cave, the Madison Limestone dips underneath Beaver Creek Canyon just down dip from the Beaver Creek Cave, the major insurgence for Beaver Creek. If the cave did continue all the way to Beaver Creek Canyon, it would likely be flooded and inaccessible to exploration. Actually, any passage development to the northeast along the major trend of the cave would likely encounter the water table only 240 m from the current eastern boundary of the cave (Fig. 3). These observations supplied us with three likely, but crude, limiting boundaries for the air-filled portion of the cave. The fourth was provided by the water table to the southeast.

Southeast of the cave, Wind Cave intersects the water table at an elevation of 1100 m (Palmer 1987). Although, divers have never penetrated the passages that continue down dip from the lakes and the deep point of the cave, it is unlikely that the cave continues an appreciable distance in that direction based on three observations: 1) there is no apparent upper level development in that section of the cave; 2) there are only a couple of places where the cave even approaches the water table; and 3) even in those areas, there is sparse cave development. This assumption may also be supported by the observation that where the water table is encountered, most cave development parallels the major trend of the cave and does not continue down dip. Based on these observations, we are assuming that the cave pinches in the southeast direction, with the water table representing the approximate southeastern boundary of the cave.

The earliest version of our cave potential map simply mapped out these four crude boundaries, while factoring in the lineplot of the cave, the location of blowholes, erosional surfaces, canyons, and the water table.

With this preliminary cave potential map in hand, we hypothesized that other geologic factors would also have had a significant effect on the development of Wind Cave. We also hypothesized that such data as the profile view of the Wind

Cave survey, cave radio location depths, surface outcrops, cave levels, airflow, and passage density would all offer additional clues on the likely extent of Wind Cave. Once we identified these additional limiting factors and data sources, individual GIS layers provided buffers and overlays for further refining potential boundaries of the cave.

LIMITING FACTORS

Several geologic factors influence or limit the potential extent of Wind Cave, including erosional surfaces, structural geologic factors, mode of speleogenesis, and paleo-injection points. In the future, as we learn more about these limiting factors, the cave potential boundaries may need further modification.

To quantify the impact that the erosional surface had upon the cave, two profiles were created, one along the dip and the other along the major trend (Fig. 3). These profiles were created by combining the surface contours from the 20-foot "Wind Cave National Park and Vicinity, S. Dak." contour map with the profile views of the Wind Cave lineplot generated in COM-PASS software (Fish 2002). The x,y base point chosen from the cave lineplot was station CA16, a station located at the intersection of the major trend of the cave with the major northwest/southeast trending lakes passages. Radio location depths and paleokarst surfaces were also incorporated into these profiles.

The structure and stratigraphy of the Madison Limestone are primary limiting factors of cave development. The thickness of the Madison Limestone, relief of paleokarst surfaces, dip of the beds, composition of individual beds, presence of folds and faults, presence of proto-cave passages, sulfate beds, and groundwater mixing zones all play major roles in delimiting the potential of Wind Cave.

The thickness of the Madison Limestone in the Wind Cave area and the relief of the paleokarst surface were important in the profile views (Fig. 3). The Madison Limestone is 80–114 m thick, with up to 46 m of vertical relief in the paleokarst surface at the top of the formation. However, the average vertical relief in the vicinity of Wind Cave ranges from 10–20 m (Palmer & Palmer 1989).

The cave slopes to the southeast between 4–5.5°, the same dip as the Madison Limestone. When the cave is examined in profile along its major trend, the cave slopes slightly to the northeast as this development does not exactly follow the stratigraphic strike (N52°E vs. N40°E). Continuing along this major trend to the southwest, a moncline dips 11° to the south at the edge of Cold Brook Canyon (Fig. 3). Several other folds lie to the west and northwest. Based on known patterns and theory, there is no reason to believe that this major trend would be abandoned with the cave trending to the west and then up to the northwest past these folds and up the significant elevation gain to Jewel Cave.

Five distinct "levels" have been identified within this three-dimensional network maze. These levels, based on morpho-

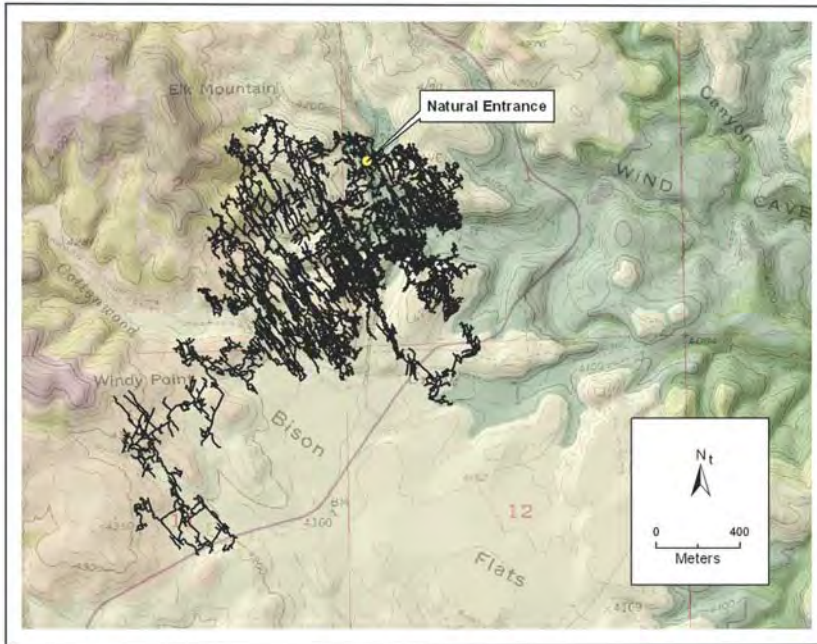


Figure 5. Wind Cave entrance location and surface relief. A DEM was used to create a surface upon which the Wind Cave USGS digital raster graphic (DRG) was draped, along with a hillshaded TIN derived from the DEM and the Wind Cave survey lineplot.

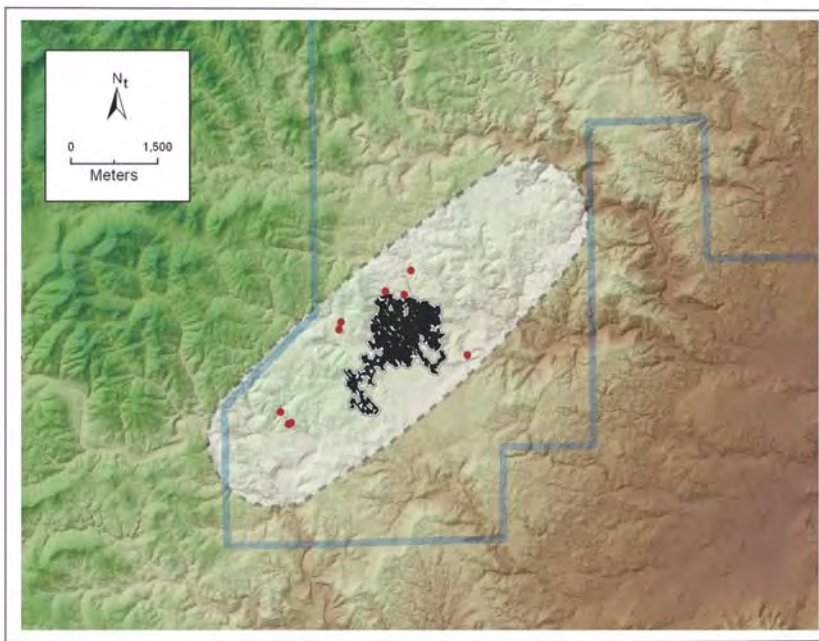


Figure 6. Cave potential boundary for Wind Cave representing the likely maximum extent of humanly accessible portions of Wind Cave. The boundary for cave development is shown in light gray. Surveyed cave passages are shown in black; blowholes are shown as red dots.

logical differences in the passages, have been attributed to the thickness, composition, bedding planes, and joints within the individual units of the Madison

Limestone. The majority of Wind Cave was developed at the middle level, which has been subdivided into the Upper Middle, Middle, and Lower Middle Levels. Lower level cave development is absent in the northwestern section of the cave, with most of the lower level developed along the major trend of the cave. Along the major trend, the vertical relief between the highest and lowest levels of the cave can vary up to 76 m.

Proto-cave passages and sinkholes were an important path for the dissolution of Wind Cave. They formed about 310 Ma, when cave passages and sinkholes in a low elevation karstic plain developed at a mixing zone between sea and meteoric waters. These Mississippian karst features were filled with basal Pennsylvanian sediment (now paleofill) during a sea level rise about 300 Ma, when the Minnelusa Formation was deposited (Palmer & Palmer 1989).

One of the densest concentrations of passages in Wind Cave, which occurs along the major trend of the cave (Fig. 2), may correlate with a sulfate zone deposited parallel with the Mississippian shoreline (Palmer & Palmer 1989). This zone later became an important mixing zone for cavern development that probably predated the canyon entrenchment (A.N. Palmer 2001 pers. comm.).

The mode of speleogenesis had a significant impact on the extent of Wind Cave. It is intuitive that such a complex cave must have an equally complex speleogenetic history. Many theories have been proposed for the development of Wind Cave (Howard 1964; Bakalowicz *et al.* 1987; Palmer & Palmer 1989; Ford *et al.* 1993). This model is based on Palmer's (2000) view of cave development.

When the plan view of the cave map is analyzed, there is a noticeable bulge in passage development towards the northwest corner, which may represent a surface injection point of waters from the northwest (Fig. 5). Palmer (1981) noticed that an old erosional valley terminates to the northwest of the cave at about the contact of the Madison Limestone with the Precambrian intrusives. He has theorized that this paleo valley supplied some of the water for the mixing zone that was a major contributor to the dissolution of the cave. Another potential injection point is along the northwest-southeast trend that runs along the lakes passage. Helictite bushes are found along this entire passage. This may be evidence of injec-

tion of thermal waters through the floor crusts of these passages (Davis 1989). Other evidence of thermal waters is the cupolas in the upper level of the cave that look like convection features (Bakalowicz *et al.* 1987). These cupolas are throughout the cave, indicating that thermal waters may have been important contributors. Even today, a thermal spring (Buffalo Gap Spring) with a temperature 5°C above the lakes in Wind Cave is only 8.8 km down dip from the cave.

USING GIS TO CREATE THE CAVE POTENTIAL MAP

A GIS was used to accomplish several tasks, including the development of a spatial model that was used to verify our preliminary cave potential map, the visualization of those results, and the development of maps to demonstrate cave potential and support management requirements and decisions. The GIS used ESRI's ArcView GIS, Spatial Analyst, 3D Analyst, and CaveTools, a third-party extension used to incorporate cave survey data into the GIS (Fig. 5).

GIS data layers were collected and derived from a variety of sources. Digital line graph (DLG) files were used to create hydrography, hypsography, and transportation layers. Contour lines from the DLG hypsography layer were used to generate a triangular irregular network (TIN) elevation model, from which slope, aspect, and other layers used for visualization were derived. Blowholes and cave entrance locations were imported from field GPS readings. Cave survey data were converted from COMPASS plot files to ESRI shapefiles format and georeferenced based on GPS locations of surface survey stations. Digitized park boundaries, digital orthophoto quads (DOQs), and geologic maps were also incorporated into the GIS.

One of the first maps produced using the GIS showed the relationship of the outcrop of the Madison Limestone to the current surveyed cave extent (Fig. 2). This map underscored the fact that the known cave does not lie below the surface exposure of the Madison, but rather is developed further down along the dip of the Madison, below the Minnelusa Formation exposures (Fig. 2).

Using the ArcView Spatial Analyst ModelBuilder, an interactive model diagram was constructed incorporating various spatial processes, such as buffering, proximity, and weighted overlays. A cave potential surface was generated by weighting proximity to certain features, such as known entrances and blowholes, and combining these derived cave potential surfaces using weighted overlays with other factors, such as geology, potentiometric surfaces, and current cave extents (Fig. 6). In addition, the volumetric constraints for cave potential were further defined by generating 3D surfaces that represented the limiting bounds of the intersection of the Madison Limestone along its strike and dip with the upper and lower limits of the historic and present water table elevations. Area calculations using the GIS were made of the known extent of the cave and the potential area for cave development, and these were used

to calculate the potential cave length based on current parameters.

DISCUSSION

An estimation of the potential extent and surveyable length of Wind Cave and a means to address the Wind/Jewel connection theory constitute the main benefit of this model. Although this exercise was also instigated because managers can not wait until a cave of this magnitude has been completely surveyed to develop their management policies, it was realized that this model has limitations.

Developing the model demonstrated that potential cave to the NE would encounter the water table, which would limit humanly accessible passage. It also demonstrated that to the SW, minor structural and erosional features would be encountered. Although these may limit humanly accessible cave or even cave development in those directions, neither would necessarily prevent them.

Recognizing the management limitations of the Wind Cave Potential Map, Wind Cave National Park has chosen to manage any surface activities above the surface exposures of the Madison Limestone or within the cave and karst watersheds of the limestone, the same way they would manage activities directly above known cave. This policy is based on the assumption that the potential exists for other sizeable caves to exist in other areas of the park or for Wind Cave to extend beyond the likely maximum boundaries identified during this project. Indeed, a blowing well was found in the north part of the Park, blowing caves exist to the southeast of the Park, and there are numerous smaller caves scattered throughout the Park.

The Wind Cave Potential Map has shown that the US Forest Service of the Department of Agriculture manages most of the potential area that falls outside of the Park. Although a minor portion falls either under private lands or down dip from those lands, the probability that the cave extends near these areas is minor. Analysis of the two Wind/Jewel Cave connection hypotheses resulted in the conclusion that either type of connection is an unlikely scenario, although such a connection could not be totally eliminated as a possibility.

Once the analysis had been completed, we used the buffers and overlays to draw an outline around the area that represents the likely maximum extent of Wind Cave, creating the Wind Cave Potential Map. Approximately 97% of those boundaries fall inside of the current boundaries of Wind Cave National Park (Fig. 6). The current boundaries of the cave were found to be 1/10th of the area of the total potential of the cave, as identified by this exercise.

By calculating passage density for the current cave boundaries and then for the maximum potential boundaries, a minimum and maximum potential surveyable length was calculated for Wind Cave. Because passage density varies among various parts of the cave, we divided the cave into four zones of similar passage densities, the North, South, Lakes, and

Southern Comfort zones. We then identified a fairly complete surveyed part of each zone. After applying those survey lengths throughout each of the zones and then adding the four zones together, we predicted that the cave could have around 400 km of surveyable passage, if the cave is not extended beyond the current boundaries. If the cave is extended to all edges of the potential boundary, Wind Cave could have nearly 1800 km of surveyable passage, assuming similar passage density throughout the potential area. Since the current 166 km of survey represents no more than 40% of the minimum predicted length of the cave or as little as 9% of the maximum predicted length of the cave, it is obvious that a tremendous amount of surveyable passage remains in the system. However, based on airflow and cave development patterns, it is unlikely that the cave will continue in all directions to the edge of the identified cave potential boundaries; and even if it did, it is unlikely that cavers would be able to physically push the cave to those boundaries.

What should be noted is that this cave potential map only reflects the *likely* maximum extent of Wind Cave. For the southwest boundary, it does not preclude the possibility that the cave could extend beyond the identified boundary, it simply states that this is unlikely to happen based on our current understanding of how the cave formed and the geology of the area. Likewise, for the northeast boundary, it does not preclude the possibility that a significant portion of the cave in that particular direction is not water-filled. Thus, our calculations are limited to the potential air-filled portion of the cave, which points out the limitation of using this model as a management tool. In the future, the cave potential boundaries will likely be modified as we learn more about the limiting factors that determined the morphological shape and extent of Wind Cave and as we gather more data from the survey of the cave.

It should be pointed out that this cave potential model can not replace actual survey and inventory work in the cave for several reasons: 1) this is a simplified theoretical cave model; 2) only in-cave survey can identify point source impacts; and 3) a more complete survey and inventory will strengthen the speleogenetic theory on the development of the cave and the understanding of the hydrology of the region. Survey work, even in the interior of Wind Cave constantly makes new scientific discoveries that add to the Wind Cave knowledge base. If every effort is made to minimize the impact from survey work, the benefits outweigh the limited impact from those activities.

ACKNOWLEDGMENTS

We wish to thank Arthur N. and Margaret Palmer, James A. Nepstad, Dwain Horrocks, David A. Herron, James A. Pisarowicz, Marc J. Ohms, Noah Daniels, Michael E. Wiles, Steve Schremp and Ed Delaney for their verbal comments or written reviews of this article. We also wish to thank Marc J. Ohms, Matthew A. Reece, and Noah Daniels for assisting with

the fieldwork, and Rene Ohms for providing Jewel Cave information.

REFERENCES

- Alexander, C., 1986, Final Report, Hydrologic Study of Jewel Cave/Wind Cave, Cave Resource Management files, Wind Cave National Park, 151 p.
- Bakalowicz, M.J., Ford, D.C., Miller, T.E., Palmer, A.N., & Palmer, M.V., 1987, Thermal genesis of dissolution caves in the Black Hills, South Dakota: Geological Society of America Bulletin, v. 99, no. December, p. 729-738.
- Brown, R., 1964, Exploration in Wind Cave, report of the 1959 expedition to Wind Cave, National Speleological Society, 47 p.
- Carter, J., & Driscoll, D.G., 2001, Hydrologic budget for the Madison and Minnelusa Aquifers, Black Hills of South Dakota and Wyoming, water years 1987-1996: USGS, Water-Resources Investigation Report 01-4119, 53 p.
- Conn, H.W., 1966, Barometric wind in Wind and Jewel Caves, South Dakota: National Speleological Society Bulletin, v. 28, no. 2, p. 55-69.
- Davis, D., 1989, Helictite bushes-A subaqueous speleothem?: National Speleological Society Bulletin, v. 51, p. 120-124.
- Fish, L., 2002, COMPASS, www.fountainware.com/compass/
- Ford, D.C., 1989, Features of the genesis of Jewel Cave and Wind Cave, Black Hills, South Dakota: National Speleological Society Bulletin, v. 51, p. 100-110.
- Ford, D.C., 1993, Uranium-series dating of the draining of an aquifer: The example of Wind Cave, Black Hills, South Dakota: Geological Society of America Bulletin, v. 105, p. 241-250.
- Howard, A.D., 1964, A model for cavern development under artesian groundwater flow, with special reference to the Black Hills: National Speleological Society Bulletin, v. 26, p. 7-16.
- La Borde, M., 1960, Project report, Wind Cave, underground passages, Garden of Eden - Elk's Room Traverse, Colorado Grotto, National Speleological Society, 14 p.
- McDonald, A.F., 1891, Unpublished diary in the Wind Cave National Park museum collection, 61 p.
- Nepstad, J., 1996, Study plan for FY96 watershed protection program funding study petroleum pollution: Unpublished proposal, Cave Resource Management files: Wind Cave National Park, p. 4.
- Palmer, A.N., 1981, Geology of Wind Cave, Wind Cave National Park, South Dakota: Hot Springs, SD, Wind Cave National History Association, 44 p.
- Palmer, A.N., 1987, Geologic interpretation of Wind and Jewel Caves: Wind Cave National Park, Unpublished report, Cave Resource Management files, 2 p.
- Palmer, A.N., & Palmer, P., 1989, Geologic history of the Black Hills caves, South Dakota: National Speleological Society Bulletin, v. 51, p. 72-99.
- Palmer, A.N., 2000, Speleogenesis of the Black Hills maze caves, South Dakota, USA, in Klimchouk, A.B., Ford, D.C., Palmer, A.N., & Dreybrodt, W., ed., Speleogenesis, evolution of karst aquifers, p. 274-281.
- Scheltens, J., 1970, Wind Cave expedition: Windy City Grotto, National Speleological Society: Wind Cave National Park, Cave Resource Management files, 16 p.
- USGS, 1957, Wind Cave National Park and vicinity, S. Dak.: 1:24,000, Contour Interval 20 and 40 feet.
- Venezky, D., 1994, An exploration of development based ground water contamination at Wind Cave: Wind Cave National Park, Cave Resource Management files, 14 p.
- Willsie, M., 1902, Unpublished report: Wind Cave National Park, Cave Resource Management files.
- Zerr, B., 1972, Unpublished diagrams, Paha Sapa Grotto files: Rapid City, SD, National Speleological Society.
- Zerr, B., 2001, Unpublished email communications: Wind Cave National Park, Cave Resource Management files.

HURRICANE CRAWL CAVE: A GIS-BASED CAVE MANAGEMENT PLAN ANALYSIS AND REVIEW

JOEL DESPAIN

Sequoia and Kings Canyon National Parks, 47050 Sierra Drive, Three Rivers, CA 93271 USA, joel_despain@nps.gov

SHANE FRYER

Hoffman Environmental Research Institute, Department of Geography and Geology, Western Kentucky University, 1 Big Red Way, Bowling Green, KY 42101USA

With the goal of minimizing impact to rare, fragile, and significant cave resources, this paper compares the location of such features in Hurricane Crawl Cave, Sequoia National Park, California, to the open and unrestricted areas of the cave as defined by the Hurricane Crawl Cave Management Plan. Geographic information systems (GIS) analysis provided statistical data on the relationship of chosen key features and resources to caver travel corridors and open areas, and thus, allowed an unbiased assessment of the appropriateness of travel closures and management restrictions. Using buffer analysis around these features, we determined that the existing plan for the cave addresses the protection of cave speleothems and paleontological features, but is not adequate in the protection of areas of biological significance.

Nearly pristine Hurricane Crawl Cave lies in a roof pendant of Mesozoic marble in the Sierra Nevada of California (Sisson 1994). The cave is one of 212 documented in Sequoia and Kings Canyon National Parks. Hurricane has 3132 m of surveyed passages, a depth of 72 m, and lies between 1320 and 1400 m msl. Its two entrances formed near the cave stream's resurgence and insurgence, respectively (Despain 2000). Hurricane developed through the piracy of a surface stream that recharges on plutonic rocks in areas of coniferous forest rising as much as 850 m above the cave (USGS 1993). The piracy occurred beneath a ridge that provides the cave with more than 150 m of overburden. The cave features breakdown, anastomotic and branchwork mazes, and paleo-phreatic upper levels 18 - 27 m above the existing vadose streams. These streams have created thousands of meters of deep, narrow canyons (Fig. 1) (Despain 2000).

The cave was found in 1988, 98 years after the area was set aside as part of Sequoia National Park. This has allowed Hurricane to be managed carefully since its discovery. The cave was closed in 1990, pending a biological evaluation, and the first management plan for Hurricane was completed in 1992. This plan was revised in 1998. Hurricane Crawl contains exceptional resources including large and delicate examples of unusual cave formations, likely endemic species, and paleontological remains. Currently, the cave has 17 closed areas and 15 sections of flagged trail as well as additional restrictions in numerous areas concerning clothing and footwear. Also, two areas considered in the subsequent analysis are restricted to one trip per year as an extra measure to protect these areas' features (Despain 1998).

The speleothems in Hurricane are exceptional. The Star Chamber upper level contains 0.3-m long vermiform and filamental helictites in profuse displays. Folia have been noted in five areas. One location is currently active at base level while another lies 25 m above the cave stream. Approximately 30

shields occur in groups in several areas of the cave. Most of these areas are in upper-level phreatic passages. The largest shields are more than 3 m in diameter (Fig. 2).

Many GIS applications in cave and karst studies examine surface relationships to karst hydrology or cave passage relationships to surface features (e.g., Szukalski & Yocum 1998; Stokes *et al.* 1999; Call *et al.* 1999; Glennon & Groves 1999; Pfaff *et al.* 2000). The dataset used in this paper examines the spatial relations of in-cave features to caver travel areas and trails. The detailed mapping and analysis that follows is probably not appropriate or necessary in most caves. This study focuses on a cave with a high level of protection, management focus, and a large number of rare and fragile features and endemic species (Despain 1998). The vast majority of caves do not have this abundance of rare formations or unique animals. However, similar analysis could be helpful in the sensitive and appropriate development of new commercial caves or the adjustment of existing trails, utilities and other infrastructure components at current commercial caves. In addition, caves with particularly rare and sensitive features or animals might also benefit from this type of GIS analysis. Such analysis could ensure that a cave's most fragile and significant features lie within closed or restricted areas.

Three types of features in Hurricane Crawl will be examined in the following analysis: 1) rare and delicate mineralogical features; 2) paleontological features, which constitute bones of unknown age and species; 3) biologically significant locations and areas of key habitat.

METHODOLOGY - DETERMINATION OF FEATURES TO BE INCLUDED IN THE ANALYSIS

This paper attempts to recognize the key Hurricane Crawl features deserving protection and to determine what percentage of these features are close to approved travel routes

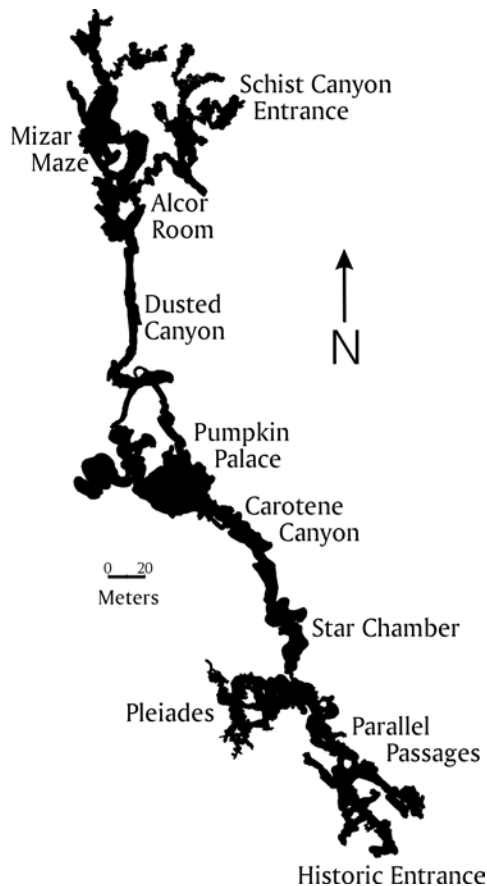


Figure 1. Hurricane Crawl Cave map, plan view.

through the cave, thus in danger of being broken or disturbed. To do this requires placing qualitative values on cave features and resources.

The relative rarity of cave formations is difficult to determine, yet this remains an important factor in assigning cave passage closures and restrictions in Sequoia, Kings Canyon, and other protected areas. Very few caves have undergone careful resource inventory and very few of these data have been published. Available for potential comparison and analysis are data from a few other caves located across the United States, including Carlsbad Caverns National Park, Jewel Cave National Monument, and Wind Cave National Park (DuChene 1997; Horrocks 2002; Ohms 2002). However, even these data present information on only a few chemically unusual caves (Palmer 1999; Jagnow *et al* 2000) and provide no comprehensive information on caves across the nation or a region. While a cave-by-cave comparison is possible using the results at these National Parks, no overall determinations of speleothem rarity are possible.

Hill and Forti (1997) make inferences concerning the relative commonness of cave features on a global scale, but provide little specific data based upon cave inventories and resource assessments. Comparison of commonness may also

be inferred from local data. Inventory work within Sequoia and Kings Canyon provide data for an overview of the features in many park caves, including Crystal Sequoia, Soldiers, Cirque, Clough, Weisraum, Carmoe Crevice, White Chief, and, to a more limited extent, Lilburn caves (Despain & Stock 1998; Vesely & Stock 1998; Despain 2001; Fryer 2001). These data also include all examples of many features (shields and helictites) that have been documented in all known park caves (Despain & Fryer 2001). In light of the lack of data on national and global occurrences of features, the study made comparisons and the determination of relative rareness using local data from the inventory of other Sequoia and Kings Canyon National Parks caves.

The determination of rareness also considered the size of individual cave mineral features in Sequoia and Kings Canyon, because larger examples of many speleothems are less common (Despain & Stock 1998; Vesely & Stock 1998; Despain 2001; Fryer 2001). Thus, the analysis included only individual larger examples of some features (such as shields).

Features determined to be rare for this analysis and the reason for that determination are below. Out of the 212 caves in the two parks, folia are found only in Hurricane Crawl, which qualifies all of these speleothems as locally rare. Pendulites occur as only poor examples in two locations in two other park caves and were, thus, included for proximity analysis in the rare category. Filamental helictites (Hill & Forti 1997) are known from only one location in the park outside of Hurricane Crawl. They were also included (Fig. 3). Raft cones, known from one other park cave, and dogtooth spar crystals, known from three other park caves, but with only one or two examples each, were included. Gypsum and hydromagnesite, found in two and three other park caves, respectively, are locally rare and, thus, included. Shields, known from six park caves, including at least 96 in Crystal Cave, were not included. However, Hurricane's largest shields, more than 2 m in diameter and the largest in the parks, were included. Other features included due to size are vermiform helictites longer than 10 cm, which are only found in Hurricane within the parks; stalactites longer than 3 m, found only in Hurricane Crawl; curtains longer than 3 m, found in two other park caves; rimstone dams more than 2 m across, found in three other park caves and soda straws longer than 1 m, currently found only in Hurricane Crawl (Table 1).

Individual cave feature data points in the proximity analysis for rare features included pendulites, raft cones, and all size-dependent features, except pools larger than 2 m. Data points for folia, filamental helictites, gypsum, and hydromagnesite deposits denote areas where the features exist, not specific individuals. In this instance, data points were created throughout the area of occurrence and have overlapping proximity buffers. Polygons represent pools larger than 2 m across due to their large size and location on the floors.

The protection of fragile features constitutes another concern in the management of Hurricane Crawl. Analysis reveals the relationship between travel corridors and the location of

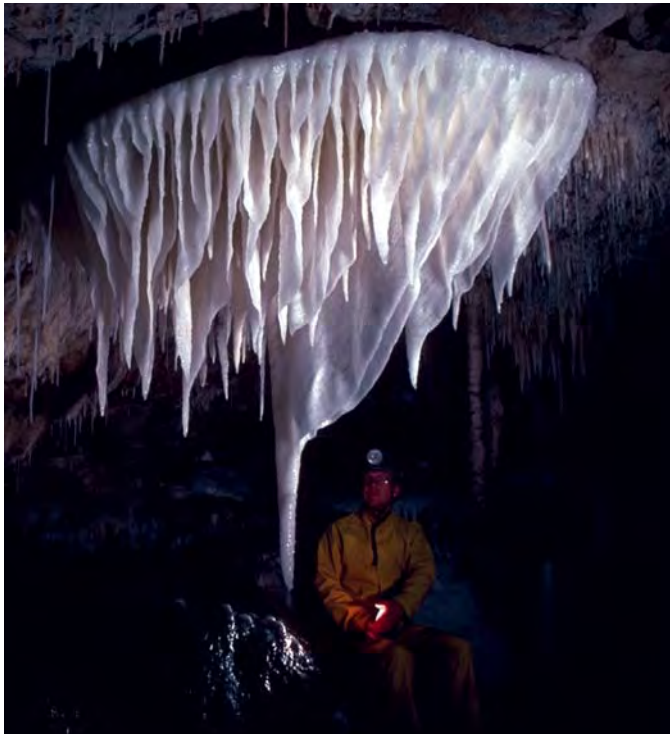


Figure 2. Large shield in the Star Chamber area of Hurricane Crawl Cave. This speleothem was included in the GIS analysis due its large size.



Figure 3. Filamental and vermiform helictites in the Pleiades area of Hurricane Crawl Cave. Filamental helictites were included in the GIS analysis due to their rarity in Sequoia and Kings Canyon, while vermiform helictites were included due to their fragility.

fragile, potentially breakable cave features. As avoiding damage to rare features is particularly important, certain routes through the cave may minimize damage and be the most appropriate to use. Formations were considered fragile if they can be damaged or destroyed through a single interaction with

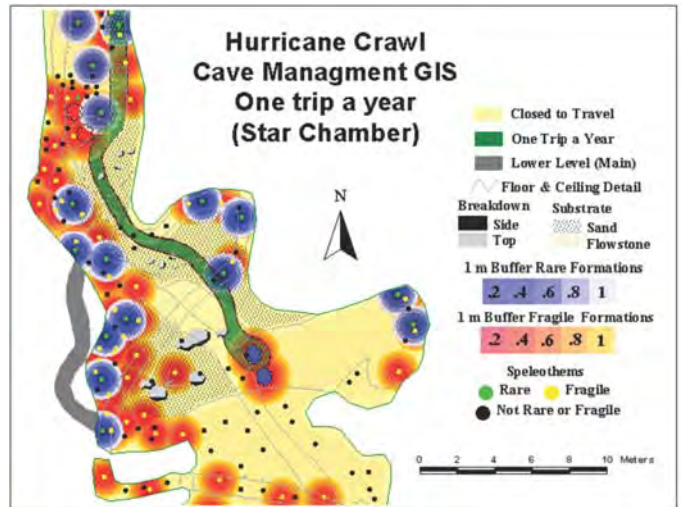


Figure 4: The upper-level Star Chamber area of Hurricane Crawl showing a segment of one-trip-per-year trail. Notice how the trail generally avoids both rare and fragile features.

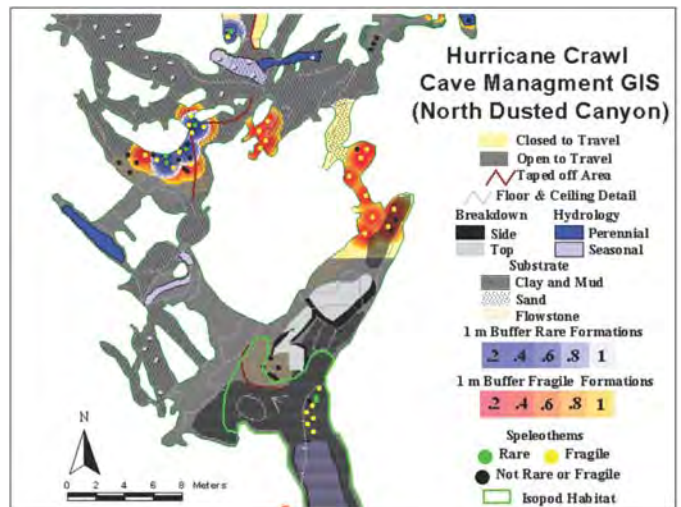


Figure 5. The north end of Dusted Canyon and the beginning of Mizar Maze. Notice the closed areas with fragile speleothems and open areas both with and without flagging but with fragile and rare speleothems. These locations are possible places for new closures and restrictions. Also notice the terrestrial isopod habitat (area with food sources) and the lack of closures or restrictions to protect these endemic animals. Finally, an area of fragile formations was removed from the study because they occur in the ceiling of the passage and are in no danger.

a caver. Formations used in proximity analysis for their fragility include all helictites, soda straws, frostwork aragonite, calcite ice, all rimstone dams, and cave pearls (Table 1). All data points in the fragility analysis represent groups or clusters of the same type of feature. Points are distributed across an area

Table 1: Secondary speleothems included for analysis, the reason for that inclusion, and how features are represented in the GIS. Rare determinations are based upon park-wide occurrences.

Included Feature	How represented	Number of points or polygons in the analysis	Category and reason for inclusion
folia	points represent groups of individual features	15	Rare - occurs only in Hurricane Crawl
pendulites	points represent each feature	32	Rare - occurs in two other park caves
filamental helictites	points represent groups of individual features	30	Rare - occurs in one other location in another park cave
raft cones	points represent each feature	8	Rare - occurs in one other park cave
dogtooth spar	points represent groups of individual features	10	Rare - known from three park caves with one occurrence each
gypsum	points represent groups of individual features	17	Rare - occurs in two other park caves
hydromagnesite	points represent groups of individual features	20	Rare - occurs in three other park caves
shields more than 2 m in diameter	points represent each feature	4	Rare due to size - occurs only in Hurricane Crawl

of occurrence so that the features have overlapping proximity buffers. Points or polygons included in the analysis that represent rare or fragile speleothems totaled 1252.

Paleontological features consist of individual skeletons in alcoves along narrow canyons and at least six skeletons in the Alcor Room. All skeletons appear to be small mammals up to 40 cm long (Table 2) (Despain 2000). They may reveal the previous presence of now extinct animals in the area near the cave, or may illuminate animal behavior that led to these individuals' deaths underground. In addition, all paleontological remains in National Park areas are to be protected and carefully managed. (NPS 1994: 156) Thus, all 8 skeletons known in the cave make up points in this analysis.

Two biologists who work with invertebrates visited Hurricane Crawl in 1991. W. Calvin Welbourn, from Ohio State University collected 24 invertebrates in the cave in July 1991. From this collection, he reported that the cave had both aquatic and terrestrial troglobitic isopods, a troglobitic millipede, and an eyeless centipede. All of these species are possible endemic and potentially new to science (Welbourn 1991). Taxonomy on these species has not been completed. In September 1991, Ubick (1991) reported a *Pimoa* sp. spider from twilight areas of the cave and possibly *Nesticus silvestrii* spiders throughout the cave. In 1999 and 2000, biological inventory plots were established in the cave and were assessed during the summers of 1999, 2000, and 2001 using the protocol of Poulson & Kane (1977) (Despain & Fryer 2002).

While these limited biological investigations provided important information concerning the biology and ecology of Hurricane Crawl, comprehensive information on the variety of species, habitat requirements and ecology is lacking. Nevertheless, while more comprehensive work is pending, management decisions and plans to protect the cave's features went forward. For endemic cave species, the need to protect these animals in a national park setting is clear (NPS 1994: 137). Food inputs into Hurricane Crawl, as in most cave environments, are very limited. Very few bats have been seen in the cave and no bat guano piles exist. Rodent feces are only in passages adjacent to entrances. However, roots are in areas over 100 m from entrances and in the Pleiades area of the cave. The cave streams also flood annually and transport organic matter

into the cave. This organic material accompanies fine, flood-deposited sediments in wide passages and coarser-grained sediments on stream bottoms. Flood deposition is most common in Pumpkin Palace, the largest room in the cave, and in the Mizar Maze complex at the north end of Hurricane (Despain 2000). The cave's two species of isopods are closely associated with these food sources. Welbourn noted aquatic isopods in sections of the cave stream floored by cobbles, sediments and organic matter, but not in sections of streams flowing across areas of clean-washed bedrock or flowstone (Welbourn 1991). In over 1000 m of stream passage in Hurricane, <10% are floored by sediments, primarily in Pumpkin Palace. Terrestrial isopods have been found in streamside plots with organic matter in Pumpkin Palace and the Mizars, but never in any other location, even by casual observations.

With the limited information available on these species and their habitat requirements, areas in the cave defined as biologically significant for this study are those locations with the potential food sources described in Table 2. Disturbance of these areas could lead to the trampling of the animals and the destruction of their food supply. These areas were incorporated in the GIS analysis as 16 polygons.

GIS DATA

Data for this project have been gathered through more than ten years of fieldwork. The cave's original survey included a specific effort to document all features, particularly mineralogical features. Information from the cave's original survey notes was augmented by field checking existing maps and during visits by biologists and geologists. Maps of the cave were originally created using the CorelDraw! 7 graphics package. These maps were converted into .dxf files and imported into ArcView, where they were organized, converted to ArcView.shp files, and geographically referenced.

The Hurricane Crawl GIS consists of eleven themes expressed on four levels including an upper level, with many heavily decorated rooms and passages, an extensive main level, and two small underlying levels. The themes include wall location and composition data; a floor theme expressing the cave's total extent; a detail theme showing slopes, drop-

offs and changes in ceiling height; a sediment theme for floor composition; a hydrology theme for streams and pools, and a breakdown and cobble theme. Additional themes include a speleothem theme composed of 44 types of secondary speleothems. A route theme shows travel corridors as polygons, and flagging tape and closed areas from the implemented Hurricane Crawl Cave Management Plan (Despain 1998). Additional themes developed for this analysis include point data for paleontological features and polygons for areas of key food availability within the cave.

Initial review of the GIS images revealed limitations to the two-dimensional rendering of the three-dimensional cave. In the cave's tall canyons, travel corridors that lie many meters below fragile speleothems were shown to intersect those deposits' buffers. In these cases, these formations were removed from further analysis (Fig 5). This problem did not apply to any of the paleontology points or biology polygons.

An additional concern with this data set was the size of the proximity buffer. How far should a given feature be from a trail and open areas to be considered not at risk and, therefore, protected? For this analysis, a 1-m buffer was used around speleothem and paleontologic points. We believe that this area around a feature will protect it from breakage or disturbance from passing cavers. No buffers were used around polygons denoting biologically significant sites.

GIS ANALYSIS

The analysis for this paper was done as grid analysis of the trail and open areas of Hurricane Crawl Cave compared to biology polygons and to 1 m proximity buffers around rare and fragile formation and paleontology points. Grid resolution in the analyzed areas was 5 cm² creating 2,793,322 data points for analysis. The total two-dimensional floor area of Hurricane Crawl Cave is 7023 m². The trail and open areas are 2454 m² or 35% of the cave.

The area of open trails in the cave that lie within 1 m of fragile mineral deposits is 11.9%, while the area of the cave trail that lies within 1 m of rare speleothems equals 2.3% of the open trail area. Risks threaten 10.8% of the cave's total fragile mineralogical resources and 7.1% of rare features because they lie within 1 m of the open trail (Table 3).

Areas of the cave limited to one trip per year contain a larger percentage of rare and fragile features. One-trip-per-year trails make up 5.2% of open areas in Hurricane Crawl. Of the areas of the cave open to one-trip-per-year, 16.7% are within 1 m of fragile speleothems, and the 1-m analysis buffer around rare features occupies 4.9% of the same section of the cave. In this case, 2.1% of the cave's total fragile mineralogical resources and 2.1% of rare features are at possible risk because they lie within 1 m of the one-trip-per-year trail (Fig. 4). These statistics imply that areas selected for one trip per year are more sensitive with a higher percentage of proximal rare and fragile features. Thus, these areas should be managed using greater restrictions compared to open trail areas.

At any given point throughout the entire cave, there is a 33.7% chance of being within 1 m of a fragile speleothem and a 10.2% chance of being within 1 m of a rare speleothem. For the trail as a whole (one-trip-per-year and open), 12.5% lies within 1 m of fragile speleothems and 2.6% is within 1 m of rare features. Thus, the trail lies in areas that are generally more free of rare and fragile formations than the cave as a whole. This implies that the total trail (including both once per year and open areas) was well chosen to avoid both fragile and rare features.

One-meter buffers around points denoting paleontological resources remain overlap 0.17% of the trail. This compares to 0.49% of the cave as a whole that lies within 1 m of paleontological resources. A total of 16% of the cave's paleontological resources lie within 1 m of open trails.

Food source and key habitat polygons for cave-adapted animals fell within 14.2% of the trail area (Fig. 5). This compares to 6% that these areas occupy within the cave as a whole. Thus, one is more likely to encounter a biologically significant area while traveling the designated trail compared to simply wandering through the cave as a whole. In addition, a total of 84% of the areas of the cave recognized to be biologically significant fall within the total trail and open areas of Hurricane Crawl (Table 4). Only 16% of the cave's biologically important sites are protected by the existing management plan.

DISCUSSION

Overall, the travel corridors and open areas within Hurricane Crawl Cave generally avoid rare and fragile cave formations. Slight adjustments to the trail routes may improve the percentage of rare and fragile features found within 1 m of the trail. Changes or alterations to existing management plans often require visits to areas under consideration for management changes, creating the potential for damage to the cave's features. However, using the existing GIS we can test other possible trail routes and open areas simply through the use of the database. Uncertainty about plan changes and trial-and-error alterations to the management of the cave might also be minimized.

Routes through the cave infringe more strongly upon currently recognized areas of biological concern and paleontological features. Based on our findings, future management of the cave will require that trails and closed areas be reconsidered. Some key biological areas, such as the north end of Dusted Canyon, and passages near both entrances may be closed in the future. In other areas, trails may be narrowed or shortened. In addition, biological work in the future may reveal other areas of concern that should be considered in the management of Hurricane Crawl. While the work of Welbourn, Ubick, and the park inventory plots do identify key areas of biological concern, these should be considered a minimum of what might be appropriate to protect in the cave. Additional data will likely reveal other areas of concern. In addition, travel routes near paleontological features may be moved or animal remains may

be carefully and obviously flagged to encourage cavers to avoid them.

In this instance, with detailed inventory data available, GIS proved to be an effective tool for the objective review of a specific cave management plan. Since this analysis examined the spatial relationships of more than 1200 cave features compared to caver travel routes, GIS was the only option available for a complete analysis of the data. We hoped and believed that the existing management plan delineated appropriate rules, restrictions, and closures to protect the cave's key features. The GIS analysis revealed that this is only partially true. We will review and examine other existing management plans for park caves using this same analysis in the future.

REFERENCES

- Call, G.K., Aley T., Campbell, D.L. & Farr, J., 1999, Use of dye tracing and recharge area delineation in cave protection and conservation on private land, Proceedings 1997 National Cave Management Symposium: Bellingham, WA, National Cave Management Symposium Steering Committee, p. 23-27.
- Despain, J.D., 1998, Hurricane Crawl cave management plan, Sequoia and Kings Canyon National Parks cave management plan, unpublished: Sequoia and Kings Canyon National Park files, p. Appendix G.
- Despain, J.D., 2000, Plan and profile maps of Hurricane Crawl Cave, Sequoia National Park, California: unpublished, Sequoia and Kings Canyon National Park files, 2 sheets.
- Despain, J.D., 2001, Plan and profile maps of Soldiers Cave, Sequoia National Park, California: unpublished, Sequoia and Kings Canyon National Park files, 2 sheets.
- Despain, J.D. & Fryer, S., 2001, Cave mineralogical features database, unpublished, Sequoia and Kings Canyon National Park files.
- Despain, J.D. & Fryer, S., 2002, Hurricane Crawl biological monitoring plots database, unpublished, Sequoia and Kings Canyon National Park files.
- Despain, J.D. & Stock, G.M., 1998, Plan and profile maps of Crystal Cave, Sequoia National Park: unpublished, Sequoia and Kings Canyon National Park files, 5 sheets.
- DuChene, H.R., 1997, Lechuguilla Cave, New Mexico, USA, in Hill C. A. & Forti, P., ed., Cave minerals of the world, 2nd ed: Huntsville, AL, National Speleological Society, p. 343-350.
- Fryer, S., 2001, Plan map of Clough Cave, Sequoia National Park, California: unpublished, Sequoia and Kings Canyon National Park files, 1 sheet.
- Glennon, J. & Groves, C., 1999, Evolving GIS capabilities for managing cave and karst resources, presentation, in 12th National cave and karst management symposium. Chatanooga, TN.
- Hill C.A. & Forti, P., 1997, Cave minerals of the world, 2nd ed.: Huntsville, Alabama, National Speleological Society, 463 p.
- Horrocks, R. & Szukalski, B., 2002, Using geographic information systems to develop a cave potential map for Wind Cave: Journal of Cave and Karst Studies, v. 64, no. 1, p. 63-70.
- Jagnow, D.H., Hill, C.A., Davis, D.G., DuChene, H.R., Cunningham, K.I., Northup, D.E. & Queen J.M., 2000, History of the sulfuric acid theory of speleogenesis in the Guadalupe Mountains, New Mexico: Journal of Cave and Karst Studies, v. 62, p. 54-59.
- Ohms, R.M. & Reece, M., 2002, Using GIS to manage two large cave systems, Wind and Jewel Caves, South Dakota: Journal of Cave and Karst Studies, v. 64, no. 1, p. 4-8.
- Palmer, A.N., 1999, Jewel Cave, A gift from the past: Hot Springs, SD, Black Hills Park and Forest Association.
- Pfaff, R., Glennon, J., Groves, C., Meiman, J. & Fry J., 2000, Geographic information systems as a tool for the protection of the Mammoth Cave karst aquifer, Kentucky, Proceedings of the 8th Mammoth Cave Science Conference, Mammoth Cave, Kentucky: Mammoth Cave, KY, National Park Service, p. 89-99.
- Poulson, T.L. & Kane, T.C., 1977, Ecological diversity and stability: Principles and management, Proceedings 1976 National Cave Management Symposium: Albuquerque, NM, Speleobooks, p. 18-21.
- NPS, 1994, Natural resource management guidelines NPS 77: Washington D.C., National Park Service.
- Sisson, T.W. & Moore, J.G., 1994, Geologic map of the Giant Forest Quadrangle, Tulare County, California: U.S. Geologic Survey Geologic Quadrangle Map GQ-1751, scale 1:62,500, 1 sheet.
- Stokes, T., Massey, N. & Griffiths, P., 1999, Digital cave/karst potential mapping in northern Vancouver Island: A strategic forestry planning tool, Proceedings 1997 National Cave Management Symposium: Bellingham, WA, National Cave Management Symposium Steering Committee, p. 170-180.
- Szukalski, B. & Yocum, M., 1998, Cave and karst GIS workshop workbook, 14th National Cave and Karst Management Symposium.
- Ubick, D., 1991, unpublished letter, to Despain, J., Sequoia and Kings Canyon National Park files.
- USGS, 1993, Giant Forest Quadrangle California - Tulare County: U.S. Geological Survey 7.5 minute series topographic map 36118-E7-TF-024, 1:24,000, 1 sheet.
- Vesely, C.A. & Stock, G.M., 1998, Cave inventory protocol for caves in Sequoia and Kings Canyon National Parks: Monrovia, California, Cave Research Foundation, 94 p.
- Welbourn, W.C., 1991, unpublished letter, to Despain, J., Sequoia and Kings Canyon National Park files.

PUBLIC DATASETS INTEGRATED WITH GIS AND 3-D VISUALIZATION HELP EXPAND SUBSURFACE CONCEPTUAL MODEL

TERRI L. PHELAN

1171 N. Maxwell Dr., Fayetteville, AR 72703 USA tphelan@arkansasusa.com

Public domain water well drilling logs were used to construct a 3-D visualization of the subsurface in a karst terrain. Subsurface displacements seen in the 3-D visualization model were shown to correlate with surface topography in the Digital Elevation Model (DEM). This methodology could improve the effectiveness of limited funding by using public datasets to contribute to conceptual hydrogeologic models. It could also identify areas that merit additional investigation which might have gone unnoticed otherwise.

Physical characteristics of the surface and subsurface environment typically affect water movement, levels, and quality. Regional population and development continue to increase in northwest Arkansas, causing changes in landuse practices. The unconfined carbonate units near the surface are subject to potential sources of pollution of groundwater caused by land-use changes. Complexities of surface-to-groundwater transport and groundwater movement are increased in karst terrain. For example, sinkholes funnel water into subsurface flow systems, while faults act as barriers or conduits for water movement. Carbonate lithologies dissolve along bedding planes, fractures, and other paths of least resistance, affecting routes of movement and development of secondary permeability. However, it has also been shown that water movement may be independent of the regional structure, and movement from an area of recharge splay laterally in all directions (Stringfield *et al.* 1979). LeGrand (1979) asserted that increased understanding of a fractured-rock system such as carbonate aquifers that are within several hundred meters of the surface is accomplished by continual data collection, observations of the system, and by making hydrogeologic inferences that lead to the development of conceptual models. Geologic structure is one factor that strongly influences carbonate rock hydrogeology. When this study began, the Arkansas Geological Commission (AGC) file contained ~2100 wells for Washington County and ~3100 for Benton County. Water well users included private rural residents, confined animal operations, RV parks, small communities, and businesses and industry. A cost-effective methodology for modeling subsurface structure using these wells could greatly contribute to the conceptual understanding of local and regional groundwater pathways by increasing the database of information within the framework of limited funding resources and manpower.

GIS facilitates data management, access, and analysis (Star & Estes 1990; Tsihrintzis *et al.* 1996). These abilities extend the research knowledge-base by allowing for the continued acquisition of data to be built on what was previously acquired, thereby improving understanding (Waite & Thomson 1993). Since earth-system processes can be exceedingly complex when trying to solve environment-related questions, spatial

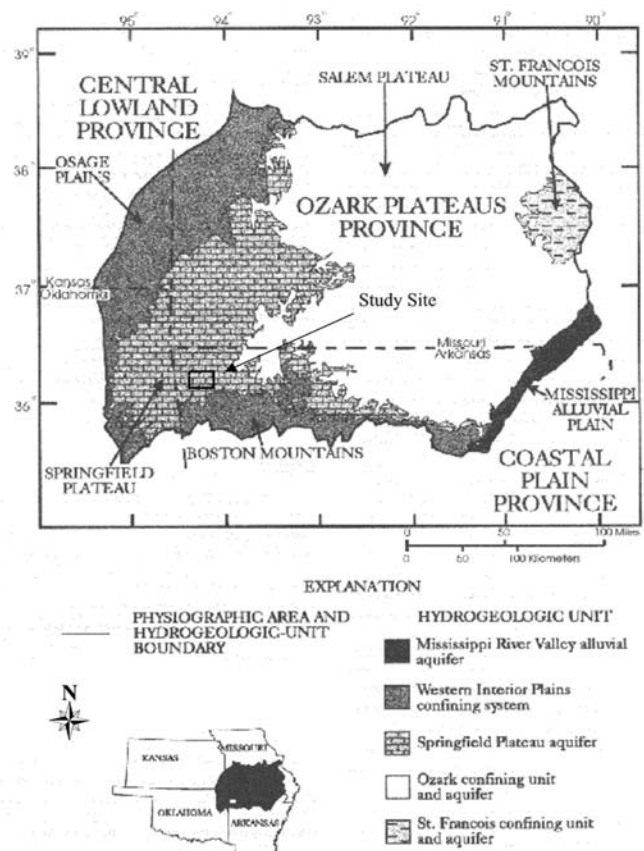


Figure 1. Regional physiographic area and hydrogeologic environment surrounding the study site (modified after Adamski 1997).

representation of them is critical for clarity (Parks 1993). The communication of information can be accomplished in a variety of ways, but visualization provides the most effective manner for conveying complex spatial relationships to the human brain (Bonham-Carter 1996). Additionally, when trying to model land-surface and subsurface hydrogeologic linkages, the inherent complexity of environmental processes is compounded by the fact that they are hidden from view and are,

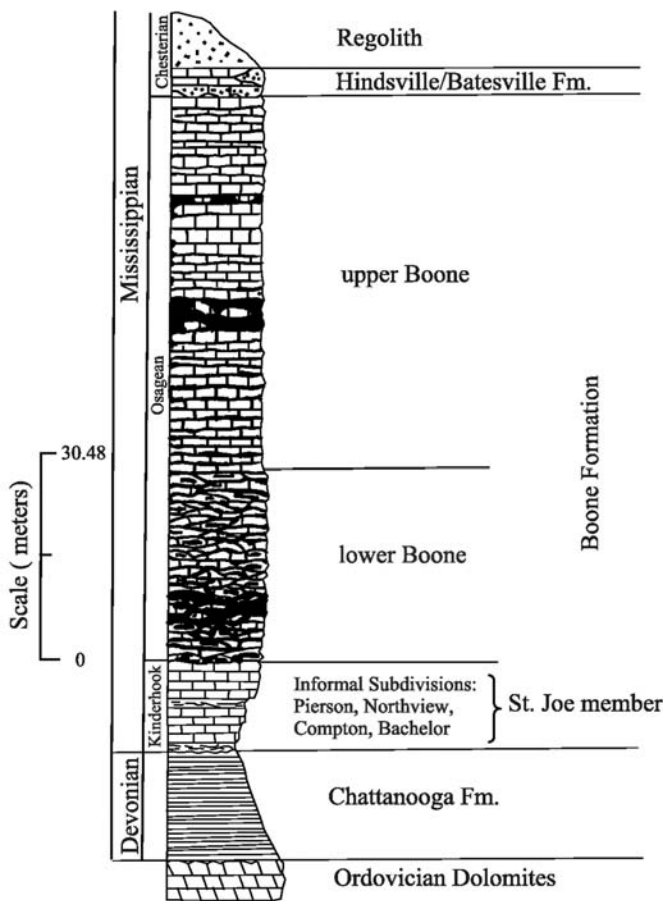


Figure 2. Generalized stratigraphic column for northwest Arkansas (modified after Bartholmey 2001).

thus, more difficult to comprehend or verify. Development of a conceptual model can reveal spatial patterns which might not otherwise be apparent (Bonham-Carter 1996). Furthermore, 2-D models have a limited functionality when attempting to convey location relationships (x and y) in space (z); thus, 3-D models are preferred. Kolm & Downey (1993) and Turner & Kolm (1991) assert that the inability to visualize in three dimensions greatly impairs interpretation of the systems. Maidment (1993) reminds us that coupling both surface and subsurface models provides a more complete understanding of the hydrosphere.

Camp *et al.* (1994) assert that the best information on the subsurface comes from wells. However, hydrogeologic investigations are typically costly and time consuming (Smith & Paradis 1989; Brahana 1997). For example, northwest Arkansas drillers charged ~\$5.00/ft for drilling (with an additional charge of \$1.00/100 ft when the depth passed 800 ft), \$5.50 per casing, and \$200 as the accessory fee (i.e., cost of cement, well cap, and drive shoe) at the time this study was concluded (1999).

Interactive viewing of complex problems is one of the most powerful capabilities of 3-D modeling (Smith & Paradis 1989). As exact subsurface representation is not possible, the

ability to identify geologic conditions and their parameters is the most important constraint in 3-D representation of the hydrogeology of the subsurface (Turner 1989). One of the major processes in characterizing the subsurface is the development of conceptual models from typically sparse datasets. When employing computerized methodologies, the ease of combining various data types is enhanced, and 3-D visualization allows interaction with the datasets so that their spatial relationships are maintained (Turner 1992). This increases the geoscientists' ability to analyze the data.

GEOLOGIC SETTING

The study area is located on the Springfield Plateau of the Ozark Plateaus Province (Fig. 1) in northwest Arkansas and covers portions of southwest Benton County and northwest Washington County. The regional stratigraphy is nearly horizontal but dips slightly ($<1^\circ$) to the south (Howard 1989) and drainage patterns are dendritic. Strata include the Upper Devonian Chattanooga Shale, which acts as the regional confining unit (USGS 1998), and Lower Mississippian St. Joe Member of the Boone Formation (Barlow & Ogden 1982) (Fig. 2). Chattanooga Shale crops out at the surface along streambeds. Limestones dominate 96% of study area surface exposures (Phelan 1999). The area is highly fractured and subject to solution enlargement of joints and fractures (Renken 1998).

METHODOLOGY

Water well log data for March 1973 to August 1997 were obtained from the Arkansas Geological Commission (AGC) in Little Rock, Arkansas. Two basic assumptions were made from the beginning: 1) the drillers were able to differentiate between the major geologic units; and 2) the wells were basically vertical and did not drift significantly. Well log data and locations were entered into a spreadsheet and sorted by geologic unit.

The dataset for this study contained all formats of location description but latitude/longitude was required for use in a GIS. Wells without a provided latitude/longitude had their location field-verified and coordinates were determined with a Trimble GPS Pathfinder Pro-XL™ global positioning system (GPS). GPS measurements could not be performed on some well locations because of restricted access at confined animal operations. When locations were confirmed for these wells, they were placed as accurately as possible on a standard USGS 7.5-minute topographic quadrangle map (datum NAD27) and later digitized.

Geologic units above and below the Chattanooga Shale unit were correlated with the driller's descriptions, and an evaluation was made as to whether or not geologic formations were correctly identified based on the descriptions and thicknesses reported on the log sheet. Each well location was required to contain a depth to the base of the shale. This was

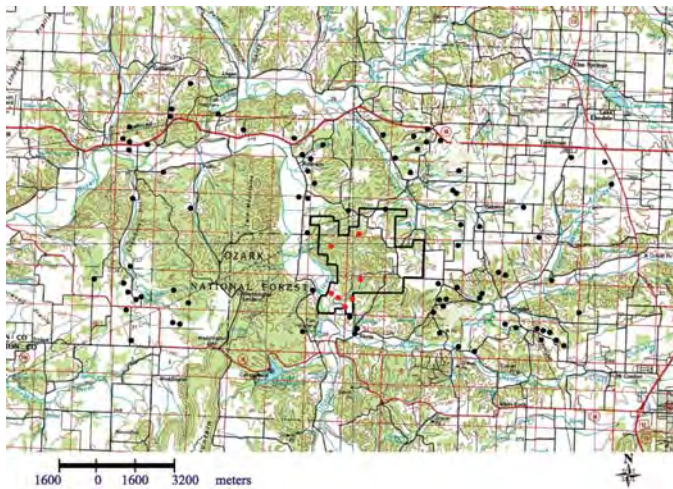


Figure 3. Study area showing water well (black dots) and control well (red dots) locations. Savoy Experimental Watershed property boundary is shown in black outline (modified after Phelan 1999).

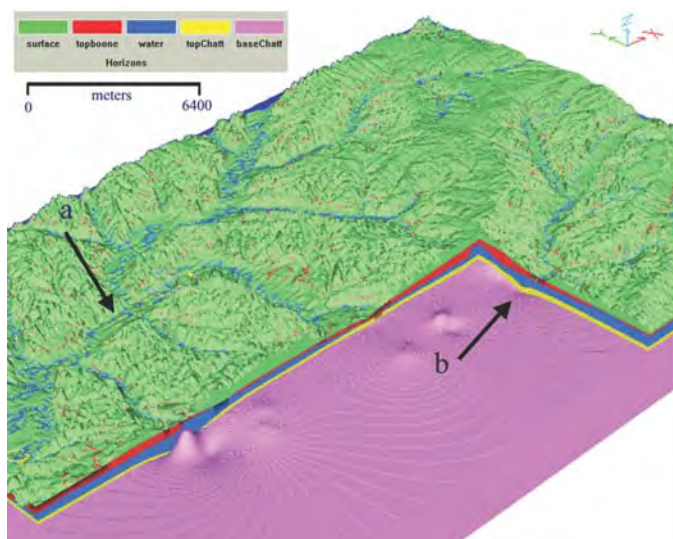


Figure 4. Chair graphic perspective viewed from azimuth 226, declination 55, Z exaggeration = 3. Arrow "a" points to where shale outcrops in the bed of the Illinois River and "b" points to apparent lineament alignment. Note that "Y" axis always points north, corresponds to latitude or northing, "X" corresponds to longitude or easting, and "Z" represents the vertical direction (elevation).

necessary for two reasons: (1) to correctly distinguish by visual means along the specific positions of the carbonate units above and below the Chattanooga Shale; and (2) to maximize the data points obtained with respect to necessary time for field verification of each well location. The initial number of log sheets for the study area totaled 174 records. After evaluating the log records, and after the field verification process eliminated additional wells, the final dataset for the study totaled to

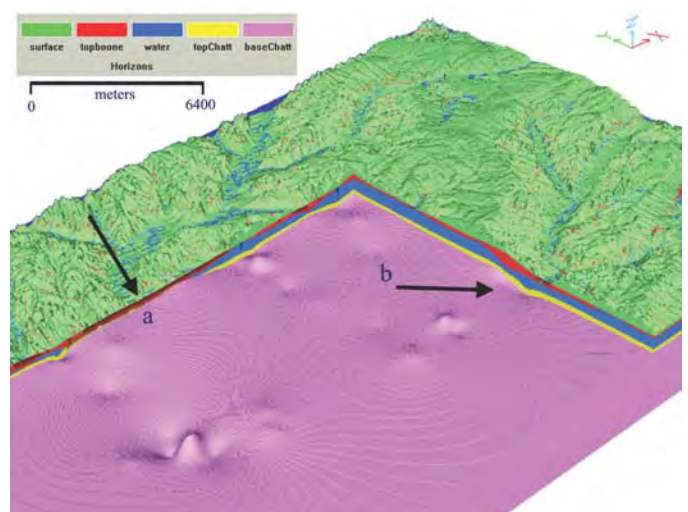


Figure 5. Chair graphic perspective viewed from azimuth 225, declination 55, Z exaggeration = 3. Arrow "a" points to where the Boone unit pinches out and shale surfaces in the bed of the Illinois River and "b" points to apparent lineament alignment. Note that "Y" axis always points north, corresponds to latitude or northing, "X" corresponds to longitude or easting, and "Z" represents the vertical direction (elevation).

83 water wells (Fig. 3). They were irregularly spaced, clustered, and biased according to anthropogenic uses. The well depths represented in the dataset are as follows:

Number of wells **Range of depth, m**

14	<91
15	91 - 122
16	123 - 152
18	153 - 183
10	184 - 213
10	>213

While the log sheet format has changed over time, the necessary basic information needed for this study — location data, date well was drilled, owner's name at the time of drilling, driller's name, total well depth, depth to top and base of carbonate and shale units, depth to water — has remained constant over time and appeared on all forms.

Arkansas climatic division 0301 precipitation records were utilized to determine if the well was drilled in a high-flow or low-flow season. Division data were used instead of individual recording station data because they were considered to be more representative of the nature of the areal distribution of precipitation and groundwater recharge for the study area. Climatic divisions are defined as relatively homogenous areas within a state. Each reporting station within a division is equally weighted with the others in the same division, and their precipitation measurements are totaled and averaged for that division. While the reporting stations within a division vary in

number and location, this method of calculating precipitation more accurately reflects the precipitation received in a physically homogenous area than relying on the nearest gauging station, which may or may not be working properly or be truly representative (Karl *et al.* 1983).

To determine if a well was completed in a low-flow or high-flow time of year, the date of completion was compared to the median statistics of the amount of rainfall for that month and year. If the amount of rainfall for the month was below the monthly median, then the well was considered to be completed in a low-flow time period. Using only low-flow completed wells as representative of base groundwater flow, an xyz point file for each geologic unit was created. Subsurface elevations for the top of the limestone unit (Boone Formation) and top and base of shale (Chattanooga Formation) for each well site were calculated from the surface elevation DEM and the reported depths to formation tops and base as indicated on the well log sheets. Subsurface elevations at each well location were then separated and grouped according to geologic unit.

A raster surface representing the top and base of the geologic units was then created using thin-plate splining. Additionally, a water surface was generated based on the recorded depth to water in the well at the time of well completion and based on the elevation of surface water features (derived from vector stream and spring files and a DEM).

Mitasova and Mitas (1993) have shown that interpolation of surfaces using bivariate and trivariate completely regularized splines with tension works well with geoscientific and scattered data. This method is a multi-grid, radial approach with global interpolation that can be segmented for large datasets. The interpolated surfaces can be "tuned" by adjusting the tension parameter which then compensates for overshoots of the data points. An increase in tension causes the data points to have influence over a shorter distance resulting in a surface that acts like a rubber sheet. A decrease in tension causes the data points to have influence over a farther distance resulting in a surface that acts like a steel plate. The change in tension allows data points to be honored. Smoothing of the data can be incorporated if desired. Whereas the data points will create peaks and dips, the interpolated surface will eventually go back to trend. Trend is a constant, is a horizontal surface, and is derived from the dataset.

The tension value was chosen so that the interpolated surface would pass through the data points or as close as possible. In order to preserve abrupt changes in elevation that could be indicators of faults, no smoothing was used.

The interpolated raster surfaces were converted to grid-format, and used to construct a 2-D geometry viewable in 3-D perspective. Geologic horizons could then be viewed interactively with cutting planes, fence diagrams, and chair graphics chosen to visually evaluate the relation of the units to one another and to the surface topography. It should be noted that these surfaces are sampling-limited, so they will become more accurately defined as more samples are input into the model (Fisher 1993).

Seven instrumented wells located at the Savoy Experimental Watershed (SEW) were used as control wells when evaluating the interpolated surfaces. SEW is centrally located to the area chosen as the study site (Fig. 3).

RESULTS AND DISCUSSION

The ability to use water well driller's logs was based on the geology of the study area being visibly discernible from one unit to another. It is doubtful that areas with less visually identifiable geologic units would be able to rely on data provided by non-geologists. Also, public domain water well log use produces data points that are irregularly spaced, clustered, and biased according to anthropogenic uses.

There were 77 points used for the Boone limestone interpolation, 79 points for the top of shale surface, and 81 points to model the base of the shale unit. The logging length represented in this study totaled 12,964 m, including: 1104 m to the top of Boone limestone; 4804 m to the top of shale; and 5914 m to the base of shale. This dataset represents an overall aggregate cost savings of ~\$229,300 (based on the cost of drilling in northwest Arkansas in May 1999). Comparison of interpolated surfaces with the 7 control well formation elevations showed differences in elevation of -18 to 15 m for top of Boone limestone, -29 to 9 m for top of Chattanooga Shale, and -12 to -2 m for base of Chattanooga Shale.

Interactive exploratory viewing of the interpolated geologic and water surfaces with and without the DEM is one main element of this study. Figures 4 through 7 demonstrate a few of the 3-D perspective views possible when visually comparing the interpolated surfaces to one another and to the surface topography. Dips and rises in the modeled surfaces can be seen to align with lineaments expressed in the surface topography. Arrows in Figures 4 and 5 point to where the top of the shale surface outcrops in the bed of the Illinois River (as confirmed in the field).

CONCLUSIONS

Free data on the subsurface in the form of water well drilling logs were successfully used to model geologic surfaces in a nearly horizontal karst environment. Additional data points are needed to continue testing the methodology. How successful this methodology would be in other geologic settings remains to be investigated.

ACKNOWLEDGMENTS

The study reported here was the result of work conducted for a Masters thesis in the Division of Geography, Department of Geosciences, at the University of Arkansas, Fayetteville, Arkansas. The stipend support provided by the university was greatly appreciated. Also, this study could not have been done without the facilities of the Center for Advanced Spatial Technology (CAST) at the university or without the coopera-

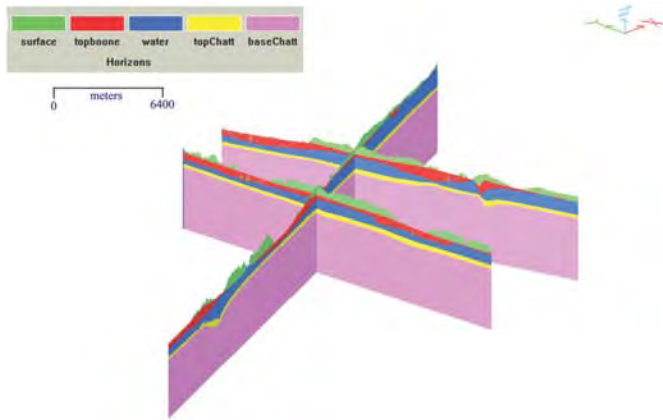


Figure 6. Iso-parametric perspective along axes. Note that "Y" axis always points north, corresponds to latitude or northing, "X" corresponds to longitude or easting, and "Z" represents the vertical direction (elevation).

tion of William Prior and Angela Braden at the Arkansas Geological Commission. Special acknowledgement is given to members of the thesis committee (John C. Dixon, J. Van Brahana, and Malcolm K. Cleaveland), who were always helpful and insightful. Software used in the study was GRASS and Intergraph's Voxel Analyst 2.0.

REFERENCES

- Adamski, J.C., 1997, Nutrients and pesticides in ground water of the Ozark plateaus in Arkansas, Kansas, Missouri, and Oklahoma: USGS water-resources investigations report 96-4313, Little Rock, Arkansas, USGS, 28 p.
- Barlow, C.A., & Ogden, A.E., 1982, A statistical comparison of joint, straight cave segment, and photo-lineament orientations: NSS Bulletin, v. 44, p. 107-110.
- Bartholmey III, E.C., 2001, Dominant factors controlling flow and transport in Stroud Spring, a resurgence in the mantled karst terrane in northwest Arkansas [MS thesis]: University of Arkansas, 105 p.
- Bonham-Carter, G.F., 1996, Geographic information systems for geoscientists, modeling with GIS. Computer Methods in the Geosciences Vol. 13: United Kingdom, Pergamon, 398 p.
- Brahana, J.V., 1997, Rationale and methodology for approximating spring-basin boundaries in the mantled karst terrane of the Springfield Plateau, northwestern Arkansas, in Stephenson, B., ed., The engineering geology and hydrogeology of karst terranes, p. 77-82.
- Camp, C.V., Outlaw, Jr., J.E., & Brown, M.C., 1994, GIS-based groundwater modeling: Microcomputers in Civil Engineering, v. 9, p. 281-293.
- Fisher, T.R., 1993, Use of 3-D geographic information systems in hazardous waste site investigations, in M.F. Goodchild et al., ed., Environmental modelling with GIS: New York, Oxford University Press, p. 238-247.
- Howard, J.M., 1989, The geology of Arkansas, the natural state: Rocks and Minerals, Arkansas Issue, v. 64, no. 4, p. 270-276.
- Karl, T.R., Metcalf, L.K., Nicodemus M.L., & Quayle, R.G., 1983, Statewide average climatic history, Arkansas 1891-1982: Historical climatology series 6-1, Asheville, NC, National Climatic Data Center, 37 p.
- Kolm, K.E., & Downey, J.S., 1993, Groundwater system modelling and management using geoscientific information systems in HydroGIS 93: Application of geoscientific information systems in hydrology and water resources, Proceedings of the Vienna Conference, April 1993. IAHS publication no. 211, p. 433-438.
- LeGrand, H., 1979, Evaluation techniques of fractured-rock hydrology: Journal of Hydrology, v. 43, p. 333-346.

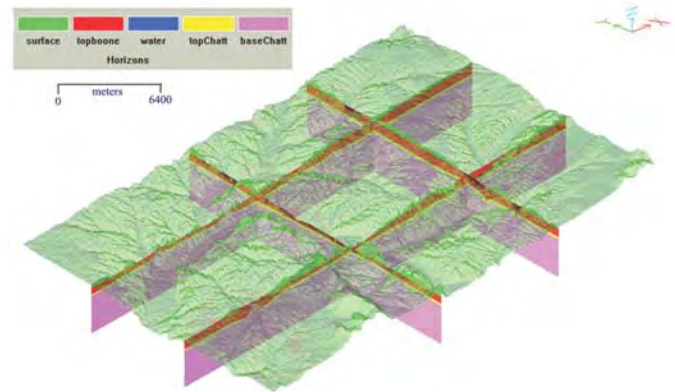


Figure 7. Iso-parametric perspective along axes with a 55% transparent surface layer. Note that "Y" axis always points north, corresponds to latitude or northing, "X" corresponds to longitude or easting, and "Z" represents the vertical direction (elevation).

- Maidment, D.R., 1993, GIS and hydrologic modeling, in M.L. Goodchild et al., ed., Environmental modeling with GIS: New York, Oxford University Press, p. 147-167.
- Mitasova, H., & Mitas, L., 1993, Interpolation by regularized spline with tension: I. theory and implementation: Mathematical Geology, v. 25, p. 641-655.
- Parks, B.O., 1993, The need for integration, in M.L. Goodchild et al., ed., Environmental modeling with GIS: New York, Oxford University Press, p. 31-34.
- Phelan, T.L., 1999, GIS and 3-D visualization for geologic subsurface static modeling in a mantled karst environment near Savoy, Arkansas [MS thesis]: University of Arkansas, 158 p.
- Renken, R.A., 1998, Ground water atlas of the United States, HA 730-F, Arkansas, Louisiana, and Mississippi, U.S. Geological Survey, http://capp.water.usgs.gov/gwa/ch_f/F-text6.html.
- Smith, D.R., & Paradis, A.R., 1989, Three dimensional GIS for the earth sciences, in Raper, J., ed., Three dimensional applications in geographical information systems: London, Taylor and Francis, p. 149-154.
- Star, J., & Estes, J., 1990, Geographic information systems, An introduction: New Jersey, Prentice Hall, 303 p.
- Stringfield, V.T., Rapp, J.R., & Anders, R.B., 1979, Effects of karst and geologic structure on the circulation of water and permeability in carbonate aquifers: Journal of Hydrology, v. 43, p. 313-332.
- Tsihrintzis, V.A., Hamid, R., & Fuentes, H.R., 1996, Use of geographic information systems (GIS) in water resources: A review: Water Resources Management, v. 10, p. 251-277.
- Turner, A.K., 1989, The role of three-dimensional geographic information systems in subsurface characterization for hydrogeological applications, in Raper, J., ed., Three dimensional applications in geographical information systems: London, Taylor & Francis, p. 115-127.
- Turner, A.K., & Kolm, K.E., 1991, Three-dimensional geoscientific information systems for ground-water modeling: American Congress on Surveying and Mapping and American Society for Photogrammetry and Remote Sensing Annual Convention, Technical papers; Baltimore, Maryland, p. 217-226.
- Turner, A.K., 1992, Applications of three-dimensional geoscientific mapping and modelling systems to hydrogeological studies, in Turner, A.K., ed., Three-dimensional modeling with geoscientific information systems, NATO Advanced Science Institutes Series C, Vol. 354, Dordrecht: Kluwer Academic Publishers, p. 327-364.
- Waite, L.A., & Thomson, K.C., Development, description, and application of a geographic information system data base for water resources in karst terrane in Greene county, Missouri: Rolla, Missouri, U.S. Geological Survey, Water-Resources Investigations Report 93-4154, 31 p.

AN EXAMINATION OF PERENNIAL STREAM DRAINAGE PATTERNS WITHIN THE MAMMOTH CAVE WATERSHED, KENTUCKY

ALAN GLENNON AND CHRIS GROVES

Hoffman Environmental Research Institute, Western Kentucky University, One Big Red Way, Bowling Green, KY 42101 USA, alan.glennon@wku.edu

Quantitative relationships describing the nature of surface drainage networks have been used to formulate flood characteristics, sediment yield, and the evolution of basin morphology. Progress has been slow in applying these quantitative descriptors to karst flow systems. Developing geographic information system (GIS) technology has provided tools to 1) manage the karst system's large, complex spatial datasets; 2) analyze and quantitatively model karst processes; and 3) visualize spatially and temporally complex data. The purpose of this investigation is to explore techniques by which quantitative methods of drainage network analysis can be applied to the organization and flow patterns in the Turnhole Bend Basin of the Mammoth Cave Watershed.

Morphometric analysis of mapped active base-flow, stream-drainage density within the Turnhole Bend Groundwater Basin resulted in values ranging from 0.24 km/km² to 1.13 km/km². A nearby, climatologically similar, nonkarst surface drainage system yielded a drainage density value of 1.36 km/km². Since the mapped cave streams necessarily represent only a fraction of the total of underground streams within the study area, the actual subsurface values are likely to be much higher. A potential upper limit on perennial drainage density for the Turnhole Bend Groundwater Basin was calculated by making the assumption that each sinkhole drains at least one first-order stream. Using Anhert and Williams' (1998) average of 74 sinkholes per km² for the Turnhole Bend Groundwater Basin, the minimum flow-length draining one km² is 6.25-7.22 km (stated as drainage density, 6.25-7.22 km/km²).

A major emphasis in geomorphology over the past six decades has been on the development of quantitative physiographic methods to describe the evolution and behavior of surface-drainage networks (Horton 1945; Leopold & Maddock 1953; Leopold & Wolman 1957; Abrahams 1984). These parameters have been used in various studies of geomorphology and surface-water hydrology, such as flood characteristics, sediment yield, and evolution of basin morphology (Jolly 1982; Ogunkoya *et al.* 1984; Aryadike & Phil-Eze 1989; Jensen 1991; Breinlinger *et al.* 1993).

Many well-developed karst aquifers display drainage characteristics that appear similar to surface networks. The degree of similarities and their consistency throughout the whole of the karst drainage network are, however, generally unknown. Quantitative descriptors, known as morphometric parameters, have long been used to describe and predict stream network behavior for surface-flow systems. The purpose of this investigation was to explore techniques by which quantitative methods of drainage-network analysis can be applied to shed light on the evolution, organization, and flow patterns in the Mammoth Cave Watershed. Since an estimated 7-10% of the world's land surface is underlain by karst aquifers (Ford & Williams 1989), understanding the processes and behaviors of karst landscapes and their subterranean stream networks may help humankind to better utilize and manage the earth's natural resources.

STUDY AREA: TURNHOLE BEND GROUNDWATER BASIN

The focus of this investigation is the Turnhole Bend Groundwater Basin, which is part of the Mammoth Cave Watershed. The Mammoth Cave Watershed consists of the Pike Spring, Echo River, Double Sink, River Styx, Floating Mill Hollow, and Turnhole Bend Groundwater Basins. Spanning 245 km², the Turnhole Bend Groundwater Basin comprises over 75% of the 317 km² Mammoth Cave Watershed (Fig. 1).

The Mammoth Cave region lies 160 km south of Louisville, Kentucky, and 160 km north of Nashville, Tennessee (Fig. 1). The karst aquifer within the Mammoth Cave Watershed has developed in an ~160 m thick unit of Mississippian limestones. The aquifer is primarily developed in the Girkin, Ste. Genevieve, and St. Louis Limestones (Haynes 1964; Miotke & Palmer 1972). The cavernous limestones are overlain by the Big Clifty Sandstone, a relatively insoluble layer of Mississippian sandstone and shale. Three physiographic subprovinces comprise the Mammoth Cave Watershed: the Glasgow Uplands in the south, the Sinkhole Plain in the central region, and the Mammoth Cave Plateau in the north (Fig. 2).

The Green River, a tributary of the Ohio River, is the outlet for the Mammoth Cave Watershed. Mammoth Cave's karst flow networks are tributaries to the Green River and are, thus, controlled by the river's location and behavior. The close com-

Table 1. Caves over one km long within the Turnhole Bend Groundwater Basin

Cave Name	Cartographers	Cave Length (m)	Lateral Stream Length (m)
Martin Ridge Cave System	Alan Glennon, Don Coons, and Steve Duncan	52,143	14,777
James Cave	Glen Merrill	16,496	*
Lee Cave	Pat Wilcox	12,875	2,199
Parker Cave	Don Coons	10,461	5,198
Smith Valley Cave	Joel Despain	4,731	1,730
Coach Cave	Glen Merrill	3,218	300m estimate, not included in total
Emerson-Gift Horse Cave	Jim Borden	3,000	612
Brushy Knob Cave	Dave Black	2,104	*
Long Cave	Tim Schafstall	1,797	*
Cedar Spring Saltpeter Cave	Don Coons	1,217	*
Diamond Caverns	Gary Berdeaux	1,207	*
Renick Cave	Jim Borden and Jim Currens	1,030	*
Neighbor Cave	Alan Glennon	1,005	9
**minor caves: less than one km in length	Alan Glennon, Bob Osburn, Don Coons, and Jim Borden	-	235
Mammoth Cave System	Bob Osburn, Pat Kambesis, and Jim Borden	50,000 in Turnhole Basin (571,327 entire system)	16,173 in Turnhole Basin
Total		161,284	40,933

* no surveyed perennial streams.

** Numerous caves, less than a kilometer in length, contain perennial streams. However, these stream lengths have a lateral length less than 5m. Surveyed exceptions include Monroe Sandstone Cave 25 m, Mickey Mouse Cave 9 m, Indian Cave 30 m, Glennon Spring Cave 5 m, Cripple Creek 91 m, Owl Cave 15 m, South Valley Cave 60 m, and Pigthistle Cave.

munication between the cave streams and Green River is exhibited in cave-level development within the caves as related to the geomorphic history of the Green River Valley. Fluvial downcutting of the Green River Valley is mirrored within the cave system, and has led to the development of tiered levels within the cave (Palmer 1981). As the Green River continuously downcuts its valley, lowering regional base level, cave streams develop conduits correspondingly deeper, and abandon higher flow routes. Consequently, the Mammoth Cave area is typified by multilevel caves, with the lowest levels containing the major active conduits hence, in general, the youngest cave passages. Beryllium and aluminum dating of quartz gravels by Granger *et al.* (2001) in the region's higher, abandoned cave levels, have found that Green River downcutting averages 30 m/Ma. These data reveal that major conduit development within Mammoth Cave's karst aquifer has been ongoing for at least three million years.

Within the Turnhole Bend Groundwater Basin, 120 individual caves possessing 10 m or greater true horizontal length have been cataloged for this project, 46 of these with perennial base-flow streams (Table 1).

METHODS

Compiling a consistently formatted dataset is one of the great challenges for the karst-aquifer modeler. In-cave survey data for the Mammoth Cave Watershed have been acquired over the last 180 years (e.g., Lee 1835; Hovey 1909; White & White 1989). Only within the last 20 years, however, have cave mappers increased survey standards to consistently include not only x and y coordinates but also elevation (z coordinates). Fortunately, since 80% or more of the cave streams within the Turnhole Bend Groundwater Basin have been discovered within the last 20 years, a majority of the dataset for this investigation includes accurate x, y, and z data.

Cave-survey data were acquired digitally from many different digital cave-data reduction programs. These included SMAPS, COMPASS, WALLS, Cave Mapping Language (CML), and spreadsheet macro-programs. Furthermore, much of the cave survey-data were available only as final paper cave maps. ArcView GIS and Arc/Info 8 were used to import these differing datasets and integrate them into a standard dataset. Each of the caves' data were imported into ArcInfo coverages and ArcView shapefiles using either AutoCAD import protocols, ArcView CaveTools, or manual digitizing.

Figure 1. Groundwater basins of the Mammoth Cave Watershed. Turnhole Bend (0083), Pike Spring (0082), Echo River (0191), Double Sink (0199), River Styx (0193), and Sand House (0200) Groundwater Basins comprise the Mammoth Cave Watershed (shaded). (modified from Ray & Currens 1998a, 1998b).

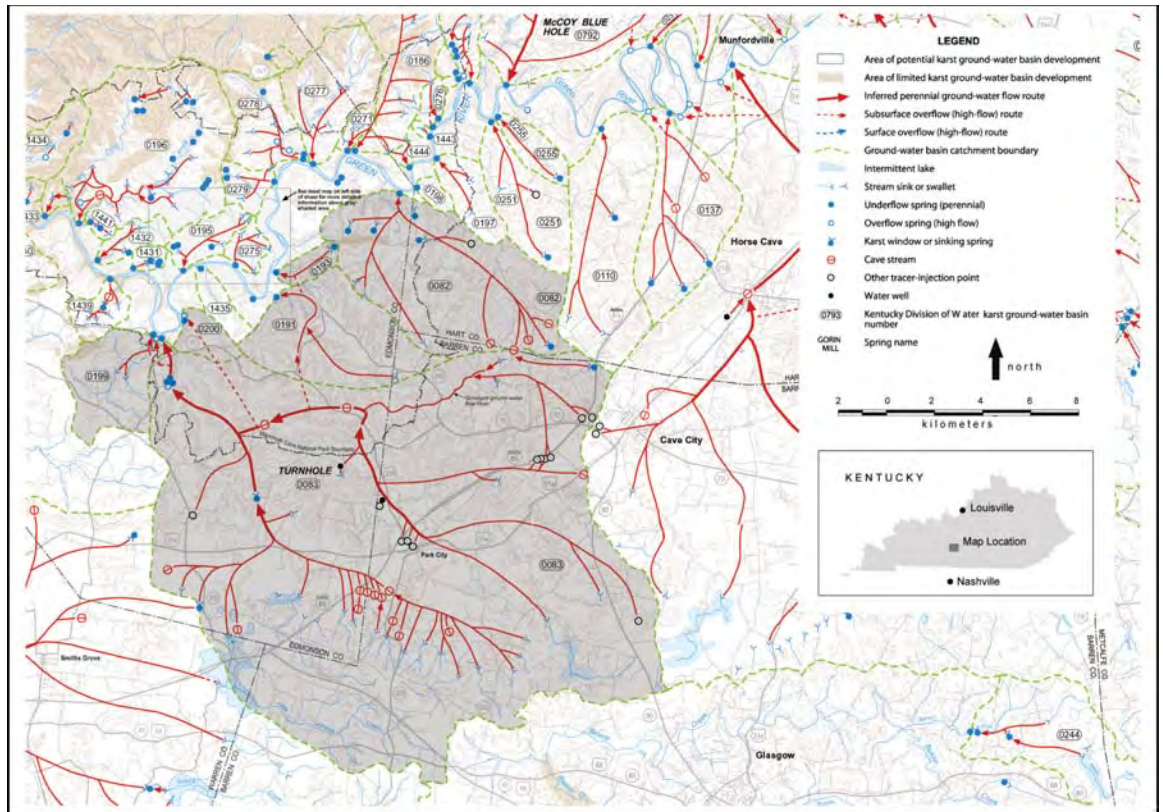
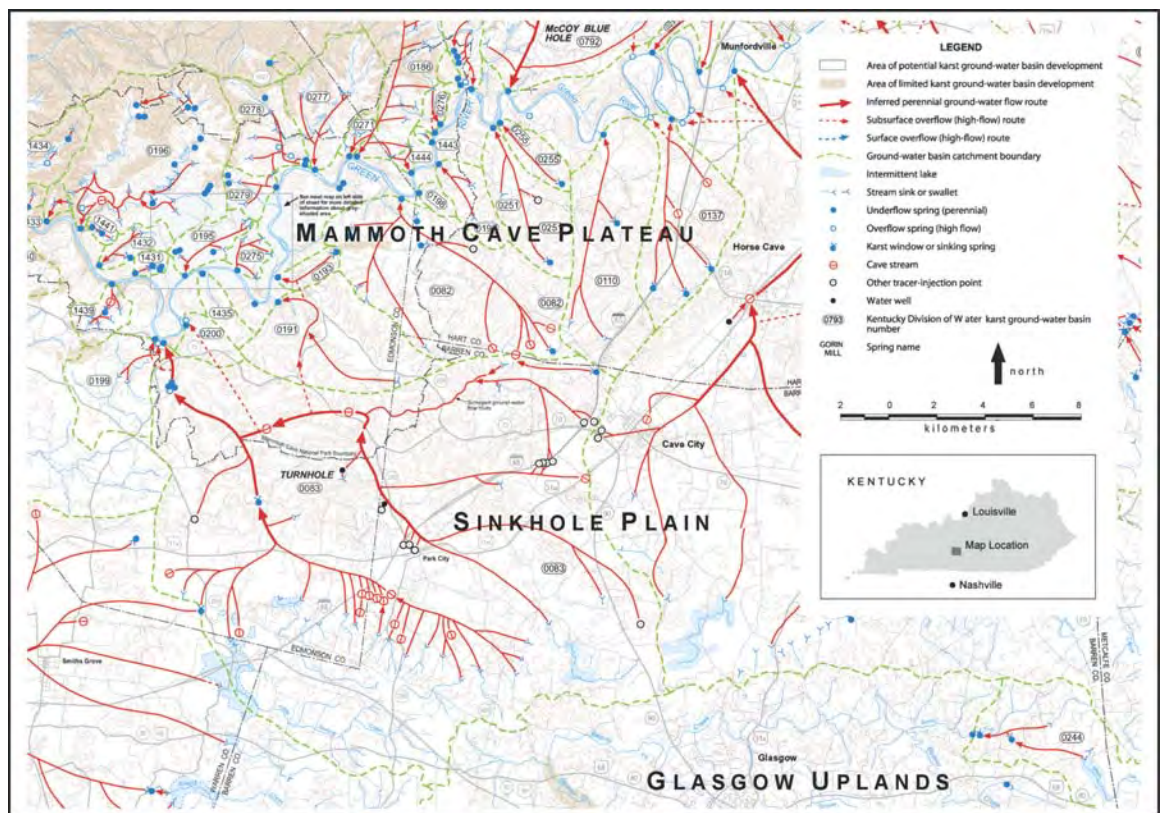


Figure 2. Location of Turnhole Bend Groundwater Basin (0083). For this investigation, the Double Sink Groundwater Basin (0199) is also included as part of the Turnhole Bend Groundwater Basin (modified from Ray & Currens 1998a, 1998b).



Cave passageways and streams were georegistered in the GIS using Universal Transverse Mercator coordinates, North

American Datum 1927, Zone 16. This projection and coordinate system were used in order to be consistent with datasets

Table 2. Drainage Density Formulas

Drainage Density (D)	Area Examined (A)	Surface Stream Length (s)	Cave Stream Length (c)	Dye Trace Length (d)
(1)	Total basin	Measured	Measured	Not included
(2)	Total basin	Measured	Measured	Straight Line
(3)	Total basin	Measured	Measured	“Smoothed” line
(4)	Total basin	Measured	Measured	Straight line * 1.5 ^a
(5)	Sub-basins total	Not included	Measured ^b	Not included

^a 1.5 represents average sinuosity of other mapped large cave streams in the basin.

^b only those stream lengths and areas with clear catchments included

Method	Drainage Density Equation	
(1)	$D = \left(\frac{s + c}{A} \right)$	<i>al.</i> 1999). Drainage basins were determined and digitized and included as ArcView shapefiles. In several cases, basins were further delineated in terms of sub-basins by normalized base-flow calculations (Quinlan & Ray 1995).
DRAINAGE DENSITY		
(2)	$D = \left(\frac{s + c + d}{A} \right)$	As a result of the nature of work performed by previous investigators and the nature of their collected datasets, this investigation focuses on two-dimensional, <i>areal</i> , morphometric relationships. Sustained research work in the Mammoth Cave area since the 1950s provided the necessary data on locations of cave streams, drainage area values, base-flow discharges, the potentiometric surface, and flood hydrographs (Meiman 1989; Quinlan & Ray 1989; Coons 1997; Duncan <i>et al.</i> 1998; Ray & Currens 1998a, b; Glennon 2001; Osburn 2001).
(3)	$D = \left(\frac{s + c + d}{A} \right)$	
(4)	$D = \left[\frac{s + c + (d * 1.5^a)}{A} \right]$	The initial attempt at calculating a quantitative parameter for the Mammoth Cave Watershed was an examination of basin drainage density. Drainage density is defined as the combined length of all streams in a basin divided by the area of the basin (Strahler <i>et al.</i> 1958). It is a measure of average length of streams per unit drainage area, and describes the spacing of the drainage ways. Drainage density has been interpreted to reflect the interaction between climate and geology (Ritter <i>et al.</i> 1995). The inverse of drainage density, the <i>constant of channel maintenance</i> , indicates the minimum area required for the development and maintenance of a unit length of channel (Schumm 1956). Due to the prior scarcity of sufficient data and processing technology for the karst aquifer, drainage density represents a previously uncalculated numerical measure describing the manner in which a basin collects and transmits water through its network.
(5)	$D = \left(\frac{c^b}{A^b} \right)$	Five different techniques were used to calculate active, base-flow drainage density given the incomplete dataset available (Table 2). For all five methods, stream-segment lengths were calculated by adding perennial stream lengths as projected onto a horizontal plane. The following paragraphs outline how stream lengths were calculated and areas defined for the drainage-density calculation for each of the five methods.

^a 1.5 represents average sinuosity of other mapped large cave streams in the basin.

^b only those stream lengths and areas with clear catchments included

produced at Mammoth Cave National Park.

Once the cave datasets were integrated into ArcView and ArcInfo, several other layers were imported or created, including: hypsography (1:24,000), digital orthophotography (1:12,000), surface catchments above the Martin Ridge Cave System (1:12,000), perennial surface streams (1:24,000), and surface geology (1:24,000) (Glennon & Groves 1999; Pfaff *et*

TECHNIQUE 1

First, the sum of mapped-segment lengths from subsurface and surface streams was calculated. Drainage density was calculated by dividing the stream-length summation by the area of the entire Turnhole Bend Groundwater Basin (Table 2). Since mapped cave streams reflect only a fraction of all streams in the karst flow network, several other approaches were devised to obtain possible drainage-density values.

TECHNIQUE 2

A second approach to calculating drainage density entailed a procedure similar to technique 1, but with the inclusion of regional dye-trace data and surface-stream lengths (Table 2). This investigation calculated dye-trace flow lengths from a digital version of the Ray and Currens (1998a, b) maps. All mapped cave streams in the Turnhole Bend Groundwater Basin were summed to include the total length of surface streams and straight-line dye-trace route lengths. The dye-trace length can be calculated using straight-line lengths from dye input points to its output receptors. As streams converged, a minimum straight line flow length geometry was maintained for each segment. Together, these represent a minimum flow length within the Turnhole Bend Groundwater Basin that considers more of the unmapped and phreatic portions of the aquifer.

TECHNIQUE 3

Quinlan and Ray (1989) derived their dye-trace routes by taking into account known caves and the potentiometric surface (Table 2). By considering the caves, potentiometric surface, and topography, the interpolated flow routes are curves approximating the regional flow routes of the Turnhole Bend Groundwater Basin.

The length of their interpolated curves was divided by the total area of the Turnhole Bend Groundwater Basin to obtain another value for drainage density. As with Technique 2, this value underestimates the actual drainage-density value for the basin because it includes only streams represented by dye tracing. In the Turnhole Bend Groundwater Basin, dye tracing has only been conducted on a regional scale. Thus, the derived value for drainage density accounts for only the largest conduits in the karst system.

TECHNIQUE 4

Straight-line dye-trace lengths do not account for the sinuosity that has been measured in known stream conduits within the aquifer. A regional groundwater flow length value can be calculated by including the sinuosity of the cave streams along individual dye-trace segments. A sinuosity value was calculated using all stream segments exceeding 500 m in the Turnhole Bend Groundwater Basin. For the average stream exceeding 500 m long, the watercourse flows 1.5 kilometers for every one kilometer of straight-line distance. A final drainage density value was calculated incorporating cave-stream sinuosity into the equation (Table 2).

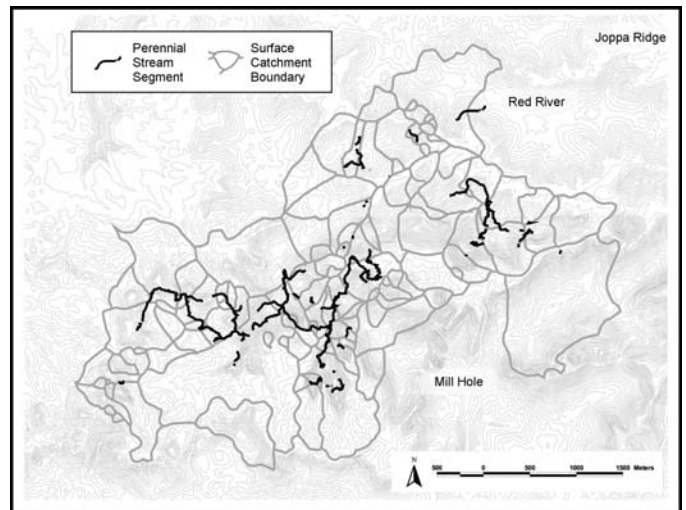


Figure 3. Surface catchments overlying perennial streams within the Martin Ridge Cave System.

TECHNIQUE 5

Lastly, a focused approach on the Martin Ridge Cave System delineated the individual catchments of the cave's mapped streams (Fig. 3). By comparing the mapped streams and their catchments, another value for drainage density was calculated. Since most of the streams discussed below were only recently discovered, the surface drained by Martin Ridge Cave has not yet been delineated through systematic dye tracing. Until additional fieldwork can be done, a provisional set of rules and assumptions has been developed to delineate the most appropriate recharge basin for each of the underground streams within the flow network. Only one stream in Martin Ridge Cave was excluded from method 5 analysis. With a recharge basin exceeding 100 km², the Red River, the downstream segment of the Hawkins River, was not used in the analysis. The remaining streams drained small to intermediate-sized catchments (Fig. 3). Streams within Whippistle Cave were examined to determine their elevation with respect to surface catchments and their most likely sinkhole recharge areas. Several streams approached the surface closely enough to allow clear determination of their recharge zone. Streams in the central portion of the system are "hemmed in" by a large karst valley. The highest elevations in the streams generally are above the level of the valley floor, so it is assumed these streams drain the valley area and the nearby surrounding ridgetop areas. These provisional methods likely overestimate drainage basin boundaries, and results of analyses using these boundaries may be subject to revision. This likelihood is especially true as basins are more firmly established by future hydrogeologic fieldwork. Catchment areas defined in this investigation provide maximum, bounding values of recharge areas for underlying streams. This logic was used to remain consistent with the objective of obtaining a minimum drainage-density value. With areas so defined, the drainage

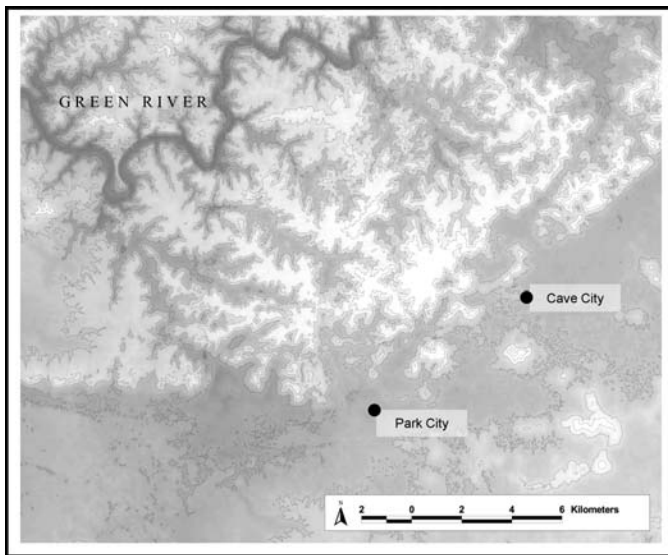


Figure 4. Elevation model of Mammoth Cave region. Lighter shades are higher elevations. The contour interval is 30 meters.

area was summed and densities calculated. Drainage density formulas are summarized in Table 2.

THE SURFACE-DRAINAGE NETWORK

In the Mammoth Cave Watershed, subsurface karst drainage appears to be influenced by the surface drainage that existed before the development of the karst landscape. Dye tracing experiments ongoing since the 1920s provide a map of current flow routes through the aquifer (Anderson 1925; Ray & Currens 1998a, b). The map shows a dendritic network of smaller-order streams draining into larger-order streams (Fig. 1). At coarse, regional scales, surface-elevation maps of the Mammoth Cave region portray an organized, dendritic surface network (Fig. 4). However, the modern Turnhole Bend Groundwater Basin is pitted with sinkholes and large karst valleys.

GIS was used to examine possible regional surface-elevation patterns. A 30-m Digital Elevation Model (DEM) was compiled of the Mammoth Cave Watershed and adjacent area (USGS 1993, 2001). The 30-m DEM is a raster dataset in which an array of 30-m x 30-m grid cells each possess a single elevation value. The grid provides a continuous surface of elevation values for the study area. In the Mammoth Cave Watershed and surrounding area, thousands of internally drained depressions exist. Likewise, in the DEM, thousands of internally drained depressions, or *sinks*, exist. These *sinks* are defined as cells (or groups of cells of equal elevation) in which all neighboring cells are higher in elevation (ESRI 1999). While GIS applications are able to determine flow direction and networks by comparing the elevations of the DEM, *sinks* are problematic for the GIS. The GIS flow-network algorithm is accustomed to stream networks converging on a single or small number of trunk streams. In the Mammoth Cave area, as

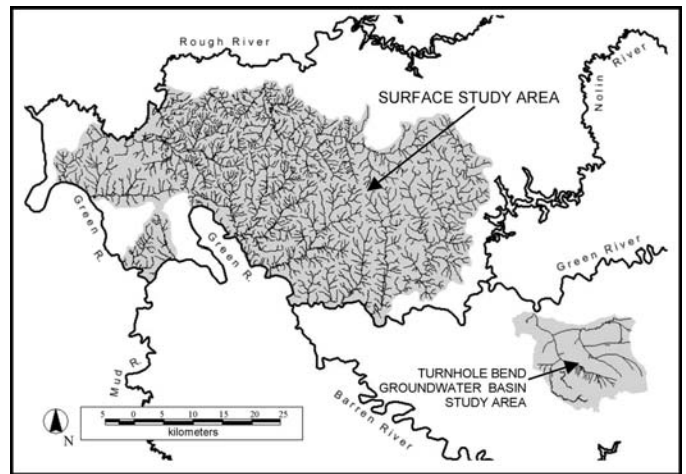


Figure 5. Location of surface study area.

a result of *sinks*, the flow-network algorithm creates thousands of disjointed streams draining into individual, internally drained basins. Therefore, the hydrologic-network algorithm used by the GIS has little use in a highly karstified landscape. However, in nonkarst landscapes, a small number of *sinks* sometimes exist in a typical DEM. These errors are common enough that ArcView and ArcInfo have functions to remove the *sinks*. The function, "FILL," is an iterative process which raises the value of a grid cell (or cell groups) until it is no longer bounded by higher elevation cells.

In order to examine the regional surface-elevation patterns that appear to exist in the Turnhole Bend Groundwater Basin, the "FILL" function was performed on the basin's DEM. The procedure effectively "smoothed" the Turnhole Bend Groundwater Basin's sinkholes and karst valleys, filling them to their lowest saddle drain. Using the GIS, a flow network was then constructed on the "FILLED" DEM. The result is a channel network that accentuates the current basin-wide surface-drainage patterns, and possibly reflects the shape of the pre-karst drainage network of the Turnhole Bend Groundwater Basin. The results section of the investigation compares the product of this model to the current and theorized historical flow network.

RESULTS

DRAINAGE-DENSITY RESULTS

Based on the equations presented in Table 2, drainage-density numbers were calculated for the Turnhole Bend Groundwater Basin. Table 3 summarizes the results. In order to compare the karst system's drainage values with a related surface network, a nearby 1880 km² non-karst site was examined (Fig. 5). The drainage-density value for this nearby climatologically similar surface-study area is 1.36 km/ km². The value includes 1856 streams analyzed with a total length of 2550 km.

Table 3. Drainage Density Formulas

Drainage Density (D)	Area Examined (A)	Surface Stream Length (s)	Cave Stream Length (c)	Dye Trace Length (d)
(1)	245 km ²	18,325 m	40,933 m	Not included
(2)	245 km ²	18,325 m	40,933 m	108,187 m
(3)	245 km ²	18,325 m	40,933 m	129,711 m
(4)	245 km ²	18,325 m	40,933 m	162,280 m
(5)	13.115 km ²	Not included	14,777 m	Not included

^a 1.5 represents average sinuosity of other mapped large cave streams in the basin.

^b only those stream lengths and areas with clear catchments included

Method	Drainage Density Equation	Result	
(1)	$D = \left(\frac{s + c}{A} \right)$	0.24 km/km ²	<p>Basin and adjacent basins. This location may represent a critical point in the geomorphic history of the Turnhole Bend Groundwater Basin. For further comparison, a map of the contemporary drainage routes is presented in Figure 8.</p> <p style="text-align: center;">DISCUSSION</p> <p>These initial efforts describe an orderly subsurface-flow network with numerical results that allow for comparison of the karst-flow network to surface fluvial systems. Additionally, quantitative examination of karst subsurface-drainage patterns and overlying surface catchments revealed several curious locations that appear to have large deviations from overlying surface valleys or possibly reflect moments of large-scale change in the development of the basin. For instance, unlike other streams in the basin, the Logsdon River flows perpendicular to overlying valleys. Most subsurface streams flow roughly parallel to the axis of surface valleys and overlying catchments. The saddle northwest of Mill Hole may also reflect a moment of great change in the geomorphic history of the Turnhole Bend Groundwater Basin. The saddle's elevation implies that the watershed for the developing Turnhole Bend Groundwater Basin was much smaller than today, but when water was able to flow underground through the karst aquifer (without regard to the elevation of the saddle), the watershed size increased dramatically. These assumptions complement the hypothesized basin-evolution model proposed by Quinlan and Ewers (1981). Critical locations like the Mill Hole Saddle display how quantitative analysis holds promise in bringing forth new hypotheses that may help unravel the geomorphic history of karst drainage basins.</p> <p>Morphometric analysis of mapped active base-flow drainage density within the Turnhole Bend Groundwater Basin resulted in values ranging from 0.24 km/km² to 1.13 km/km². A nearby, climatologically similar, non-karst surface-drainage system yielded a drainage density value of 1.36 km/km². Since the mapped cave streams necessarily represent only a fraction of the total of underground streams within the study area, the actual subsurface values are likely to be much higher. Also, in the Turnhole Bend Groundwater Basin, of the 40.3 km of mapped cave streams, only 1 km of physically mapped cave</p>
(2)	$D = \left(\frac{s + c + d}{A} \right)$	0.68 km/km ²	
(3)	$D = \left(\frac{s + c + d}{A} \right)$	0.77 km/km ²	
(4)	$D = \left[\frac{s + c + (d * 1.5^a)}{A} \right]$	0.90 km/km ²	
(5)	$D = \left(\frac{c^b}{A^b} \right)$	1.13 km/km ²	

IDENTIFYING SURFACE-ELEVATION TREND ANOMALIES

Based on the sinkhole "FILL" drainage pattern developed from the 30-m DEM of the Turnhole Bend Groundwater Basin, a drainage map was produced (Fig. 6). From this map, a key location was identified to the northwest of Mill Hole Karst Window. By eliminating the existing saddle northwest of Mill Hole Karst Window, another "FILL" drainage network map was created (Fig. 7). The resulting map shows drainage flowing through Cedar Spring Valley toward Turnhole Bend. By comparing the two "FILL" maps, the elevation of the saddle northwest of Mill Hole represents a point of great influence over flow directions within the Turnhole Bend Groundwater

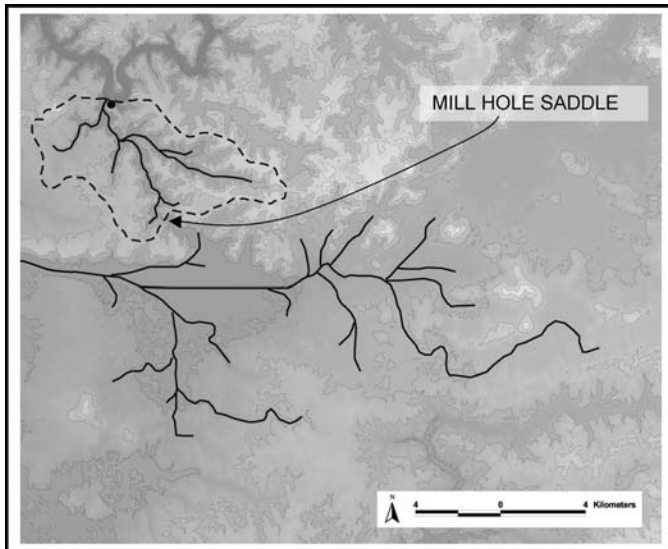


Figure 6. “FILLED” stream network. Lighter shades are higher elevations. The contour interval is 30 meters. The dashed line represents the watershed boundary draining to the Green River near Turnhole Bend Spring. Turnhole Bend Spring is denoted (•). Solid lines represent stream networks derived by the GIS from the 30-meter DEM.

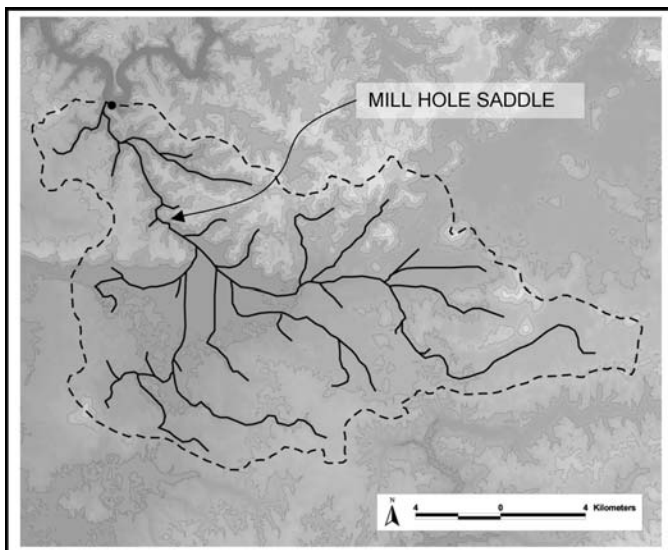


Figure 7. “Lowered saddle - FILLED” stream network. Lighter shades are higher elevations. The contour interval is 30 meters. The dashed line represents the watershed boundary draining to the Green River near Turnhole Bend Spring. Turnhole Bend Spring is denoted (•). Solid lines represent stream networks derived by the GIS from the 30-meter DEM.

streams lies in the phreatic zone. Cave divers’ future mapping in underwater cave passages will provide data to adjust the model, thereby reducing the current bias toward the vadose

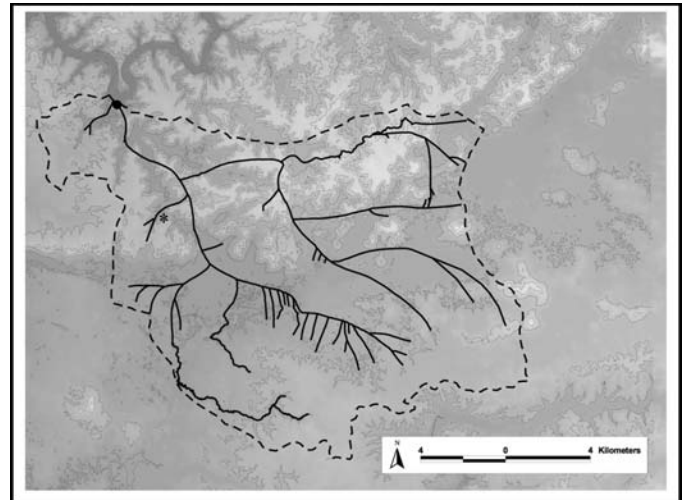


Figure 8. Contemporary Turnhole Bend Groundwater Basin. Lighter shades are higher elevations. The contour interval is 30 meters. The dashed line represents the hypothesized groundwater basin boundary. Solid lines represent either perennial streams flowing on the surface or hypothesized subsurface flow routes from dye traces. Turnhole Bend Spring is located at (#). The saddle north-west of Mill Hole is denoted by a (*). (Modified from Ray & Currens 1998a,b).

areas of the karst aquifer. For future researchers, careful examination of abandoned phreatic tube complexes may provide a reasonable alternative for wholesale underwater cave mapping.

A MODEL FOR CALCULATING A MAXIMUM DRAINAGE DENSITY FOR THE TURNHOLE BEND GROUNDWATER BASIN

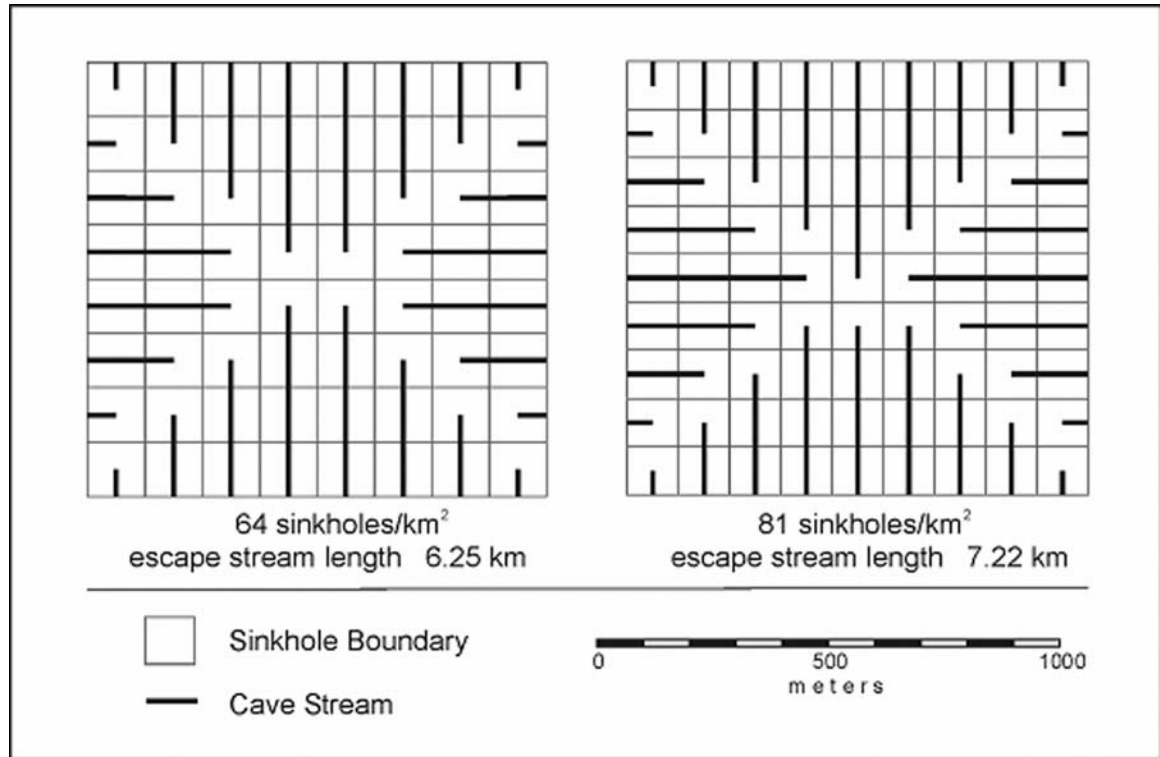
While it is assumed that the Turnhole Bend Groundwater Basin drainage-density value will increase beyond the surface study site value as more streams are mapped, not enough data exist to determine a maximum drainage density value. To provide insight on the upper limit of perennial drainage density in the Turnhole Bend Groundwater Basin, a 1 km² hypothetical model was developed to calculate a maximum drainage density within the Sinkhole Plain (Fig. 9). For this investigation, the initial model makes the following assumptions and constraints:

- 1) That within the Turnhole Bend Groundwater Basin, the Sinkhole Plain has a higher drainage density value than the Mammoth Cave Plateau or Glasgow Uplands (Fig. 2). This assertion is based on the assumption that there is lessened evapotranspiration on the Sinkhole Plain because, unlike the Glasgow Uplands and Mammoth Cave Plateau, the Sinkhole Plain contains no surface streams. More available subsurface water is likely to create a longer subterranean stream network. Thus, the value obtained for the Sinkhole Plain will represent a maximum drainage density for any part of the basin;

- 2) That each sinkhole in the 1 km² possesses an identical square shape and size;

- 3) That each sinkhole drains one first-order stream that

Figure 9.
A model for calculating maximum drainage density within the Turnhole Bend Groundwater Basin.



originates in its center; and

4) That each stream will follow the most-direct route to the edge of the 1 km² model in two-dimensional space. This constraint yields a minimum flow length for the streams to leave the 1 km² area.

For the Turnhole Bend Groundwater Basin Sinkhole Plain, Anhart and Williams (1998) counted an average of 74 sinkholes per km². In order to follow the constraints of the model, where each sinkhole has an identical square shape, two 1-km² sinkhole plains were created (Fig. 9): one with 64 sinkholes/km² and one with 81 sinkholes/km². The drainage density for the 74 sinkholes/km² number lies within the range of the two models. By following the constraints of the model, the 64 sinkholes/km² plain yielded a value of 6.25 km streams. The 81 sinkhole/km² plain yielded 7.22 km of streams. Therefore, for a 1-km² area containing 74 similarly shaped sinkholes, the flow-length lies in a range between 6.25 and 7.22 km (stated as drainage density, 6.25-7.22 km/km²).

CONCLUSIONS

In this investigation, the researcher examined the use of GIS to store, analyze, and visualize surface- and subsurface-spatial data for the Mammoth Cave Watershed. GIS was used to store information and hydrologic attributes for all known caves within the Turnhole Bend Groundwater Basin.

Our work proposes preliminary drainage-density values for the Turnhole Bend Groundwater Basin. These values range from 0.24 km/km² to 1.13 km/km². Drainage density for a nearby non-karst basin yielded a value of 1.36 km/km². As

more streams are discovered, explored, and surveyed within the Turnhole Bend Groundwater Basin, the drainage density value is likely to exceed the nearby surface value. In order to assess a potential maximum drainage density value for the karst aquifer, a theoretical model was developed to describe the amount of two-dimensional stream length necessary to drain a square-kilometer of the Turnhole Bend Groundwater Basin Sinkhole Plain. Given this theoretical model, a maximum drainage density value for the Turnhole Bend Groundwater Basin is 6.25-7.22 km/km².

This work also describes the use of GIS to assess and uncover regional surface-elevation trends and anomalies within a karst watershed. For the Turnhole Bend Groundwater Basin, the GIS analysis highlighted a location immediately northwest of the Mill Hole Saddle that may have played a pivotal role in the development of the current flow regime of the watershed.

All data collected and analyzed for this investigation suggest that karst aquifers, though complex, are consistent with an orderly system. Like surface drainage networks, the karst drainage system exists to reduce potential energy most efficiently. Seemingly unusual patterns exist within the network not as a reflection of disorder, but as a reaction to the hydrogeologic setting of its flow path.

ACKNOWLEDGMENTS

The authors wish to thank the numerous cavers, scientists, and survey projects that provided data for this work: particularly, Cave Research Foundation, Central Kentucky Karst

Coalition, Martin Ridge Cave Project, James Cave Project, and the Science & Resource Management Office of Mammoth Cave National Park. We also would like to acknowledge Don Coons, Bob Glennon, Rita Glennon, Deana Groves, Joe Meiman, and Rhonda Pfaff for their support.

REFERENCES

- Abrahams, A.D., 1984, Channel networks: A geomorphological perspective: *Water Resources Research*, v. 20, p. 161-168.
- Anderson, R.B., 1925, Investigation of a proposed dam site in the vicinity of Mammoth Cave Kentucky, *in* Brown, R.F., ed., Hydrology of the cavernous limestones of the Mammoth Cave area, Kentucky, U.S. Geological Survey Water-Supply Paper, p. 1837- 64.
- Aryadike, R.N.C. & Phil-Eze, P.O., 1989, Runoff response to basin parameters in southeastern Nigeria: *Geografiska Annaler, Series A*, v. 71A, p. 75-84.
- Breilinger, R., H. Duster, & Weingartner, R., 1993, Methods of catchment characterization by means of basin parameters (assisted by GIS) - empirical report from Switzerland: Report - UK Institute of Hydrology, v. 120, p. 171-181.
- Coons, D., 1997, "Whigpistle Cave" [map], 1"=100', Unpublished, Mammoth Cave National Park Museum Collection, three ~30"x72" sheets p.
- Duncan, R.S., Currens, J., Davis, D., & Eidson, W., 1998, Trip reports and cave descriptions of Jackpot Cave, E-mail correspondence with the author from 1996-1998.
- ESRI, 1999, Sink discussion, *in* ArcView 3.2 help [digital documentation within software]: Redlands, CA.
- Ford, D.C. & Williams, P., 1989, Karst geomorphology and hydrology: Winchester, Massachusetts, Unwin Hyman Ltd.
- Glennon, J.A. & Groves, C.G., 1999, Evolving geographic information systems capabilities for management of cave and karst resources, *in* Paper presented at the 12th National Cave and Karst Management Symposium, Chattanooga, Tennessee.
- Granger, D., Fabel, E.D. & Palmer, A.N., 2001, Plio-Pleistocene incision of the Green River, Kentucky, from radioactive decay of cosmogenic ²⁶Al and ¹⁰Be in Mammoth Cave sediments: *Geological Society of America Bulletin*, v. in press.
- Haynes, D.D., 1964, Geology of the Mammoth Cave quadrangle, Kentucky: U.S. Geological Survey.
- Horton, R.E., 1945, Erosional development of streams and their drainage basins: Hydrophysical approach to quantitative morphology: *Geological Society of America Bulletin*, v. 56, p. 275-370.
- Hovey, H.C., 1909, Kaemper's discoveries in the Mammoth Cave: *Scientific American*, no. May 22, 1909, p. 388-390.
- Jenson, S.K., 1991, Applications of hydrologic information automatically extracted from digital elevation models: *Hydrological Processes*, v. 5, p. 31-41.
- Jolly, J.P., 1982, A proposed method for accurately calculating sediment yields from reservoir deposition volumes, Recent developments in the explanation and prediction of erosion and sediment yield, *Proceedings of Exeter Symposium*, July, 1982. IAHS Publication 137, p. 153-161.
- Lee, E.F., 1835, Notes on the Mammoth Cave, to accompany a map: Cincinnati, James & Gazlay, 30 p.
- Leopold, L.B. & Maddock, Jr., T., 1953, The hydraulic geometry of stream channels and some physiographic implications: U.S. Geological Survey Professional Paper 252, 57 p.
- Leopold, L.B. & Wolman, M.G., 1957, River channel patterns: Braided, meandering, and straight: U.S. Geological Survey Professional Paper 282-B, 85 p.
- Meiman, J., 1989, Investigation of flood pulse movement through a maturely karstified aquifer at Mammoth Cave National Park [MS thesis]: Eastern Kentucky University, 343 p.
- Miotke, F.D. & Palmer, A.N., 1972, Genetic relationship between cave landforms in the Mammoth Cave National Park area: Wuerzburg, Germany, Boehler Verlag, 69 p.
- Ogunkoya, O.O., Adejuwon, J.O. & Jeje, L.K., 1984, Runoff reponse to basin parameters in southwestern Nigeria: *Journal of Hydrology*, v. 72, p. 67-84.
- Osburn, R., 2001, Mammoth Cave Cartographic Program (including draft maps of Mammoth Cave System and minor caves within Mammoth Cave National Park), Cave Research Foundation.
- Palmer, A.N., 1981, A geologic guide to Mammoth Cave National Park: New Jersey, Zephyrus Press, 210 p.
- Pfaff, R.M., Glennon, J.A., Groves, C.G., Anderson, M., Fry, J. & Meiman, J., 1999, Landuse and water quality threats to the Mammoth Cave karst aquifer, Kentucky. *Proceedings of the 12th National Cave and Karst Management Symposium: Chattanooga, Tennessee.*
- Quinlan, J.F. & Ewers, R.O., 1981, Hydrogeology of the Mammoth Cave region, Kentucky, *in* Roberts, T.G., ed., GSA Cincinnati '81 field trip guidebook 3: Falls Church, Virginia, American Geological Institute, p. 457-506.
- Quinlan, J.F. & Ray, J.A., 1989, Groundwater basins in the Mammoth Cave region, Kentucky: Friends of the Karst Occasional Publication, v. 1, p. map.
- Quinlan, J.F. & Ray, J.A., 1995, Normalized base-flow discharge of ground water basins: A useful parameter for estimating recharge area of springs and for recognizing drainage anomalies in karst terranes, *in* Beck, B.F. & Stephenson, B.F., ed., *The Engineering Geology and Hydrogeology of Karst Terranes*: Rotterdam, A.A. Balkema, p. 149-164.
- Ray, J.A. & Currens, J.C., 1998a, Mapped karst ground-water basins in the Beaver Dam 30 x 60 Minute Quadrangle, Kentucky Geological Survey.
- Ray, J.A. & Currens, J.C., 1998b, Mapped karst ground-water basins in the Campbellsville 30 x 60 Minute Quadrangle, Kentucky Geological Survey.
- Ritter, D.F., Kochel, R.C. & Miller, J.R., 1995, *Process geomorphology* 3rd edition: Dubuque, IA, W.C. Brown Publishers, 539 p.
- Schumm, S.A., 1956, Evolution of drainage systems and slopes in badlands at Perth Amboy, New Jersey: *Geological Society of America Bulletin*, v. 67, p. 597-646.
- Strahler, A.N., 1958, Dimensional analysis applied to fluvially eroded landforms: *Geological Society of America Bulletin*, v. 69, p. 279-299.
- USGS, 1993, Digital elevation models—data users guide 5: Earth Science Information Center: Reston, Virginia, U.S. Geological Survey.
- USGS, 2001, US GeoData available through the internet, factsheet: Reston, Virginia, (<http://mac.usgs.gov/mac/usb/pubs/factsheets/fs04600.html>), U.S. Geological Survey, 2 p.
- White, W.B. & White, E.L., 1989, Karst hydrology: Concepts from the Mammoth Cave area: New York, Van Nostrand Reinhold, 346 p.

OBITUARY - WILLIAM L. WILSON (1953-2002)

William L. Wilson (NSS 12231FE) passed away on Friday, March 15, 2002. He was stricken with a heart attack exactly one week earlier while on a karst field trip, and did not recover. Bill began caving in 1968. He earned his BSc in geology in 1976 from Indiana University, and worked for 7 years as a field and project geologist for energy extraction companies in West Virginia, Wyoming, and Colorado. He went back to graduate school in 1983, and in 1985 he received a MSc in geology from Indiana State University. His thesis was titled "Lithologic and base control of groundwater flow paths in the Garrison Chapel area, Indiana", with the late Dr. Don Ash as his advisor.

Bill went to Florida in 1986 to begin work as a Research Geologist at the Florida Sinkhole Research Institute at the University of Central Florida. He branched off in 1987 to start his own business, Subsurface Evaluations, Inc. [SEI], which by 2002 had grown into a major geophysical consulting company. SEI provides geophysical surveys and geological evaluations for geotechnical and environmental applications, and specializes in the detection of karst geological hazards, such as sinkhole precursors, and karst hydrogeology. Bill was the first person to provide ground-penetrating radar as a commercial geophysical service in central Florida. Bill was a certified cave diver, and licensed as a professional geologist in Indiana, Florida, and Kentucky. He was the lead scientific diver on many cave diving expeditions including Deans Blue Hole, Red Snapper Sink, and one of the early Wakulla Expeditions.

Bill made substantial contributions to the science of karst and caves. At SEI, along with his wife Diane and others, he provided expert advice to people concerned with collapse sinkholes in the State of Florida and beyond. He maintained a large digital database on sinkhole occurrence, and developed an actuarial method for predicting the likelihood of sinkhole collapse. More recently, his work focused on evaluating the carbonate aquifer as a whole. His thoughts on this topic were just published in a paper entitled "Conduit morphology and hydrodynamics of the Floridan Aquifer: Moving to the next level - conduit modeling" [Karst Waters Institute Special Publication 7, p. 5-8], which he presented as a keynote opening address at a karst conference in Gainesville, Florida, just two days before he was stricken. His goal was to develop a dual-permeability model of the Floridan Aquifer that accurately predicts the effects of conduit networks on groundwater flow.

A scholarship in Bill's name, to support student research in caves and karst, has been established by the Karst Waters Institute in cooperation with Bill's family. Tax-deductible donations will be accepted at: Karst Waters Institute - Wilson Scholarship; PO Box 537; Charles Town, WV 25414. The purpose of the scholarship is to bring new, young scientists into karst research to continue the work that Bill had dedicated himself to. Bill is survived by his wife Diane and their son Robert, his mother Sylvia Motta, grandmother Mary Wilson,



Brothers Greg and Kevin Wilson, and sister Robin Grider.

Bill was an original thinker and a pioneer. He worked quietly and developed both a database and the ideas that illuminated new approaches to understanding karst. He was a steadfast friend to those around him and to the discipline. His good cheer and dedication to cave science will be greatly missed.

John Mylroie and Ira Sasowsky

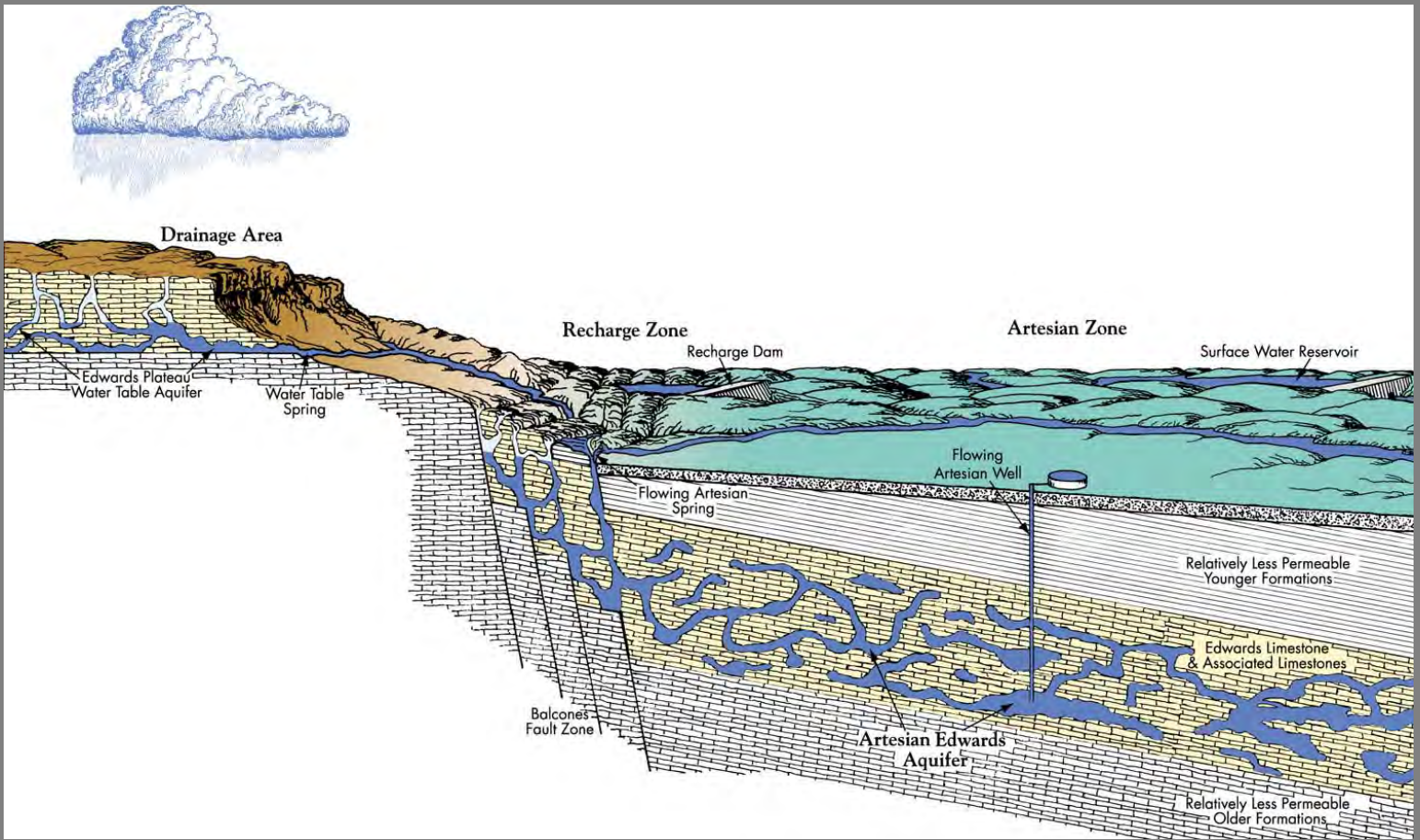
NEW JCKS CONSERVATION EDITOR

The *Journal of Cave and Karst Studies* welcomes a new Associate Editor for Conservation, Julian J. Lewis. A cave biologist by training, Dr. Lewis operates a cave, karst, and groundwater biological consulting company in Indiana. He has published over 90 articles, many of them related to cave conservation issues. His contact information is available on masthead of this issue.

JCKS ADVISORY BOARD ADDS NEW MEMBERS

Three prominent cave and karst scientists have accepted appointments to the *Journal's* Advisory Board for terms extending 2002-2004. They are hydrochemist Malcolm Field from the EPA in Washington D.C., paleontologist Donald McFarlane of Claremont Colleges in California, and geologist William White from Pennsylvania State University. Ending three-years of service to the *Journal* are Douglas Medville, John Mylroie, and Elizabeth White.

Members of the Advisory Board frequently provide advice and suggestions through e-mail conferences throughout the year. They help to form policy, provide insight on complex problems facing the *Journal*, and advise on the selection of new editors. It is an active group whose wisdom and experience has proven invaluable to the editorial staff. We thank the scientists who volunteer their time to help raise the standards of the *Journal of Cave and Karst Studies*.



GEOLOGIC CROSS-SECTION OF THE EDWARDS AQUIFER

National Speleological Society
2813 Cave Avenue
Huntsville, Alabama 35810-4431